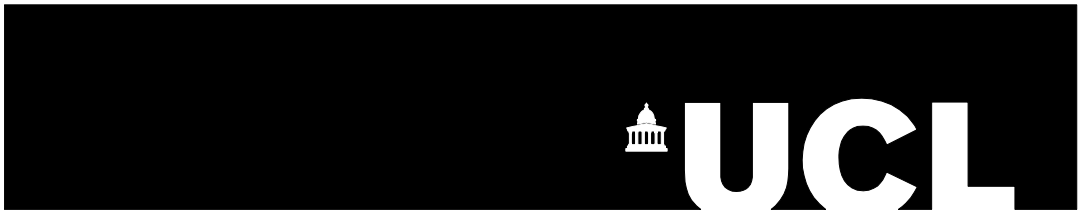

Effect of Gasoline Fuel Additives on Combustion and Engine Performance

Mart Mägi

Submitted for the degree of

Doctorate of Philosophy (Ph.D.)

in

Mechanical Engineering

2015

I, Mart Mägi confirm that the work presented in this thesis is my own. Where information has been derived from other sources, I confirm that this has been indicated in the thesis.

_____

Acknowledgements

I would like to use this page to say a few *thank yous* to the people that have helped me during my Ph.D. and beyond.

Firstly, I would like to thank my supervisors Rama Balachandran and Nicos Ladommatos. Their assistance and advice throughout the project has been invaluable and is greatly appreciated. I would like to thank Innospec Fuel Specialities and especially Trevor Russell and Anthony Cooney for their expertise and support during the Ph.D. years. I am also grateful to the staff at UCL Mechanical Engineering department.

A big thank you to Baptiste and everybody else in the labs. Aadil, Aaron, Anne, Elina, Midhat, Paul and Taaha, your input both academically and otherwise has not gone unnoticed. The 12 o'clock lunches, endless Costa breaks and the quotations on the wall will stay with me for years to come!

On a personal level I would like to thank my family for always, even from distance, being there for me and encouraging me to get to where I am today. I would like to thank Konstantin and his parents Regina and Ralph, whose support has been truly invaluable. And last but not least, I want to thank Echo without whom the past years simply would not have been the same.

Thank you all.

Abstract

Ever increasing emissions regulations and demand for fuel economy have brought about great advances in fuel and engine technologies. Improving engine efficiency through the use of fuel additives has been practiced for nearly a century but advances to direct injection gasoline engines have presented new obstacles that need to be overcome. With direct injection systems often suffering from reduced timescales allowed for combustion processes, atomisation and vaporisation characteristics have become of paramount significance.

Present study aimed at adding to the field of knowledge by experimentally investigating commercial fuel additives of different functionalities against their effects on fuel atomisation and combustion characteristics. Fuel atomisation was evaluated through the use of a laser diffraction system and measurement of fuel viscosity and surface tension. Additives from six functional groups were investigated. Additionally, effects of anti-knock and ignition promoting additives on gasoline combustion behaviour were studied in a constant volume combustion vessel and a single cylinder research engine. Flame speed, heat release rate and emissions output were compared for three commercially available combustion improvers.

Investigation into the effect of fuel additives on the physical properties and therefore on fuel atomisation and sprays revealed that in commercially employed quantities, no significant change in recorded Sauter Mean Diameter could be observed. Combustion investigations in a combustion vessel demonstrated that the low temperature reactions initiated by ignition promoting additive reduced CO emissions up to 37.7 % which could be attributed to possible reduced flame quenching near combustion chamber walls. However, in high quantities this reduction in CO levels was not experienced. Addition of anti-knock additives resulted in increased NO_x emissions, which was thought to result from increased combustion durations. Present work has clarified fuel additive function and interactions with combustion processes and has demonstrated that gasoline fuel additives do not interfere with combustion processes outside their intended functionality.

Contents

Table of Images

Table of Tables

Nomenclature

Abbreviations

AS	Anti-Static(s)
ATC	Technical Committee of Petroleum Additive Manufacturers in Europe
BTDC	Before Top Dead Centre
CCD	Combustion Chamber Deposit(s)
CI	Combustion Improver(s)
CF	Carrier Fluid(s)
CFD	Computational Fluid Dynamics
CVCV	Constant Volume Combustion Vessel
CVHC	Constant Volume Hot Cell
CVPC	Constant Volume Pre-Combustion Cell
DCA	Deposit Control Additive(s)
DI	Direct Injection
DRA	Drag Reduction Agent(s)
EGR	Exhaust Gas Recirculation
FM	Friction Modifier(s)
GDI	Gasoline Direct Injection
HC	Hydrocarbon
HRR	Heat Release Rate
IC	Internal Combustion
ICCD	Intensified Charge couple device
IMEP	Indicated Mean Effective Pressure
KI	Knock Intensity
LD	Laser Diffraction
NO_x	Oxides of Nitrogen
ORE	Optical Research Engine
ORI	Octane Requirement Increase
PDA	Phase Doppler Anemometry
PDIA	Particle/Droplet Image Analysis
PFI	Port Fuel Injection

PM	Particulate Matter
PMT	Photomultiplier Tube
PN	Particulate Number
PPM	parts per million, mg/L
PT	Pressure Transducer
RCM	Rapid Compression Machine
SG	Shadowgraph(y)
SI	Spark Ignition
SMD	Sauter Mean Diameter
SOI	Start of Injection

Symbols

A	Area	(m^2)
A	Constant. 25.1 for pintle nozzles, 23.9 for hole nozzles, 22.4 for throttling pintle nozzles.	
B, C	Constant determined by nozzle geometry	
f	focal length	
ν	Kinematic viscosity of fuel	(m^2/s)
σ	Surface tension	(N/m)
ρ	Density	(kg/m^3)
μ	Viscosity of fuel	(Pa*s)
θ	Half cone angle of spray/ Contact angle	(°)
ΔP	Mean pressure drop across the nozzle	(MPa)
Q	Injection quantity	(m^3/stroke)
Q’	Injection quantity	(kg/s)
t	Liquid film thickness at plane of discharge from nozzle	(m)
V	Volume of fuel per cycle per cylinder	(m^3/stroke)

Subscripts and Superscripts

a	Air
c	Critical
eff	Total effective for all nozzle holes at ΔP
f	Fuel

fc	Fuel per cycle per cylinder
g	Gas
l	Liquid
orf	Total for all nozzle holes

Chapter 1

Introduction

The discovery of crude oil in the middle of 19th century and the subsequent development of the internal combustion engine have led the use of fossil fuels to increase exponentially. Figure 1.1 displays the increase in the number of cars and fuel usage throughout the last century in USA. Similar trends can be seen throughout the

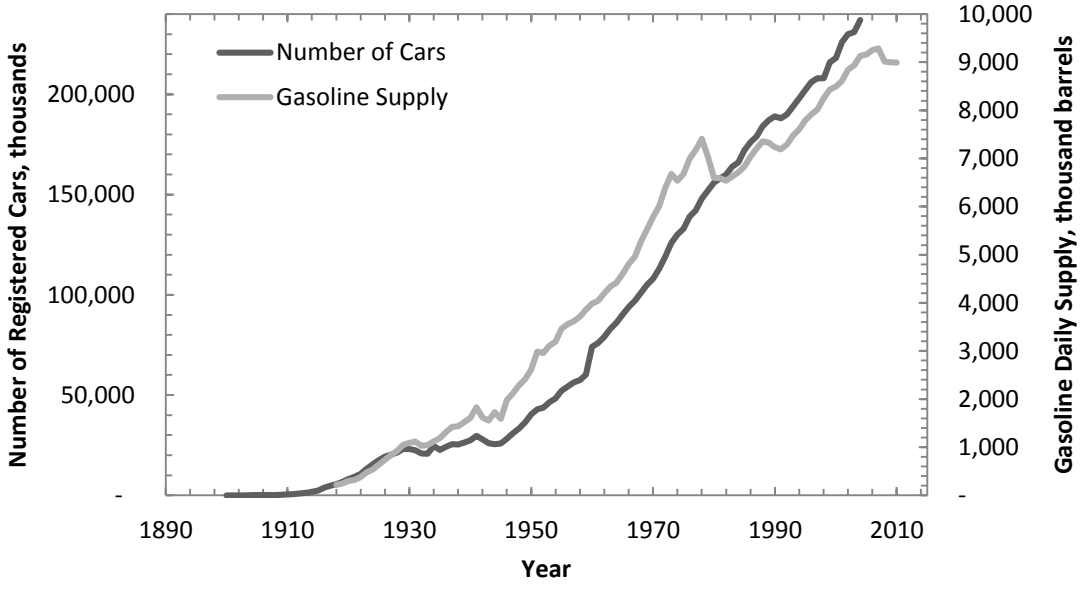

Figure 1.1: Fuel Usage and Number of Cars in the USA throughout 20th century [1, 2]

developed world. It has been widely accepted that the emissions from burning fossil fuels contribute towards climate change and air pollution. As a result increasingly stringent regulations, for instance the EURO 1-6 emission standards shown in Table 1.1, concerning fuel efficiency and emissions are imposed on new vehicles. The need for compliance with the regulations has been among driving forces behind advances in engine and fuel technologies. Among techniques employed to improve the fuel's performance is the use of fuel additives. They are a chemical tool used to improve fuel properties and offer great advantages from environmental and economic point of view.

Standard	Date	CO	HC	HC+NOx	NOx	PM	PN
Euro 1	1992	2.72	-	0.97	-	-	-
Euro 2	1996	2.20	-	0.5	-	-	-
Euro 3	2000	2.30	0.2	-	0.15	-	-
Euro 4	2005	1.0	0.1	-	0.08	-	-
Euro 5	2009	1.0	0.1	-	0.06	0.005	$6.0x10^{11}$
Euro 6	2014	1.0	0.1	-	0.06	0.005	$6.0x10^{11}$

Table 1.1: Regulated exhaust gas emissions within the EU for gasoline powered passenger cars. A given standard applies to all new cars sold within the EU after a given date. PM and PN emissions are only applicable to engines with direct injection. All emissions are measured in g/km, except for PN which is measured in #/km [3]

1.1 Background on Additives

Fuel additives are chemicals used in very small quantities to enhance or add properties to base fuels. The quantity of additive added to base fuels is referred to as a treat rate and is typically in the range of 1-20,000 mg/l. According to Barnes et al. [4], improving engine efficiency and emissions through the use of fuel additives has been practiced for nearly a century. The earliest additives were lead based organometallic compounds that reduced auto-ignition in spark ignited combustion systems but concerns with pollution and legislation changes mean in the developed world only organic compounds are now employed. Since the early days, additives that function also in areas outside the combustion chamber have been developed. Along with aiding combustion reactions and pathways, additives are utilised to address issues

arising from deterioration or failure of fuel delivery system components due to wear or accumulation of deposits. For optimum operation, this is especially important in modern fuel metering systems, where high pressure direct injection systems and electronic control and monitoring mechanisms are sensitive to deviations from normal operational characteristics. Additives additionally provide benefits in refineries, where lower-refined fuels can be made to offer similar if not better physical and chemical properties compared to their highly refined derivatives.

Typically, additives are supplied to oil companies as pre-prepared packages tailored to customers' specifications and often are only mixed with the fuel at the final stages of the supply chain which enables great cost savings and product differentiation. In general, irrespective of their function, additives are employed to affect the overall performance of internal combustion engines. Additive functional groups include combustion and lubricity improvers, detergents and carrier fluids and characteristic chemistries often comprise polymeric compounds with polar head groups and fuel soluble long chain tails. In some cases oxygenates that are added to fuel in quantities of up to 50% by volume are referred to as additives but in present work only the performance modifying compounds used in the parts per million (PPM) range are considered. A detailed overview of the different additive groups investigated in the present study will be given in Chapter 2.

1.2 Objectives

A good understanding exists of fuel additive effects on the overall engine performance and combustion process. The investigations mainly include vehicle field tests and single cylinder research engines. Although such methods give a good representation of the overall effects, the de-coupled effects of fuel additives on the individual stages of the combustion process are not fully represented.

The spark-ignited combustion can be separated into four sub-stages: fuel atomisation; air-fuel mixing and fuel evaporation; ignition; and flame propagation. The first two stages largely depend on the fuel delivery system and the physical properties of the fuel such as density, surface tension and viscosity, while the latter two are controlled by chemical reactions. It is generally believed that only combustion improvers, which divide into ignition promoters and anti-knocking additives, have a direct effect on combustion processes. Both types of combustion improvers are

chemically active and alter the radical pool mainly in the ignition stage of the combustion process. Ignition promoters are used in diesel fuels and provide chain branching radicals that enhance auto-ignition. The anti-knock additives are used in spark ignition engines to prevent auto-ignition by providing chain terminating radicals. A more detailed overview of combustion improvers is given in Chapter 2.

Although it is unlikely that additives from other functional groups have a significant effect on ignition or flame propagation, some additive groups comprise long chain polymeric compounds that can affect fuel viscosity, surface tension and density (although quantities used often mean the effect might be small) and can as a result have an effect on the atomisation, air fuel mixing and fuel evaporation which in turn affects the latter stages of the combustion process.

The additive effect on the physical properties of the base fuels is especially important in modern direct injection (DI) fuel delivery systems where fuel is injected directly into the combustion chamber. According to Aradi et al. [5], gasoline direct injection method allows for fuel consumption reductions of up to 35% when running in stratified mode, but the short timescales allowed for fuel atomisation and evaporation can inhibit sufficient air-fuel mixing. Consequently several problems such as poor running of engine, spark plug wetting and soot formation can arise. Soot forms as a result of excessively fuel rich areas within the combustion chamber oxygen starvation causes the fuel to nucleate from vapour to solid phase [6]. This soot in turn translates into smoke emissions from exhaust as well as deposits in the lubricating oil through exhaust gas blow-by. Insufficient air-fuel mixing can additionally contribute towards increased unburned hydrocarbon and carbon monoxide emissions. Lefebvre [7] has described in detail how changes in viscosity and surface tension of fuels affect the atomisation characteristics of fuels.

The research into the de-coupled effects of additives on the combustion processes is limited. Up to date, no published data on gasoline atomisation characteristics with different fuel additives could be found, though, limited investigations on the effects of additives on diesel sprays are available. Felton et al. [8] identified detergents as additives that due to their surfactant nature could alter atomisation characteristics of diesel sprays. Their investigations, although based on a small data set, concluded that detergent additives could affect the droplet size and evaporation rates. Higgins et al. [9, 10] carried out experiments on changes to spray liquid length and cone angle (detailed descriptions given in Section 2.3) with ignition

promoters. They found no effect on physical properties outside experimental repeatability.

In addition to the effect additives have on the physical properties of the base fuel, significant changes in combustion behaviour can be seen. Colucci et al. [11] showed an improvement in gasoline performance under cold start conditions with the addition of a diesel ignition promoter without affecting the base fuel auto-ignition characteristics. They claim a complete removal of cold start misfires with the addition of 2-ethylhexyl nitrate (2-EHN) in low quantities. Higgins et al. [9, 10] showed atomisation and evaporation characteristics to be unaltered by ignition promoters and as such, the effect can be assumed to originate from chemical reactions. However, Colucci et al. [11] provide no mechanism through which the improvements in cold start characteristics are achieved.

To date, majority of DI spray investigations have been based on diesel atomisation. Although no significant effects on fuel sprays from additives have been noted, the high injection pressures used with diesel injection systems could mean the effect of additives is overpowered by the injection pressure effect. Development and deployment of gasoline DI systems in the recent decades warrants a new study into the effects of fuel additives on gasoline atomisation characteristics where typical injection pressures can be an order of magnitude lower than in diesel DI systems. In addition, an improved understanding of the mechanisms through which ignition promoters and anti-knock additives affect combustion characteristics could provide basis for new and enhanced additive chemistries to be used in gasoline-like fuels. Usage of biofuels in modern fuel compositions results in further unknowns about fuel sprays and knowledge of fuel blend composition effects on atomisation quality could enable improved injector designs as well provide valuable information to additive manufacturers about the effect different concentrations of additive in base fuel have on the properties of the blends.

In this light, the aim of the present study was to assess the usage of gasoline fuel additives for suitability with latest engine technologies and emissions legislation. In order achieve this, the present study has sought to advance the understanding of fuel additive interactions with combustion processes by looking to fulfil the following objectives:

- Investigate the effect of fuel additives on fuel spray quality through droplet sizing methods under varying injection pressures and fuel additive treat rates
- Investigate the effect of fuel additives on fuel viscosity and surface tension
- Investigate atomisation characteristics of single component fuel binary mixtures and diesel fuel under varying injection pressure and fuel temperature conditions in light of future alternative fuel demands and to explain results obtained from fuel additive investigations
- Investigate the effect of fuel additives on fuel combustion behaviour and emissions at varying additive treat rates
- Investigate the effect of fuel additives on emissions characteristics

In summary, the present study was carried out in order to contribute to current understanding of fuel additive interactions with gasoline fuels with atomisation characteristics in direct injection systems and combustion characteristics with ignition promoters and anti-knock additives being the special items of interest.

1.3 Thesis Layout

Chapter 1 has offered an overview of the current project. In order to provide a more in depth view of the current understanding of fuel atomisation and combustion and the interactions with fuel additives, Chapter 2 presents the background on the wider research on the topic. This includes a detailed description of the fuel additives studied in present work and research methods used in literature for fuel atomisation and combustion characteristics studies. Chapter 3 presents the hardware employed in the work and explains reasoning behind the selection. In Chapter 4, the experimental methods are explained for spray and combustion investigations. Throughout the chapter base fuel is investigated under various conditions in order to develop methods to effectively understand how additives affect the spray formation and combustion characteristics of the base fuel. Chapters 5and 6 then describe the study into study the effects of additives on fuel atomisation and combustion, respectively. Finally, in Chapter 7 conclusions are drawn from the previous work and a summary of results is offered. This chapter also provides some recommendations for future studies in the same field. High speed shadowgraph imaging was employed in this work for providing

qualitative information, an example of which is displayed in Appendix A. Dimensional analysis explaining spray characteristics is presented in Appendix B.

Chapter 2

Literature Survey

Chapter 2 seeks to present background theories and research relating to the current project. First, the function of fuel additives and the research in the field is offered. Then fuel spray formation features relevant to IC engines are explained and the chapter concludes with combustion characteristics.

2.1 Fuel Additive Review

Fuel additives are chemicals added to fuels in small quantities in order to enhance their performance or add properties that were not present in the base fuel. Improving combustion characteristics would enable reduction of emissions through for example reduced burning temperatures or reduction of deposits. The latter, if present, could increase combustion temperatures and/or contribute towards an increase of unburnt hydrocarbons.

The first fuel additives to find their way into wider use were antiknock additives in gasoline, first found in 1921. Combustion in gasoline engines is initiated by an external energy source. However, given certain conditions, it is possible for a gasoline fuel to self-combust as a result of high pressures and temperatures. Such event is called ‘knocking’. Gasoline engines in general are designed for pressure levels far

lesser than the diesel engines and self-combustion in gasoline engines often results in sudden pressure hikes and can damage the engine. In order to prevent this from happening, antiknock additives are used in gasoline fuels.

Fuel additives can be grouped based on different functional criteria. The most common separation is made between diesel and gasoline fuel additives. There are some species of additives that only contribute towards one group of fuels but many, such as lubricity or deposit control additives, have properties that work well with either of the fuels. Fuel additives can also be classified into 'distribution' and 'vehicle fuel system' additives. The former group are the ones that are used in refineries to produce fuels of specific specification at optimum cost levels. The latter group are used in the vehicle's fuel system and only provide benefits when the fuel enters the engine inlet system or the combustion chamber.

Typical fuel system additives include deposit control additives, combustion improvers and lubricity additives whilst distribution system additives include drag reducing agents and often anti-static additives. In some cases oxygenates such as methyl t-butyl ether (MTBE) are added to fuels to increase their octane rating [12] but are, due to the volumes in use, not considered additives but fuel compounds. Typical performance additives treat rates fall within the 1-10,000 mg/L (often referred to as ppm) range whereas some oxygenates and bio-fuel blends can be treated at rates of more than 50 % by volume.

Additives are usually sold to oil companies as a package satisfying the specified requirements. Due to financial gains, most oil companies share refineries and only add additives into fuels before fuel retail stations. This allows for great cost efficiencies and product differentiation.

The following sections will aim at giving a better understanding of the additives that this project is concerned with. The additive groups under investigation are deposit control additives, combustion improvers, anti-statics, drag reducing agents, friction modifiers and carrier fluids.

2.1.1 Deposit Control Additives

The presence of deposits within an internal combustion engine has been known since the beginning of 20th century when most effective way of removing deposits was thought to be 'burning out cylinders' with pure oxygen [13]. Since then deposit control additives (DCA) have been developed. They are designed to remove deposits from

vehicle fuel systems and the combustion chamber. By removing different oxides from fuel they also provide corrosion resistance. DCA are petrol soluble chemicals that in most cases are also preferred to be soluble in lubricating oil. DCA are the most researched additive group with approximately 57 % share of all patents and patent applications in 2002 [14].

Although most deposits are likely be derived from the fuel and combustion, some also originate from crankcase lubricant.

Gasoline DCA are mostly detergents and dispersants often combined with carrier fluids. Typical additives come from chemical groups like amides, amines, amine carboxylates, polybutene succinimides, polyether amines and polyolefin amines [4, 15, 16, 17]. The molecule consists of a long fuel soluble hydrocarbon tail and a polar head group [4, 18]. The two parts of the molecule have different solubility within the fuel and as a result often occur as an inverse micelle. Both detergents and dispersants function similarly in that they trap deposit precursors (which are due to insolubility in fuel attracted to the DCA molecules) within the micelles. For smaller particles (20-50 nm) DCA create a thin film around the deposits in fuel preventing deposit coagulation. Particles of size >50 nm often carry a surface charge that attracts detergent and dispersant additive molecules. By doing so, the further coagulation of deposits is inhibited by charge repulsion [18]. A further mode of action is that DCA coat the surfaces of the fuel system, reducing the available surface area for the deposits to be attracted towards. Concentration of additives in fuel can vary between 30-20,000 ppm [19, 20, 21]. Dispersants are often referred to as ashless due to the lack of metals to form metal oxides during a combustion event, while detergents often use magnesium and calcium in their composition. A typical dispersant molecule has a longer hydrocarbon tail than a detergent and as a result can hold up to 10 times the amount of deposit particles.

Deposit control additives for gasoline fuels are divided into 3 main categories based on the area of action:

i. Fuel Metering System

Fuel metering system includes carburettors and injectors. Deposits in these areas if large enough can obstruct fuel flow into the induction system or in case of direct injection to the combustion chamber, resulting in higher air-fuel ratios, reduced power output and in more extreme cases, injector failure [22, 23]. The additives in these areas work as dispersants or detergents. Also, coating surfaces is possible

whereby a layer is created on the surfaces of the metering device that prevents accumulation of deposits. Additives used for these areas include low molecular weight amines and amine carboxylates.

ii. Induction System

Induction system comprises any areas between the injector/carburettor and the combustion chamber, i.e. intake manifold, intake ports and intake valves. It has been reported poorly formulated additives can cause build up around intake valve seat area and become viscous at low temperatures preventing valve movement [24]. Further, deposit build up in this area can inhibit closing the valve in other IC engine strokes than the intake, resulting in loss of compression. This can affect the running of the engine or further promote formation of deposits within the combustion chamber, as shown by Fukui et al. [25] who found that lower pressure conditions exhibit higher tendency of deposit build up. This could be explained by lower combustion efficiency at lower compression ratio conditions. Additives designed for the induction system operate on the principle of detergents but also coat the induction system surfaces, thus preventing new build-up of deposits. Longer chain higher molecular weight additives such as polybutene amines are used [14].

iii. Combustion Chamber

Deposits in this region accumulate on the piston tops, cylinder head area, spark plugs and exhaust valves. It has been widely reported that combustion chamber deposits (CCD) contribute towards ignition through deposit induced hot spots [26, 27, 28], the subsequent fuel octane requirement increase (ORI) [29, 30] and emissions increase [31, 32]. ORI results from thermal insulation of metal parts by deposits and possible heat storage which can ignite the air-fuel mixture before the spark event causing pressures hikes and raised temperatures leading to engine pre-ignition and knock [33, 34]. Additives aimed at reducing CCD neutralise acidic compounds derived from combustion that can act as deposit precursors [35]. Bert et al. [30] claim an ORI of up to 15 % could be experienced in an engine due to deposit build up within the combustion chamber. Raised temperatures within the combustion chamber can increase the engine's NO_x output as nitrogen from the air breaks down to monatomic nitrogen. This in turn could further contribute towards CO emissions if some of the carbon is unable to form CO_2 because oxygen assumed available for combustion is used up previously by nitrogen. The importance of lubricating oil and additive composition in formation of CCD was emphasised by Bartleson and Hughes [36].

However, that was nearly 60 years ago and in recent times no significant study has been found except for that of [25], where a 2-stroke engine was used for the experimental work. It could be assumed that increased engine manufacturing tolerances have prevented significant leakage of lubricant into the combustion chamber.

Zerda et al. [26, 37] carried out two experiments using derivatives of polyether amine and polybutene amine on the effect of DCA on the microstructure of CCD. They showed that the highly porous nature of deposits results in the total inner surface area of approximately 300 m^2/g of deposit. They argued that the volume available within the deposits promotes incomplete combustion and HC emissions whereby part of the air-fuel mixture is locked in the available space and remains unburned. Reduction in available surface area with the use of an additive was noted. Further, polyether amine additive showed a decrease of intake valve deposits compared to base fuel of 73 % while a 21 % increase in CCD was experienced. No data on intake valve deposits from polybutene amine was enclosed but a 10 % increase in CCD was reported. HC emissions can increase further if CCD build-up hinders full closure of exhaust valves letting some of the air fuel mixture to leak into the exhaust manifold.

It has been shown that DCA used with conventional PFI injection systems is ineffective in reducing CCD while DI equipped cars can see a significant reduction in CCD when same additives are used [4]. As such, in PFI engines, often the benchmark for performance is neutrality whereby no new CCD occurs. Development of GDI engines has caused a shift in research such that in 2001 – 2005 nearly half of all detergent patents aimed at removing CCD were designed for GDI engines [38]. Typical additives against CCD are the same as for previous two groups and include different amines and alkenyl succinimides.

Development since the introduction of DCA in the 1950's has been significant but several unknowns and discrepancies in research exist. Lewis and Honnen [39] describe an additive formulation that is effective in the fuel metering and induction systems but does not contribute towards CCD, whilst the need for additives that are simultaneously suitable for carburettor, PFI and GDI fuel metering technologies has also been recognized [21]. Although it is thought that ashless dispersants, due to their lack of metals, discourage ash formation on combustion [18], Fukui et al. [25] found that at combustion pressures of 1.5 MPa an ashless dispersant produces up to 50 % more CCD than a metal based additive. They mention, however, that under regular

engine operating conditions such pressures are improbable. Zerda et al. [26] found that additives with head groups of lesser polarity are more effective at reducing CCD than those with higher polarity but are unable to provide a mechanism to explain the phenomenon. Similar results were reported by Martin et.al [40] who found that polarised sulphur compounds in fuels promote deposit formation.

It is evident that DCA is a very important and widely investigated group of additives. It is also clear that testing of effectiveness only applies to suitability against the designed criteria. Effects on combustion and spray formation are unknown and advances to DI systems mean whole set of additives designed to be used in the induction system are made redundant.

2.1.2 Combustion Improvers

Combustion improvers (CI) are in broad terms additives that improve fuel's combustion characteristics. In gasoline fuels, CIs primarily improve a fuel's octane number which in practice relates to its knock resistance. As such, CIs in gasoline are often also called anti-knock additives. Gasoline combustion is based upon a single source of ignition that initiates flame kernel growth and the subsequent flame propagation. Fuels that auto ignite prior to this can cause violent combustion that can raise the pressure beyond the designed values and damage the engine. According to Zhen et al. [41], knocking over a prolonged period causes damage mainly to piston rings, cylinder head and piston crown erosion, piston melting and increases the emissions levels.

Knocking in gasoline IC engines occurs when enough energy is present to cause stable molecules within the fuel to break down without an external energy source. This usually occurs within the air-fuel mixture in a cylinder that is reached latest by the propagating flame front, called the end gas [42]. Due to increasing pressure and temperature conditions as a result of piston movement and flame propagation, the end gases can reach an energy state high enough to initiate combustion reactions which produce highly reactive radicals before being consumed by the propagating flame, resulting in knocking. Chain initiating reactions are followed by propagation and chain-branching reactions, where the aforementioned radicals react to form products and new radicals. In the propagation reactions, the number of radicals consumed is equal to that produced while in chain branching reactions more radicals are produced than consumed. The final termination reactions

take place when fewer radicals are produced than consumed. This process will continue until all unstable radicals are converted into stable reaction products.

CI anti-knock additives are molecules that break down at lower temperatures than knocking conditions and provide radicals that either consume chain initiating radicals or cause chain debranching, thus preventing auto ignition [43]. However, as Benson [43] further explains, the additives are often limited in the temperature range. A shift in a temperature conditions can initiate a different path of reactions that could in fact support chain initiating reactions.

Initially an organometallic additive Tetraethyl Lead was used but starting with legislation changes from 1996 up to 2005, lead anti-knock additives have been banned from being sold within the EU. This is due to an increase in concentrations of lead in the bloodstreams of people living in urban environments which has a negative effect on the human intellectual development [44]. It has been reported that an increase of 1 µg/dl blood lead level can decrease the average intelligence quotient (IQ) by 0.25 points [45]. Although this effect can be considered low, Rosen [46] argues that it applies to a very large proportion of population and affects the number of people with exceptional IQ score. This has caused a market change towards lead replacement additives but has also indirectly created grounds for an increase in the use of diesel fuel.

According to Dabelstein et al. [47], other metallic compounds have been used as anti-knock additives but can exhibit similar shortfalls to lead compounds. Furthermore, ashless (non-metal containing) nitrogen based aniline additives can be used, though, their effectiveness is often reduced in small quantities and higher treat rates are economically unviable in comparison. Moreover, it has been found that fuel bound Nitrogen compounds have a capability to increase NO_x emissions [48, 49]. Ickes et al. [50] argue, however, that any increases in emissions levels due to additives are offset by the benefits offered by using the additives. In some countries, oxygen containing compounds, such as ethers are used instead of CI additives, although the quantities involved mean they are not considered as fuel additives but fuel components.

Further improvements can be seen by using metallic additives that work based on a catalytic effect, although the use has been stopped in developed countries. May [51] explains the catalytic effect of iron and magnesium based CI additive with excitement of outer layer electrodes. At the start of combustion these electrodes

acquire energy states higher than that of surroundings. They then release this energy to reach a degenerate state, thus maintaining the required reaction activation energy level and reducing the effect of quenching or other thermal losses that would hinder completion of combustion reactions.

Due to possible metal phase sintering under high temperature conditions during combustion but also financial viability, typical treat levels of organometallic catalytic CI fall below 1,000 ppm [52] although effects can be seen from treat levels as low as 0.005 ppm [53]. Lyons and McKone [54], using organic compounds of selenium, animony, arsenic, bismuth, cadmium, tellurium, thallium and tin, argue that concentrations of at least 10-400 ppm need to be reached before instantaneous effects can be seen. However, they note that in time, with build-up of catalytically active deposits, it is possible making lower treat rates of additive effective. This conclusion is further supported by field tests by May and Lang [55] who saw a delay of a 'few days' before full effect of additive was experienced. The additives in this case included combinations of magnesium and iron and pure iron. Typical additives used as catalytic CI are alkali or other metal salts although it has been noted that some metal containing detergents can also act as CI [14, 56, 57].

In diesel fuels, CIs improve the fuel's cetane number, which constitutes as ignition quality. Unlike in gasoline fuels, diesel combustion relies upon auto-ignition. The higher the cetane number the easier the fuel will ignite and shorter the ignition delay (time between SOI and start of combustion). CI are unstable molecules that can easily break down at relatively low temperatures to provide free radicals in combustion reactions to enable faster conversion of a hydrocarbon fuel into CO_2 and H_2O [58]. Typical diesel CIs include organic nitrates and organic peroxides, with the most common compound being 2-ethylhexyl nitrate (2-EHN) [59, 60].

CI can reduce emissions in diesel engines. May and Lang measured a reduction in NO_x emissions of over 75 %. They contributed the effect to lower combustion temperature due to enhanced lean burning capabilities of the fuel. Gonzales [56] similarly found an advantageous effect of a CI additive with a 25.1 % decrease in NO_x emissions. This, however, was contributed to an increased resonance radiation from the core of the flame which would result in a cooling effect along the outer edges of the flame. A further explanation is proposed by May [61], whereby the enhanced reaction speeds reduce the time available for NO_x formation. May & Lang and Gonzales further found a decrease in other controlled emissions (see Section 2.4.4)

and improved fuel consumption. Higgins et al. [10] showed that 4,000 ppm of 2-EHN additive in low cetane number fuel reduced the ignition delay for low pressure and temperature conditions compared to equivalent high cetane number fuel. Furthermore, the increased nitrogen from the additive composition was observed to increase the NO_x emissions.

Although cetane improvers are designed to promote auto ignition in diesel combustion, in some cases adding these additives to gasoline fuel has been found to be advantageous. Colucci et al. [11] show that using 2-EHN in gasoline, the ignition properties of the fuel can be significantly improved. They found that at 100 ppm treat rate, misfires during the cold start period have been completely removed. Moreover, it is claimed that the additive would enable reduced cycle-to-cycle variations during normal running. However, no mention is made of the limiting engine operating conditions where auto ignition could start occurring. According to Aradi and Roos [62] 2-EHN only survives at temperatures up to 625 K. They argue that improvement in engine efficiency could be achieved if additives that dissociate near the ignition temperatures of around 800 K were utilised. Furthermore, Morsy [63] displayed the usefulness of diesel orientated CI as tools to control combustion in homogeneous charge compression ignition (HCCI) engines where gasoline-like fuels are utilised and Becker [64] demonstrated the use of cetane improvers in high octane fuels to be beneficial for multi fuel engines.

Due to similar nature of base fuel and their combustion process, CI are suitable for most liquid fuels including gasoline, diesel, kerosene and others [65, 66]. However, some CI additives are fuel insoluble and can contribute towards fuel system deposits. As such, they are often used in conjunction with carrier fluids. Kitchen [67] uses small quantities of naphtha and polyalphaolefin synthetic oil for such purpose along with combustion enhancing manganese linoleate. More detailed description of carrier fluids will be offered in Section 2.1.6.

2.1.3 Anti-Statics

Due to low electrical conductivity characteristics of hydrocarbon fuels, static build up during handling and distribution processes can lead to ignition of the fuel or even an explosion [68]. Desulfurization of modern fuels has reduced their natural electrical conductivity even further. Low conductivity promotes electrostatic charges,

which often result from pumping operations, to form as a result of charge separation [69].

Good explanation for such phenomenon is offered by Leonard [70, 71]. It is believed that static charge originates from ionic impurities present in the hydrocarbons. At stationary conditions, such impurities locate between the surface of the fuel container and the fuel itself. Since negative and positive charges of the impurities are equal in numbers, a neutral total charge prevails. However, under flow conditions in a high shear environment the portion of an impurity molecule attracted to the container walls remains attached to it whilst the other is swept away. Ions attached to the container walls can dissipate their charge to the ground through the walls whereas those in the fuel remain charged, thus giving a negative or positive charge to the hydrocarbon. Charge build up can occur if electrical conductivity of the hydrocarbon is in the range 0.1-10 pS/m or less. Without sufficient dissipation, significant potential can be stored and in case of an eventual discharge to a grounded object through a flammable air-fuel vapour mixture, can result in ignition [72].

Early attempts to reduce static charge build-up included changes in design of handling devices [73] and more recently vehicle fuel system components that dissipate electrostatic charge [74]. However, in modern fuels anti-static additives (AS) are used. AS additives increase the electrical conductivity of the fuel, thus, reducing probability of charge accumulation. Leonard [71] reports an increase in electrical conductivity of over 50 pS/m or more with an addition of only 1 ppm of AS additive while safe limit is considered to be above 40 pS/m. Early AS included heavy metals but environmental concerns have resulted in a shift towards additives which include chromium materials, polymeric sulphur and nitrogen compounds [4, 75, 76]. Schwab and Kyaw [77] note that the most commonly used AS agent is a sulphur based Stadis® brand as sold by Innospec Fuel Specialities. However, possible problems with sulphur based additives rise form generating additive performance packages, as often preferred in modern fuels. These compounds are highly reactive with nitrogen based additives, such as those used in CI and hence could lose their effectiveness in increasing a fuel's electrical conductivity. They propose using a strong acidic compound in conjunction with the AS additive to neutralise some of the nitrogen-containing compounds. Typical additive treat levels are in the region of 0.5-20 ppm.

2.1.4 Drag Reducing Agents

Drag reducing additives (DRA) are high molecular weight (typically exceeding 1 x 10^5) polymers added in low concentrations to single or multiphase fluids to reduce frictional pressure losses in pipes and ducts [78]. Energy is needed to overcome such pressure losses and is taken directly from the fluid pressure. In water, the pressure loss over a meter of pipe with an increase in mass flow rate from 10 g/s to 20 g/s, increases approximately 300 % [79]. Pressure drops in pipes increase with increasing flow rate until they equal to the fluid supply pressure. Using DRA has enabled a reduction in frictional losses and an increase in production rate of crude oil by increasing the flow rate of oil for a given pressure drop or lowering the pressure drop for a given flow rate. The additives, other than in petroleum based products, are known to be used in flood water disposal, biomedical systems, field irrigation, firefighting and other applications [80]. In general, DRA can, due to their large molecular weight, be considered viscosity modifiers if used in large enough quantities, although in concentrations used in industry a notable effect is unlikely.

Although effect of drag reducing additives is known, the drag reducing mechanism is not fully understood [81]. Losses in pipes and ducts are thought to result from friction created by turbulent processes in the flow. Warholic et al. [82] believed these to be caused by Reynolds shear stresses and velocity fluctuations normal to the pipe wall resulting from small scale flow disturbances along the walls that develop to form large scale turbulent structures. Drag reduction increases as the Reynolds shear stress tends towards zero. They conclude from their experiments that drag reduction results from aggregates of additive molecules being broken up. This means entangled additive molecules are separated in turbulent flow, dissipating energy from turbulent flow sections. Further, this explains the degrading nature of some drag reducing additives. Their experiments using a polyacrylamide and sodium-acrylate co-polymer showed up to 10 % reduction in drag with additive concentrations as little as 0.25 ppm whereas maximum reduction in drag was seen at concentrations of 13 ppm and 50 ppm.

Similarly to drag reducing mechanism, the effect of concentration or molecule size is yet to be agreed upon. Al-Yaari et al. [83] showed, however, that with a 3 x 10^5 molecular weight a small negative effect can be seen due to greater rate of dispersion of different liquid phases, whilst molecular weights of 4 x 10^6 and 8 x 10^6 kept

different liquid phases stratified and displayed an increase in drag reduction with increasing molecular weight as well as increasing concentration. These results are in good agreement with Deshmukh et al. [84] who show an increase in drag reduction of up to 65 % with increasing concentration and Shanshool and Al-Qumaje [85] who showed an increase of 6.3 % in drag reduction with an increase in molecular weight from 2.6×10^6 to 5.2×10^6. The decrease in frictional losses can be assumed to result from enhanced entanglement of additive molecules with larger molecular weight or quantity of molecules.

Deshmukh et al. [84] further investigated the bio- and shear degrading of DRA. Due to degradation, the effect on frictional pressure losses disappears whilst the heavy molecules remain in fuel and as Al-Arji [86] has shown, can contribute towards deposit build up in the internal combustion engine intake valves and combustion chamber. Deshmukh et al. [84] conclude that up to 32 time increase in bio- and shear degradation resistance can be achieved if graft copolymer derivatives of guargum and polyacrylamide are used instead of their commercially available versions.

According to Hoyt et al. [87] DRA additionally work as anti-misting AM agents. AM agents are mainly used in jet fuels to inhibit formation of fine fuel mists that can occur after aircraft crash landings [88]. The high molecular mass of the additives increases the fuel viscosity and as such also affects the morphology of the fuel droplets generated in such conditions. Little et al. [89] bring out the quantities used as the difference between DRA and AM agents. DRA usage remains within the ppm range while AM agents can be used in concentrations of several tenths of a per cent by volume.

2.1.5 Friction Modifiers

Desulphurisation of modern fuels has instigated the need for use of friction modifiers (FM). Low sulphur levels are mandated in gasoline and diesel fuels both, with Ultra Low Sulphur Diesel consisting as little as 15 ppm or less of sulphur [90]. However, it is argued that sulphur itself does not directly contribute towards the lubricant properties of the fuel. Wei et al. [91] describe a study which concluded that the drop in fuel lubricity results from removal of oxygen-containing and other polar materials that are inevitably removed as bi-products during the desulphurisation process. In vehicle fuel delivery systems, pumps and injectors rely nearly solely on fuels for lubrication. However, hydrocarbon fuels have a low viscosity and consist of

nearly no polar components resulting in poor hydrodynamic and boundary layer lubricating properties.

Whilst in some heavy duty diesel machinery significant efficiency gains could be experienced as a result of FM use, in gasoline engines, where fuel pressures only reach a fraction of the pressure, key benefits lie within reliability and extended life expectancy of fuel pumps and injectors. Gustavsson et al. [92] showed with different fuels that factory coatings used in high pressure fuel system components exhibit good to excellent lubricating characteristics, but under sufficient contact pressure can wear out in as little as 10,000 piston strokes.

As described by Williams [93], hydrodynamic lubrication is where a viscous film is created between two surfaces, keeping them apart completely. Friction can be expressed as:

$$\mu = k\sqrt{\frac{LU\eta}{W}} \qquad 2.1$$

where W/L stands for the specific load, U the relative sliding speed of the given two surfaces, η is the Newtonian viscosity of the liquid and k a constant that depends on the surface geometry of the given surfaces. Reducing speed or increasing specific load would enable lower friction coefficient but to a limit, after which the viscous film becomes unsustainable, reaching thicknesses of only a few molecules. Although remarkable progress has been experienced in engine tribology and possible lubricant film thicknesses can be as little as 1×10^{-7} m, sliding surfaces touching each other can eventually occur [94].

This leads to boundary lubrication mode. Williams [93] states that fuel properties such as viscosity and density play little role in this mode while significance of chemical composition rises. Fuels themselves are unable to support lubrication in this mode, with an increase in friction coefficient as much as 100 times and hence FM additives are used [94]. Their mode of action is very similar to that of lubricant oil additives and aims to provide a very fine film on all surfaces with film thicknesses about 0.0025 µm. According to Totten et al. [35], FM can interact with available surfaces through physical absorption or chemical reaction.

In case of physical absorption, the polar head groups associate themselves with metal surfaces and keep their structural integrity. In case of chemical reaction, new molecules are created on the metal surfaces, changing the structure of the additive as

well as the surface on which the reaction takes place. The hydrocarbon chains of the additives extend into the fuel and also associate with each other which results in a fine but strong film on the metal surfaces.

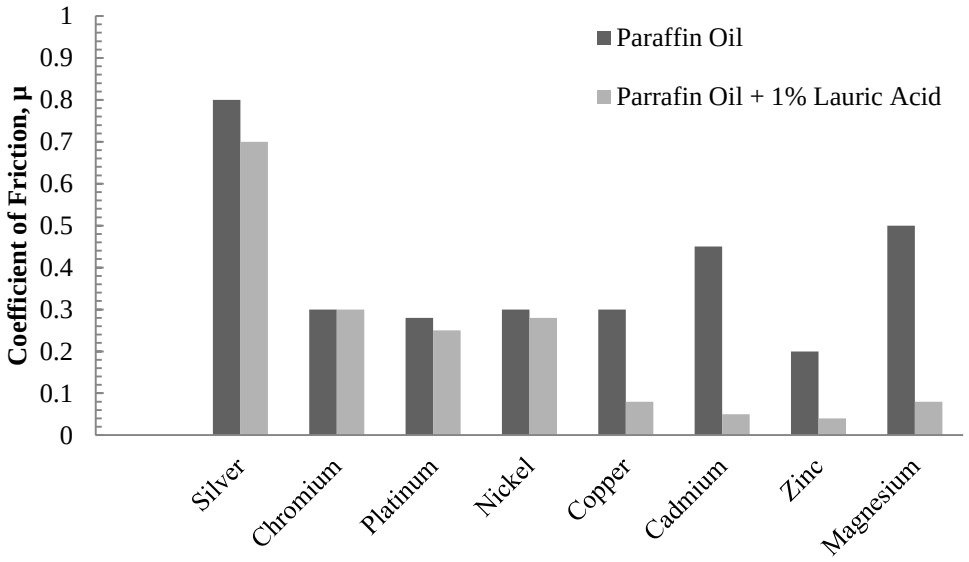

Figure 2.1: Change in coefficient of friction with a friction modifier for different materials [95]

Type of additive used depends highly on the surfaces it is meant to protect. Bowden and Tabor [95] describe experiments with lubricating oil and chemically surface active FM additives. Lauric acid interactions with different material surfaces were investigated. Results are reproduced in Figure 2.1. Silver, Chromium, Platinum and Nickel, which were expected to not react or only show little reaction with the acid, show only minor occurrence of interactions whilst copper, cadmium, zinc and magnesium displayed far greater reductions in the coefficient of friction.

Representative chemical groups in additive composition include fatty acids, amines and other ashless long chain polar compounds [4, 18, 96, 97]. Treat rates typically fall below 1,000 ppm range.

2.1.6 Carrier Fluids

Carrier fluids (CFs) are used in conjunction with other additives. CF are also known as solubilising agents and are used to mix fuel insoluble additives into hydrocarbon fuels. Need for CF is determined by the chemistry and not the functionality of the additive and as such are mixed with different type of additives. Abramo et al. [98] describe a polyalkenyl succinimides based DCA mixed with a CF

consisting mineral or synthetic oil, polyether, ester and a polymer or copolymer of an olefin hydrocarbon. McLean [99] suggests use of a CF containing mineral oil or synthetic oils such as polyesters or polyethers, or hydrocracked or hydroisomerised base stocks in concentrations of 30-60 % by additive compound weight (where total treat level of compound is 2,000 ppm) with a n-butylamine oleate based FM. A further use of CF has been described by Palmer and Heikoff [100] where piperidine is used as CF to make a protective coating containing methacrylic or acrylic/methacrylic polymer for nuclear fuel rod soluble in water.

Published research on CFs is limited and most information available comes from development of other types of additives. However, according to Barnes et al. [4] typical CF include polyalphaolefins, polyethers, mineral oils and esters.

2.1.7 Measuring Effectiveness of Additives

An overview of measurement techniques for additive effectiveness can be seen in Table 2.1. No defined method for CF additives exists. However, as mentioned in previous sections, the typical chemistry, irrespective of the additive used in conjunction, remains similar. As such it can be assumed that reasonable solubility from all chemistries can be expected and most appropriate method of testing is trial and error.

FM performance is most commonly assessed by the High Frequency Reciprocating Rig (HFFR). A ball is oscillated against a metal plate while submerged in fuel. The diameter of the wear mark on the ball from the contact under a 2 N load at 60 °C is then measured and used to characterise the lubricating properties of the fuel [101]. In Europe, the maximum diameter of the wear scar on the ball from an EU standards EN590 diesel fuel is 460 μm.

CI characteristics are evaluated against the fuels cetane or octane numbers in diesel and gasoline fuels, respectively. As described in Section 2.1.2, octane number is a measure of the fuel's resistance to knock under high pressure and temperature conditions in spark ignition engines. Test fuel knock-resistance is compared to that of a blend of reference fuels isooctane (octane number 100) and n-heptane (octane number 0). Octane number found in such way is referred to as Research Octane Number (RON).

Additive	Function	Treat Rate (ppm)	Test Method
Friction Modifier	Reduce frictional losses in fuel systems and improve operational life of fuel system components in gasoline and diesel fuels	25 - 1,000	HFFR
Combustion Improver	Improve combustion characteristics of gasoline and diesel fuels	100 - 1,000	Octane number in gasoline fuels and cetane number and the ignition delay in diesel fuels
Carrier Fluid	Transport fuel non-soluble additives in diesel and gasoline fuels	50 - 2,000	-
Anti-Static Additive	Reduce static charge build-up by improving electrical conductivity of diesel and gasoline fuels	1 - 40	Measurement of electrical conductivity
Deposit Control Additive	Reduce and prevent carbon and other deposit build-up in fuel systems	100 - 1,000	Measurement of injector flow characteristics, weight of intake valves
Drag reducing Agent	Used in pipelines to reduce frictional pressure losses	10 - 50	Measurement of fuel flow rate in oil lines, pumping pressure requirements

Table 2.1: Fuel additive types with characteristic usage and testing information

Cetane number relates to a fuel's ignition quality in mainly compression ignition engines and similarly an engine test at standard operating conditions is used. Any test fuel is referenced to a blend of n-cetane and 1-methylnaphtalene to find a combination that matches in ignition quality [64].

DCA additive effectiveness is tested mainly on engine tests. Either 60 hr dyno tests or road tests after which the intake valves are weighed for deposit formation. Although these tests successfully display the effectiveness of the additive in the intake regions, they do not take into account of the CCD either in the same engines or GDI equipped engines. According to Barnes et al. [4], difficulties arise from signal to noise ratio in such cases but the aforementioned tests in modified forms (such as ASTM D 6201 standard test) can be carried out. An alternative test that can be carried out is to characterise injector fuel flow properties for reference fuel and that of one with an additive.

No specified method of testing DRA additives seems to have been developed, although an often noted parameter is the frictional pressure drop in pipes or alternatively the drag-reduction (DR), which can be expressed as [81]:

$$DR = \frac{\Delta P_{without\ DRA} - \Delta P_{with\ DRA}}{\Delta P_{without\ DRA}} \quad 2.2$$

Here ΔP stands for a frictional pressure drop in a pipe and DR is expressed as a percentage improvement in drag reduction with an additive.

All fuels need to adhere to a set of standards that would also include a target for the electrical conductivity. AS additives can be tested following the procedure outlined by the ASTM D4308-12 standard [102]. By this method, a fuel is placed in a cell which is connected in series to a power source and a sensitive direct current ammeter is used to measure the electrical conductivity.

2.2 Fuel Metering Systems

Vehicle fuel delivery systems comprise of a fuel storage facility, fuel pump(s) and metering devices. Fuel delivery systems in automotive engines are responsible for controlling the amount, location and method of fuel introduced to the combustion chamber. The method through which fuel is introduced to the combustion chamber

ultimately determines several important characteristics of engines such as the fuel consumption, power output and emissions.

Due to hydrocarbon fuels not having high enough volatility to rapidly produce fuel vapour, successful air-fuel mixture is created through a fuel atomisation process. This means breaking liquid up into small droplets that can mix with air and evaporate easier than the fuel in liquid form. Atomisation is achieved through high relative velocities between the fuel and the ambient air. This can be realised through dispersion of fuel at high speed into a relatively slow-moving air, such is the case with pressure and rotary atomisers or alternatively expose a slow moving liquid fuel to high moving stream of air [103]. The following sections will briefly discuss the three prominent fuel metering systems used in gasoline internal combustion engines.

2.2.1 Carburettor Systems

Carburettors are the earliest fuel delivery systems used in internal combustion engines. They rely upon a Venturi effect created in the air inlet duct. Fuel delivery pump into carburettor is often connected to camshaft or the distributer, supplying volumes of fuel proportional to engine speed. Narrower section in the inlet duct increases the air velocity through it as the lowering piston generates suction, while the connection to the float chamber of the carburettor induces a vacuum effect and sucks in fuel. Often the idling characteristics mean not enough suction is created and additional ducts and orifices are used for compensation.

Inherently, carburettors lack in fuel metering accuracy and additionally provide for low efficiency air-fuel mixing. Defrance and Versille [104] addressed mixing issue with a heated charge-mixing device, fitted in line between the engine and the carburettor to increase homogeneity of air-fuel mixtures and enable reductions in fuel consumption. Although reliable and simple in construction, lack of accurate fuel metering control means that carburettors in modern automobiles are nearly completely superseded by more fuel efficient mechanical or electronic fuel injection systems.

2.2.2 Gasoline Indirect Injection

Gasoline indirect injection refers to pressure atomiser systems where the air-fuel mixture is created outside the combustion chamber. This can be achieved through either a single-point injection system or more commonly a multi-point injection/port

fuel injection (PFI) system. In single-point systems, one injector per engine is used in the intake manifold, whilst PFI systems use an injector per cylinder whereby fuel is injected directly behind the inlet valves on each of the cylinders. Typical fuel pressures are 2-3 bar above atmospheric. Using injectors instead of carburettors enables much greater control over fuel quantities used and further improves atomisation characteristics of fuel sprays. Control mechanisms for PFI systems include continuous mechanical systems such as Bosch KE-Jetronic where injectors open mechanically under sufficient fuel supply pressure and a fuel distributer is used, or electronically controlled systems such as Bosch L-Jetronic where electromagnetically actuated injectors are employed [105].

Due to low fuel pressures, relatively simple and inexpensive electronic control units can be employed. Injecting fuel into the intake manifolds allows for sufficient time periods during which fuel vaporisation and air-fuel mixing can occur and leads to achieving homogeneous mixtures prior to combustion. This enables maximisation of power output but lacks the capability of running an engine at very lean conditions that would help with fuel economy. As such, the future of injection technologies, especially when applied to road going vehicles, is seen in direct injection systems although issues with increased particulate matter emissions need to be resolved.

2.2.3 Gasoline Direct Injection

Gasoline direct injection (GDI) refers to systems where gasoline is injected directly into the combustion chamber. First GDI equipped spark-ignition (SI) engines were developed in 1950s but complex injector control electronics meant commercial use in light duty vehicles was not achieved on large scale until the end of 20th century. An extensive review of spark ignited direct injection gasoline engines was carried out by Zhao et.al. [106]. They bring attention to better atomisation of fuel with GDI compared to PFI due to higher injection pressures. Injection pressures of 250 bar and above can be reached [107]. Typical droplet size mean values are around 16 μm for GDI as opposed to 120 μm for PFI technology enabling faster evaporation of fuel [108, 109, 110]. This leads to reduced wetting of cylinder walls and significantly improved low temperature unburned hydrocarbon emissions. Unburned hydrocarbon emissions reductions of up to 70 % have been reported when experimentally used in a 2-stroke engine [111].

In case the fuel is injected during the induction stroke, injection strategy is called homogeneous, whilst if in compression stroke, it is stratified. Stratified injection strategy allows for overall lean air-fuel ratios whilst stoichiometric conditions are achieved around the sparking point, enabling for air-fuel ratios as high as 25:1 compared to stoichiometric 14.7:1. Reduced NO_x emissions are thought to be possible with direct injection through charge cooling whereby relatively cool fuel is injected into the combustion chamber, thus reducing temperature within the cylinder. However, often the improved lean-burn capability and the subsequently increased availability of ambient nitrogen in GDI engines results in higher quantities of nitrogen oxides.

Two types of injectors are used with GDI technology – pressure-swirl and multi-hole injectors [105]. Pressure-swirl injectors use a single hole at the tip of the injector with an internal nozzle geometry that gives the fuel a high angular velocity at exit from the nozzle, thus, creating a swirl effect. Swirl effect in pressure-swirl injectors is used to enable better air entrainment during mixing. As the fuel leaves the nozzle, it mostly produces a hollow conical sheet that can easily break down to create small droplets. As will be explained further in later sections, fuel mixing is directly related to atomisation of fuel spray which in turn is a function of the injector nozzle geometry. In multi-hole type injectors, several smaller diameter holes are used in the nozzle geometry. Air is entrained by dispersing several smaller jets into a wider volume and swirl effect is not needed. Additionally, smaller diameter nozzle holes will produce smaller size distributions during atomisation which increases fuel evaporation rates.

In research and especially when spray characterisation is concerned, single-hole injectors are often preferred over multi-hole injectors. Difficulties with multi-hole injector analysis arise from the need to separate the spray plumes which can otherwise interact with one another resulting in non-symmetric radial velocity and drop size distributions at given distances from the nozzle exit. A non-symmetric radial drop size profile was measured by Fdida et.al. [110], who carried out experiments on drop sizing with a 6-hole GDI injector using laser diffraction and phase Doppler anemometry techniques. Serras-Pereira et al. [112] avoided interactions between spray plumes by using a custom-made ‘bowl’ to collect all but one spray plume and Patel [113] replaced a 6-hole diesel injector nozzle with a custom made 2-hole one where injection directions were radially 180° apart. Baert et al. [114] compared spray

characteristics between one multi hole injector with a 'bowl' that blocked all but one spray plume and another with the holes welded closed. They found welding the holes to increase the momentum force of the spray by almost 10 % and as such recommended the 'bowl' type spray plume blocking technique.

Due to high injection pressures, reliability of fuel pumps and injectors can become problematic and subsequently great expectations are put on the properties of fuel for removing deposits and lubricating the moving components of the fuel system. Additional disadvantage of the GDI system is its high dependence of accurate spark timing in stratified mode whereby early spark could miss the spray completely or late one be influenced by spark plug wetting due to high liquid fuel concentration. Furthermore, due to possibility of liquid fuel combustion, high level of soot formation is possible. Advantages include accurate fuel metering control and the possibility of very lean fuel mixtures promises greatly increased fuel economy and reduced emissions.

2.3 Spray Characterisation

The previous section described the different fuel introduction and atomisation strategies available to IC engines. Although carburettors allow for excellent air-fuel mixing characteristics, lack of control over fuel quantity and the subsequent reductions in fuel efficiency mean that the use in modern engines has all but stopped and the following sections will concentrate on fuel spray development through pressure atomisers. Furthermore, variables that affect atomisation quality and methods in determining droplet sizes are presented.

2.3.1 Fuel Atomisation

Dependent upon the injection pressure, fuel and ambient conditions, sprays go through the process of liquid flow ejection, primary and secondary spray plume and droplet break-up. The liquid jet leaving a nozzle will start to deform on the liquid interface. As the spray progresses, the disturbances on the jet surface grow and result in the jet breaking into fragments and ligaments. This mechanism is referred to as the primary break-up of the spray. The size of these fragments is influenced by liquid density, ρ_l, dynamic viscosity, μ_l, flow velocity, u and a characteristic dimension D. This can be described by a dimensionless Reynolds Number, Re:

$$Re = \frac{\rho_l u D}{\mu_l} \quad 2.3$$

After primary separation of fragments and ligaments from the liquid jet, the elements can further disintegrate into smaller droplets. This process is the secondary break-up regime and can continue to take place until the surface tension forces are strong enough to withstand the disruptive hydrodynamic inertial forces [115]. The ratio between the inertial and surface tension forces can be expressed as the dimensionless Webber number, We:

$$We_g = \frac{\rho_g u^2 \mathrm{D}}{\sigma_l} \quad 2.4$$

Weber number can also be expressed in terms of the liquid properties at the spray boundary where the subscript 'g' would be replaced by 'l' [116]. A critical Weber number above which secondary droplet break-up occurs has been shown to be around 12 [117]. However, the ranges of Weber numbers within which different secondary droplet break-up mechanisms can occur vary widely, as reviewed by Jaalal and Mehravaran [118]. The review refers to varied droplet generation techniques employed by different researchers as the principal cause. Acroumanis et al. [119] suggest a classification of secondary droplet break-up mechanisms as shown in Table 2.2.

Weber Number	Break-Up Mechanism
We < 12	Vibrational
12 ≤ We < 18	Bag
18 ≤ We < 45	Bag-and-Stamen
45 ≤ We < 100	Chaotic
100 ≤ We < 350	Sheet Stripping
350 ≤ We < 1000	Wave Crest Stripping
We < 1000	Catastrophic

Table 2.2: Secondary droplet break-up mechanisms based on Weber number

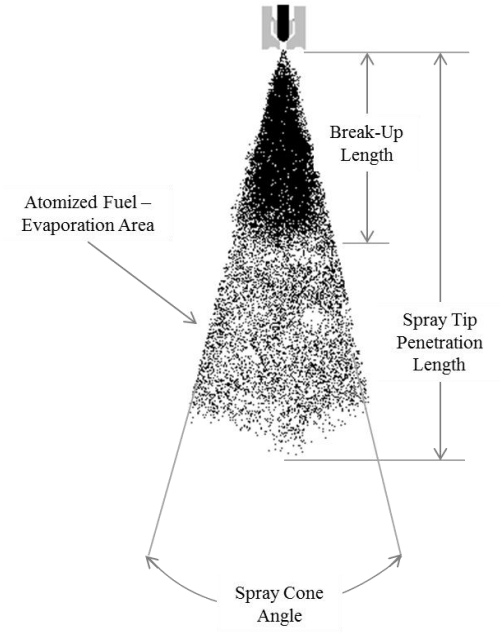

Figure 2.2: Schematics of fuel spray and key parameters

An additional dimensionless relationship to relate the viscous and surface tension effects is the Ohnesorge number, Oh:

$$Oh = \frac{\sqrt{We_l}}{Re} = \frac{\mu}{\sqrt{\rho_l \sigma_l D}} \qquad 2.5$$

Due to the Ohnesorge number completely disregarding the gas phase properties, it is assumed that $\mu_g << \mu_l$ [117]. Van Romunde [116] proposes additionally using gas phase Weber number or liquid to gas density ratio to obtain improved understanding of spray characteristics.

The fuel is introduced into the combustion chamber or intake manifold through one or several nozzle holes. Figure 2.2 displays a typical fuel spray through a high pressure injector and lists the key parameters associated with the spray development.

As the liquid fuel leaves the injector nozzle it is rapidly accelerated to high velocities due to the high pressure difference to the ambient conditions and becomes turbulent. Fuel jet leaving the injector nozzle entrains ambient gases and spreads out and small drops will start developing along the outer edges of the jet.

The liquid fuel leaving the injector will for a given geometry and pressure conditions disintegrate as a result of turbulence and air entrainment at a finite distance

from the injector nozzle. This is called the spray *break-up length*. Break-up in sprays relates to the phenomena where intact fuel jet breaks up into ligaments and droplets. Lin and Reitz [120] conclude that spray properties depend on a large number of parameters including nozzle internal flow effects resulting from cavitation, jet velocity profile, turbulence at the nozzle exit and the physical and thermodynamic states of the liquid and the ambient gases. Although particularly important in high-speed break-up regimes, nozzle internal flow effects have only been incorporated into break-up theories empirically. Break-up phenomena in liquid jets has been divided into 5 distinguishable groups, as shown in Figure 2.3.

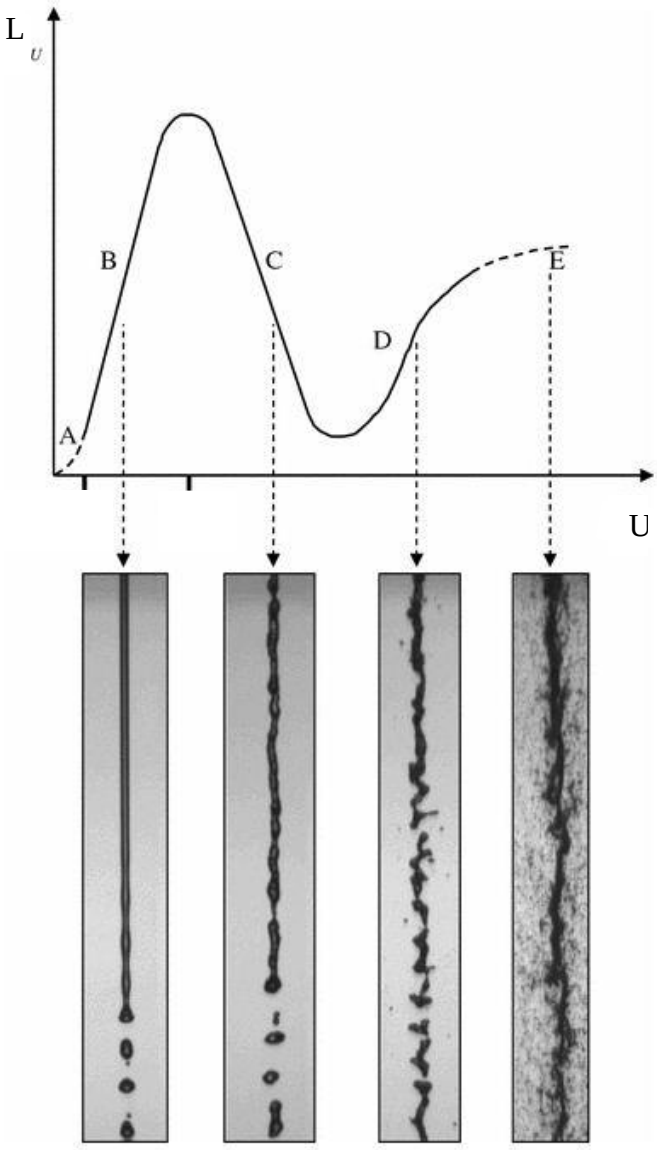

Figure 2.3: Liquid jet break-up regimes [115]. L and U represent the break-up length and jet velocity, respectively. B) Rayleigh break-up; C) First wind-induced regime; D) Second wind-induced regime; E) Atomization regime

Initially, only dripping of liquid drops occurs and no defined liquid core length can be defined, as displayed by dashed lines in Figure 2.3 (A). In the Rayleigh break-up regime, (Figure 2.3 {B}) the jet velocities are slow and a smooth jet exits from the nozzle. Rayleigh [121] showed that this results from surface tension induced hydrodynamic instability and in droplets with a constant size of 1.98 times the jet diameter. Break-up length increases to a maximum at which point aerodynamic forces begin to have an effect and break up length starts decreasing.

The first wind-induced break-up regime (Figure 2.3{C}) is reached with increased jet velocity that enables aerodynamic forces between the jet and ambient gases in conjunction with surface tension forces to result in equivalent drop sizes to the jet diameter. The jet break-up length is shorter than in the Rayleigh regime. In both the Rayleigh and the first wind-induced break-up regimes drop formation is thought to be caused by capillary pinching at the end of the jet.

In the second wind-induced break-up regime (Figure 2.3{D}), with yet higher jet velocities, a divergence of spray jet after the intact section occurs. This is due to flow of liquid within the nozzle reaching critical Reynolds number and becoming turbulent. Larger jet velocity and increased aerodynamic forces promote unstable growth of short wavelength waves that result in smaller than jet diameter droplets. However, break-up length becomes increasingly difficult to evaluate.

Figure 2.3(E) represents the final break up regime - the atomisation regime. This is reached with further increase in jet velocity and formation of a conical spray due to increased aerodynamic forces and droplet sizes are much smaller than the nozzle diameter. Although some researchers have found liquid length to approach zero in this regime, others have noted an increase in the break-up length. This has been explained by an increased dependence on flow conditions within the nozzle [122]. Due to high injection pressures, it is expected that spray break-up in current project occurs in the atomisation regime.

Yule and Filipovic [123] note that liquid core break-up length in DI engines under the atomisation regime can be as much as the distance from the injector nozzle to the piston surface meaning liquid spray core can accumulate on the piston surface. This wetting of the piston surface can contribute towards decreased fuel economy and increased unburned hydrocarbon emissions. Moreover, due to slow vaporisation of un-atomised fuel, burning of liquid spray core can occur which results in high levels of

soot formation [124]. As the spray progresses, more air is entrained within the fuel jet and it further spreads out.

The spray density around the exit of the injector nozzle can be very dense and results in optical methods such as phase Doppler technique or Particle Imaging Velocimetry being unsuited for analysis [125]. This means photographic techniques are often used to measure spray cone angle or spray penetration length instead.

The angle between the outer edges of the spray tip and the injector exit is called the *spray cone angle*. Large cone angles are preferred because of air entrainment needed for spray atomisation and better fuel distribution within the combustion chamber. At lower pressures where the fuel carries less momentum and the effect of aerodynamic drag forces is larger the cone angle is larger. Cone angle is dependent upon fuel injection pressure, ambient pressure and fuel viscosity [126, 127]. Roisman et al. [125] note that ambient pressure seems to have much larger effect on the cone angle than the injection pressure.

Patel et al. [128] note that the elliptical shape of the spray often results in different cone angles being measured with varying downstream distance from the injector nozzle. As a result, comparing the maximum width of the spray was deemed more relevant. Similar technique of measuring spray plume width but at 30 mm downstream from the injector nozzle was employed by Zeng et al. [129].

A further parameter used for characterisation of sprays is the *spray penetration length*. This determines the maximum distance of any part of the spray from the injector nozzle. The spray penetration length depends on the fuel injection pressure and ambient back pressure. The higher the back pressure or lower the injection pressure the shorter the penetration length. The fuel speed reaching this point reduces rapidly with increased distance due to aerodynamic drag forces applied to the fuel droplets.

In general short distances are sought after in order to avoid impingement of fuel on piston crowns and the subsequent increase in unburned hydrocarbon and soot emissions. Park et al. [130] carried out tests on a second generation spray guided direct injection system on a single cylinder research engine and found at pressures above 200 bar fuel penetration length to be enough to reach the piston crown and advised for use of particulate filter in order to meet emissions regulations.

2.3.2 Droplet Size

Droplet size is often represented on the basis of a diameter of an equivalent sphere [131]. Dependent upon method the equivalence can be based on maximum or minimum length, weight, volume, surface area or other properties. However, the process of obtaining the diameter of equivalent sphere from non-spherical droplets often relies on several assumptions and in case of some optical methods (Section 2.3.3) can provide basis for inaccurate analysis.

The commonly used parameter to characterise the spray is the Sauter Mean Diameter (SMD). SMD represents the diameter of a fuel droplet with the same volume to surface ratio as the total spray. It is most applicable in cases such as liquid fuel sprays where specific surface area, due to its relevance to evaporation rates, is important. It follows the form [132]:

$$D[3][2] = \frac{\Sigma nD^3}{\Sigma nD^2} \qquad 2.6$$

The *n* term denotes the number of particles of a certain size.

Reduced SMD refers to smaller droplet diameters and increased total droplet surface area, meaning higher fuel evaporation rates and improved fuel mixing. Enhanced evaporation and mixing characteristics are especially important in the case of direct injection where much reduced time periods compared to PFI systems are involved. Smaller droplets are expected to occur with increased injection pressures. Controversially, Zhang et al. [133] found that while increased fuel injection pressure reduced unburned hydrocarbon emissions, CO and NO_x emissions increased. It is thought CO increase is a resultant of increased fuel-wall impingement with increased fuel pressure, while NO_x increase results from increased amount of fuel being available within the cylinder as a result of injection duration being kept constant. A more thorough description of emissions will be given in Section 2.4.4 (Page 67).

Fuel atomisation into a large number of small droplets is important in order to create a large surface area on which the fuel can rapidly evaporate. Willauer et al. [134] carried out experiments on flammability of aerosols produced by rotary atomisers. They found the droplet size to have a profound effect on the flammability limit, combustion rate and temperature averages reached during combustion. Reduced droplet size was seen to increase the concentration of fuel vapour, thus, enabling easier

air-fuel mixing and at high fuel flow rates. 75 % decrease in droplet size could increase the average temperature of the hot gases and aerosol mixture by nearly 800 %. Larger droplets inhibited fuel atomisation and as a result the propagation of pilot flame and sustainable burning of fuel was hindered. Similar effect of atomisation quality on flammability limit was experienced by Park et al. [130]. The tests on lean burn capability of a spray guided direct injection system showed that at 200 bar injection pressure φ = 3.0 could be achieved. However, at 100 bar injection pressure the flammability limit was reached at only φ = 1.5.

In most cases, the evaporation rate of the fuel follows the D^2-Law. The size of the fuel droplet can be expressed as [135]:

$$D^2 = D_0^2 - \lambda t \qquad 2.7$$

where D is the final droplet diameter, D_0 is the droplet initial diameter, λ is the evaporation constant and t the evolution time. It is clear from this relationship that droplet size decreases over time proportionately to the constant λ. Furthermore, λ is expressed in terms of [m^2/s], indicating clearly its dependence on total droplet surface area of the fuel jet and hence the atomisation quality on the evaporation rate.

2.3.2.1 Fuel Viscosity

Viscosity is among the main physical properties of fuels and other liquids to determine the droplet size. As can be seen in Figure 2.4, an increase in viscosity of the

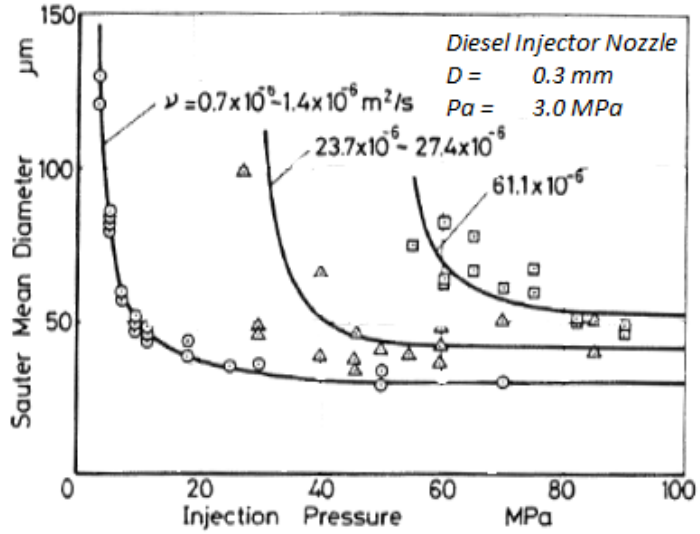

Figure 2.4: Effect of viscosity on Sauter Mean Diameter with varying injection pressure [136]

fuel is accompanied by an increase in the droplet size. This, according to Lefebvre [137], originates from the dampening effect viscosity has on either short or long surface waves that precede atomisation phenomena. According to Lefebvre and Ballal [138], liquid jet break-up occurs when the magnitude of disruptive forces, originating from aerodynamic interactions, overcome the consolidating surface tension and viscosity forces.

For a given experimental set up, such aerodynamic forces are solely affected by the pressure drop across the injector nozzle. Everything else remaining equal, for a given pressure drop, an increase in viscosity is likely to increase the viscous forces. This means an increase in the level of disruptive forces required for liquid jet break-up and as such increased droplet size, as demonstrated in Figure 2.4. Furthermore, Yao et al. [126] note a decreased spray cone angle with increased liquid viscosity that inhibits air entrainment and the subsequent atomisation processes.

2.3.2.2 Fuel Surface Tension

Although early research would suggest that droplet radius of curvature has an effect of surface tension [139] it is accepted that droplet size is affected by the surface tension and that similarly to viscosity, an increase in surface tension provides for larger droplets [140]. Lu et al. [141] believe this to be derived from the increased cohesion of fuel molecules on the surface of the fuel.

Lefebvre [137] explains this by the resistance to distortion or disturbance, such as surface waves, on the liquid surface. As shown in Figure 2.5, this results in a delayed ligament formation and subsequent atomisation, causing larger diameter droplets to occur for a given pressure drop.

2.3.2.1 Fuel Injection Pressure

The effect of an increase in injection pressure can be observed from Figure 2.4 and Figure 2.5. Increasing injection pressure reduces the size of droplets with a non-linear relationship prevailing. Larger changes are experienced initially but the effect diminishes at high pressures. Lu et al. [141] explain reduction in SMD with reduced surface viscosity and cohesion between fuel molecules. The injection pressure effect can additionally be seen in Table 2.3. The negative power of ΔP term in the equations demonstrates the reduction in droplet size with increasing pressure difference between injection and ambient pressures.

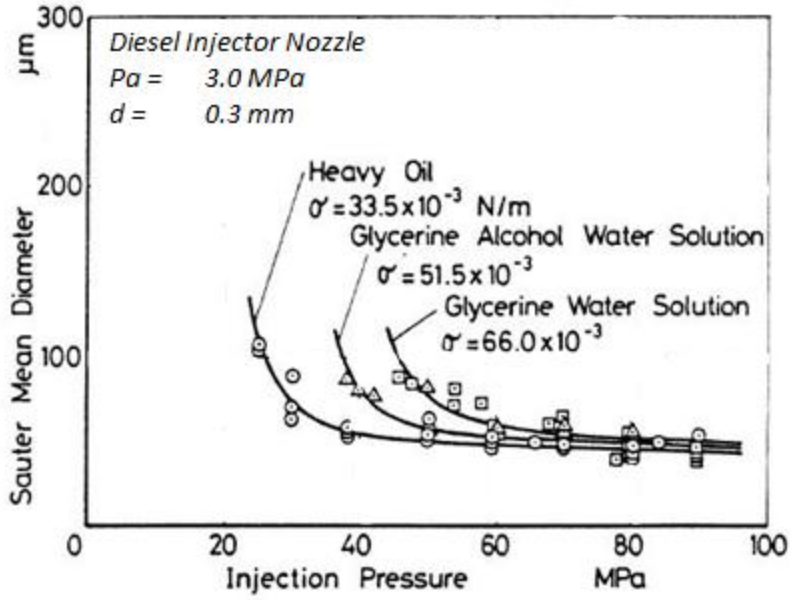

Figure 2.5: Effect of surface tension on Sauter Mean Diameter with varying injection pressure [136]

Researcher	Equation	No.
Knight (1955)	$SMD = 1.605 * 10^{6}(\Delta P)^{-0.458} Q'^{0.209} \nu^{0.215} \left(\frac{A_{orf}}{A_{\text{eff}}}\right)^{0.916}$	2.8
Hiroyasu and Kodota (1974)	$SMD = A(\Delta P)^{-0.135} \rho_a^{0.121} V_{fc}^{0.131}$	2.9
Elkotb (1982)	$SMD = 6156\nu^{0.737}\sigma^{0.385}\rho_f^{0.737}\rho_a^{0.06}\Delta P^{-0.54}$	2.10
Lefebvre (1987)	$SMD = B\left(\frac{(\sigma^{0.5}\mu_L)}{\rho_A^{0.5}\Delta P_L}\right)^{0.5} (t cos\theta)^{0.25} C\left(\frac{(\sigma\rho_L)}{\rho_A \Delta P_L}\right)^{0.25} (t cos\theta)^{0.75}$	2.11

Table 2.3: Empirical relationships for SMD and researches that established them [7, 136, 142, 143]

2.3.2.2 Fuel Temperature

Temperature is a parameter that affects the droplet size through effects on other fuel properties. Increased temperature is known to affect both viscosity and surface tension of liquids and for a given injection pressure, a higher temperature fuel will

result in lower droplet size. Moreover, according to Sazhin et al. [144] increased droplet surface temperature reduces the surface tension resulting in increased vaporisation speeds and hence smaller droplets.

2.3.2.3 Empirical Relationships

Several experimental studies have been carried out to establish a relationship between different fuel and injection properties and the droplet size. According to Lefebvre [7], owing to the complexity of various physical phenomena involved, much research into droplet sizing follows empirical methods. Five equations for the Sauter Mean Diameter have been displayed in Table 2.3.

It is clear from the equations that the importance of viscosity compared to surface tension on droplet size is much larger. The equations are mainly aimed at estimating droplet sizes in diesel sprays and might prove inaccurate when applied to other fuels, especially those with higher volatility characteristics. Also, the equations do not take into account of the location of the measuring point and try and estimate a global droplet size. As will be shown in later chapters, measurement location affects the droplet size. Further, the established relationships are derived from a given set of experiments and are highly dependent upon achieving same conditions. The effect of injection pressure is relatively close between Elkotb and Knight but greatly reduced for the case of Hiroyasu and Kodota [143].

Moreover, although pressure difference across the nozzle is expected to affect the SMD, Araneo et al. [145] found flash boiling to have a significant effect, especially at below atmospheric ambient conditions, whereas above 800 kPa ambient pressure did not affect SMD further. Wang and Lefebvre [146] found the ambient pressure increase above atmospheric to increase the size of droplets to a maximum value initially before a decline. This would suggest that the ΔP term in the presented equations is limited in its range which, however, is not demonstrated in the equations.

Lefebvre [7] and Wang and Lefebvre [147] also argue that the liquid sheet disintegration at exit from an injector nozzle is in addition to aerodynamic forces affected by turbulent or other disruptive forces within the liquid itself and proposed Equation 2.11. They acknowledge, however, the difficulty arising from experimental difficulties of measuring the liquid film thickness for purposes of the analysis.

It is evident all researches only fit the equation to their specific experiments and admit different relationship might be more appropriate compared to other

researchers. The accuracy/suitability of the relationships presented will be compared against the current study in Section 5.1.

2.3.3 Droplet Sizing Methods

The following section introduces optical methods used for determining droplet size and droplet size distribution. The three most commonly used methods described here are Particle/Droplet Image Analysis, Phase Doppler Anemometry and Laser Diffraction.

2.3.3.1 Particle/Droplet Image Analysis

Particle/droplet image analysis (PDIA) is an image based method of determining the droplet size. Particle detection algorithms allow for usage of digital imaging of small regions of the spray. Kashdan et al. [148, 149] applied PDIA and Phase Doppler Anemometry techniques to sprays produced by a pressure-swirl GDI injector with droplets in the region of 5-30 µm. They found good agreement between the results. They also found good response of the PDIA system to large and non-spherical droplets as well as coping with greater droplet size ranges. According to Anand et al. [109], this makes the PDIA system suitable to PFI sprays where large and often non-spherical droplets are expected.

Downsides to the PDIA system include inaccuracies caused by incorrect distance between particle and the focal plane that makes detection and contour defining of unfocused droplets difficult [150]. Also, small region imaging results in

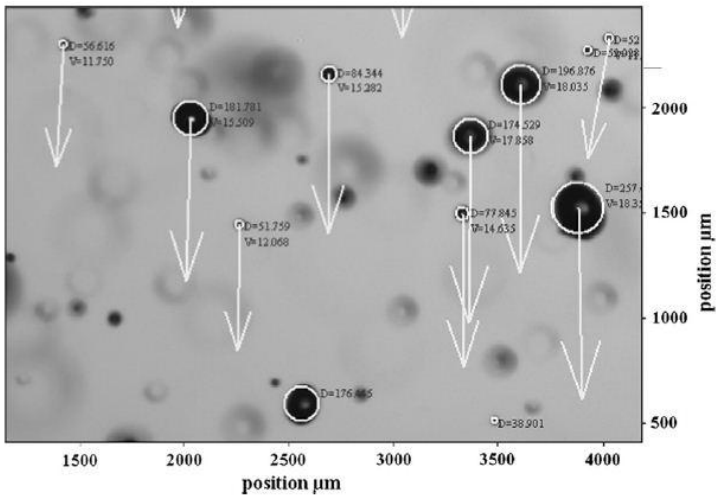

Figure 2.6: PDIA image with identified droplets [109]

only a very few droplets being measured, meaning a distortion in droplet size distribution is possible. A sample image from a PDIA system can be seen in Figure 2.6.

2.3.3.2 Phase Doppler Anemometry

Phase Doppler anemometry (PDA) uses a split light source directed through a small volume of the spray. The interference caused by the spray creates a scattered light signal that can be translated into spatial and temporal data on droplet size, location and velocity [151]. A typical PDA set-up can be seen in Figure 2.7. Two detectors are positioned on the y-z plane out of the incident beam at an angle φ, and at symmetric ±ψ degrees from the off-axis angle. However, as pointed out by Damaschke et al. [152], PDA systems can produce unreliable results if non-spherical droplets are present and determination of local droplet number density and volume flux can be difficult. Non-spherical droplets can further force the PDA system to reject data, meaning often large numbers of repeat spray events are necessary [153]. Due to the very small sampling volume of the PDA system, large numbers of repeats are always necessary for a statistically relevant result [154].

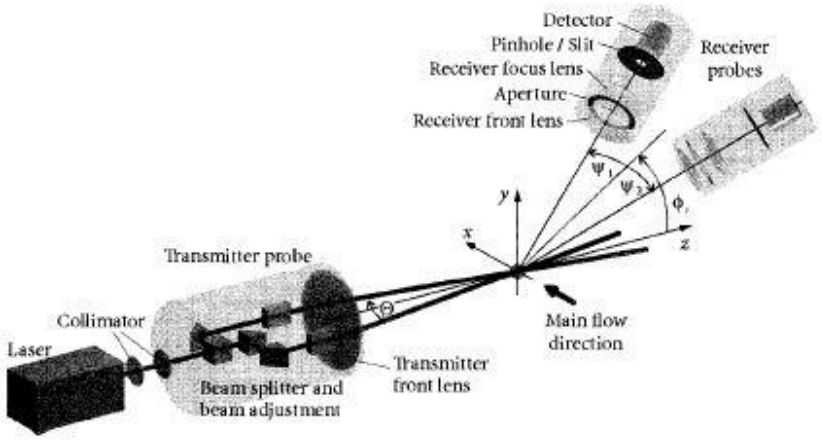

Figure 2.7: PDA optical arrangement [155]

2.3.3.3 Laser Diffraction Granulometry

Laser diffraction (LD) systems calculate particle size and distribution from the light forward scatter pattern. It is a line of sight technique that averages a volume

defined by the intersection of the spray and the laser beam. A typical laser diffraction set-up can be seen in Figure 2.8.

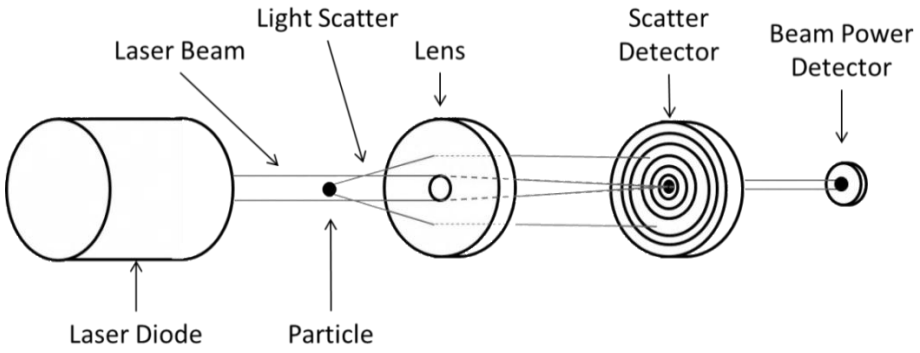

Figure 2.8: Basic principle of Laser Diffraction Granulometer

A diode-produced cylindrical laser beam is directed trough the working section. As the light hits a particle it is deflected at an angle proportional to its surface radius of curvature and is collected by the scatter detector. The light scatter is analysed based on the Mie Theory to predict a droplet size and size distribution. Smaller droplets with larger curvature will deflect light more and will be detected by the outer rings while larger droplets will be caught by inner.

LD systems are very easy to set up and quick for obtaining experimental results. Also they can offer very high acquisition rates and offer particle size ranges from 0.1-2,000 μm [156]. Further, unlike PDA and PDIA, LD systems, due to their relatively large laser diameters, enable analysis of relatively large volumes that can provide for better representation of spray characteristics. However, this also reduces their spatial resolution compared to other techniques.

Comparative studies between PDIA, PDA and LD techniques were carried out by Fdida et al. [110, 153] and Dodge [157]. Good to excellent correlation between results was seen between the aforementioned techniques. It has been noted that droplet sizes found with the LD method can be of smaller diameter than those of PDA or PDIA [110, 116].

Limitations of the LD method arise with the presence of the beam steering effect [158]. This is especially prominent phenomena with volatile fuels. Beam steering is caused by the evaporation of droplets that effects the local gaseous phases and changes the refractive index. The resultant small deflections of the beam result in

the system having exaggerated readings on the inner most detection rings, thus, skewing the results. Unlike background noise, this effect cannot be eliminated. Fdida et al. [110] found beam steering to produce a bimodal droplet size distribution with higher peak occurring from droplets in the range $90 < D < 130$ µm. PDA measurements, however, showed the droplets to be in $4 < D < 45$ µm range. This knowledge allowed for some of the out most detection rings to be discounted from further analysis.

As mentioned in Section 2.2.2, however, PFI injectors produce droplets within this beam steering region. It could be argued that fuel evaporation as a result of large droplets would not be a prominent issue but if possible droplet sizing of PFI sprays would as a result be advised to be analysed by alternative drop sizing methods.

A further limitation of the LD technique is the multiple scatter effect resulting from measuring dense sprays [159]. Multiple scatter refers to situation where a deflected light beam is further deflected off another droplet before reaching the light detector, thus giving a false reading [160]. According to Triballier et al. [161] this phenomena comes into effect when the transmission of light from the laser to the detector below 40 %. Commercial software packages include a correction algorithm for such cases. It is claimed this allows for droplet size analysis at transmission levels as low as 2 % whilst remaining within a 1 % margin of the true droplet diameter value [162].

2.3.4 Fuel Additive Effects on Atomisation Characteristics

Research into the effects of fuel additives on fuel spray characteristics is limited. This is partly due to the quantities of additives involved compared to that of the base fuels but also due to the proprietary nature of the chemicals in use. Higgins et al. [10, 9] investigated the effect of ignition promoter 2-EHN on liquid length and the cone angle of non-combusting hot diesel sprays. At treat rates of 4,000 ppm of additive in fuel, the conclusion drawn was that the additive does not alter the fuel spray beyond the experimental repeatability. Any effect that was seen was a resultant of ignition promoting radicals that 2-EHN provides and not of physical nature. Felton et al. [8] studied the effects of two detergent additives on droplet size and evaporation mixed into two diesel-type fuels. They found that at high treat rates the additives had the capability to hinder evaporation of fuel and increase droplet size but that it was also highly dependent on base fuel characteristics and only applied to the fuel with

high aromatics content. The diesel fuel with more common characteristics to modern automotive fuels did not exhibit any noticeable change in evaporation or atomisation characteristics.

The effect of additives on fuel atomisation is not fully understood. Although the quantities involved are small, properties such as viscosity and surface tension could be altered significantly and a study into the effect of additives from a variety of functional groups on fuel atomisation would provide valuable insight into the mechanisms at work.

2.4 Combustion Analysis

Combustion characteristics are dependent on a number of factors including physical and chemical properties of fuels. Physical processes inherently affect combustion characteristics through effects on fuel spray atomisation and subsequent air-fuel mixing. Additional contributions to variations in combustion quality arise from changes in fuel chemistry. Such changes affect the way a fuel behaves and what chemical reaction paths are promoted or suppressed during oxidation processes. In this section methods of analysing combustion characteristics and efficiency are introduced, including techniques that are used involving optical and non-optical methods.

2.4.1 Heat Release Analysis

The most widely used technique for determining combustion efficiency and characteristics in IC engines is heat release analysis. In cases where optical access is not possible or suited, pressure change caused by the combustion can be used to characterise the combustion rate. Stone [163] explains that heat release analysis allows for calculation of the quantity of heat required to cause an observed pressure change within a control volume. Applying the 1st Law of Thermodynamics to a control volume with no mass transfer allows the heat released by a combustion event to be expressed as:

$$\delta Q_{hr} = dU + \delta W + \delta Q_{ht} \qquad 2.12$$

Assuming the reactants and products have same properties and that there is no temperature gradient throughout the gas mixture, the terms in Equation 2.12 can be evaluated as follows:

$$dU = mc_v dT \tag{2.13}$$

and

$$\delta W = p\, dV \tag{2.14}$$

Rearranging the equation of state, $pv = mRT$, gives:

$$mdT = \frac{1}{R}\,(pdV + VdP) \tag{2.15}$$

Substituting Equation 2.15 into Equation 2.13:

$$dU = \frac{c_v}{R}\,(pdV + VdP) \tag{2.16}$$

Substituting Equations 2.14 and 2.16 into Equation 2.12 gives:

$$\frac{dQ_{hr}}{dt} = \frac{c_v}{R}\left(p\frac{dV}{dt} + V\frac{dp}{dt}\right) + p\frac{dV}{dt} + \frac{dQ_{ht}}{dt} \tag{2.17}$$

Assuming $\gamma = \frac{c_p}{c_v}$, $R = c_p - c_v$ and $\frac{dQ_{net}}{dt} = \frac{dQ_{hr}}{dt} - \frac{dQ_{ht}}{dt}$, Equation 2.17 can be expressed as:

$$\frac{dQ_{net}}{dt} = \frac{\gamma}{\gamma - 1}\,P\frac{dV}{dt} + \frac{1}{\gamma - 1}\,V\frac{dP}{dt} \tag{2.18}$$

Equation 2.18 includes both, the pressure and volume change terms and takes into account of heat lost to the cylinder walls. Frequently, the in-cylinder pressure data of an engine is coupled with the piston position to determine the instantaneous volume of the cylinder. In that case, the net heat release is usually represented in terms of incremental crank angle change, dϑ, instead of time, dt. Heat release analysis can also be used in conjunction with optical methods and is utilised in rigs other than research engines [164].

2.4.2 Optical Combustion Characterisation

Several optically accessible rigs can be utilised to enable the investigation of combustion characteristics under engine-like conditions. The rigs can be divided into piston and non-piston based rigs. The benefit of optical access arises from the capability of imaging of flames and the application of laser diagnostic methods that can reveal and explain fundamental processes during combustion.

2.4.2.1 Optical research Engine

The most commonly used piston-based optical rig is the Optical Research Engine (ORE) which, due to its operational characteristics, are closest to normal IC engines. Optical access to the combustion chamber can be achieved through several techniques. Most commonly a window in the piston crown is employed [165, 166, 167, 168], although optical access can also be gained through cylinder head or cylinder walls/liner [165, 169]. Advantages include analysis of combustion in engine conditions that might not be possible in other rigs. However, the optical windows and cylinder liners can be very expensive and fragile, thus, limiting operational conditions.

2.4.2.2 Rapid Compression Machine

A further piston based rig used is the Rapid Compression Machine (RCM). The RCM utilise a single rapid compression stroke to achieve test conditions. Due to the lack of valve train requirement, very good optical access can be gained to the combustion chamber [170]. However, Mittal and Sung [171] discuss that a very rapid pressure rise is necessary in order to avoid significant heat losses to the vessel walls and combustion reactions from occurring before the compression process has been completed. The timescales available are in the order of 10s of ms and as a result very complex designs using hydraulic and pneumatic actuators need to be used [171, 172] . Although RCMs closely replicate turbulence seen in IC engines, the rapid piston movement experienced often causes vibrations that have been reported to limit the use of laser techniques [114, 173].

2.4.2.3 Constant Volume Combustion Vessel (CVCV)

Non-piston based systems include mainly Constant Volume Combustion Chambers (CVCVs) either set for pre-combustion or heated conditions. The chamber

sizes vary although typically a much larger working section volume than in an engine is utilised. Constant volume heated chambers (CVHC) tend to be smaller in size due to low thermal inertia of the usually stainless steel walls and high energy needs in heating the vessel [114]. Conditions suitable for diesel combustion can be reached, with temperatures and pressures of over 590 °C and 75 bar, respectively, having been reported in the literature [174, 175]. In constant volume pre-combustion chambers (CVPC), a pre-determined mixture of lean stoichiometry fuels is combusted to reach high temperatures and pressures and the fuel is injected into the products of the preceding combustion and ignited [176]. Heated chambers can run repeat experiments at much higher frequency than pre-combustion chambers while pre-combustion chambers can achieve experimental conditions faster and simulate engine-like conditions closer. It has been reported that that compared to other optical methods, CVCV allow for highest degree of control over the test conditions and the subsequent reduction in variables makes the technique very well suited for fundamental combustion studies [113, 114].

2.4.3 Optical Diagnostic Techniques

The following sections offer a brief overview of techniques used in optical combustion investigations. The methods most relevant to current project are direct imaging of flames, shadowgraphy and Schlieren imaging. Shadowgraphy and Schlieren imaging both utilise backlight illumination as the light source making use of the change in the density gradient in the working section resulting from either sprays or combustion. A brief description of a few other methods is additionally given in Section 2.4.3.4.

2.4.3.1 Direct High Speed Imaging

The simplest technique to follow when studying combustion optically is to use high speed imaging to capture the flame luminosity directly. The method relies upon the flame or combustion to produce enough luminosity for the aperture to capture and has been shown to work well with both gasoline and diesel combustions [177, 178]. When luminosity has been found problematic, a sufficient increase in luminosity levels has been achieved through an addition of selected salts to the fuel that are thought not to affect flame propagation [179]. Winklhofer and Fuchs [180] state that with shutter speeds of 10 µs or faster allow for good imaging of the flame structure under the

influence of turbulent flow field but make note of the high requirements of the optical aperture because of short exposure times.

2.4.3.2 Shadowgraphy

Shadowgraphy implies that a light source faces the camera directly or often through a diffuser to generate equal light distribution. A beam of light is directed through the working section and is refracted due to density changes that affect the refractive index of the working environment. Schematics of a simple shadowgraphy set-up can be seen in Figure 2.9 [181]. The method does not produce a focused optical image of the object but instead produces a shadow of the investigated phenomena. Its response to the second spatial derivative of the refractive index makes it well suited for experiments with large density gradients. Although sometimes applied to combustion analysis [182], as demonstrated by several researchers, shadowgraphy is mostly used for fuel spray analysis [183, 184, 185].

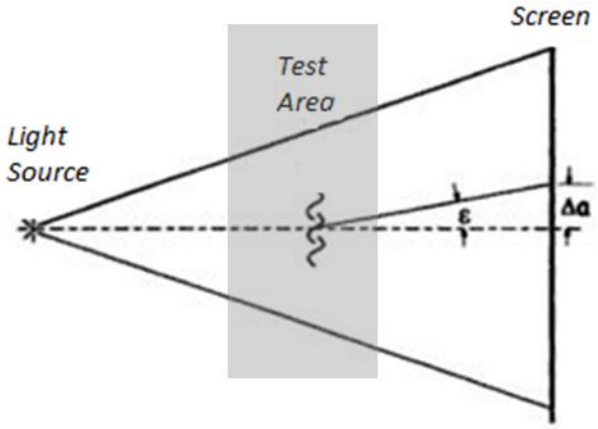

Figure 2.9: Diagram of Shadowgraph method [181]

2.4.3.3 Schlieren Imaging

Schematics for the Schlieren system can be seen in Figure 2.10 [186] where ε represents the refraction angle of light rays. Schlieren system works on the same principal of variation in refractive index as shadowgraphy but uses twin concave mirrors or lenses to form a collimated beam of light that travels through the working section. Before being reaching the camera again, the light rays are re-focused.

A light source is directed through a condenser lens to create a collated light or alternatively a collated light source is used, is sent to the first concave mirror that reflects it as a parallel beam through the working environment. The second concave

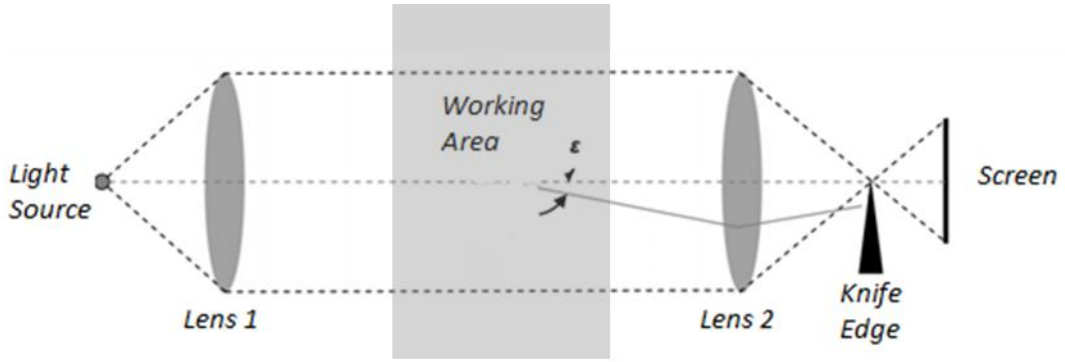

Figure 2.10: Schlieren system aperture schematics [186]

mirror focuses the beam at which point part of the light is cut off by a knife edge or graded filter. This effectively acts as means to control the contrast in light intensity. The remaining light is allowed to reach the Schlieren camera. Images respond to the first derivative of refractive index and as a result possess much higher sensitivity to changes in density than shadowgraph images. Furthermore, the Schlieren system produces a 1:1 scale of the studied object and according to Kostiuk and Cheng [187], unlike in shadowgraph images where detail is often reduced, it is emphasised.

2.4.3.4 Other Techniques

Direct, shadowgraph and Schlieren imaging of flames allows for overall characterisation of combustion reactions but often understanding of specific reactions and species present during those reactions is sought after.

In such cases numerous laser techniques can be employed [151]. Laser induced fluorescence (LIF) uses a laser source to excite radicals that then can be captured by an intensified charge couple device (ICCD) camera. If enough energy from the laser is available this can further be converted to a planar laser induced fluorescence technique (PLIF), where a point source is converted to a laser sheet, enabling view of the cross section of the flame. Radicals such as CH, CH_2O and OH have been associated with inner flame front, preheat and oxidation/post flame zones, respectively [188]. Dependent upon the wavelength of the laser, different radicals can be excited which enables visualisation of the reaction zones and as a result characterisation of the flame structures under various conditions. Moreover, simultaneous OH and CH_2O fluorescence imaging can be used to evaluate the local heat release rate [189].

A series of experiments on diesel combustion in a constant volume combustion vessel were carried out at University of Valladolid [190, 191]. Using 306 nm and 430

nm band-pass filters on two Hamamatsu 9536 photomultiplier tubes (PMTs) to detect the OH* and CH* radical chemiluminescence, respectively, to measure the auto-ignition time of diesel sprays. The time-resolved signal traces of the OH* and CH* radical chemiluminescence were compared to that of pressure and mechanical vibrations and good agreement was found.

Several other combustion characterisation methods are used. Hentschell [192] applied the use of optical fibres within a modified head gasket. About 100 optical fibres were used to form an optical grid covering the cross section of the engine. The flame position could be resolved spatially by using a tomographic reconstruction algorithm. Fibres were also used by Spicher and Velji [193] for flame detection but were built into the walls of the combustion chamber of a single cylinder SI engine. They bring out the possibility of a three-dimensional resolution to the flame propagation analysis compared to other optical techniques.

2.4.4 Emissions

Vehicle emission levels have increasingly been one of the driving forces in engine and fuel technology research. All countries within the EU follow the same regulations for new cars. The regulated emissions include carbon monoxide, unburned hydrocarbon, nitric oxide, nitrogen dioxide and particulate emissions. Additionally from the start of EURO 6 standard, the total number of particulates (in addition to weight) will also be measured. As briefly mentioned in Section 2.1, fuel additives can be successfully utilised to reduce regulated emission levels.

2.4.4.1 Carbon Monoxide

Carbon monoxide (CO) primarily results from incomplete combustion that is caused by oxygen starvation during combustion that would allow for complete oxidation of the fuel. However, slow burning rates could also result in an increase in emissions. Incomplete combustion is mostly reached during cold start periods as well as transient events during full load situations where fuel rich mixtures are employed. Better burning rates and lean mixtures enable lower CO levels. Ji and Wang [194] experimented with hydrogen addition to fuels to improve the lean burn limits of gasoline. They found reductions of CO emissions by more than 75 % were possible with 4.5 % hydrogen in gasoline. Furthermore, reduction in cold start emissions was reported by Chen et al. [195] with gasoline-ethanol blends, where ethanol

concentration was between 20-30 % in fuel. Similar results were reported by Al-Hasan [196] where 20 % ethanol blend gave lowest CO emission levels. Emissions are of great interest and even diesel-gasoline fuel blends have been studied for effects on cold start CO release rate [197].

2.4.4.2 Unburned Hydrocarbons

Unburned hydrocarbon (HC) emissions are an outcome of several processes. HC can result from leakage of air fuel mixture during the compression stroke through exhaust valves, small crevices within the combustion chamber, un-atomised fuel, layers of lubricant oil on combustion chamber walls or other cold surfaces that can quench flames [198]. Shen et al. [199] found the fuel hydrocarbon composition to have a profound effect on HC emissions through the aforementioned methods. They reported a decrease in HC emissions of up to 45 % with decreasing aromatic levels and increasing olefin levels in gasoline fuels.

Cold start HC emission levels were investigated by Henein and Tagomori [200]. HC emissions were contributed to low temperature combustion instability at start up. Additionally, low efficiency of the three-way-catalyst at low temperatures was mentioned. In order to reduce heat up time, in high performance vehicles this has resulted in catalytic converters being fitted on the exhaust manifolds or very near them [201, 202].

2.4.4.3 Nitrogen Oxides

Nitrogen oxides (NO_x) that result from combustion are nitric oxide (NO) and nitrogen dioxide (NO_2). It is widely accepted that the oxides form as a result of oxidation of atmospheric nitrogen although in small quantities, it is possible for NO_x emissions to originate from fuel bound nitrogen compounds [48]. Increased NOx emissions are contributed to increased combustion temperatures that enable oxidation of atmospheric nitrogen into nitrogen oxide and nitrogen dioxide. NO_2 emissions are only notable in compression and not in SI engines. NO_x output is dependent upon temperatures within the combustion chamber. Main heat induced reactions that contribute towards NO formation are [203]:

$$N_2 + O \leftrightarrow NO + N \qquad \textbf{2.19}$$

$$N + O_2 \leftrightarrow NO + O \quad \textbf{2.20}$$

$$N + OH \leftrightarrow NO + H \quad \textbf{2.21}$$

Further possibilities have been proposed where recombination process of N_2 and O occurs [198, 204]:

$$N_2 + O + M \leftrightarrow N_2O + M \quad \textbf{2.22}$$

$$N_2O + O \leftrightarrow NO + NO \quad \textbf{2.23}$$

And

$$N_2 + H + M \leftrightarrow NNH + M \quad \textbf{2.24}$$

$$NNH + O \leftrightarrow NO + NH \quad \textbf{2.25}$$

Several investigations have been carried out under different conditions and with different fuels to see effects on NO_x emissions. Chen et al. [205] studied the effect of alcohol-gasoline fuel blends and measured NO_x reduction of up to 30 %. However, this was accompanied with a 10 % reduction in torque and even greater output losses and increased emissions were recorded under high load conditions. Wang et al. [206] investigated the effect of gasoline mixed with hydrogen or hydrogen-oxygen mixture on engine performance and emissions. They found a decrease in CO and HC emissions but up to 70 % increase in NO emissions with hydrogen-oxygen blends. This was contributed to increase combustion chamber temperature and increased air availability within the combustion chamber.

The primary technique used in modern automotive engines to reduce the NO_x emissions is exhaust gas recirculation (EGR). Part of the clean air introduced to the engine is replaced by exhaust gases from the previous cycle. This increases the water vapour content and reduces available oxygen levels in the cylinder. Although small gains can be achieved through depletion of available oxygen, the main advantages result from addition of water vapour. The water vapour increases the heat capacity of the gas mixture within the cylinder and as a result, the peak temperatures reached are reduced, thus, reducing NO_x emissions [207].

Three-way catalysts used in modern vehicles have proven to be inefficient in reducing NO_x emissions in lean burn engines [208]. Problems arise from the increased amount of atmospheric nitrogen in the air fuel mixture resulting in increased nitric oxide levels and the efficiency of catalyst at high exhaust oxygen concentrations. However, research is on-going in finding more efficient ways in which to tackle the issue both experimentally as well as by modelling methods [209, 210] and has in part been addressed by the creation of the lean NO_x trap (LNT) [208, 211] and the Selective Catalytic Reduction (SCR) technology [212, 213]

LNT technology allows for NO to oxidise on the alkali metal and alkaline earth promoters present in the catalysts to form NO_2. The oxidation is followed by formation of stable nitrites with the alkali metals or alkaline earth materials. The trap has, however, an absorption limit and will need to be 'purged' after a while which currently is achieved by reducing the air-fuel ratio for short periods of time. The SCR technology injects a reducing agent (typically urea) into the exhaust of a vehicle with reported reductions of up to 50 % in NO_x been reported [214]. However, these technologies are primarily still in early stages of development and can come at a significant cost.

2.4.4.4 Particulate Emissions

According to Myung et al. [215], particulate matter (PM) and particulate number (PN) formation in gasoline engines is related to DI engines. Namely, the emissions are related to non-uniform fuel air mixture and wetting of combustion chamber walls that can inherently occur under cold start and transient high fuel injection rate conditions. Cold conditions inhibit evaporation of fuel which hinders air-fuel mixing and results in fuel rich areas where insufficient oxygen levels cause pyrolysis of fuel to occur. Their experiments with liquefied petroleum gas addition showed significant promise of the fuel to reduce PN concentrations by up to 99 %. Further improvements can be achieved by improved injector design. Using multi-hole DI injectors and spray-guided (as opposed to wall guided) injection systems where fuel is injected towards the ignition source can significantly reduce wetting of cylinder walls.

2.4.5 Fuel Additive Effects on Combustion

Additives are directly or indirectly aimed at improving the efficiency of an internal combustion engine. However, direct effects on the combustion characteristics are only assumed to come from the combustion improvers, be it through improving the fuel's cetane or octane number. Ickes et al. [50] and Higgins et al. [10, 9] have shown that 2-EHN cetane improver can significantly improve diesel fuel's ignition characteristics but also contribute towards NO_x emissions. However, the additive derived emissions are often offset by improvements in overall emissions resulting from enhanced combustion characteristics. Colucci et al. [11] used a cetane improver in gasoline in small quantities and completely eliminated misfires under cold start conditions, thus significantly improving unburned hydrocarbon emissions. They argued that the fuel anti-knock properties under low treat rates are not affected but provided no quantitative information regarding a possible change in octane rating.

Fuel consumption, emissions and efficiency of internal combustion engines is also indirectly affected by additives other than CI. As previous review has revealed, significant increase in ORI can result from CCD build up, meaning DCA are required for smooth running engines. Rang and Kann [14] bring to attention the catalytic effect some organometallic DCA can exhibit meaning additives could affect engine running outside their functionality. Similar analogies could occur in ashless additives that use nitrogen in their composition. Since many CI chemistries include nitrogen compounds, improvements in combustion characteristics could result from additives of different primary functionality that contain similar molar groups.

2.5 Summary

The research published on fuel additives and their interactions with fuel spray and combustion development is limited. In order to be able to successfully develop and employ new additives, an improved understanding of the phenomena is needed.

Research on sprays with additives in the fuel has shown very little effect from additives. However, the only additives found investigated in the literature include 2-EHN, which is a combustion improver and two deposit control additives of an unknown chemistry. Effect of additives on spray formation from other functional groups seems not to have been studied. Moreover, all published research thus far on fuel additive effects on sprays has been carried out using diesel fuels. The extent to

which the physical properties of gasoline with additives would be altered is currently unknown. It is likely that the higher volatility and lower viscosity of gasoline compared to diesel fuel would result in more significant changes to atomisation characteristics. This could especially be true for additive groups such as friction modifiers and drag reducing agents where long chain polymers are used.

Although an extensive amount of combustion investigations with additives in fuels have been carried out, majority of these have studied the additive effectiveness against their function. Anti-knocks were the first additives to commercially find their way into fuels. Similarly, ignition promoters in diesel fuels have been extensively investigated. Some interesting developments have been reported with combustion improvers where diesel ignition promoters have successfully been used in gasoline fuels to eliminate cold start misfires. Intrinsically, adding ignition promoters to fuels increases their cetane rating while the octane rating reduces. The relationship between the two can be represented by the Wilke equation [216]:

$$CN = 60 - 0.5\,x\,MON \qquad 2.26$$

where CN and MON stand for cetane number and motor octane number, respectively. It can be seen that an increase in CN would be accompanied by a decrease in MON and a subsequent knocking behaviour of the fuel would be expected. A study into the effects of ignition promoters in gasoline would help understand the fundamental processes responsible for the improved characteristics of gasoline combustion.

Anti-knock additives have been studied extensively since their introduction, although majority of published work remains on metallic compounds, the use of which is now forbidden in developed countries. The mechanisms of auto ignition suppression are thought to be well understood in both metallic and organic compounds, while the effects on other combustion properties such as fuel efficiency, heat release and emissions characteristics seems to have often been neglected.

It is evident that gaps exist in understanding the full effects of fuel additives. Modern direct injection fuel systems and emissions regulations mean an improved understanding of additives is vital. Current project, therefore, has aimed at improving the understanding of additive effects through the investigations of changes to the

physical and chemical properties of base fuel under varying conditions and additive quantities.

Chapter 3

Experimental Facility

Chapter 3 introduces the experimental facility. It begins by presenting equipment employed in spray investigations and finishes with combustion investigation apparatus. The chapter additionally describes considerations behind design work and explains reasoning for hardware selection and its characteristics.

All the spray investigations and part of the combustion analysis was carried out in the UCL constant volume combustion vessel. The remaining combustion studies were carried out in a single cylinder research engine.

The constant volume combustion vessel is a 300 mm inner diameter cylindrical stainless steel vessel with four orthogonal quartz windows for optical access. The vessel is displayed in Figure 3.1. Working pressures of up to 50 bar could be reached by introducing various gases through up to eight available gas injection ports. Dependent upon requirements, two methods of heating the gas mixtures within the vessel could be used:

- 5 kW in line gas heater producing air/nitrogen temperatures of 700 °C
- A gas mixing manifold for pre-combustion events.

A more detailed description of the aforementioned methods is given in Section 3.2.1.

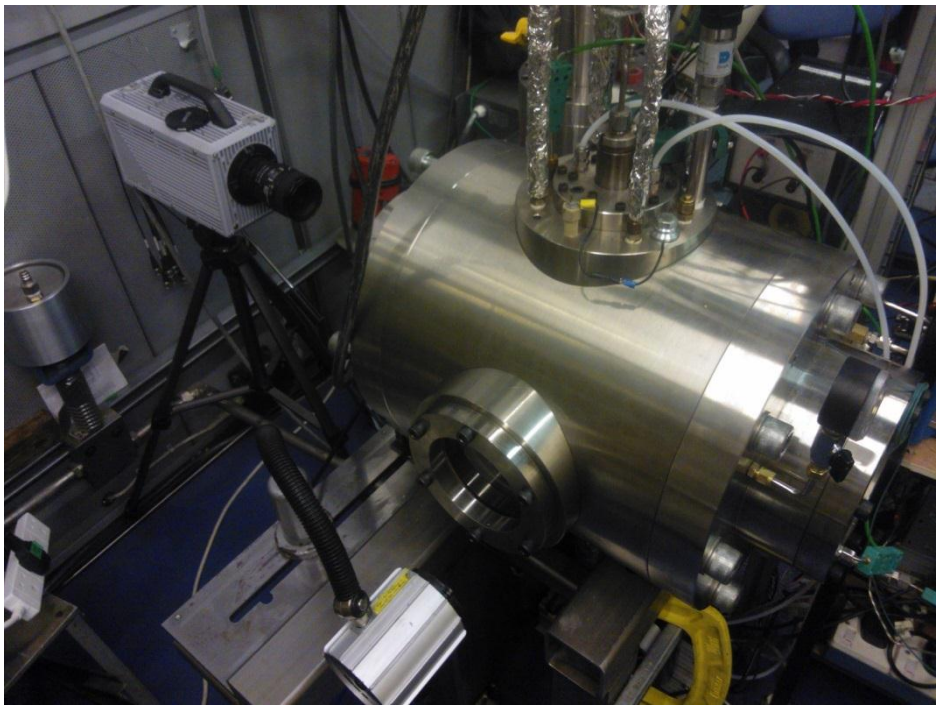

Figure 3.1: UCL constant volume combustion vessel

Constant volume combustion vessel was chosen due to its flexibility in operating conditions. Shadowgraph and direct imaging of sprays and combustion at different ambient conditions and fuel injection pressures is easily achieved, while different laser diagnostic methods are also readily employable. In addition to optical methods, heat release analysis can be carried out. To conclude the analysis of additive effects, testing in a single cylinder research engine was carried out. The engine used was a Ricardo E6 research engine allowing for heat release, knock intensity and emissions analysis.

3.1 Spray Investigation

The combustion vessel had previously been designed and built for diesel spray investigations. Modifications were carried out to enable gasoline spray characterisation with additives. This included a new fuel delivery and control systems.

3.1.1 Injection System

The fuel injection system was built based on a gasoline direct injection (GDI) system. Although modern GDI systems make use of spray guided multi-hole injection systems,

a single-hole wall-guided DI injector was reasoned more suitable for the current study. This was due to factors described in Section 2.2 on interactions between spray plumes but also with combustion experiments in mind. Due to the very large volume in the combustion chamber with respect to engine conditions at the end of compression stroke and a single source of ignition, the wall-guided injection system was employed as a spray-guided injection system. The selected injector was a Bosch single-hole GDI injector rated at 110 bar injection pressure. A custom water-cooled injector mount was designed and manufactured for the chosen injector. The mounting assembly can be seen Figure 3.2.

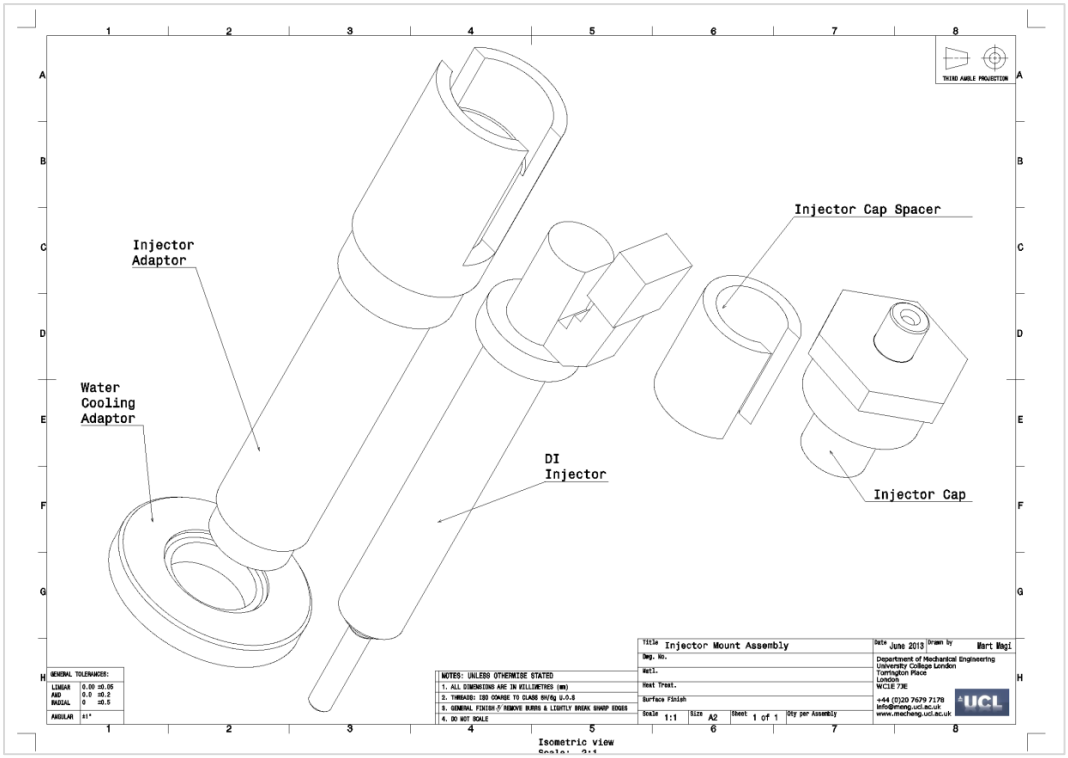

Figure 3.2: Injector mount assembly. Components as named in the figure

It was anticipated that some if not all of the additives used in the testing might carry a memory effect. This would potentially distort results and as a result a full fuel system clean up using an ultrasonic bath was used between different additives. Consequently, the fuel was pressurised using an in-house designed fuel pressure accumulator [217]. A larger piston is pressurised directly from a nitrogen supply which then amplifies the pressure as the force is transferred to a smaller piston. This system allowed for nitrogen supply pressure to be stepped-up by a factor 7 while all components in contact with fuels could explicitly be cleaned. Cleaned components

included fuel injector, injector cap, high pressure fuel line, pressure transducer mount and fuel accumulator parts that were in contact with the fuel. This is presented in Figure 3.3.

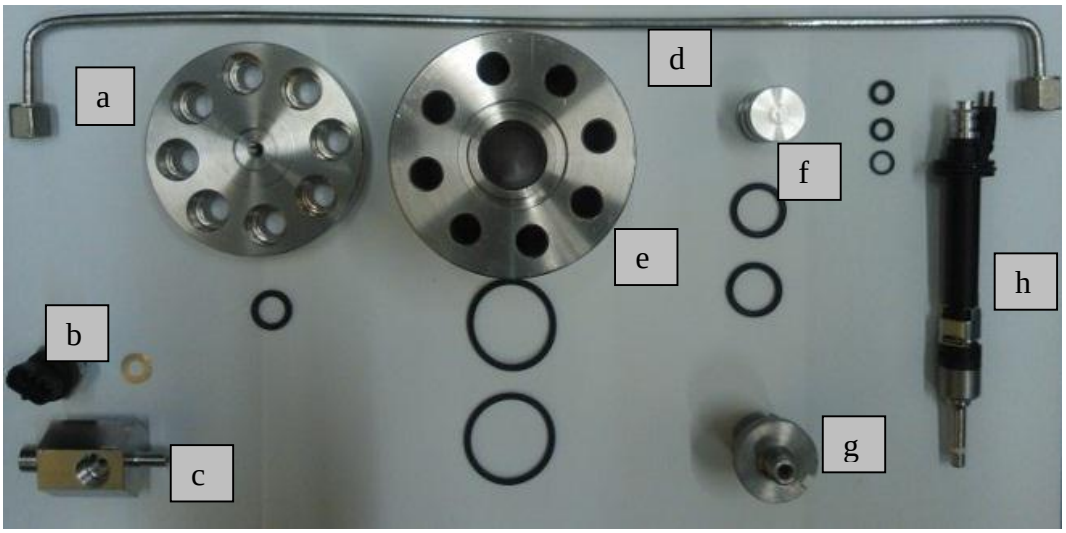

Figure 3.3: Fuel system components cleaned in the ultrasonic bath. Components include: a) high pressure fuel tank lid, b) common rail fuel pressure transducer, c) pressure transducer mount, d) high pressure fuel line, e) high pressure fuel tank main body, f) fuel side small piston, g) injector cap, h) DI injector

3.1.2 Injection System Characteristics

Injector characteristics were quantified in order to be able to distinguish between hardware variability and additive effects. Additionally, this data could be used to determine experimental conditions. Figure 3.4 represents the shot-to-shot

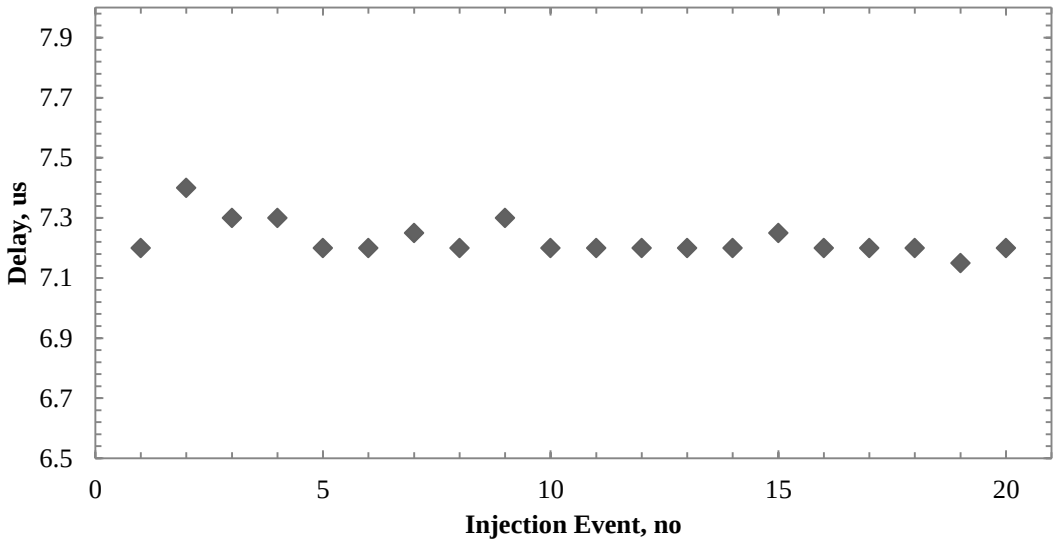

Figure 3.4: Injection signal to injector driver output signal delay

variability of start of injection signal to start of injector signal. An average delay was found to be 7.2 μs with a standard deviation of 0.79 %. This, in comparison to the injection signal duration (in ms range), was considered not significant.

Figure 3.5 displays the increase in fuel velocity with increasing injection pressures. The data was obtained from shadowgraph images at each injection pressure and was measured to reflect time taken to reach 60 mm from the injector nozzle. Each point was measured from a 20 image average that was found large enough sample to eliminate the effect of spray-to-spray variability. The measured spray tip velocity varied nearly linearly between 38.5 km/h and 51.9 km/h. Shadowgraph images of typical injections for 50 bar and 110 bar injection pressures can be seen in Appendix A.

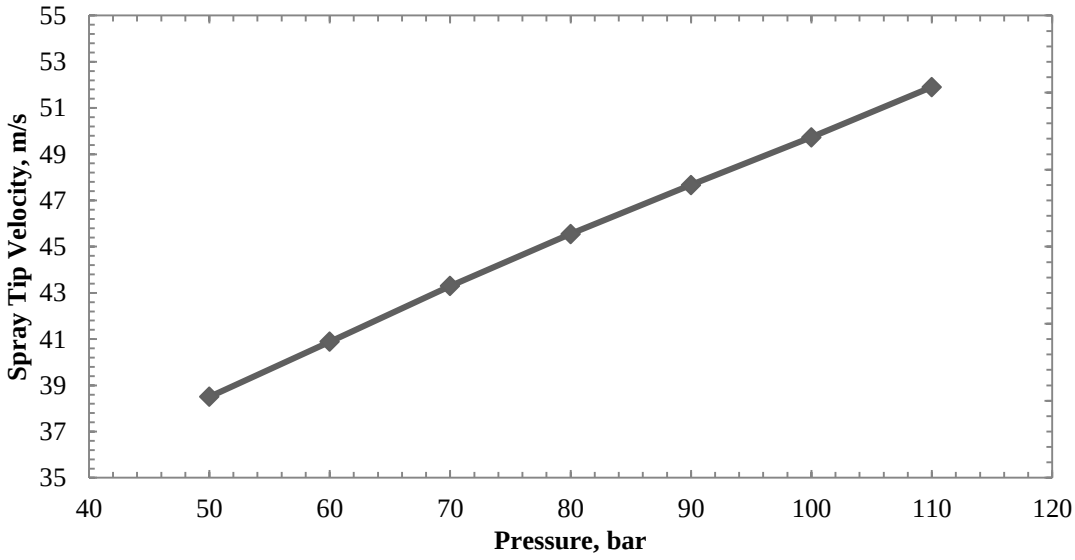

Figure 3.5: Spray tip velocity at increasing fuel injection pressure as measured to 60 mm from the nozzle

3.1.3 Droplet Sizing

As was discussed in Section 2.3.2, droplet size is the primary microscopic characteristic of spray atomisation quality. Droplet size analysis characterisation was carried out using a Malvern Instruments Spraytec laser diffraction system. The system uses a 660nm wavelength 10 mm diameter laser beam directed through the working section and sampled on a 32 ring receiver. Maximum sampling rate of the system is 2,500 Hz. Initial testing showed great difficulty in aligning the laser through the 88 mm thick quartz windows due to diffraction of light at different laser to rig alignment angles. If normal positioning between the two was not achieved, small deflections in

the laser beam caused the inner most rings of the receiver to misread the input and give false readings in the form of large droplets. As a result, two of the windows were removed and the testing carried out under ambient pressure and temperature conditions.

3.1.4 Viscosity and Surface Tension Measurement

In order to better understand drop size behaviour between different additives and fuels, measurements were carried out on viscosity and surface tension. As explained in Section 2.3.2 these are the two prominent physical properties of liquids that affect the droplet size and can change in a non-linear manner to their constituent composition. Viscosity measurements were taken with a *Brookfield DV – III Ultra* programmable shear rheometer combined with a heated bath for temperature control. The principle of operation is using a calibrated spring to drive a spindle [218]. The liquid is placed within a cylinder and a rotating spindle is lowered into it. As the spindle rotates, the liquid exerts a measurable torque on it which is converted into shear rate and viscosity of the liquid. The rheometer gave accuracies to within two decimal places.

Surface tension of the fuels was measured with a *Kimble & Chase Surface Tension Analyzer*. The analyser works on the principle of capillary action, whereby a liquid fuel is forced vertically up a tube and then let fall down due to gravitational forces [219]. In this process wetting of the capillary walls occurs and the surface tension induced tensile stress tends to pull the liquid free surface towards the solid surface. This encourages formation of a curved meniscus and, if the capillary diameter is small, creates a capillary rise. The surface tension could be calculated using an equation proposed by the manufacturer and followed the form:

$$\sigma = \frac{1}{2}\rho ghr \qquad 3.1$$

where: σ – surface tension ρ – density of sample, g – acceleration due to gravity, h – distance between menisci and r – radius of the capillary. It was claimed that accuracies to within 20 % of true values were possible with the analyser.

3.1.5 Spray Apparatus Overview

The overall schematics of the experimental facility, used for droplet size analysis, can be seen in Figure 3.6. The equipment includes a constant volume combustion vessel (CVCV), Malvern Spraytec laser diffraction system, GDI high pressure swirl-type injector and a fuel pressure accumulator.

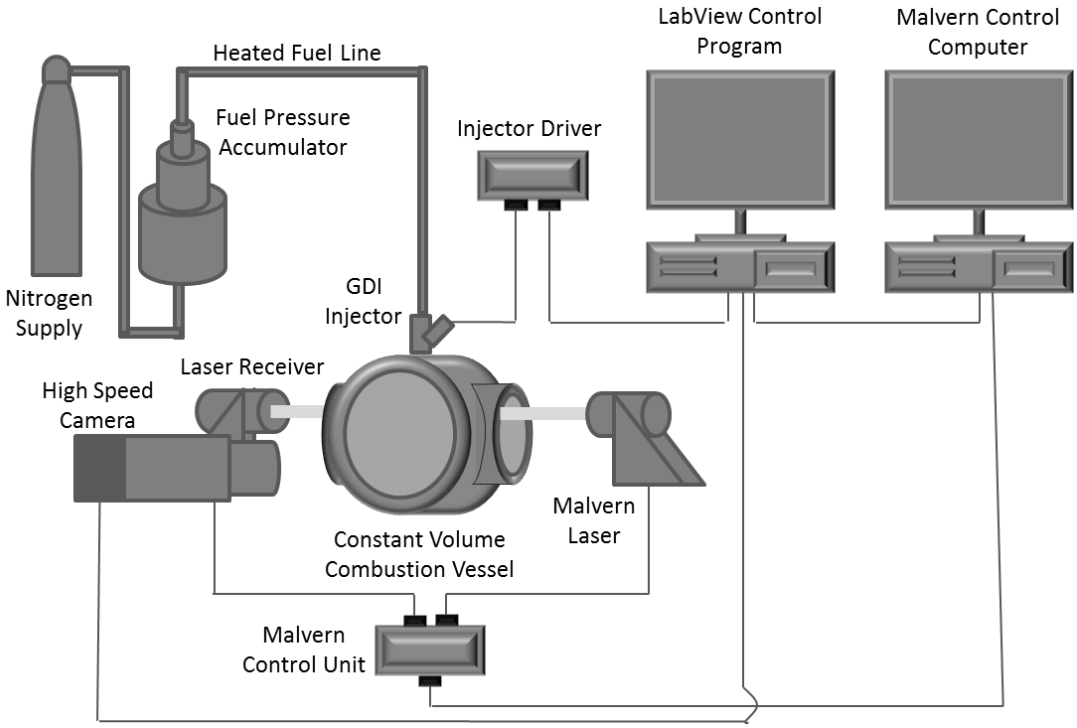

Figure 3.6: Schematics of experimental facility for spray analysis

The injector was powered by a LifeRacing GDI driver and injections controlled through a LabView control program. The software was additionally used to send a signal to the Malvern system for triggered data acquisition. The same program was also used to monitor fuel pressure and ambient conditions. Shadowgraph images were taken with a Photron APX-RS high speed camera coupled with a Nikon 50 mm f/1.8 lens.

3.2 Combustion Experiments

Combustion experiments were carried out in the UCL constant volume combustion vessel (or the bomb) and a single cylinder Ricardo E6 research engine. The following sections will describe the set-up used with each of the methods.

3.2.1 Constant Volume Combustion Vessel

The set-up for combustion experiments comprised of an ignition system and appropriate control methods for temperatures and pressures prior to a combustion event. Two types of gasoline combustion were carried out in the vessel:

- Gasoline spray combustion
- Gasoline vapour combustion

Spray combustion involved using the gasoline direct injection system introduced in Section 3.1.1. Fuel was delivered in liquid jet form and sprayed into the combustion vessel at pre-determined gas conditions for stratified combustion. Alternatively, the gasoline was introduced into the vessel via a syringe pump and vaporised for homogeneous gas combustion.

Due to above atmospheric pressures used with both methods, vessel gas leakage characteristics were determined. This is displayed in Figure 3.7. Over a 4 hour period at ambient temperature, a projected 8 % drop in pressure occurred. The experimental duration in current study was estimated to be 25 minutes for spray combustion (combustion event every 30 seconds, 50 repeats in total) and less than 10 minutes for gasoline vapour combustion (fuel pumped in at 0.5 ml/min, 2-8 ml of fuel – dependent upon pressure/air-fuel ratio conditions required prior to combustion, single combustion event) during which pressure losses of less than 1 % were expected.

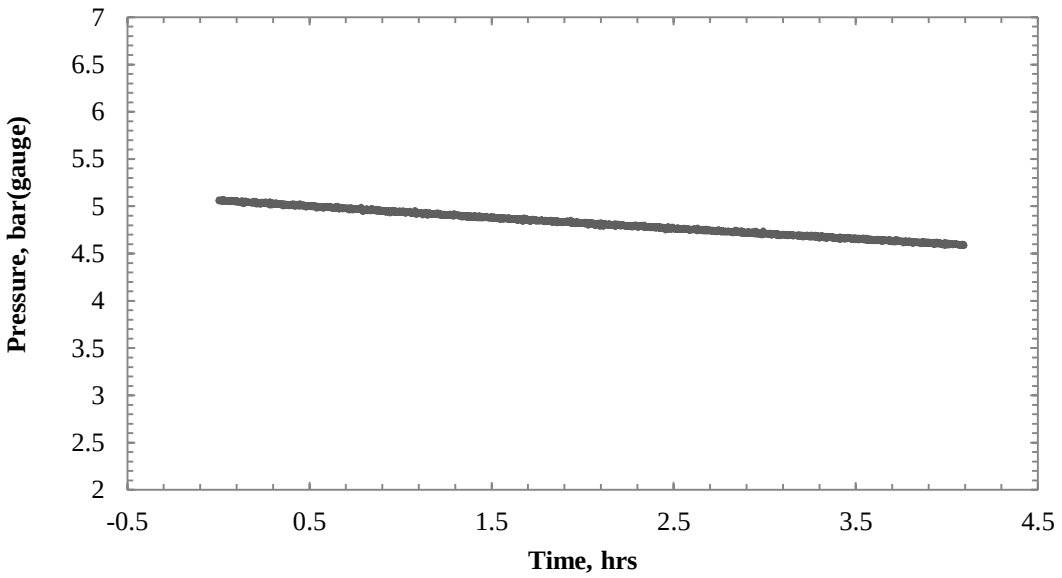

Figure 3.7: Combustion vessel leakage characteristics at ambient temperature

3.2.1.1 Gas Preparation

Gas conditions in the combustion could be controlled using two methods:

a) Heating the air up using an inline air process heater and

b) Pre-combustion in the vessel under lean conditions.

The heater and the gas mixing manifold can be seen in Figure 3.8. The air process heater enabled reaching temperatures of up to 700 °C at the exit from the heater and dependent upon set-up inside the combustion vessel and heat losses in the gas injection lines, temperatures above 250 °C could be achieved within the chamber for short periods of time. Vessel was heated up by running heated high pressure air through the

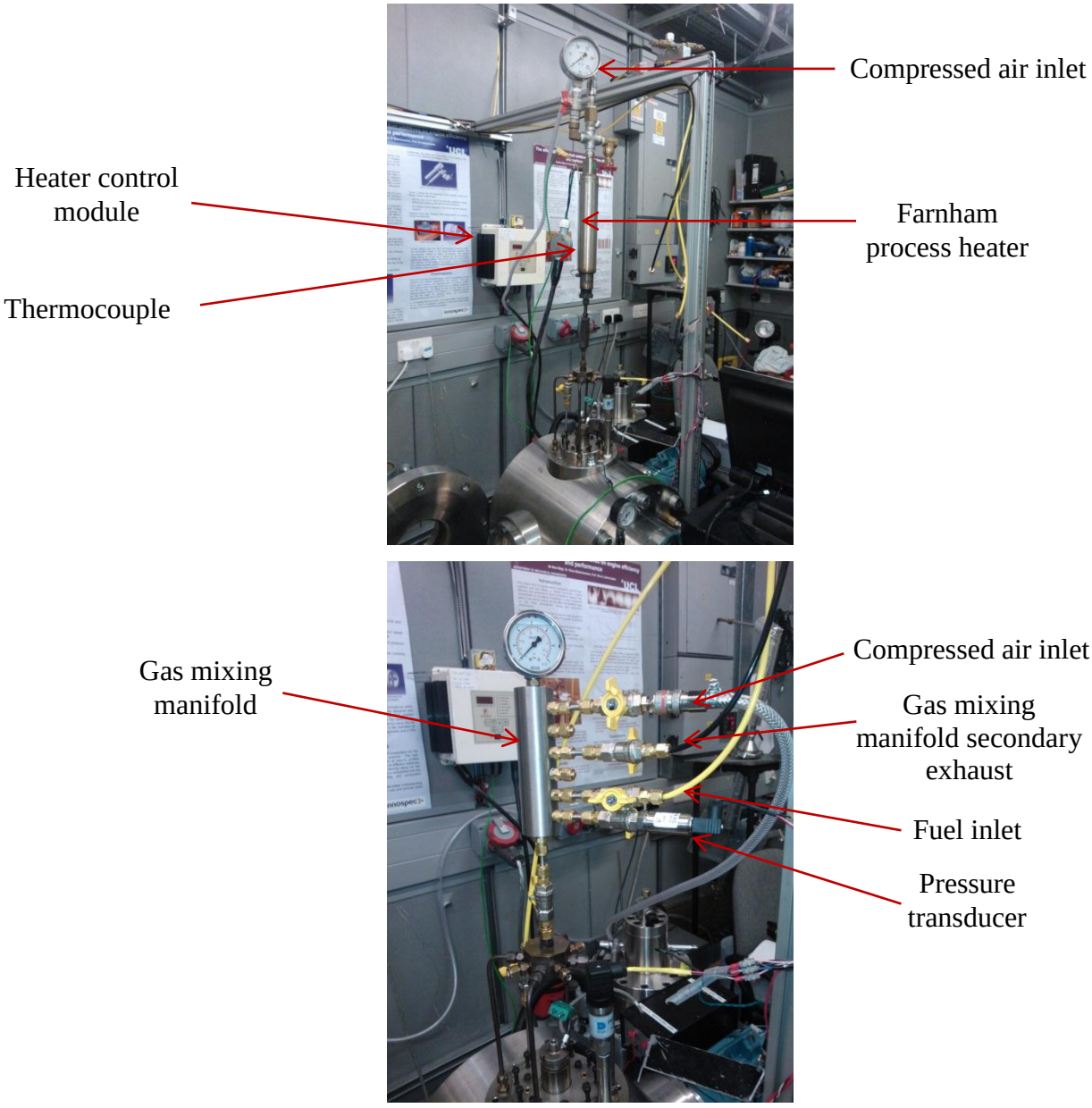

Figure 3.8: Top: Farnam air process heater, Bottom: gas mixing manifold

system until certain wall and air temperatures were achieved. The low thermal inertia of the rig meant that up to 3 hours was required to reach 80 °C wall temperature but also that the temperature could be maintained throughout spray and gasoline vapour combustion events without experiencing a significant drop. The large volume of the vessel (22.5l) enabled large number of spray combustions before oxygen levels were depleted to a critical level, thus speeding up experimental time. This was especially true for raised initial air pressures.

The pre-combustion method allowed for much increased pressure and temperature conditions for a short time period. A lean mixture of gaseous fuel was ignited, giving EGR-like conditions before spray combustion. This method can potentially simulate engine conditions better than the heater method but repeat experiments under same conditions are time consuming. The pre-combustion gaseous fuel mixture could be prepared based on partial pressures. Dalton's law of partial pressures states that the ratio of partial pressures of air and fuel is the same as their molar ratio [220]. This can be expressed as:

$$P_f = \frac{n_f}{n_{air}} \times P_{air} \qquad 3.2$$

Generally the pre-combustion method suits better diesel combustion where spray variability does not play as much a role as in gasoline combustion where it is additionally accompanied by spark variability and as a result a larger number of repeats is required for a statistically relevant average [114].

Additionally to spray combustion, a combination of syringe pump and heater was used for gasoline vapour combustion. Heated fuel would be pumped at a constant rate into the pre-heated vessel where it would evaporate and result in a homogeneous air-fuel mixture. Although typical experimental timescales involved were an order of magnitude longer per combustion event, the pressure rise from the pre-mixed gasoline combustion event was more than 2 magnitudes of order higher. As a result the error deriving from limitations in pressure transducer sensitivity was reduced.

The air-fuel mixing was aided by a 70 mm brass fan, driven by a 1.3 kW 3,000 rpm electric motor. The fan mount replaced one of the quartz windows to allow for improved gas mixing while filling the vessel with pre-combustion gases/ gasoline vapour. The fan location is as shown in Figure 3.9.

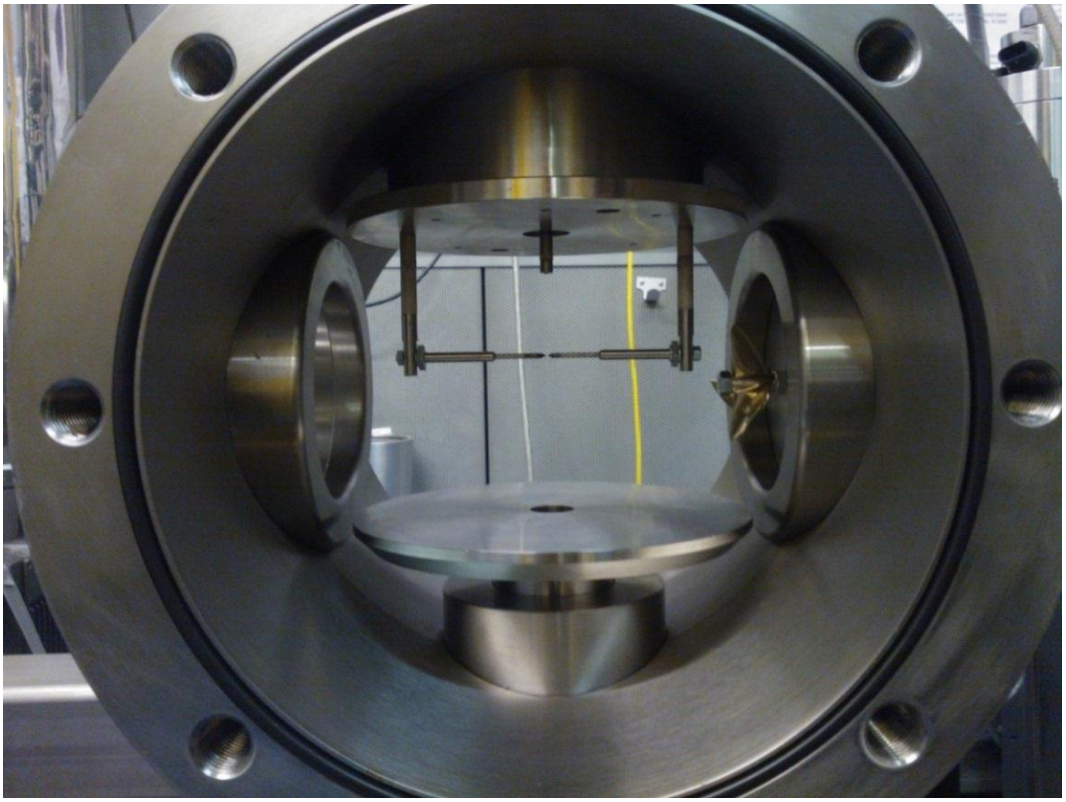

Figure 3.9: End view of combustion vessel. Visible items: injector nozzle, electrodes & mixing fan

3.2.1.2 Ignition System

Figure 3.9 displays the electrodes in the combustion vessel. The electrodes were placed 55mm vertically below the injector nozzle, close to the centre of the vessel. For spray combustion, the electrodes were rotated slightly to shift the electrode gap towards the fringes of the spray where a more favourable air to fuel ratio, compared to the centre of the spray plume, was experienced. This is due to electrode wetting occurring at the central position that terminates the spark without ignition occurring. Electrode gap was fixed at 1mm for all experiments.

Ignition system included a set of purpose built electrodes and a commercially available ignition coil. The electrodes were adjustable in the horizontal and vertical directions through different sized spacers and current carrying anode and cathode were separated from the pressure chamber through PEEK isolating rods. Although the anode in the circuitry was grounded to the pressure chamber and would not need isolation, for manufacturing purposes both the anode and cathode were manufactured following the same design. An assembly of the system can be seen in Figure 3.10.

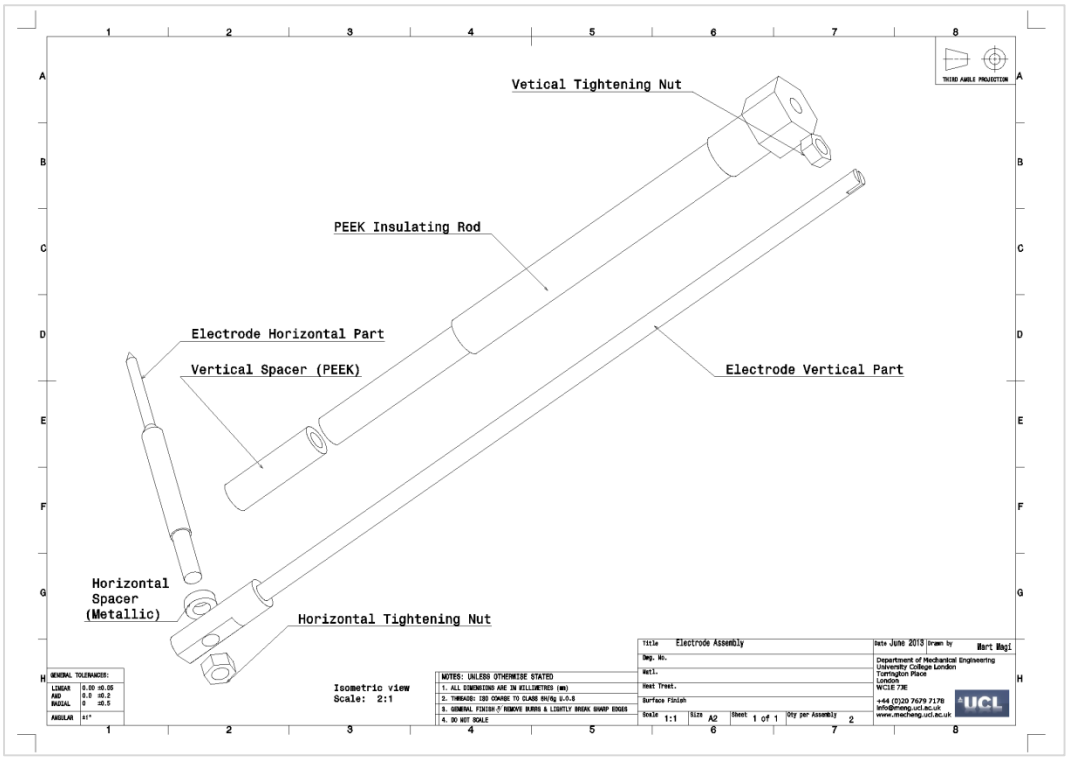

Figure 3.10: Electrode assembly drawing

The spark was generated through a commercially available coil-on-plug (COP) type inductive ignition coil. The system benefitted from easy set-up, low cost and readily adjustable spark duration through changes in dwell timing (coil charge time). This was especially important when spray combustion was concerned. Although Dale et al. [221] state that shorter spark durations are more efficient as less energy is lost to the electrodes, longer discharge periods increase ignition probability by exposing larger fraction of the air-fuel mixture to the related deviations in combustion characteristics, spark energy measurements for all combustions were performed.

Available spark discharge energy can be found by using the following relationship:

$$E_{Spark} = \int [(V_{Probe} - I_{Probe} \times R_{Electrode}) \times I_{Probe}]\, dt \qquad 3.3$$

Energy is calculated over the duration of the spark. Spark duration is defined as the time during which the measured current is above 0 A. Spark voltage and current data was obtained using a Tektronix P6015A high tension probe and Pearson Model

110 current monitor and sent to a Tektronix DPO3014 digital oscilloscope for data display and storage.

A typical voltage and current traces obtained with the aforementioned hardware with a signal trigger signal as a reference are presented in Figure 3.11. At t_1 the coil charging commences with voltages around 300-400 V applied to the electrode gap. A magnetic field, which is created between the primary and secondary windings of the ignition coil during this stage, collapses once power to the primary coil is removed, as represented by the end of spark signal. This leads to the pre-breakdown phase [221]. In this stage the potential difference between the anode and cathode caused by the collapsing magnetic field causes the free electrons in the gap to accelerate towards the anode. The higher the voltage input the higher the number of molecules that are ionised. Once the electrode gap impedance has been reduced to the point where current starts flowing, breakdown phase (t_2) of the spark discharge phenomena is reached. In this stage the current and voltage increase rapidly and further ionise molecules between the electrodes. The energies in the arc channel are reported to be high enough to fully ionise the gas molecules and raise the temperature to 60 000 K [221].

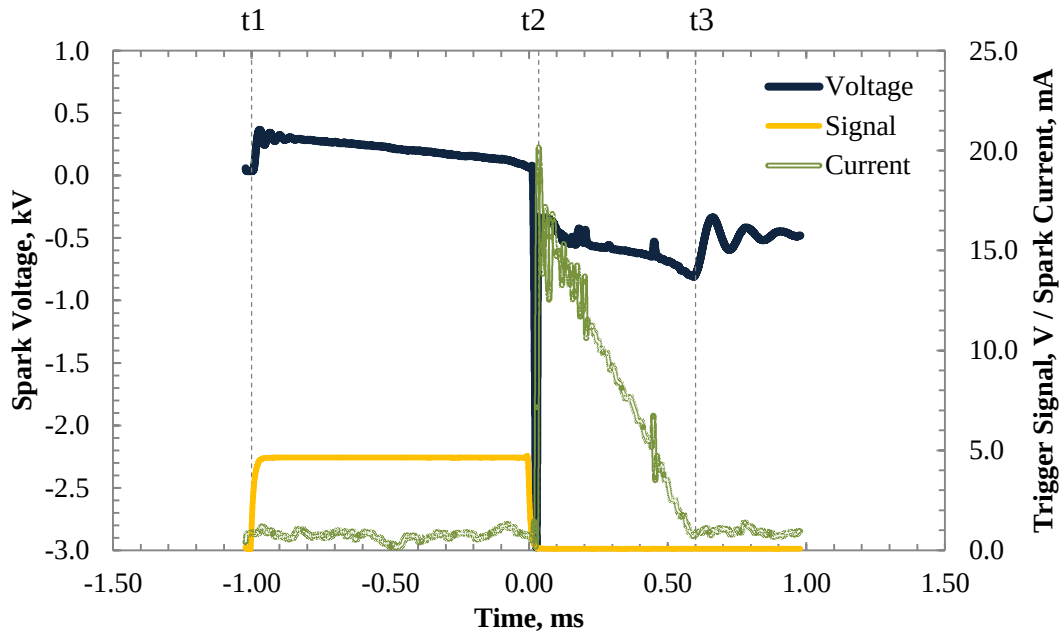

Figure 3.11: Current and Voltage traces from the COP-ignition coil

Arc phase follows with lower voltage and current characteristics. The added energy applied to the spark gap during the breakdown phase reduces the voltage

required to maintain the arc from >2-3 kV to typically around 100-200 V. Due to increased timescales involved in this phase, the total energy released is greater, although peak power output is reduced. In the final, glow phase, of the spark discharge, power output reduces further still due to the finite nature of energy stored. This results in fewer molecules being ionised and less current being carried. Consequently, an increase in voltage is often experienced. This phase lasts until no more ionised gas molecules are available and current stops flowing, represented by t_3 in Figure 3.11. As mentioned previously, spark occurs when measured current is positive which is defined as the time interval from t_2 to t_3.

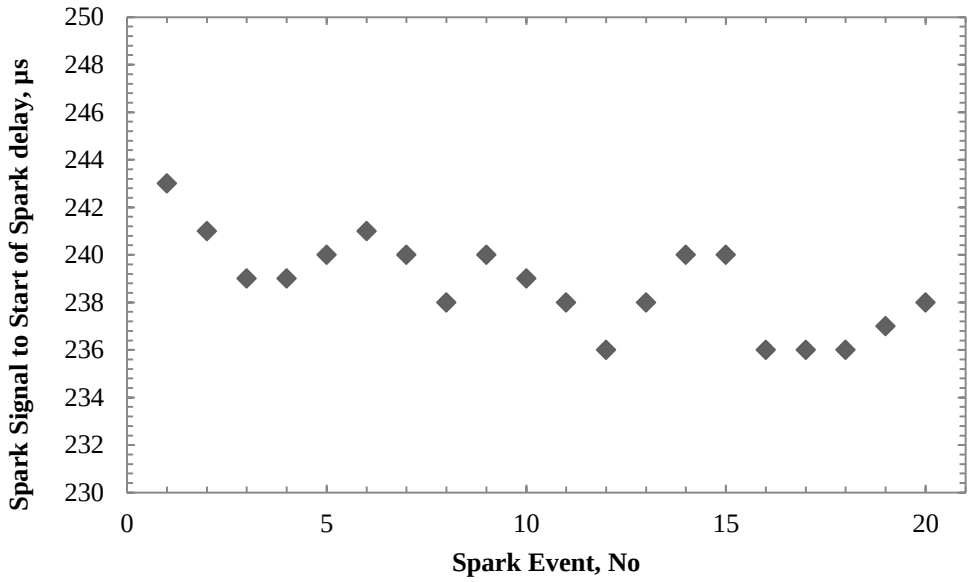

Figure 3.12: End of spark signal to beginning of spark delay. Dwell time 0.8 ms.

Figure 3.12 displays typical delays from end of spark signal to start of spark at 0.8 ms dwell time. The spark-to-spark average delay was measured as 238.75 µs with a standard deviation of 0.81 %. The delay could be shortened with longer dwell time due to higher potential differences being achieved in the electrode gap as a result of larger magnetic field being created between primary and secondary windings of the ignition coil.

3.2.1.3 Emissions Analysis

Emissions were analysed using a Horiba MEXA 9100 HEGR gas analyser. The analyser measures NO_x emissions through chemiluminescence. CO and CO_2

content is established using non-dispersive infrared analyser. The analyser can further measure unburnt hydrocarbon content using the flame ionisation method. Due to the distance of the gas analyser from the combustion vessel, fuel condensation in gas lines was likely, resulting in false hydrocarbon readings. Furthermore, the GDI combustion method means misfires can occur as a result of spray variability and any hydrocarbons detected might not represent additive effects. Therefore, no hydrocarbon emissions were measured for any set of combustion experiments.

The combustion efficiency could additionally be evaluated by analysing the soot contents with a Cambustion DMS500 particulate spectrometer. The device produces output in terms of particle size, number and mass.

3.2.1.4 Combustion Apparatus Overview

Schematics of the experimental rig for the combustion experiments can be seen in Figure 3.13. Main changes included an ignition and pre-heating systems. High speed imaging was used with spray combustion as a means of qualitative analysis. Quantitative analysis is carried out based on methods describe in Section 2.4.1 using pressure data.

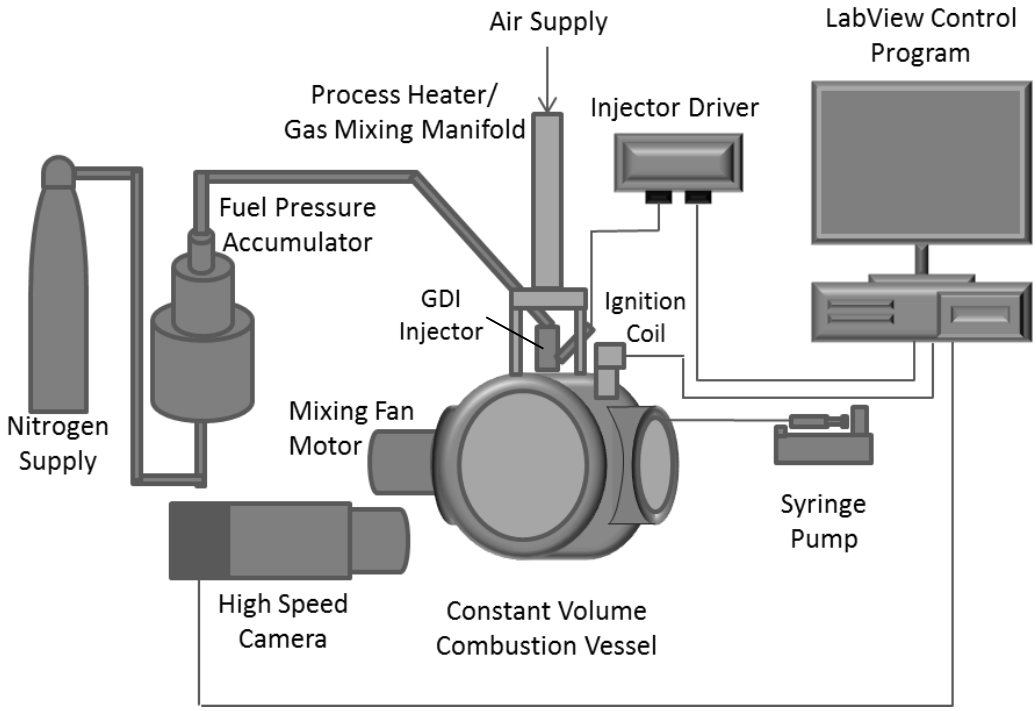

Figure 3.13: Schematics of experimental facility for combustion analysis

Gas pressure was monitored through three pressure transducers:

a) Druck PMP1400 0-100 bar, 0-5 V – bomb pressure
b) Kistler 701A piezoelectric PT, 0-250 bar pressure range, 84 pC/bar sensitivity, coupled with Kistler 5015A charge amplifier – dynamic bomb pressure
c) Omega PXM319 0-2 bar, 0-10 V – gas mixer pressure

Temperature was monitored in two locations within the vessel and in one location inside the vessel walls. This data was only useful when the air process heater is used. Pre-combustion events occur in timescales shorter than the thermocouple response time and the rig wall temperature is unaffected by high combustion temperatures due to low thermal inertia. Additionally, fuel temperature within the injector could be monitored. Injector mount was surrounded by a water cooling jacket enabling high temperature air flow into the vessel without raising fuel temperature to very high temperatures.

3.2.2 Engine Facility

In addition to the combustion vessel, part of the combustion experiments was carried out in a Ricardo E6 research engine, shown in Figure 3.14. It is a single cylinder, variable compression ratio engine with a 3 inch bore and 4 3/8 inch stroke

Figure 3.14: Ricardo E6 research engine

that can be run in compression and spark ignition modes [222]. The engine employs a similar ignition set up to the combustion vessel but spark discharge is performed through a spark plug. Fuel injection can be carried out using PFI or carburettor fuel delivery systems. Cylinder pressure data is logged for heat release analysis and emissions are analysed using the Horiba gas analyser and Cambustion DMS500 particulate spectrometer. For more information on the device, the reader is directed to Ref. [223].

3.3 Summary

Chapter 3 has presented the experimental equipment used for the characterisation of the effects of fuel additives on gasoline DI sprays and combustion. Figure 3.15 displays the overall work split schematics and methods and equipment used for each type of analysis.

The physical properties of fuels were tested through measuring changes in surface tension and viscosity and their effects on fuel sprays through droplet size analysis. Chemical kinetics were evaluated through combustion analysis. Heat release and emissions analysis were primary methods of study in the combustion vessel and also in the single cylinder engine. Additionally, combustion vessel tests with vaporised gasoline allowed for high speed imaging to be used for flame speed analysis.

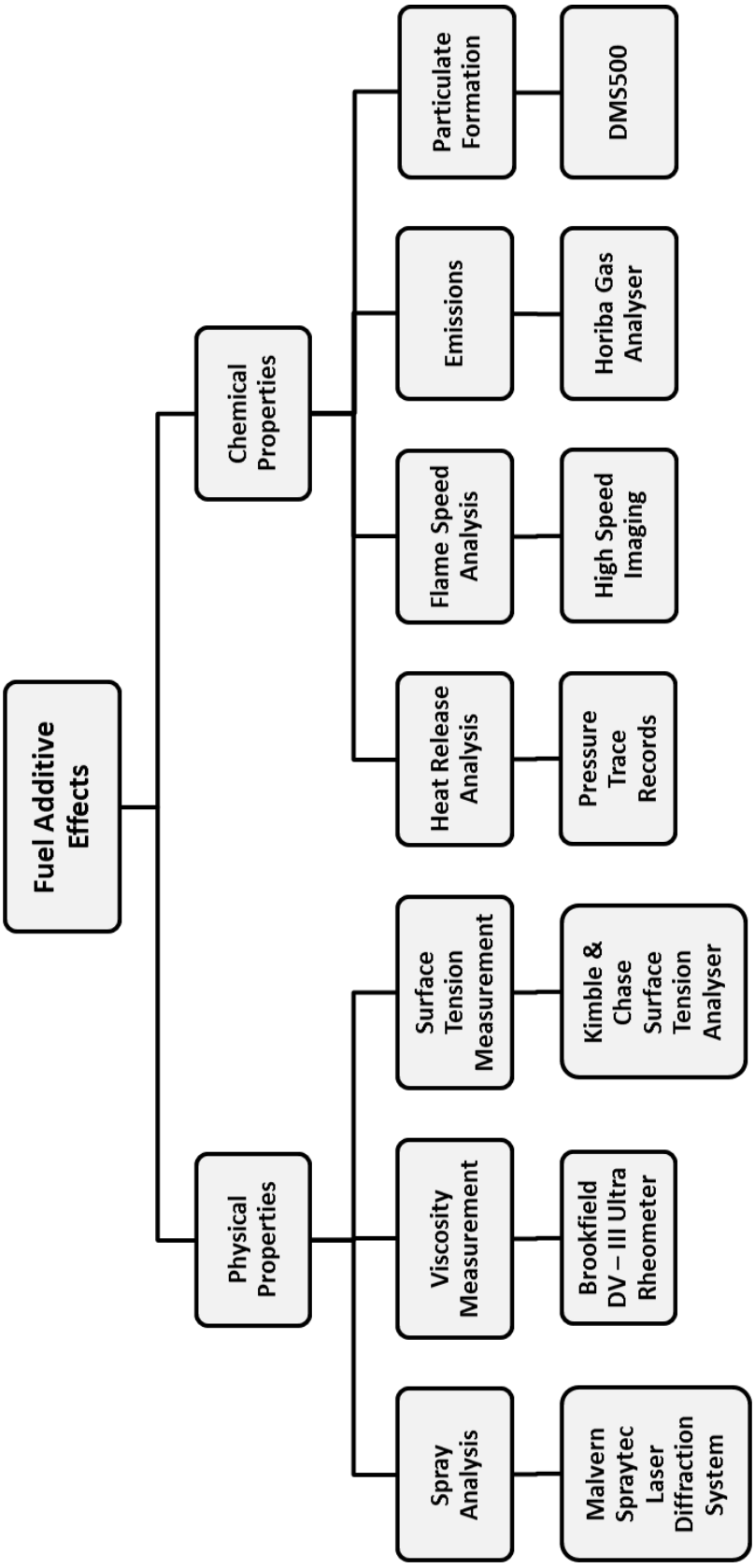

Figure 3.15: Project schematics for measurement focus and associated hardware

Chapter 4

Base Fuel Characterisation

This chapter explains the base gasoline fuel spray and combustion characteristics. The aim of the work was to establish conditions under which it was possible to successfully study the effects of fuel additives on fuel spray formation and combustion characteristics. First, the spray features are discussed and the experimental methodology for droplet size analysis for the subsequent additive investigations is presented. Thereafter, methods used in combustion investigations are explained. This includes combustion vessel experiments under ambient, heated and pre-combustion conditions as well as some selected engine testing.

4.1 Spray Features

In order to determine conditions under which additive effects on fuel atomisation could successfully be assessed, base fuel characterisation under several different conditions was carried out. This included a study into the effect of fuel injection pressure and measurement location on droplet size where measurement location was defined as the spatial position of the laser beam within the spray plume in the x-z plane, as shown in Figure 4.1. For all experiments, injection period was kept at 2 ms. This time was found to be sufficient to allow for spray development and, as

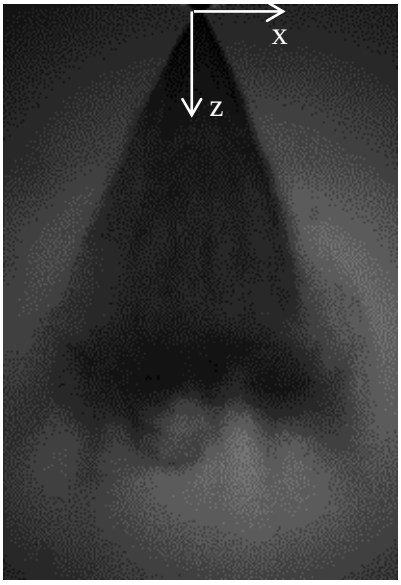

Figure 4.1: Fuel spray plume and measurement location definition

will be explained in the following sections, capturing first spray measurement while injector was still activated. It is also representative of conditions in GDI engines [116, 224].

As described in Section 2.3.2, for large injection pressures the effect of pressure drop across injector nozzle on droplet size diminishes. As such, additional tests at lower pressures, where possible additive effects would be more prominent, were carried out. Injection pressure was varied between 50-110 bar in 10 bar steps. Pressures below 50 bar were considered too low for practical engine applications and as such were not considered for the analysis. Although at different injection pressures the quantity of fuel varies, it was thought that under identical experimental conditions between different additives no additional benefit could be gained from adjusting injection duration to injection pressure.

4.1.1 Effect of Location and Injection Pressure on SMD

For the Malvern laser diffraction system to work reliably, transmission of light to the detector/receiver needs to be above 2 %. This proved difficult along the central axis of the spray with the chosen injector and location off the centre axis had to be used instead. Although recommended practice for GDI spray characterisation involves measurement along the central axis [225], for the purpose of the current comparative study where changes in fuels are investigated, an off axis location was still considered suitable. It was desired that the injector was still active at the time of acquisition of the

first SMD data and a location as close as possible to the central axis was used. A distance of 60 mm from the injector nozzle and 10 mm from the central axis was found to be the closest possible location to satisfy the aforementioned criterion. Similar measuring locations were used by Suh et al. [226] and Chen et al. [227] although neither author has given reasoning for the selection. The following analysis will show the effect varying x and injection pressure at z = 60 mm, where x and z denote the spray jet radial and axial directions, respectively. The point (0, 0) was defined as the injector nozzle tip.

Figures 4.2 and 4.3 display the effect of location on the transmission of light at 50 bar and 110bar injection pressures, respectively. Shadowgraph images of spray development at 50 bar and 110 bar can be seen in Appendix A. It can be detected for both pressures, that initial rapid decrease in transmission to a minimum value is followed by a less rapid increase in transmission back towards 100 %. Also, it can be seen that transmission is higher for locations further from the central axis, suggesting the presence of less fuel in these regions. Furthermore, it can be seen that higher pressure accounts for extra fuel which is represented by the lower transmission values for a given location.

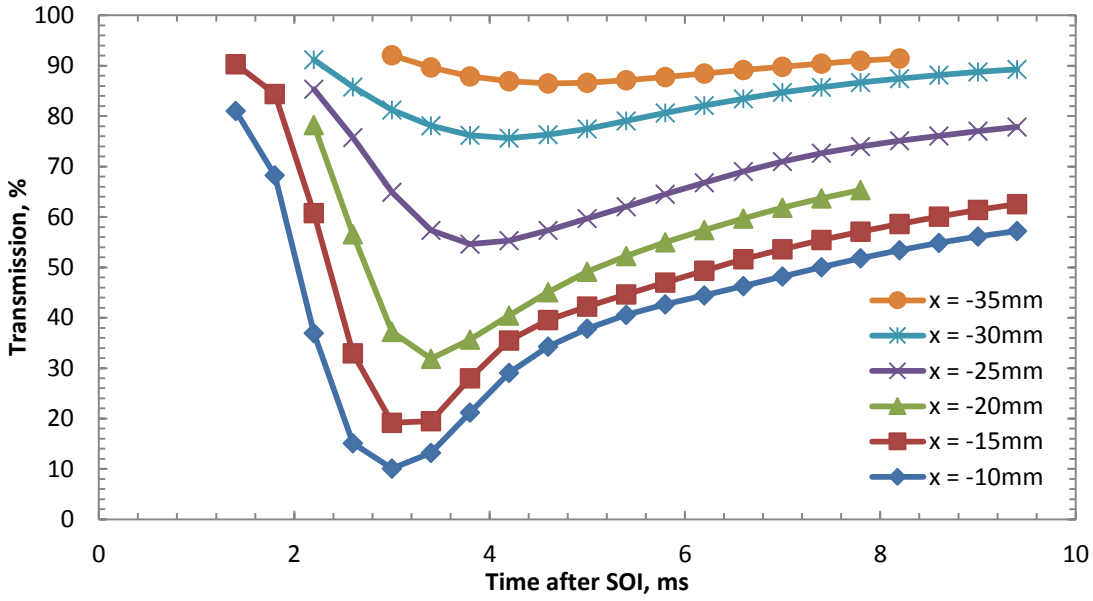

Figure 4.2: Effect of location on transmission at 50 bar injection pressure

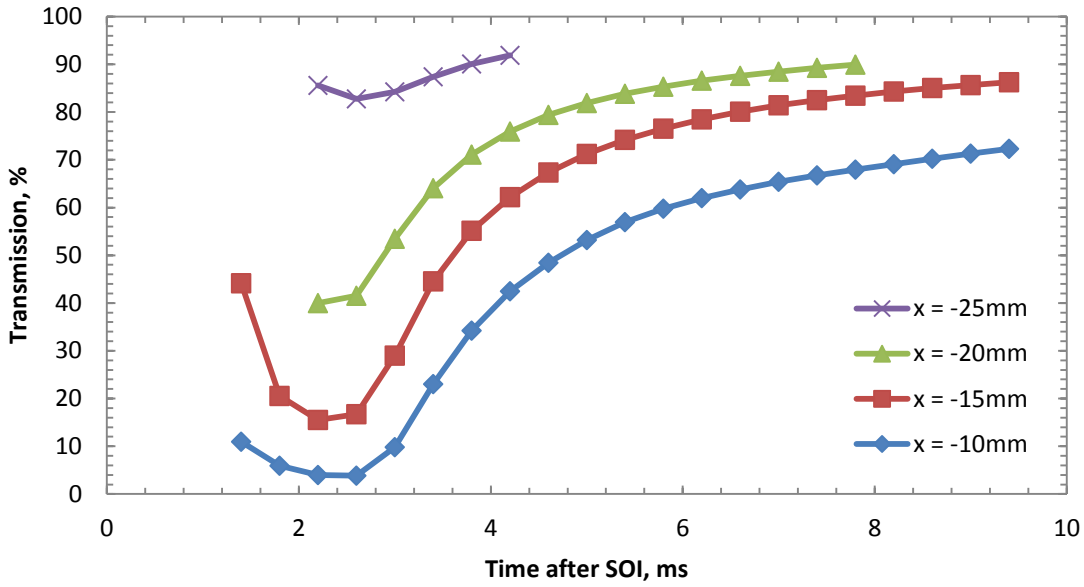

Figure 4.3: Effect of location on transmission at 110 bar injection pressure

It is noteworthy that two extra readings were made at 50 bar injection pressure compared to 110 bar. This is due to fuel quantities in the measurement location being below the Malvern system cut-off threshold of minimum 5 % laser obstruction. Appendix A displays a typical injection at 50 bar and 110 bar. No difference in the spray cone angle could be noted up to an axial distance of around 25 mm but with increasing axial distance from the nozzle it is thought the lower momentum carried by the fuel with 50 bar injection pressure caused an increase in radial movement of fuel droplets due to aerodynamic drag compared to 110 bar injection pressure. This meant that at 110 bar at locations x = -30 mm and x = -35 mm, spray density was too low to be reliably measured.

Figures 4.4 and 4.5 display the effect of location on measured SMD for 50 bar and 110 bar, respectively. It can be seen that initially large droplets are present followed by small droplets for short period of time. Before reaching a plateau value for the duration of measurement, a short period of increased droplet sizes occurs. It is evident that this feature diminishes as measurement is taken at a further off axis position. This is likely to be due to the fact that the measurements were taken on the fringe of the spray jet, if not completely outside the spray focus area where only small quantities of fuel are present and aerodynamic force effects on the fuel droplets are greatly increased. As a result, lower droplet velocities are experienced and greatly reduced temporal variation of droplet size is observed.

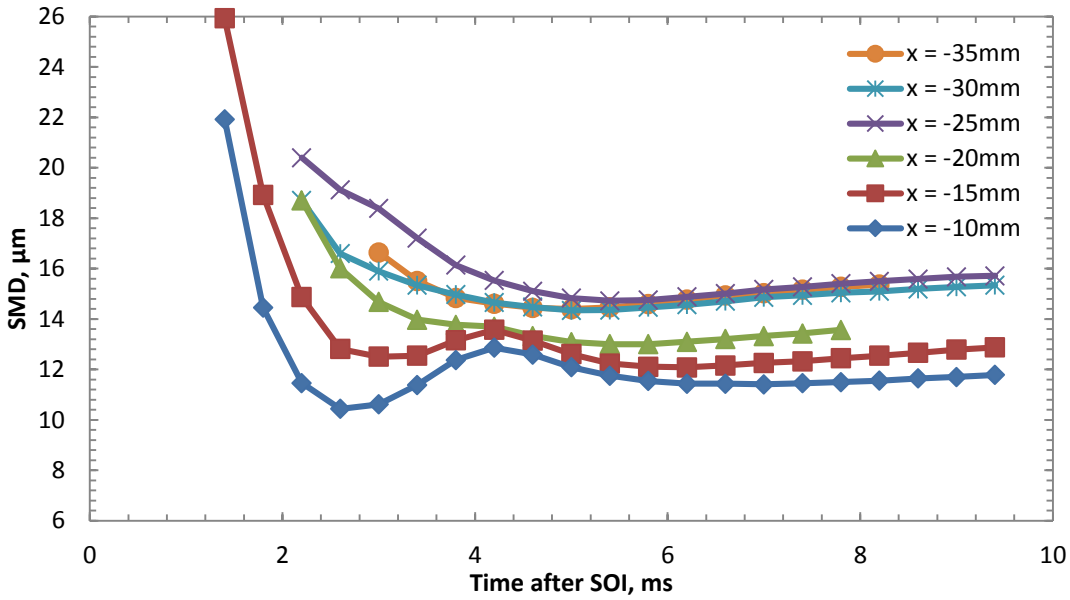

Figure 4.4: Effect of location on droplet size at 50 bar injection pressure

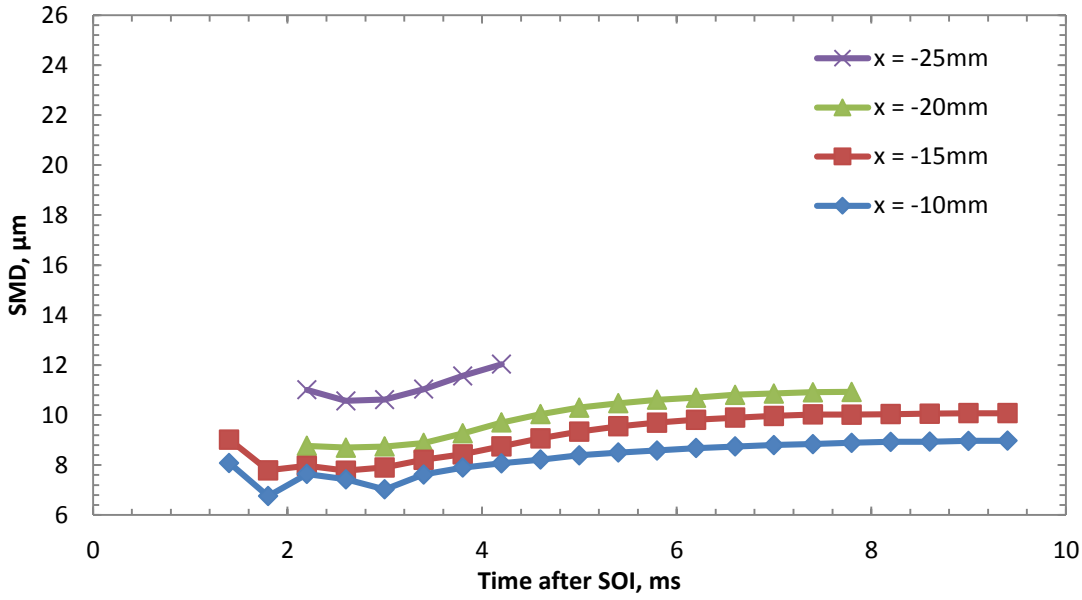

Figure 4.5: Effect of location on droplet size at 110 bar injection pressure

Furthermore, an increase in droplet size was seen with increasing distance from central axis. This phenomenon was investigated by Moon et.al. [228]. They carried out CFD analysis on gasoline direct injection spray formation and its dependence on airflow effects at ambient temperature and 90 bar injection pressure. They found it to generate a static low pressure region in front of the spray that creates pockets of entrained air and also pushes small droplets from the edges to the central regions of the spray.

Another explanation for large droplets to occur on the edges of the spray could be the velocity profile. Lu et al. [141] used a PDA system to obtain a spray velocity profile under atmospheric back pressure and 60 bar injection pressure conditions and found a much reduced droplet velocities on the edges of the spray compared to those along the centre line. As was described in Section 2.3.2, spray atomisation quality depends on droplet primary and secondary break-up that in turn depends on the aerodynamic interactions between the air and fuel droplets. Due to higher velocities observed along the central regions of the spray, smaller droplet sizes are expected in these areas.

4.1.2 Experimental Conditions

SMD measurements were taken at a location of x = -10 mm; z = 60 mm, as displayed in Figure 4.6. Among main considerations regarding analysis of fuel additive effects was the timing of SMD measurement during a spray event. Fdida et al. [110] found significant temporal variation in SMD in their experiments and advised against averaging over total acquisition period as a result. The following analysis explains the temporal variation in SMD values with the chosen experimental set-up.

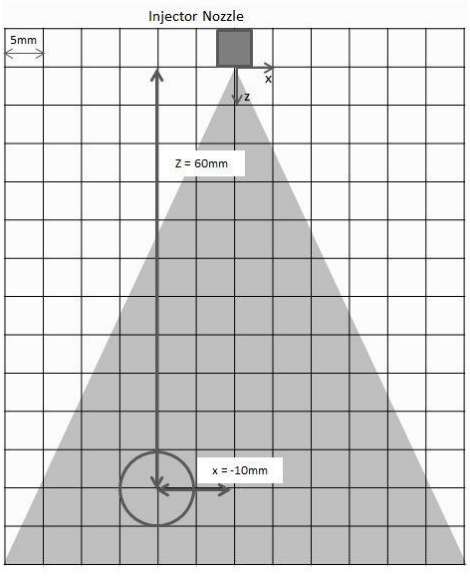

Figure 4.6: SMD measurement location

Figure 4.7 displays variation in droplet size and transmission with shadowgraph images for better understanding of fundamental processes during a spray event. In Figure 4.7, at t_1 there is no spray passing the laser beam and transmission is

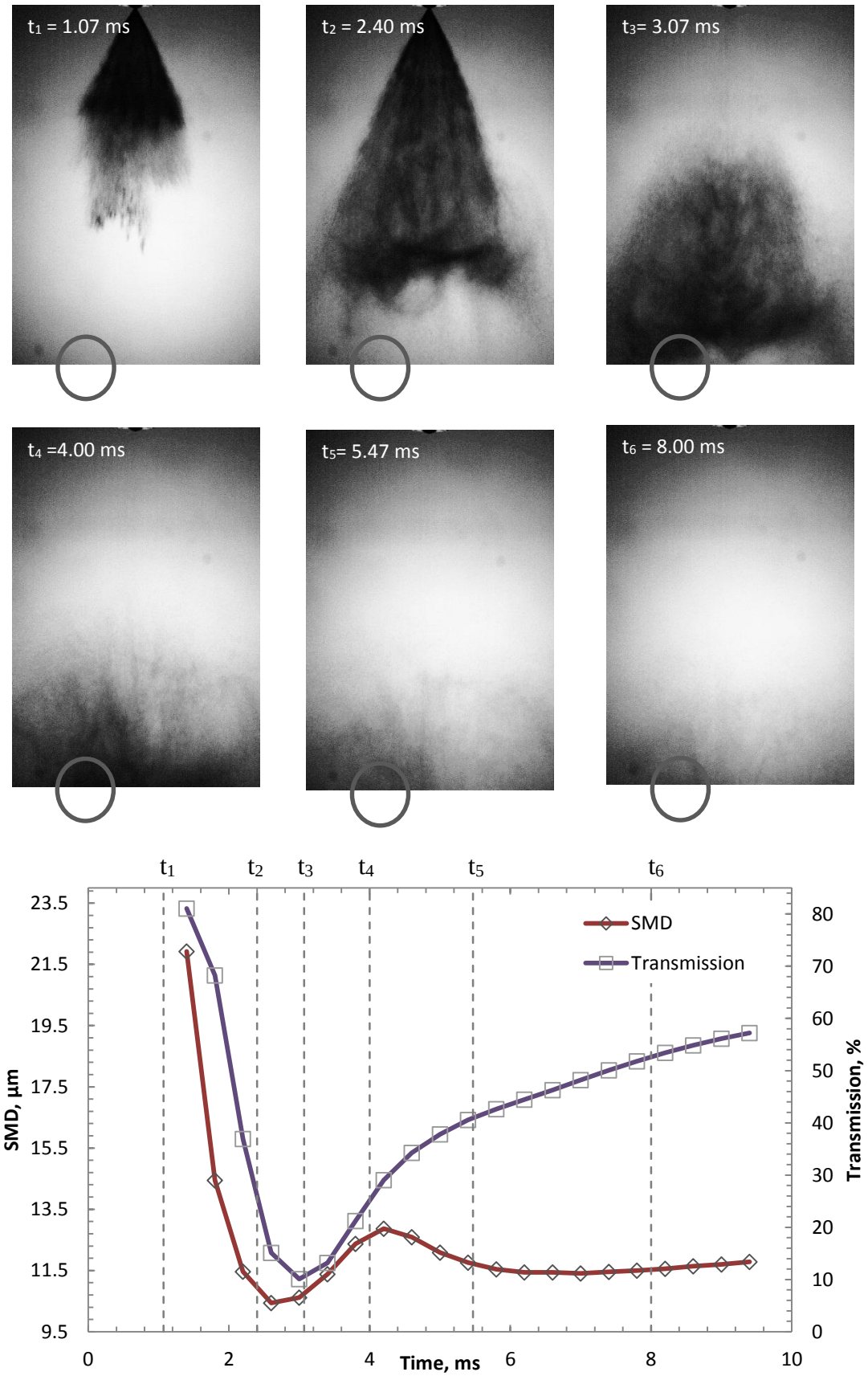

Figure 4.7: Relationship between transmission and droplet size with shadowgraph illustrations at x = -10 mm, z = 60 mm and injection pressure 50 bar

at 100 %. It can be seen from the image that the leading edge of the spray jet carries higher velocity than the rest of the spray. Lee and Park [229] noted similar phenomena and thought it to result from transient motion of the injector needle opening. At t_2 the large droplets have already passed the laser beam and a mist of small droplets is seen. These droplets originate from partial break-up of the early large droplets.

Smallest droplets in early stages of spray are seen just before t_3 when the maximum amount of fuel passes the laser. It is evident from the graph that droplet size starts to increase from this point to just after t_4 where it peaks. One of the causes for the increase in SMD is believed to be the dense fuel portions entraining less air which hinders fuel evaporation. Although current experimental work was carried out at ambient temperatures, the high volatility of gasoline means that significant evaporation of droplets can still take place [110, 230]. Furthermore, any air that is entrained would be increasingly affected by momentum exchange with fuel droplets, thus reducing relative velocities between air and fuel. Pribicevic and Sattelmayer [231] note that this results in diminished aerodynamic forces that would otherwise promote primary and secondary droplet break-up. A further cause for the increase in SMD is likely to be coalescence. This is a phenomena where, upon collision, two droplets merge into one. Coalescence is dependent on the We number and an impact parameter, B, that depends on droplet radius and separation distance of the colliding droplet centres. It can be seen from Appendix B that the We numbers experienced in this study varied between 26 – 47, which, dependent on parameter B, Qian and Law [232] have shown to be a region where possible coalescence occurs.

At time instants t_5 and t_6 it can be seen that fuel quantity decreases (corresponding to increasing transmission) and, at least initially, as a result of increased aerodynamic forces and improved evaporation characteristics, a decrease in SMD is experienced. Due to the slowing fuel spray and reduced aerodynamic effects, the SMD values remain relatively constant around t_6 as We number is reduced and the rates of secondary break-up and coalescence converge. Because of the number of conditions involved, it was deemed useful to compare the SMD results based on a single value for each injection pressure. However, as previously explained, temporal change in SMD occurs and it was agreed that finding a mean SMD for the total duration of the spray would not be representative of actual spray conditions.

Comparison of Figure 4.4 and Figure 4.5 revealed that at 50 bar and 110 bar injection pressures, fuel sprays went through same characteristic phases but occurred

at different time bases. Analysing further, Figures 4.2 and 4.3 showed that maximum fuel quantity for 50 bar injection pressure passed the laser 0.4 ms later than for the 110 bar case (2.6 ms vs 3.0 ms). This suggested that comparing SMD values on temporal basis at different pressure conditions would not produce comparable results, as different phases of the spray formation would be considered.

A better method, therefore, was thought to be comparing SMD values for a given transmission value. Most relevant SMD value was considered to when transmission was at its lowest, thus representing a time instant when maximum quantity of fuel per pressure passes the laser beam. A further point was selected where transmission was at 50 % towards the end of the spray. Although this instant marks a different stage in the spray formation for different pressures, it was thought it could provide information on the effects of fuel pressure on equal quantities of fuel. Due to the large distance from nozzle to the measuring location, the time of measurement for both chosen conditions occurred after the end of injection.

Figure 4.8 displays the change in minimum transmission levels as the injection pressure is increased. A transmission value 10.25 % can initially be seen which decreases to 4.21 % for 120 bar injection pressure. It is apparent that the decrease in transmission levels at higher pressures is smaller than that of lower injection pressures. This could be as a result of limitations in the injector fuel flow rate at pressures close to and above the rated 110 bar.

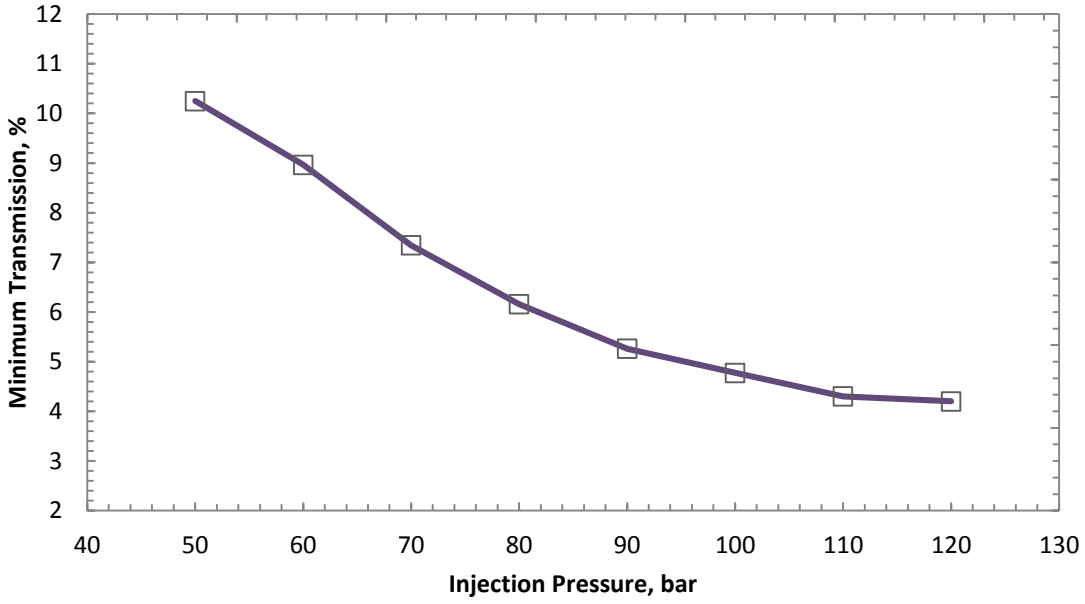

Figure 4.8: Change in minimum transmission levels with increasing injection pressure

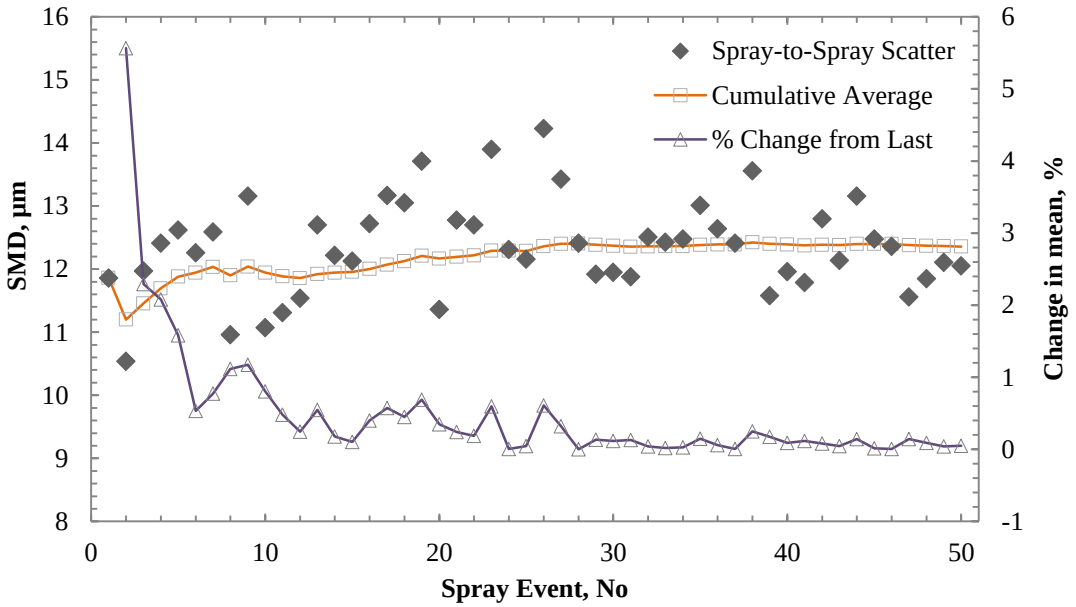

Figure 4.9: Droplet size shot-to-shot variation at 50 bar and minimum transmission

Figure 4.9 displays the analysis of shot-to-shot variation for 50bar injection pressure at minimum transmission. This helped set a suitable number of spray events to obtain a reliable and representative droplet size figure per given condition as well as quantify experimental repeatability. This analysis was only carried out at the extremes of 50 bar and 110 bar only. An overall standard deviation for 50 injections at 50 bar injection pressure was found to be 0.74 µm (SMD = 12.36 µm) and 0.69 µm (SMD = 7.01 µm) at 110 bar. A cumulative average was calculated along with % change for each subsequent point for 50 sprays. For both pressures % change after 30 injections was below 0.3 %. Because of some earlier results that showed a possibility of an outlier result occurring that could affect the overall average SMD, the total number of repeats per condition was increased to 50 sprays.

4.1.3 Base Gasoline Fuel Characteristics

Figures 4.10 and 4.11 display the SMD averages for base fuel at minimum and 50 % transmission, respectively. At both transmission levels the droplet sizes were found to behave in a very similar manner.

It was found that increasing injection pressure from 50-110 bar at minimum transmission reduced the droplet size by 39.1 % and 37.3 % at 50 % transmission. The experimental repeatability had largest standard deviation at 50 bar and 50 % transmission case of 0.64 µm. Smallest occurred at 110 bar and minimum transmission

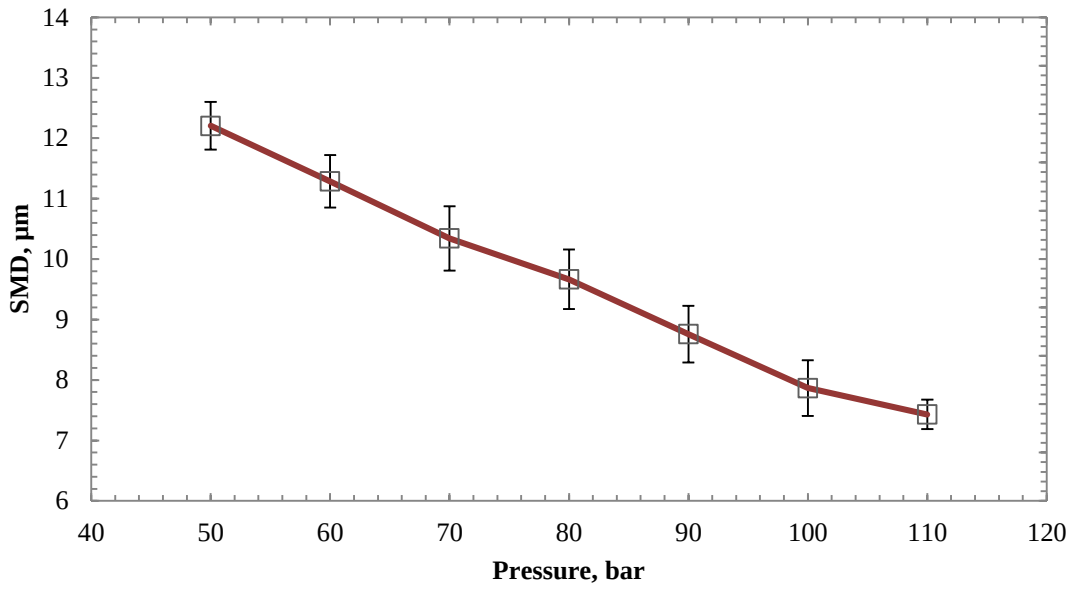

Figure 4.10: Overall average base fuel droplet size at minimum transmission point with test-to-test standard deviation to represent repeatability of the system shown for each pressure point

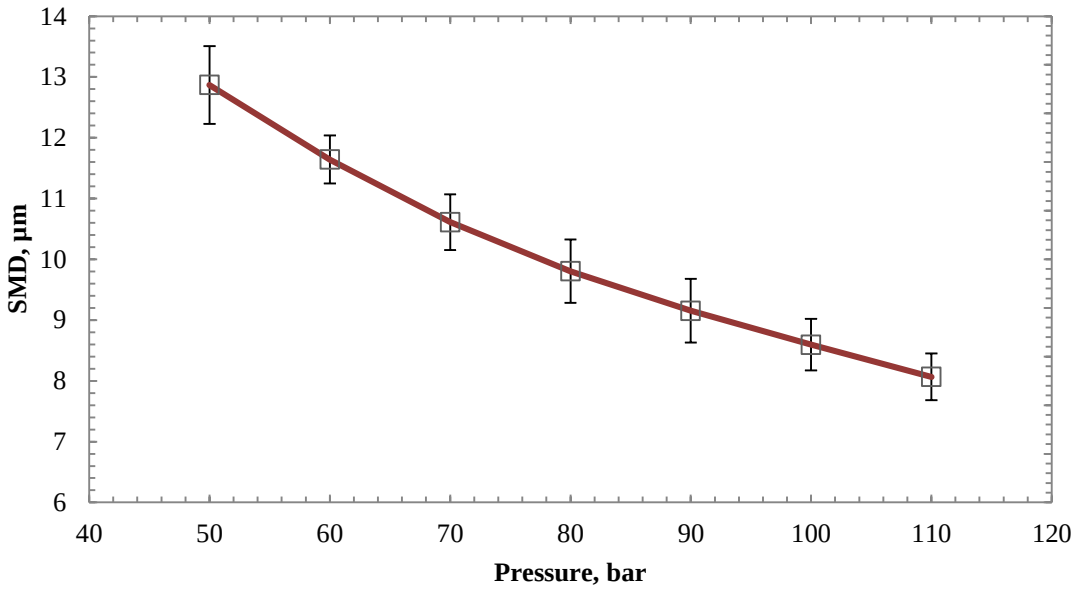

Figure 4.11: Overall average base fuel droplet size at 50% transmission point with test-to-test standard deviation to represent repeatability of the system displayed for each pressure condition

of 0.24 µm. For the purpose of comparison of behaviour of fuels with additives, it was assumed that any changes measured that lie within or very close to the repeatability limits were considered not to be significant. It should be noted, however, that test-to-test, the measured base fuel SMD values could vary over 20% as can be seen in Figure 4.12 and Figure 4.13.

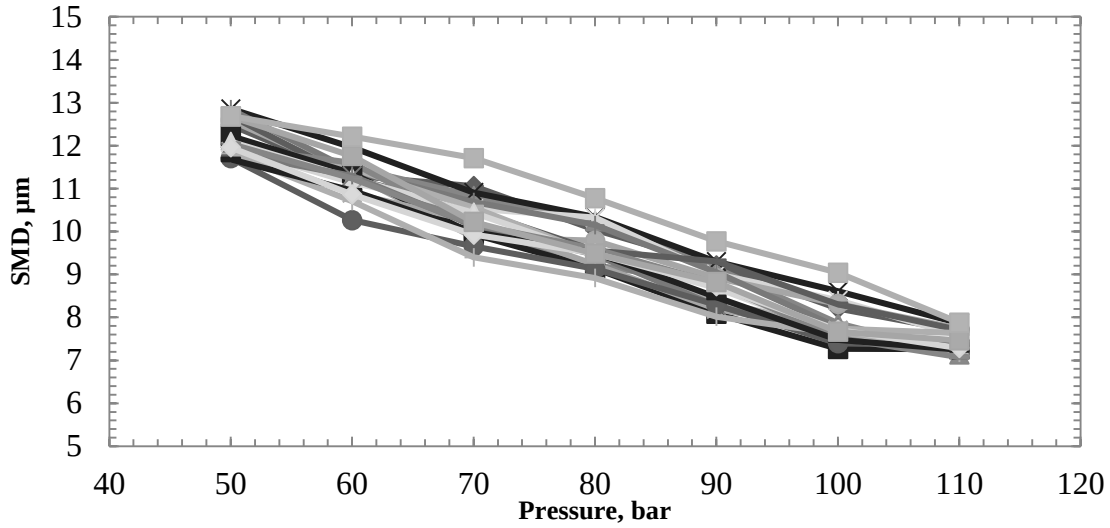

Figure 4.12: Measured SMD values for all base fuels at minimum transmission

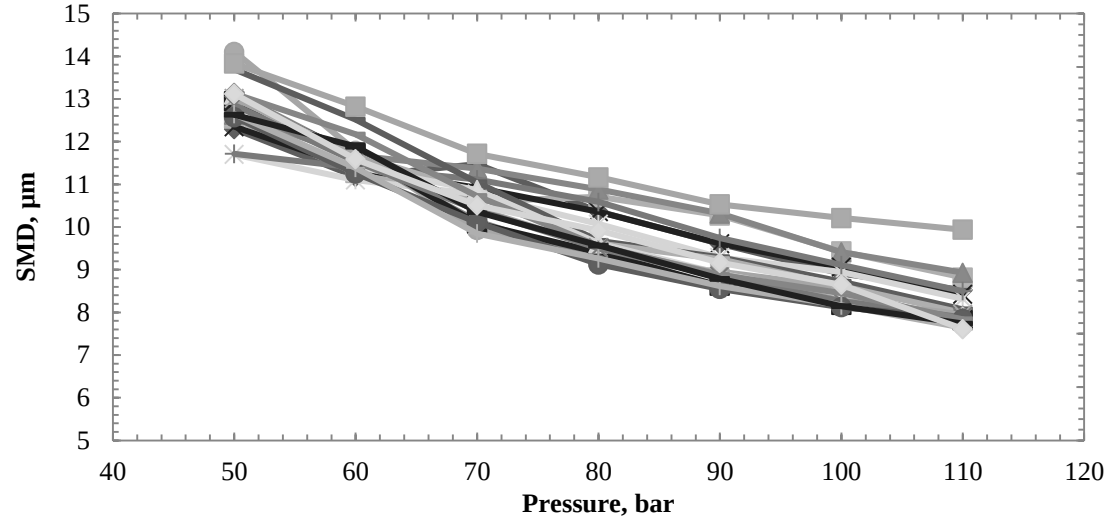

Figure 4.13: Measured SMD values for all base fuels at 50% transmission

SMD for the 50 % transmission level is at all times larger than that of at minimum. However, as demonstrated by Figure 4.14, the droplet sizes are further most apart at the low and high end of the pressure range and smallest in the middle at 80 bar. This could be explained by the trigger settings used for laser diffraction system data acquisition. It was clear form Section 4.1.2 that the required transmission levels at different pressures were reached at different time instants. The delay of reaching minimum transmission at 50 bar compared to 110 bar was 0.4 ms which corresponds to the laser diffraction system data acquisition rate. However, the same trigger timing between injection and laser diffraction system activation was employed throughout all pressure conditions. It can also be seen that this effect is more prominent at minimum

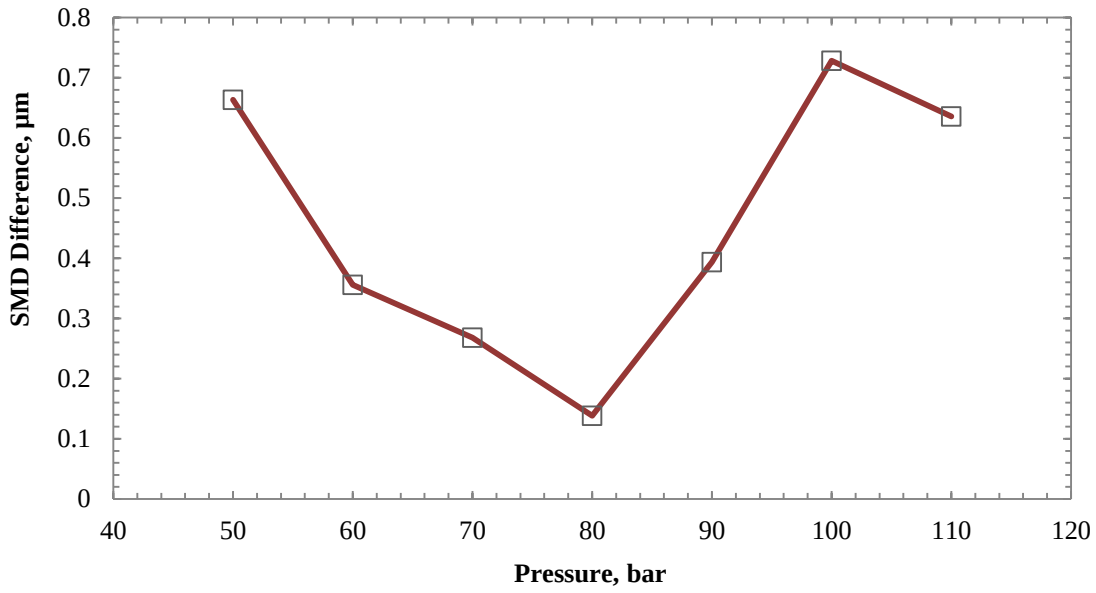

Figure 4.14: Droplet size difference between minimum and 50 % transmission levels

transmission. This could be explained by the more transient events occurring at much higher droplet velocities during the earlier stages of a spray event where aerodynamic forces are higher and the resulting droplet primary and secondary break up processes take place. 50 % transmission was reached up to 8 ms after SOI for 50 bar injection pressure and the measurements were taken on the trailing edge of the spray. It is worth mentioning, however, that this cyclic variation was, based on standard deviations for all pressure conditions, within or very close to the experimental repeatability limits and as such no additional benefit was thought to result from adjusting laser system timing to sprays any further. Furthermore, for future presentation of results, it was decided that unless specifically stated, SMD at 50 % transmission was not further considered and SMD only at the minimum transmission level was analysed.

Comparison of the base fuel characteristics against empirically established relationships discussed in Section 2.3 is presented in Figure 4.15. Since all empirical relationships are profoundly dependent upon experimental set up, data is normalised against the maximum droplet size value in each set to enable direct comparison of pressure effect on droplet size.

Very good agreement is seen between the results that of Knight and Elkotb [142] and the current study while Hiroyasu and Kodota [143] found pressure dependence to be of lesser effect. It is worth mentioning that when comparing the actual calculated values, Hiroyasu and Kodota's [143] were in fact the closest to

current study while Elkotb's [142] equation produced droplets over three times the size. This is displayed in Figure 4.16.

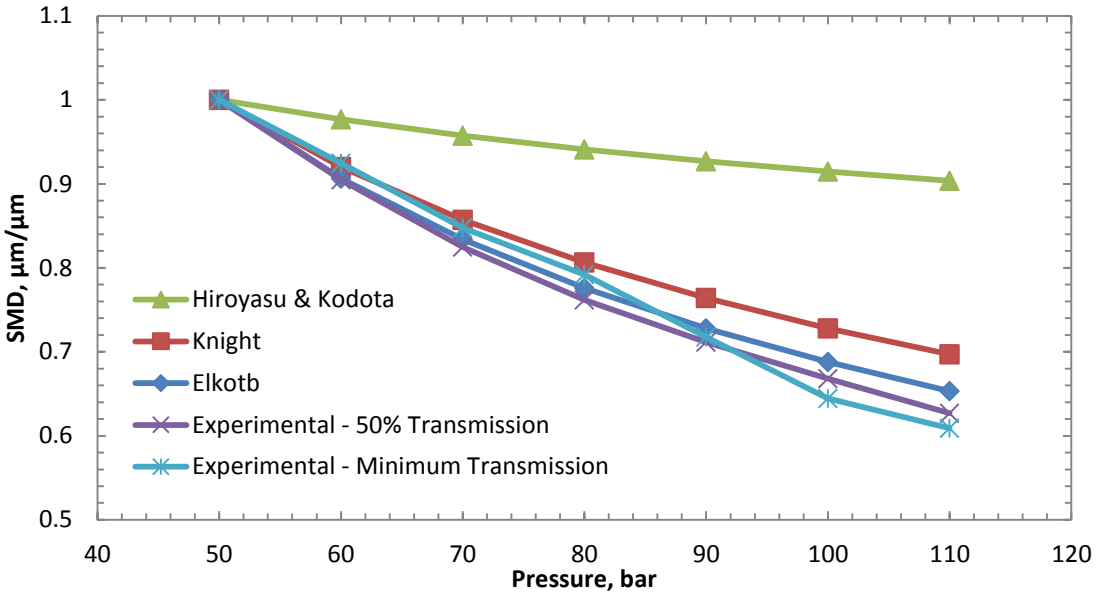

Figure 4.15: Comparison of experimental base fuel droplet size and empirically established relationships. All data normalised to maximum droplet size in each data set

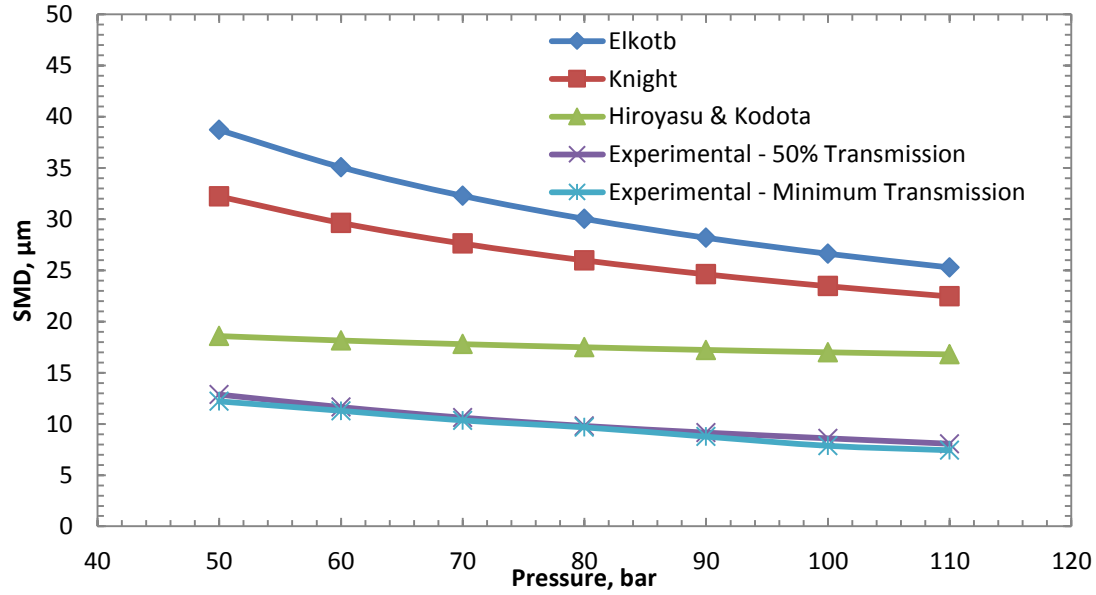

Figure 4.16: Comparison of experimental base fuel droplet size and empirically established relationships. Actual values of each data set displayed

4.2 Combustion Investigations

Combustion investigations were carried out using the equipment described in Chapter 3. Three methods for combustion analysis were employed. The combustion vessel was used for GDI spray and gasoline vapour combustion while the single

cylinder research engine was used to examine the additive effects under engine conditions. Throughout the following sections, the base fuel characteristics are explained and methodology for the following analysis described. All pressures in this chapter and Chapter 6 (analysis of effects of fuel additives on combustion) are expressed in terms of gauge pressure, unless explicitly specified.

4.2.1 Spray Combustion

Initial combustion investigations were carried out using the DI fuel delivery system. Fuel was pressurised to the rated 110 bar and air in bomb raised to 5 bar. This configuration allowed for numerous combustion events to be carried out under closed vessel conditions without the diminishing oxygen levels having an effect subsequent combustions. Also, as described by Ghasemi et al. [233], increased back pressure results in an increased ambient density and leads to a wider spray cone angle. As a result of a wider cone angle, more of the quiescent air is entrained by the spray jet and lower localised equivalence ratio is achieved. In the current study, this improvement was observed through a reduced number of misfires.

Typical pressure and heat release rate traces under ambient temperature conditions can be seen in Figure 4.17 and high speed imaging for a similar event in Figure 4.18. The pressure displayed was above the vessel starting pressure of 5 bar. A peak pressure of just below 0.04 bar was observed. This amounts to less than 1 % of what is experienced in a gasoline engine. Furthermore, over 20 combustion events, a standard deviation in peak pressure of more than 15 % and over 30 % in peak heat release rate was experienced. This is likely to be caused by the spray and spark variability. Peak heat release rate was experienced at around 35 ms after start of ignition signal and total combustion duration was approximately 90 ms. This is significantly longer compared to engine conditions where peak heat release can be reached in 2-3 ms and total duration remains below 10 ms [234, 235]. This was likely caused by the dense fuel spray not enabling close to stoichiometric air-fuel ratios in the central areas of the spray, thus, affecting combustion characteristics. Furthermore, the low energy state of the combustion environment would have had an effect as well as seen in previous sections, fuel spray delivery from the injector nozzle to the combustion region could have hindered the processes.

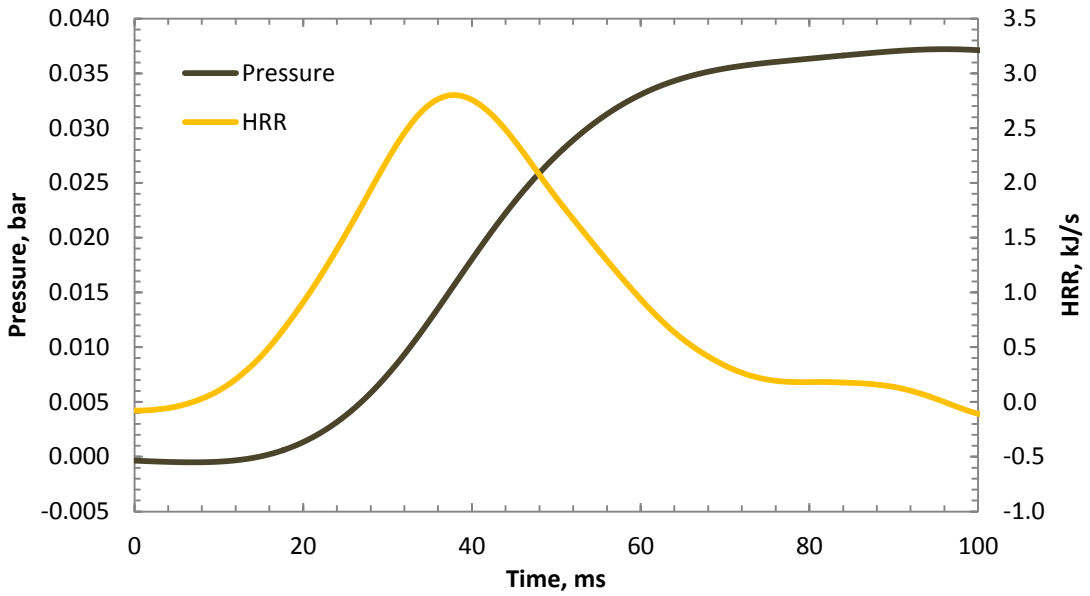

Figure 4.17: Heat release and pressure rise traces for spray combustion under ambient temperature and 5 bar (gauge) air pressure conditions

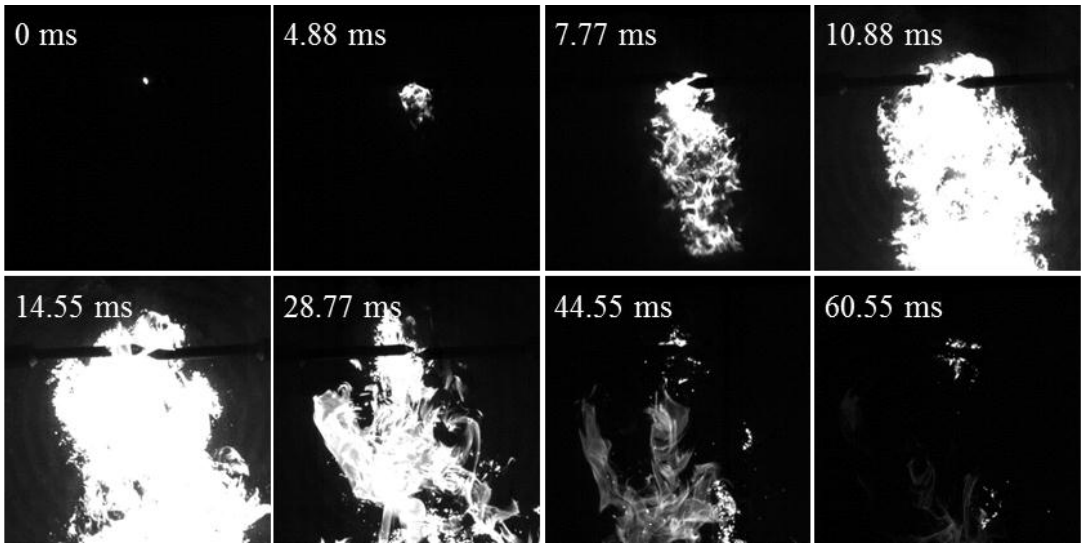

Figure 4.18: Gasoline spray combustion under ambient temperature and 5 bar (gauge) air pressure. Images taken at 9,000 fps with Nikon 60 mm f/1.8 lens

Although successful combustion could be reached at low temperatures, high soot content and low experimental repeatability was seen. As such, further studies under heated air and pre-combustion environments were conducted. Figure 4.19 displays a spray combustion using the pre-combustion method described in Chapter 3 with hydrogen as the fuel. Hydrogen pre-combustion prior to the spray caused the spray combustion duration to decrease by around 10-15 ms although peak pressure change due to the combustion event remained below 0.1 bar. Spray combustion with

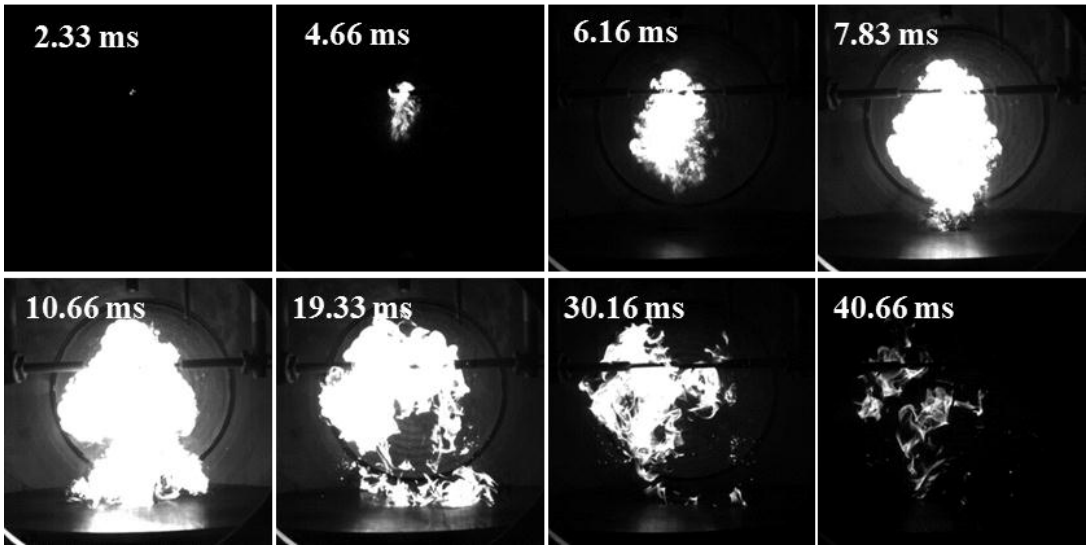

Figure 4.19: Gasoline spray combustion using hydrogen pre-combustion (hydrogen-air mixture φ = 0.3) (Not same as Figure 4.17) Images taken at 6,000 fps with Nikon 50 mm f/1.2 lens

heated air produced similar results. As previously mentioned, the full range of the pressure transducers used in the study was 0-100 bar and 0-250 bar raising concerns over the accuracy of readings at such low pressure change levels. Although the dynamic sensor could support low pressure changes, the second 0-100 bar transducer could only offer accuracies of 0.25 % or 0.25 bar which was up to 5 times higher than the measured pressure rise as a result of a combustion event.

4.2.2 Gasoline Vapour Combustion

In order to reach significant pressure rises and reduce experimental variability, gasoline vapour combustion investigation was performed in the combustion vessel. A fully pre-mixed gaseous mixture was prepared and in addition to pressure, heat release and emissions analysis, flame propagation speed was computed from direct high speed imaging. In current study the spherically expanding flame was analysed in terms of turbulent flame speed. According to Ferguson and Kirkpatrick [236] the relationship between the laminar and turbulent flame speed can be expressed as:

$$\frac{S_t}{S_l} = a \left(\frac{U_t}{S_l}\right)^b \qquad 4.1$$

where S_t is the turbulent flame speed, S_l the laminar flame speed, U_t turbulent intensity and a & b are constant that depend on the geometry and specific conditions in the combustion chamber. The difference between the laminar and turbulent burning velocities can be 3-30 times [236]. Although laminar flame speed could be derived from the measurements, it was considered not to offer additional benefits as comparative fuel properties were under investigation and not each fuel separately.

Flame images were used to calculate the cross sectional area and the circumference of the propagating flame and on the assumption that the flame propagates spherically, radius increase per time step could be found. All raw images were background corrected and the threshold used for flame front detection was set based on the intensity of the specific combustion event. Electrode size was used for calibrating the pixels/mm value.

A sample of the image processing and time series of a combustion event can be seen in Figure 4.20. Figure 4.21 displays the radius change in time based on the two methods described. It can be seen that the circumference based measurement method produced calculated radius values twice as large as the area based method. This was likely to have been caused by difficulties in flame edge detection. It was especially prominent feature at the beginning of the combustion event and at time instants after 35-40 ms, where high spark and flame intensities, respectively, caused misinterpretation of images due to limitations of the threshold values used. Furthermore, a much steadier change in radius was found with area based calculations.

As such, it was decided that only the area based calculation of flame speed would be used, where the typical averaging time period was between 15-35 ms. Figure 4.22 displays typical pressure and heat release rate traces for gasoline vapour combustion. It can be observed that the peak pressure reached was two orders of magnitude larger than that for spray combustion. Additionally, repeatability in peak pressure and heat release rate over five combustions was found to be less than 2% which was thought to be low enough for the current investigations. Furthermore, using a Lambda sensor, exhaust gas analysis showed that around 1.3% error in pre-combustion gas mixture composition was experienced over the same number of combustion events.

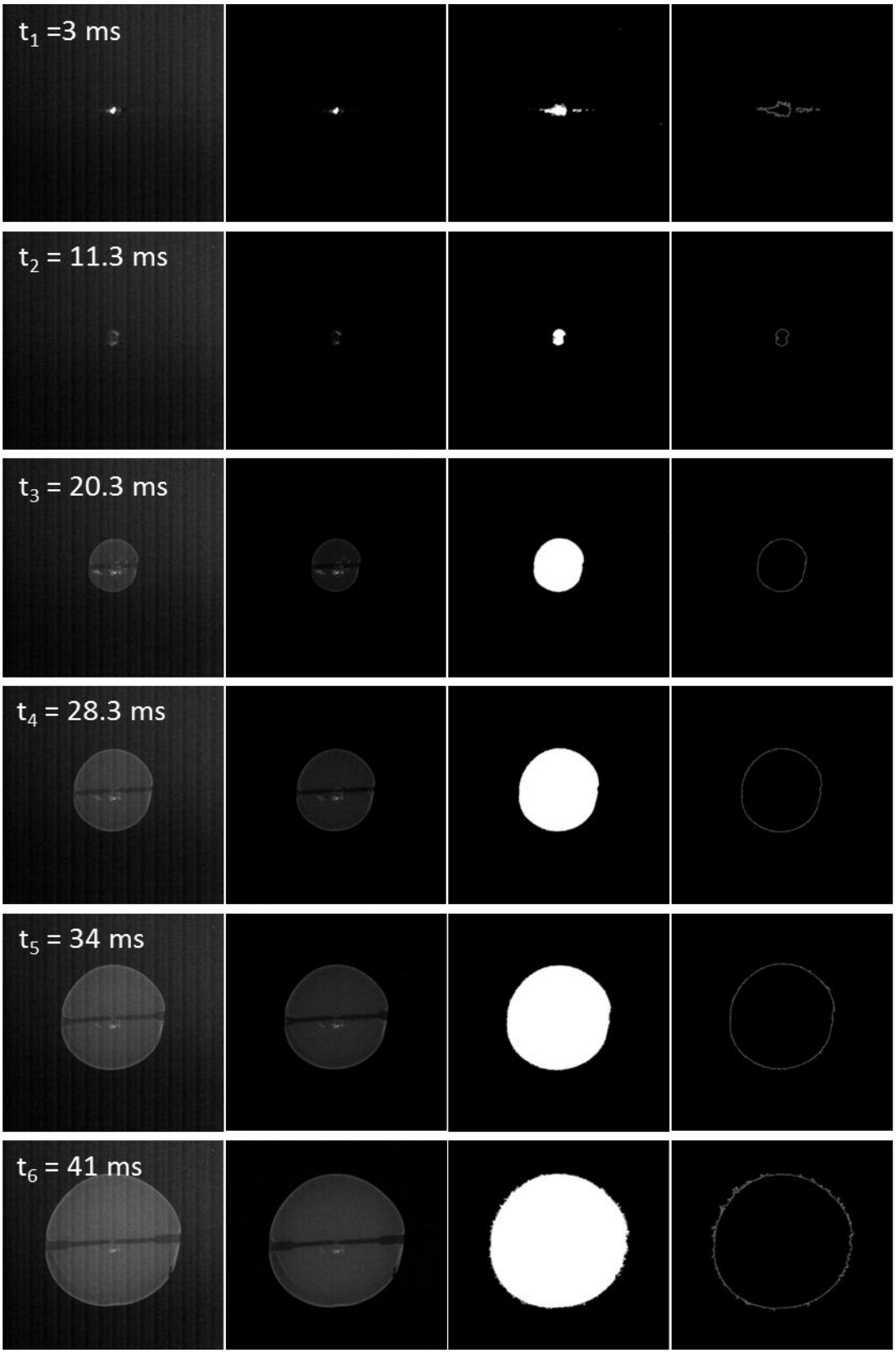

Figure 4.20: Time series of sample gasoline vapour combustion with initial pressure of 0.7 bar. Left to right, image processing procedure: raw image; background corrected image; binarised image for area based radius calculation; binarised image for circumference based radius calculation

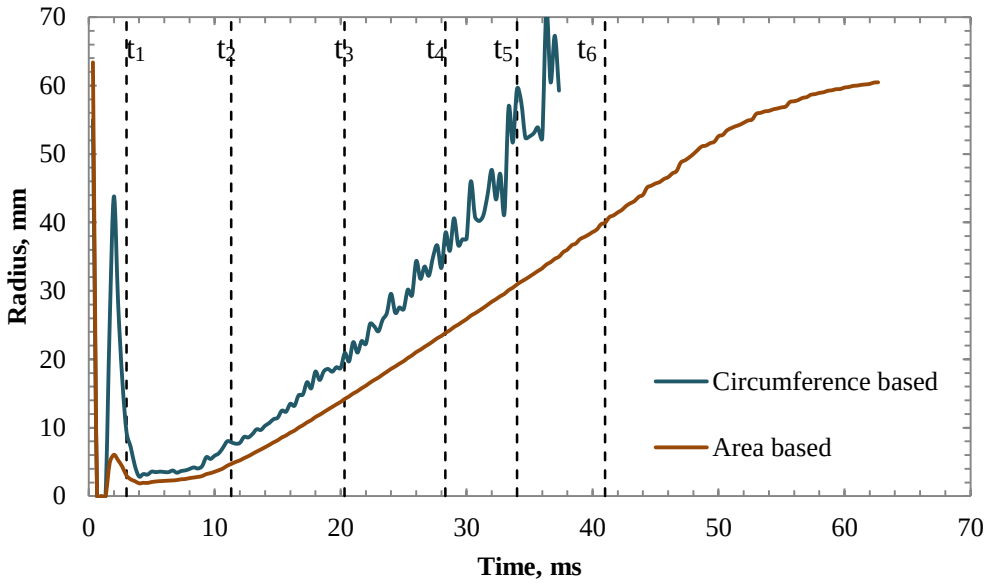

Figure 4.21: Radius change in time for area and circumference based calculation methods. Time points t_{1-6} correspond to those shown in Figure 4.20

Initial base fuel characterisation was carried out under ambient initial pressure conditions. Although this was suitable for pressure/heat release rate and flame propagation speed analysis, it was found that emissions analysis suffered due to the output from mainly the oxygen sensor being flow dependent. It can be observed from Figure 4.22 that after a combustion event the pressure dropped very quickly to pre combustion levels. This meant that without opening air inlet to the combustion vessel,

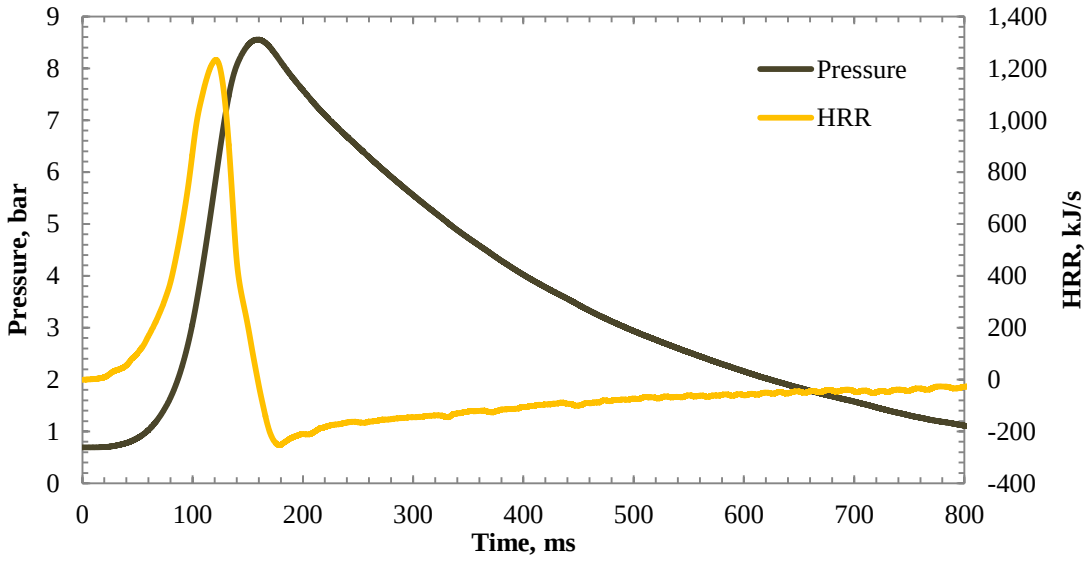

Figure 4.22: Sample pressure and heat release rate traces for gasoline vapour combustion in combustion vessel at raised initial pressure and φ = 0.8

vacuum pressures were generated by the analyser which affected the readings. Furthermore, allowing for extra air to be pulled into the vessel (to avoid vacuum pressures) diluted the exhaust gases quickly, and no stable readings could be recorded.

Therefore, initial pressure was raised to 0.7 bar which was found to be sufficient to allow for up to a 60 second period during which stable readings could be logged. Characteristic emissions recordings for raised initial pressure conditions can be seen in Figure 4.23.

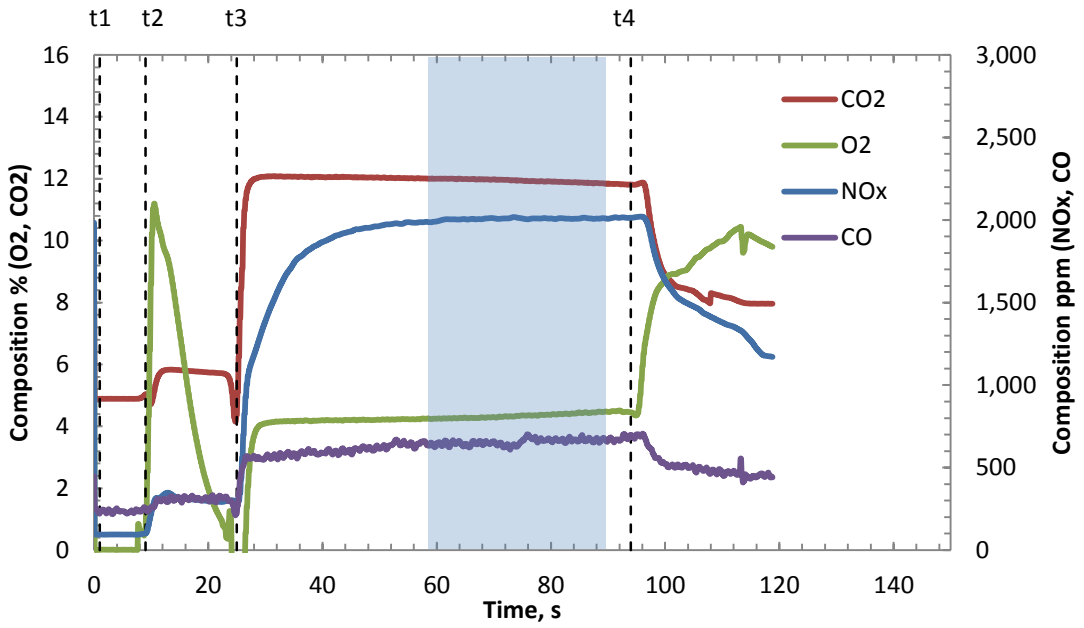

Figure 4.23: Emissions readings from combustion vessel. At t_1 data logging commences, at t_2 the gas analyser sampling is activated and vacuum pressure is generated in gas supply line, at t_3 the exhaust gases are released from the vessel and at t_4 air inlet to the combustion vessel is opened to avoid vacuum pressures occurring. Typical area used for averaging is displayed by the shaded area

Figure 4.24 displays the peak pressures for different equivalence ratios at atmospheric and raised initial pressure conditions. For both cases, the ignitability limits were found to be from around $\varphi = 0.8$ to $\varphi = 1.8$ and peak pressure occurred at around $\varphi = 1.5$ after which a sharp decrease in the pressure was observed. Due to soot production at higher than stoichiometric equivalence ratios, additive comparison tests were carried out under lean conditions. Any soot produced would give rise to errors in emissions analysis of subsequent combustion events, where burning of soot from the vessel walls could increase CO and CO_2 readings. Moreover, this could affect

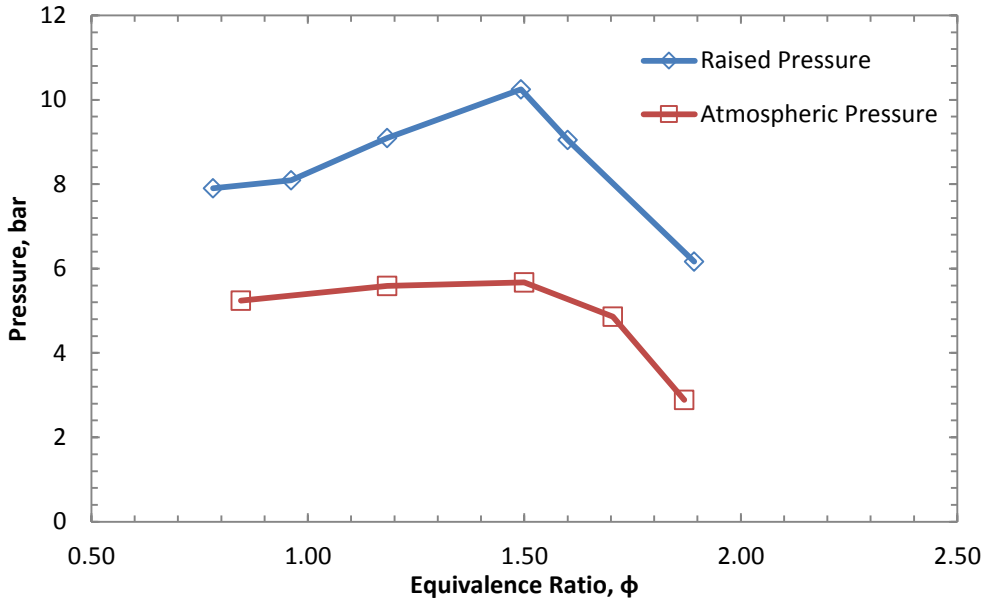

Figure 4.24: Peak pressures for atmospheric and raised initial pressure conditions at different equivalence ratios

pressure readings and constant depositing of soot on the vessel windows would mean significant timescales needed to clean the vessel. As such, tests were carried out at leanest possible condition which for raised initial pressure conditions meant 3 ml of gasoline fuel per vessel filling, giving an equivalence ratio of 0.79.

4.2.3 Engine Testing

The final stage of the research included testing the CI additives under engine conditions using the Ricardo E6 single cylinder research engine. The conditions used during testing have been summarised in Table 4.1. Figure 4.25 displays pressure and heat release rate characteristics at the aforementioned criteria. In Figure 4.26 peak pressure, peak heat release rate, knock intensity and IMEP at different spark advance angles can be seen. It can be observed that with increasing spark advance, higher peak

Fuel Delivery System	*Carburettor*
Engine Speed	*1,200 rpm*
Compression Ratio	*9:1*
λ	*1*
Engine Load	*30%*
No of cycles for Data Acquisition	*300*

Table 4.1: Engine testing conditions

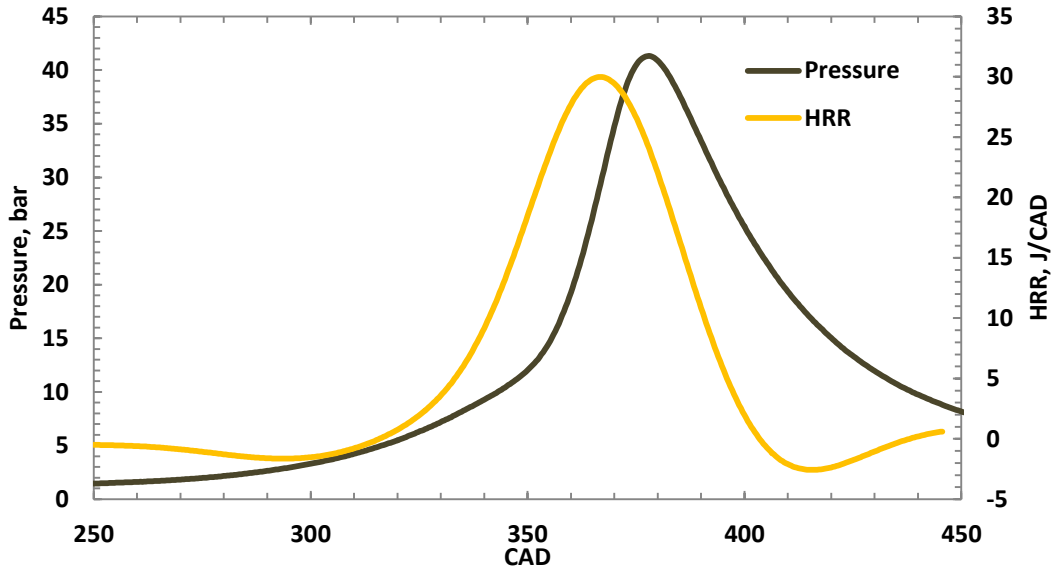

Figure 4.25: Sample pressure and heat release traces, averaged over 300 cycles at spark timing of 40° BTDC

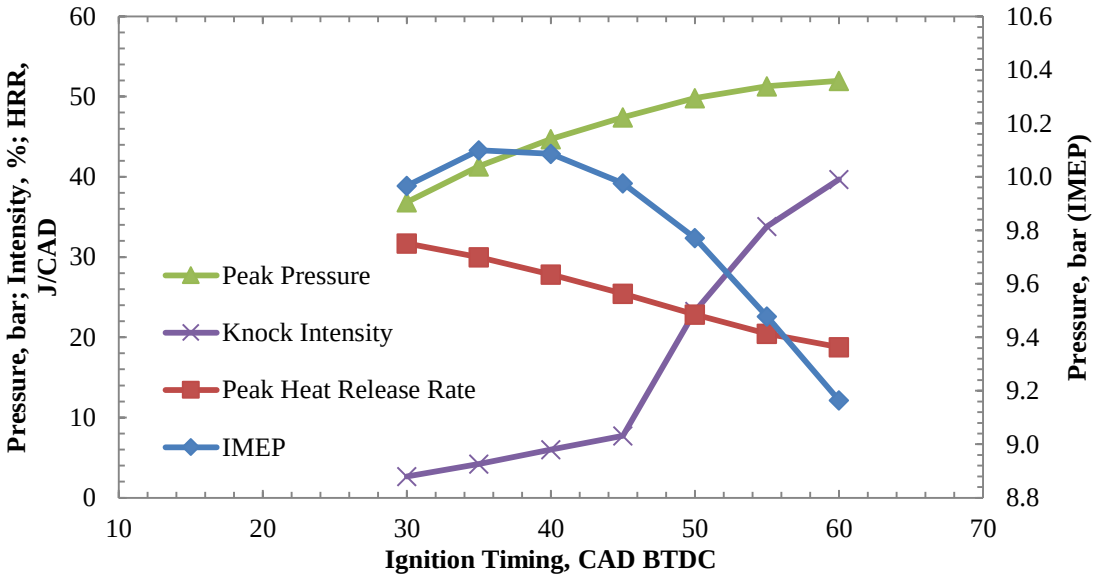

Figure 4.26: Peak pressure, knock intensity peak heat release rate and IMEP characteristics for base fuel with different spark timing

pressures were reached while the peak heat release rate decreased. This was due to the time instant when the combustion event occurred. As spark was advanced, more of the combustion occurred in the compression stroke. This meant that higher pressures were reached within the cylinder. Similarly, the heat release rate decreased with advancing the spark timing. Heat release rate is dependent upon the conditions within the cylinder and by advancing the timing of spark lower pressures and subsequently lower temperatures were experienced at the time of spark [29, 194]. IMEP could be seen to

initially increase and then decrease as the spark was advanced. It is evident that the optimal spark timing occurred at 35 CAD BTDC. Although advancing spark further resulted in higher measured peak cylinder pressures, Ji et al. [237] describe that the negative work on the piston reducing the IMEP values. Similarly, retarding the spark results in a retarded peak pressure occurrence and less work can be transferred to the piston.

The spark timing additionally affected the knock intensity readings. The intensity was defined as the percentage of cycles where knocking occurs. As the spark was advanced and higher pressures were experienced in the cylinder, more of the cycles went through rapid pressure rise that caused the end gases to auto-ignite.

4.3 Conclusion

This chapter aimed to describe in detail the characteristics of base gasoline fuel under various fuel injection and combustion strategies and also introduce the conditions under which fuel additive study would be undertaken.

Fuel spray atomisation characteristics were investigated through laser diffraction technique at ambient pressure and temperature conditions. A fuel quantity based method was developed to analyse possible SMD changes caused by additives under varying injection pressures between 50 – 110 bar. The results of the additive analysis and a selection of pure component fuels are presented in Chapter 5.

Three combustion strategies were investigated for suitability to analyse effect of additives. These included gasoline spray and vapour combustion in the combustion vessel and engine testing in a single cylinder research engine. It was found that spray combustion in the CVCV could not produce the repeatability levels needed to confidently compare additive effects. Therefore, a method based on homogeneous mixture of air and gasoline vapour combustion in the vessel under lean conditions was developed. Test conditions were determined as 3 ml of fuel per vessel filling with an initial charge pressure of 0.7 bar before ignition. Finally, tests under engine conditions were carried out. Conditions for the engine testing were summarised in Table 4.1. The results of the analysis with additives are presented in Chapter 6.

Chapter 5

Droplet Sizing with Additives and Alternative Fuels

Chapter 5 describes the results from an investigation into the fundamental effects of fuel additives on GDI spray formation. In Section 5.2, analysis of four single component fuels and a base diesel fuel is additionally presented to enable better understanding of the effects that fuel additives exhibited on base gasoline. The equipment and methods used in the experimental and data analysis are identical to those described in Chapters 3 and 4. In Section 5.3, surface tension and viscosity measurement analysis and discussion is presented.

5.1 Gasoline Spray Investigations with Additives

The need for better efficiencies and ever increasing government regulation on fuels and emissions has made use of fuel additives the norm in modern engines. Although often overall benefits are known to result from the use of additives, the mechanisms at work are often not understood. This is especially true for recent utilisation of DI fuel systems in gasoline engines. The first part of the current study on fuel additive effects was to determine the extent to which fuel additives affect the

physical properties of fuels through analysis of fuel sprays under various conditions. The following sections will present the findings of the investigations.

5.1.1 Experimental Additives

Fuel additives used in the current study are mostly in commercial use. The categories are as described in Section 2.1: deposit control additives, friction modifiers, combustion improvers, drag reducing agents, anti-static additives and carrier fluids. Additives are added to base fuel in quantities of parts per million. In current study this is equivalent to adding a milligram of additive per litre of fuel. Base gasoline fuel used in the study corresponds to European Standards EN228.

Table 5.1 displays the additives and the labelling system used for experimental work. Due to their proprietary nature, it is not possible to disclose the exact

Additive Group	Additive	Treat Rate (1X), mg/L
Anti-Static Additive	AS-A	2
Carrier Fluid	C-B	100
Combustion Improvers	CI-E	250
	CI-F	250
	CI-H	250
	CI-I	1000
Deposit Control Additives	DCA-A	100
	DCA-B	100
	DCA-C	100
	DCA-G	100
	DCA-M	100
	DCA-N	100
Drag Reducing Agents	DRA	30
	DRB	30
Friction Modifiers	FM-A	100
	FM-N	100
	FM-O	100
Viscosity Modifier	Lauric diethanolamide	1000

Table 5.1: Additives and treat rates as used in droplet sizing experiments

composition of the additives. However, it is known that all additives were of ashless type, meaning no metals were present in the chemical composition and that friction modifier FM-O was a chemically reactive acidic compound while FM-A and FM-N worked on the physical absorption principle. Combustion improver CI-I is known to be an organic anti-knock compound.

The additive composition in fuel mixture is called the treat rate. In present study, the fuels were treated with commercially employed quantities of additive (1X) and at ten times the amount (10X). It can be seen that the treat rates for the anti-static additive and drag reducing agents are low compared to other type of additives. Highest treat rates used were for combustion improvers. All experimental work on additives included a base fuel comparison to additive bearing fuel at 1X and 10X treat rates.

5.1.2 Experimental Protocol

Experiments were carried out on base gasoline fuel without an additive which was compared against an additive bearing base fuel with a selection of additives. Experimental protocol followed for the additive tests was the same as described in Section 4.1. SMD measurements were taken at instants of minimum and 50 % transmission (end of spray) values for injection pressures of 50-110 bar in 10 bar intervals. 50 repeat injections were carried out per condition.

Base fuel tests were carried out between each additive. This allowed for detection of any drift in SMD values that could occur but also enabled calculation of overall test-to-test variation. Base test after an additive was used as the base before the next additive. Overall, nineteen base tests were carried out, the standard deviation of which was used to represent repeatability of the measurements. Any additive results that lied outside the standard deviation were considered to be significant.

Each new fuel was injected into the combustion chamber for at least 50 times to clear the injector nozzle of any residue from precious fuels, should there still be any present. Cleaning of the whole fuel system was carried out between each fuel/additive in an ultrasonic bath.

5.1.3 Effect of Additives on Base Gasoline Fuel

Fuel additive effects were initially tested through droplet sizing methods. All additive measurements were preceded by base fuel tests, after which the base fuel with

the additive at the recommended treat rate and then ten times the treat rate was tested. Base fuel data obtained between all additive experiments was used for estimating experimental repeatability and additive measurements were compared against its standard deviation (displayed as dashed lines in this section).

The largest experienced change to SMD from additives was seen for drag reducing agent DRA. SMD results for minimum transmissions have been displayed in Figure 5.1. It can be seen that although the changes are very small in relation to the base fuel, DRA at 10X seems to suggest an increase in droplet size. Similar change in SMD could be seen for the 50 % transmission case.

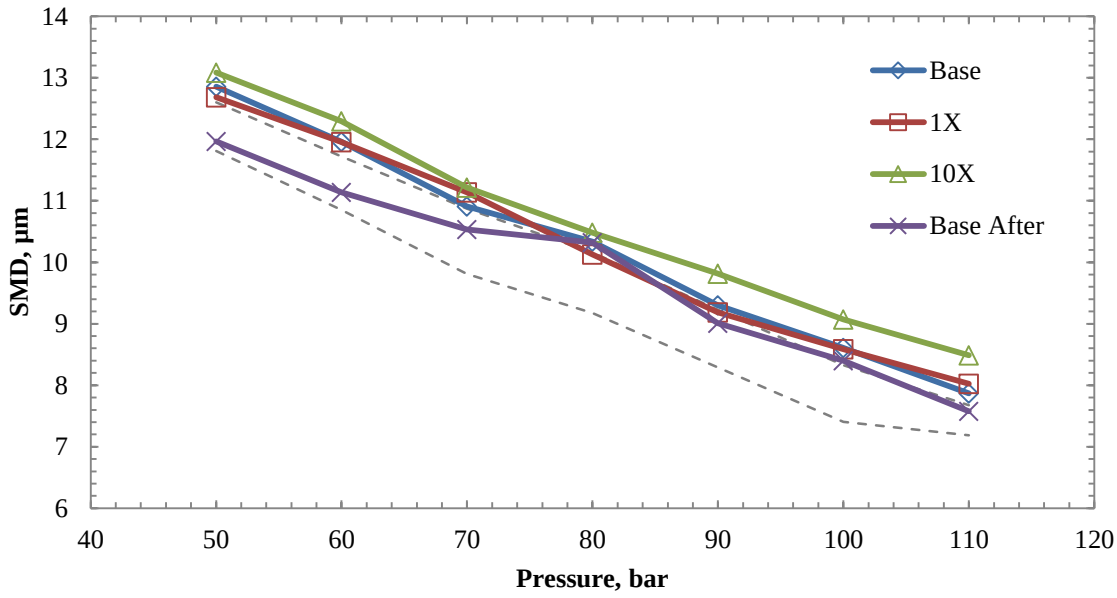

Figure 5.1: SMD for gasoline with DRA additive at minimum transmission

Same behaviour could not be fully seen for DRB additive as displayed in Figure 5.2. As discussed in Section 2.1.4, drag reducing agents can break down under turbulent conditions. It is shown in Appendix B that Reynolds numbers of up to 23,000 were experienced in present investigations, suggesting very high levels of turbulence that is thought to cause the breakdown of agglomerates of the drag reducing agents. This might suggest that the DRA agglomerates are larger or more shear resistant than those of DRB.

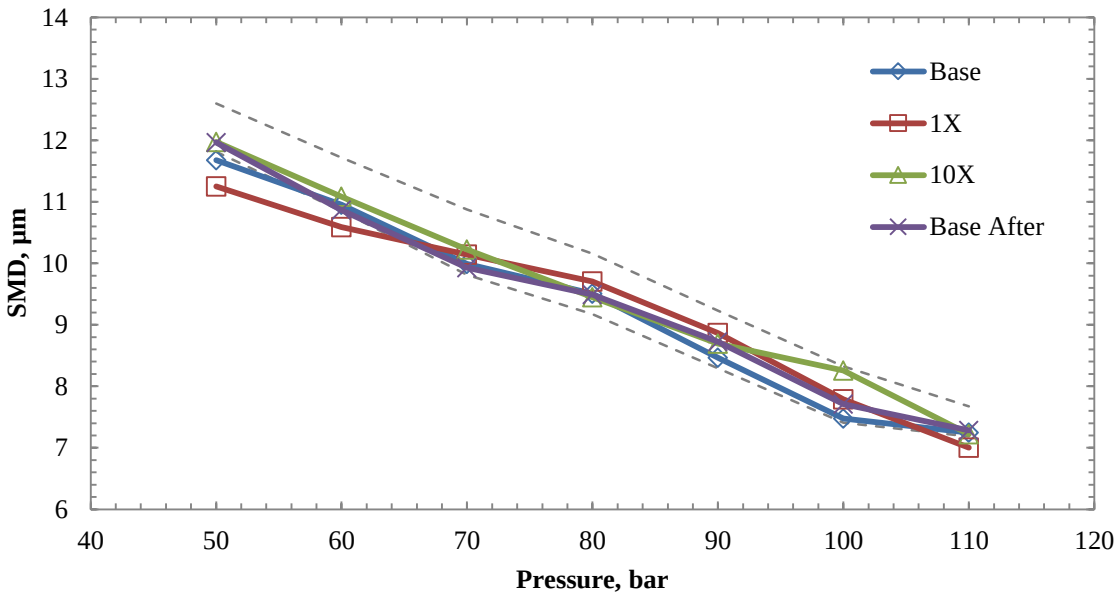

Figure 5.2: SMD for gasoline with DRB additive at minimum transmission

A non-fuel additive lauric diethanolamide, a commercially available viscosity modifier, was further investigated for possible effects on droplet size. It was hoped that the additive would be more shear resistant than the drag reducing agents and changes in SMD measurements would be noted. The results are displayed in Figure 5.3. Treat rate was taken as the maximum used in test fuels (CI-I). At the tested 1,000 ppm treat rate no change to droplet size was noted. It can be noted, however, that

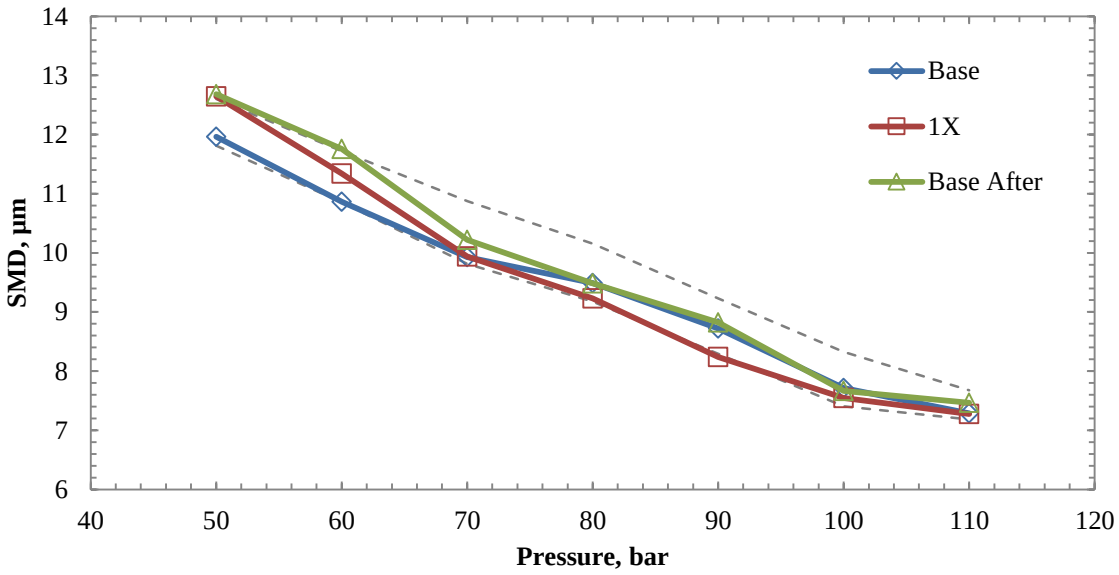

Figure 5.3: SMD for gasoline with 1,000 ppm lauric diethanolamide at minimum transmission

industrially, lauric diethanolamide treat rates of more than two orders of magnitude higher are employed [238, 239] but due to reduced proximity to fuel additive quantities employed commercially, no further study was carried out.

In general, the pressure effects from the high pressure injection system seemed to overpower any additive effects that might have been present. Representative SMD results of gasoline sprays with additives from different functional groups can be seen in Figures 5.4 – 5.8. It should be added that for typical PFI fuel metering systems,

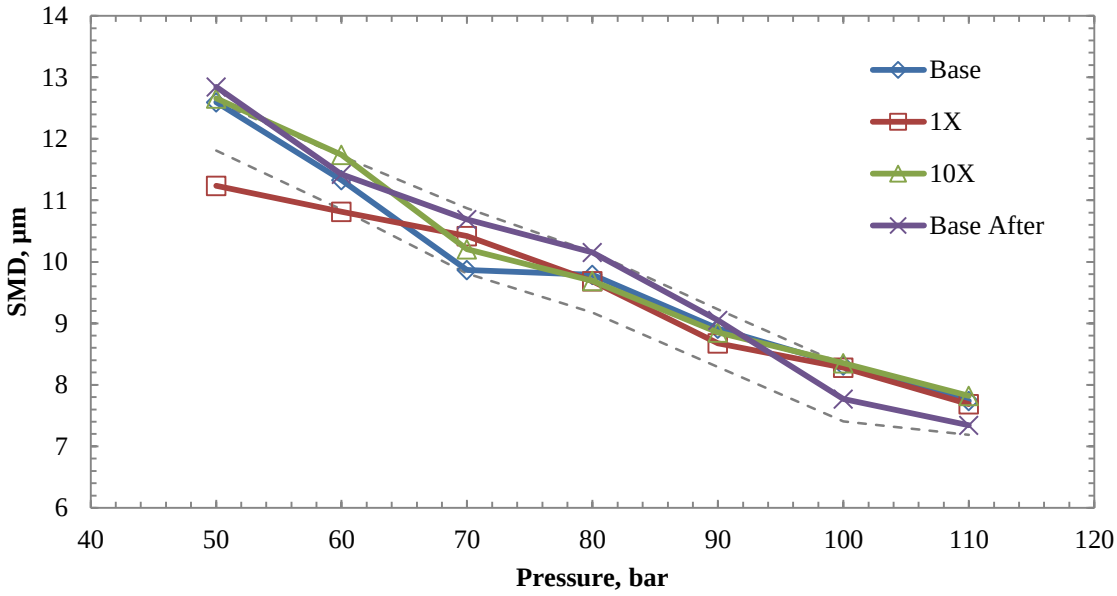

Figure 5.4: SMD for gasoline with DCA-B at minimum transmission

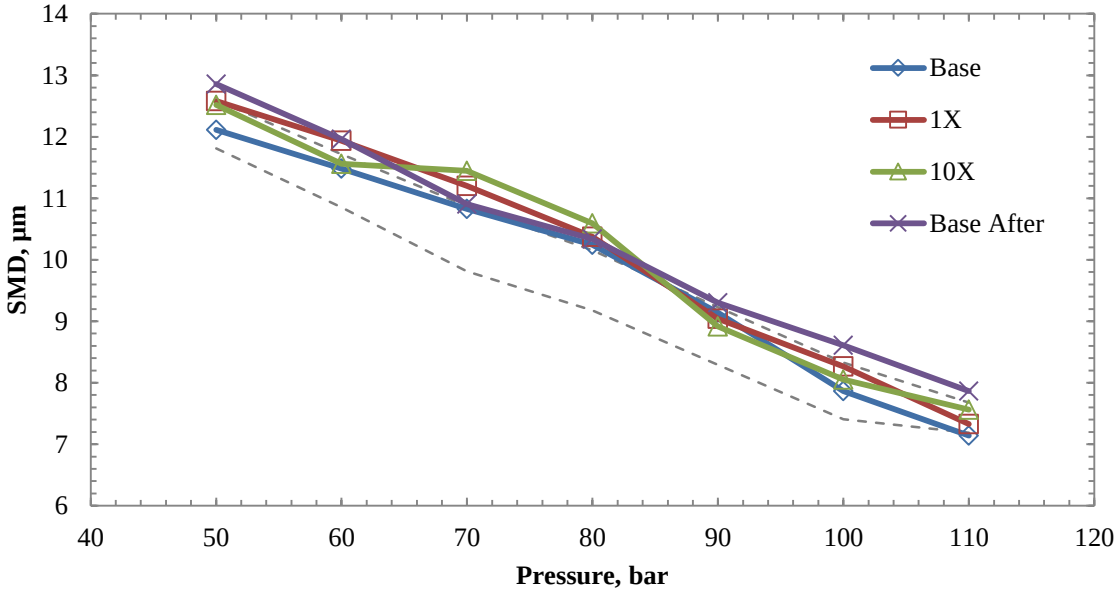

Figure 5.5: SMD for gasoline with C-B at minimum transmission

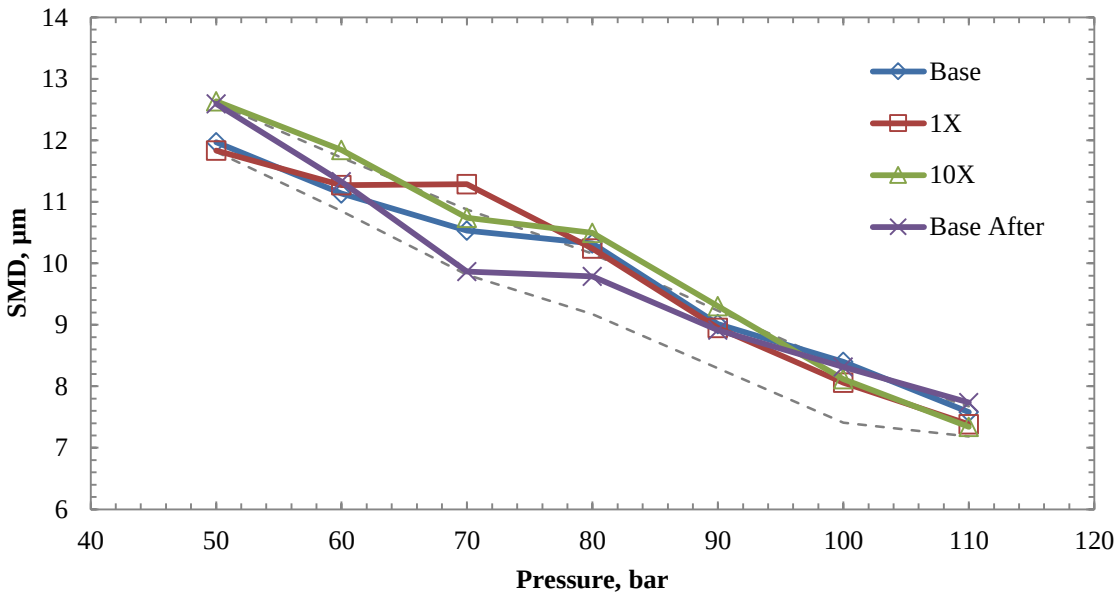

Figure 5.6: SMD for gasoline with AS-A at minimum transmission

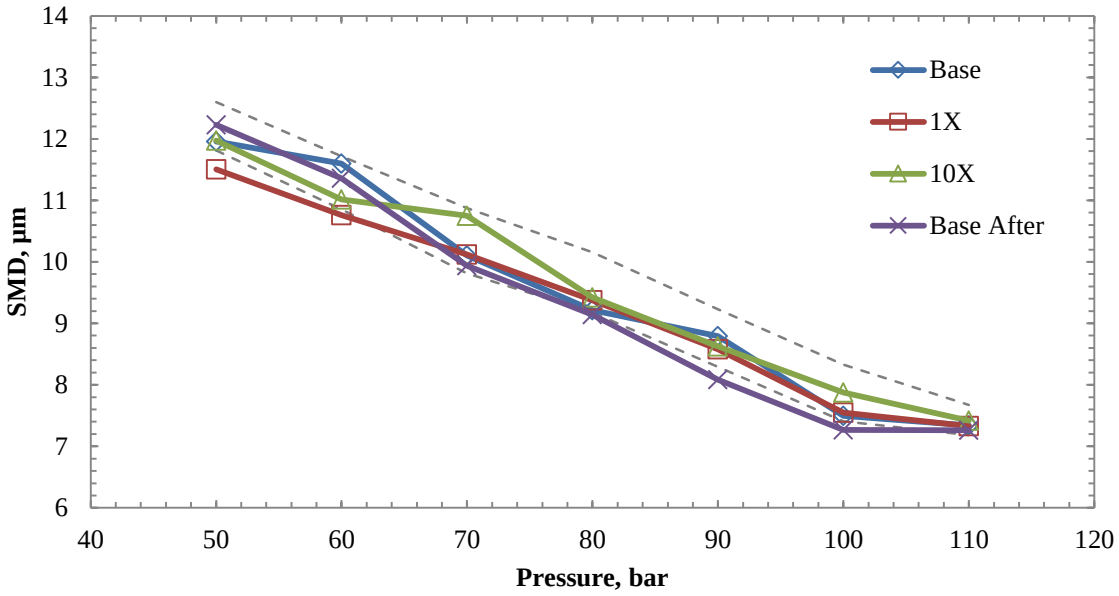

Figure 5.7: SMD for gasoline with CI-I at minimum transmission

where injection pressures are much lower, changes in droplet sizes should be expected with high treat rates of DRA and DRB additives. However, treat rates as high as those in the current work are unlikely to ever occur in practice, especially as these additives are used in distribution systems and are unlikely to make it into vehicle fuel systems without degradation. Consequently, investigating the effect of the aforementioned additives with a PFI system any further was thought to offer no additional benefit.

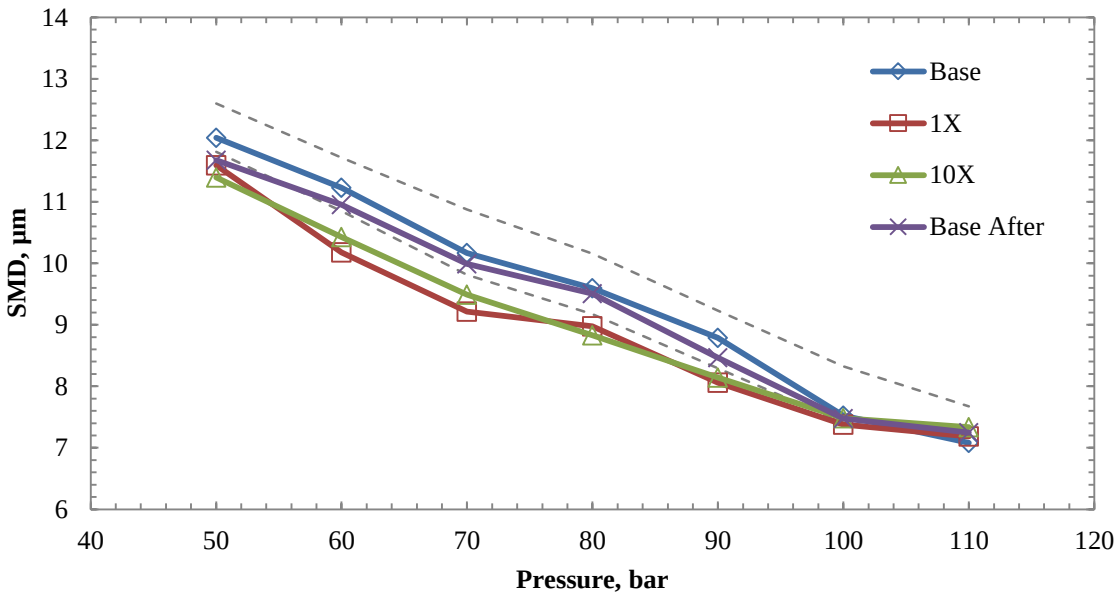

Figure 5.8: SMD for gasoline with FM-O at minimum transmission

5.2 Droplet Sizing with Alternative Fuels

This section describes droplet sizing results with fuels other than gasoline and gasoline additives. Previous work with gasoline bound additives showed that very little if any effect can be seen from usage of additives. Since it is essential to understand effects from various sources under varying conditions on fuel sprays, it was deemed useful to carry out further tests to see what and to what extent does affect fuel atomisation. The droplet size analysis was carried out under the same conditions as described Chapter 4.

Moreover, temperature effect of some fuels and binary mixtures was investigated. Due to the effect of temperature on fuel viscosity and surface tension and its effects in turn on SMD. Overview of the fuels tested is given in Table 5.2.

5.2.1 Diesel Fuel

Among alternative fuels investigated was diesel fuel. Globally, it is estimated that 2/3 of all new passenger cars are diesel vehicles [240] and consequently it was considered valuable to compare diesel sprays under identical conditions to gasoline sprays. Diesel fuel was tested at injection pressures of 50-120 bar and SMD measurements taken at minimum and 50% transmission instants. In addition, temperature effect on SMD was investigated. This was carried out to study the effect of viscosity change on SMD. Whilst evaporation rates are bound to be affected by

Fuel	Carbon Chain Length	Density, kg/l	Boiling Point, °C	Flash Point, °C	Autoignition Temperature, °C
Gasoline	C4-C12	0.72-0.79	25-220	-40	280
Diesel	C8-C21	0.83	170-390	55	210
Hexene	C6	0.673	63	-15	272
Dodecane	C12	0.75	214-218	83	205
Heptane	C7	0.68	98	-4	223
Toluene	C7	0.87	111	6	215

Table 5.2: Properties of base fuels used in the project

increased fuel temperature, it was believed that the high boiling and flash point temperatures for diesel would mean that at ambient conditions no significant effect would be experienced.

Figure 5.9 displays the effect elevated temperature had on droplet size under varying injection pressures. A proportional-integral-derivative (PID) controller was used on the high pressure fuel line together with a tape heater and set at 118 °C and 205 °C. Later analysis showed that the actual temperatures in the injector before

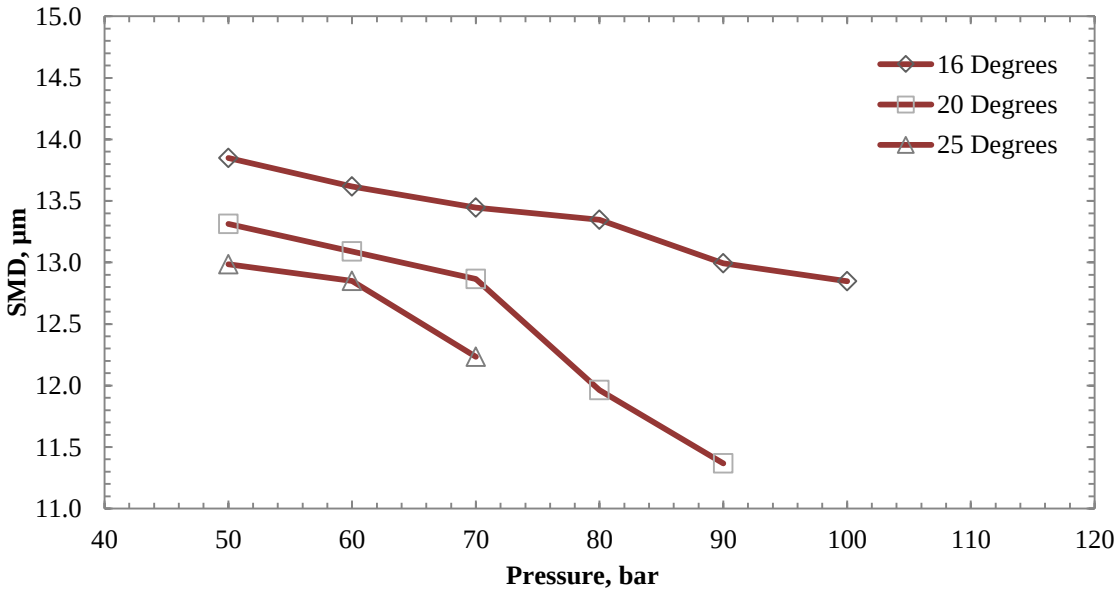

Figure 5.9: Diesel fuel SMD at room and elevated temperatures for various pressures at minimum transmission

injection would only have increased to 20 °C and 25 °C, respectively. However, it is clear that droplet size decreases with increased temperature. Higher temperatures resulted in lowered viscosity, which in turn increased the quantity of fuel being injected for a given pressure condition. The increased fuel quantity meant that in some cases, the transmission of light from the laser dropped below 2 %. Since this is outside the measurement range for the laser system, these data points were ignored.

These results are in good agreement with theory in Section 2.3.2. Increased temperature has an effect on SMD, through what is thought to be a viscosity modifying effect. This is because of changes in laser power levels that decreased significantly for given pressure conditions as a result of improved flow conditions within the injector nozzle. The transmissions at different injection pressures can be seen in Figure 5.10.

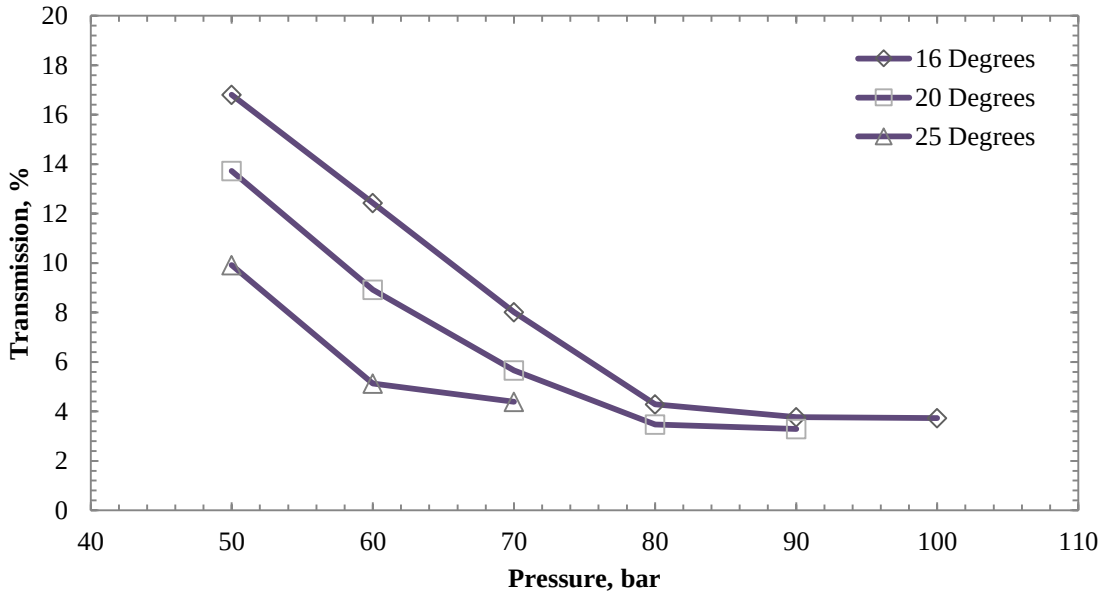

Figure 5.10: Minimum laser transmission levels at different temperature and injection pressure conditions

It is evident that fuel quantities are higher for higher temperature conditions at the measured location. It can also be noted that at higher temperatures much reduced decrease in transmission levels is experienced. This could be a result of injector internal flow characteristics whereby a throttling effect occurs. Reduction in viscosity enabled increased flow rates up to a certain value, after which increases in fuel injection pressure were not followed by increases in fuel quantity to the same degree. Interestingly, droplet size did not appear to be affected by this phenomenon and reductions in SMD of similar magnitude continue to occur even past the point where

transmission levels seem to flatten out. It should be pointed out that this behaviour was not seen in gasoline fuels where the transmission levels decreased evenly throughout the pressure range.

In order to obtain better understanding of fuel viscosity changes, experimental values for diesel viscosity changes with temperature, as found by Esteban et.al. [241], were compared to the temperatures obtained in current experiments. This can be seen in Figure 5.11. It shows that viscosity can be estimated to reduce by at least 10 % with each of the temperature increases. This would suggest at 50 bar injection pressure, a 20 % decrease in fuel viscosity is followed by a decrease of 7.1 % in SMD. At higher pressures a general trend of even larger SMD decreases with increased temperature seems plausible.

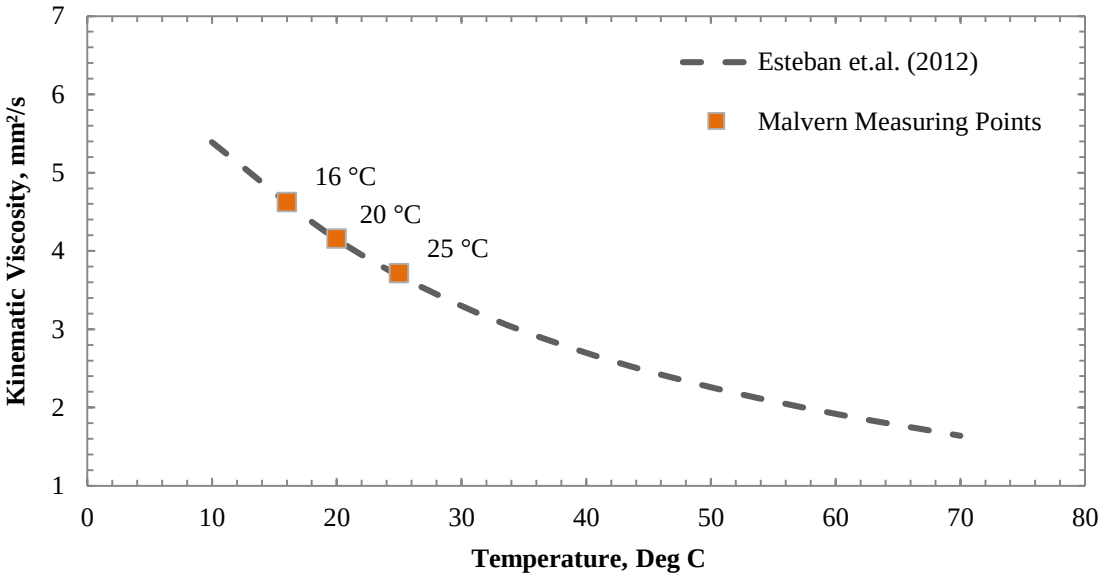

Figure 5.11: Comparison of diesel fuel viscosity dependence on temperature and estimated Malvern measurements conditions

5.2.2 Mixtures of Single Component Fuels

Several pure fuels were investigated in order to see effects of fuel carbon chain length and molecular structure. Additionally experiments were carried out on temperature effects and binary blends on SMD. All mixtures were prepared by volume. Experiments on hexene and dodecane were carried out to investigate effects of carbon chain length and hence volatility on SMD. Additional mixtures at 25 %, 50 % and 75 % hexene were analysed. Hexene boiling point is about a third of that of dodecane and it was expected to produce smaller droplets as a consequence of

improved evaporation. Mixtures of heptane and toluene were carried out in pure and in a 50 % mixture forms. The main aim of the investigations was to determine SMD for pure and mixture forms in order to understand if physical properties of the fuels can be used to explain the effects combustion, as found by Hellier et al. [242]. Furthermore, it was thought such fundamental study would enable better explaining results obtained from droplet sizing with additives.

5.2.2.1 Hexene and Dodecane Binary Mixtures

The pressure dependence at minimum transmission of the pure forms and blends can be seen in Figure 5.12. Evidently, hexene produces smaller droplets than dodecane under the same experimental conditions. Binary blends at higher pressures separate nearly evenly between pure forms but at lower pressures, especially at 50 – 70 bar, seem to tend towards the SMD size of dodecane. It is possible that this is caused by the hexene portion of the fuel blend evaporating faster than the dodecane portion, thus, the tendency towards the dodecane SMD. However, this effect should be seen throughout the pressure range, which is not the case for the current set of experiments. As such, the results can more likely be explained by limitations in experimental repeatability rather than fuel blend effects.

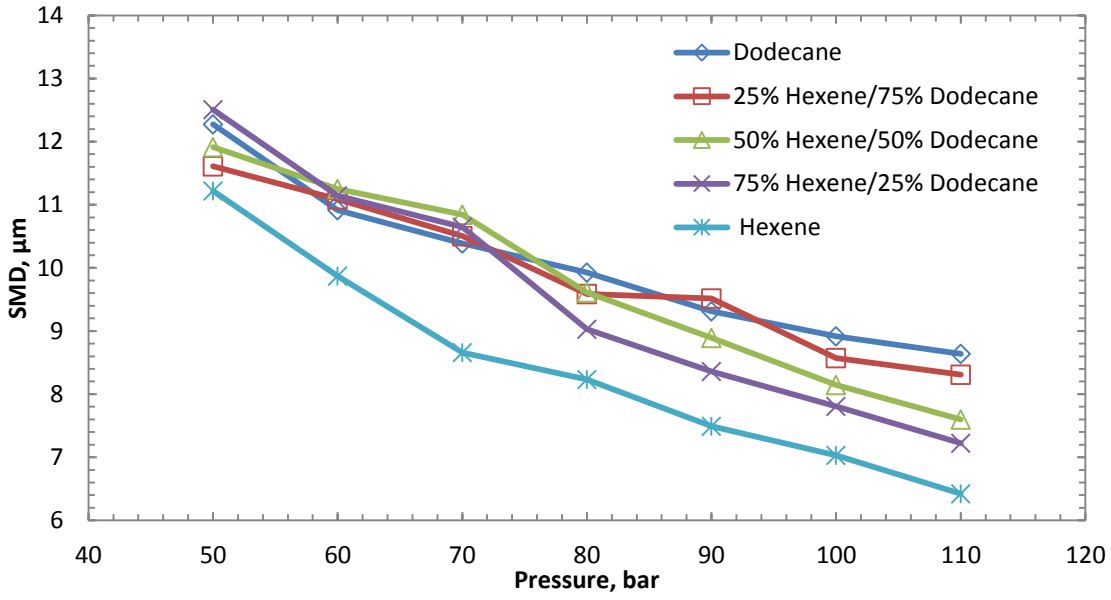

Figure 5.12: Pressure dependence of hexene and dodecane in pure and blended forms at minimum transmission

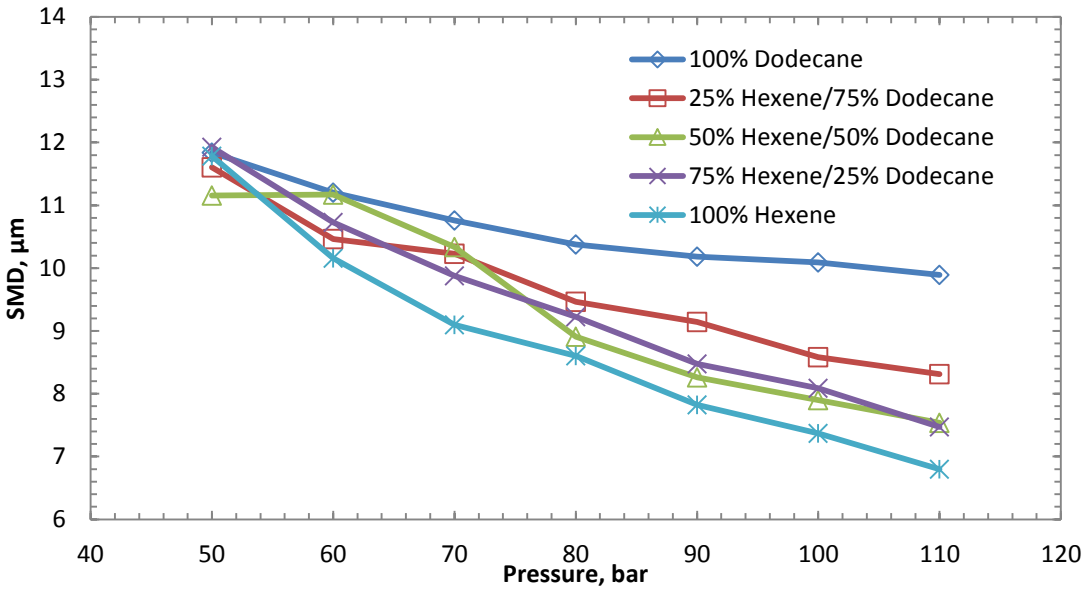

Figure 5.13: Pressure dependence of hexene and dodecane in pure and blended forms at 50% transmission

Due to the SMD values' tendency to incline towards pure dodecane values at minimum transmission, also 50 % transmission results were analysed. This can be seen in Figure 5.13. At 50% transmission, separation of SMD was similarly experienced at higher pressures. However, no trend for fuel blends to tend towards either of the pure fuel forms under any injection pressure could be noted, although the SMD values did seem to converge at lower pressures. This could be explained by different evaporation rates for hexene and dodecane. Fuel vaporisation rates are dependent on total spray surface area which is higher at increased injection pressures as a result of improved atomisation characteristics. Both, the flash and boiling points for hexene are lower than for dodecane, meaning superior evaporation rates at ambient conditions. It is possible that as a result of improved atomisation quality, the effect of evaporation rate differences was amplified and divergence in SMD values is seen at higher injection pressures. The results at 50 % transmission suggest that previously mentioned experimental repeatability limits could be used to explain pure hexene SMD values at minimum transmission.

Furthermore, it is known that the main properties to affect droplet size, besides injection pressure, are the fuel surface tension, viscosity and density. Alptekin and Canacki [243] and Tat and Van Gerpen [244] measured surface tension, viscosity and density of different binary fuel blends and found that all the aforementioned properties change proportionately and linearly to their constituent components. Although this

would suggest similar changes in SMD with incremental composition variation could be expected, it should be noted that changes in flash points [245, 246, 247] and boiling points [248, 249] for binary mixtures are not linear. However, due to limitations in experimental repeatability, the effect of this was not reflected in the results.

Additional investigation into the effect of fuel temperature on dodecane and hexene was carried out. For these sets of experiments only a 50/50 binary blend of hexene and dodecane was studied. All sprays were carried out at 110bar injection pressure. For hexene temperature was increased to within 20 °C of fuel boiling, for the 50/50 mixture to the boiling temperature of hexene and for dodecane to the maximum system capability of just under than 90 °C. The fuel temperature was measured with a K-type thermocouple placed through the injector cap into injector reaching just behind the needle mechanism to give the most accurate reading during the experiments.

Dodecane and hexene SMD dependence on temperature is presented in Figure 5.14. For both pure fuels and the 50/50 mixture, a larger temperature increase is necessary to produce a similar reduction in SMD as for diesel.

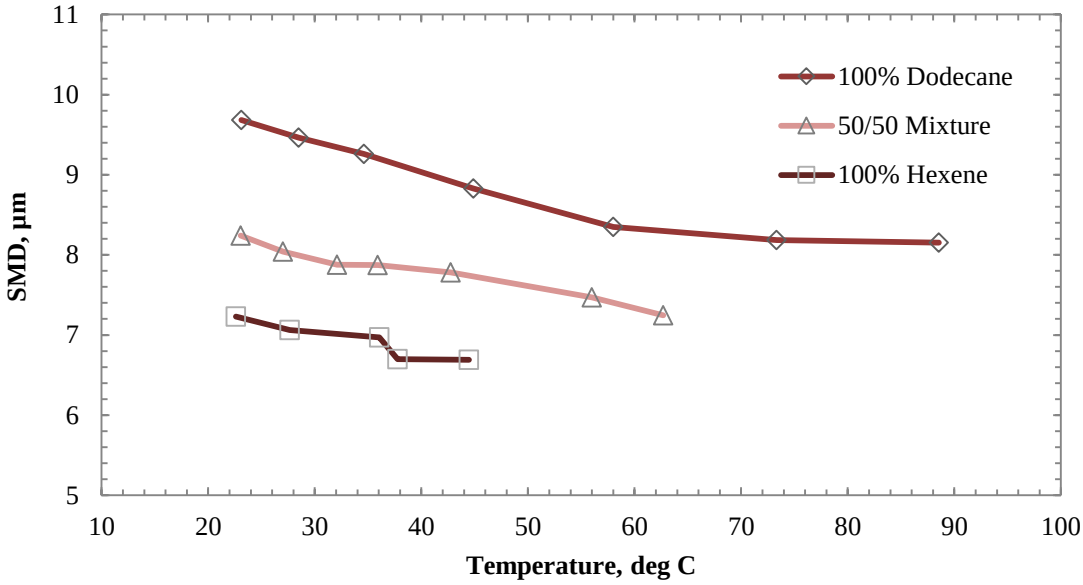

Figure 5.14: Temperature dependence of hexene and dodecane fuels in pure and 50% binary blend form on SMD at minimum transmission

Table 5.2 demonstrates closeness of hexene (and dodecane to an extent) properties to that of gasoline rather than diesel. This is especially evident in their density and carbon chain length. Viscosity measurements displayed in the following sections further validate this claim. Wang and Lefebvre [250] found, when comparing

diesel and gasoline fuels, diesel to be more affected by temperature changes. This was thought to be due to much higher initial viscosity of diesel compared to gasoline (also hexene and dodecane for current set of experiments) that for the same temperature range will decrease more rapidly. However, the SMD values measured for different temperatures exhibit very good agreement with the theory that fuel properties change proportionately to their constituent components. The SMD for the 50/50 mixture clearly lies in the middle of the two pure component fuels without any clear tendencies towards either.

5.2.2.2 Toluene and Heptane Binary Mixtures

Further experiments with toluene and n-heptane with an additional 50% binary mixture were carried out. Results are presented in Figure 5.15. Although similar in carbon molecule number and boiling point, toluene and n-heptane differ greatly in molecular structure. Hellier et al. [242] found a 75% n-heptane / 25% toluene binary mixture to cause two stage ignition and more than 50% toluene in the mixture to suppress ignition altogether.

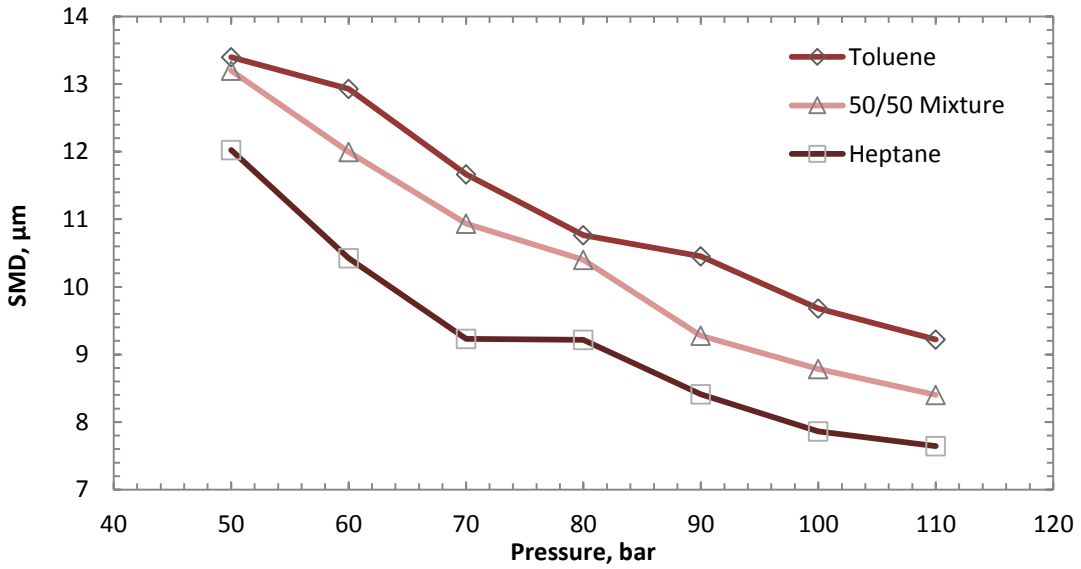

Figure 5.15: Droplet size for of toluene, heptane and a 50% binary mixture at minimum transmission

Measurements were carried out to look for any significant changes in binary mixture physical properties that would explain the combustion phenomena but similar proportional relationship of the components in the mixture to the pure fuels as previously was seen. As such, changes to ignition characteristics were attributed to

changes in chemical properties in fuel where radical absorption by toluene was suspected.

5.2.3 Experimental Error Assessment for Droplet Sizing

As explained in Section 4.1, over 50 injections, the cumulative average of measured SMD was reduced to below 0.3 % of mean value. Thus, the effect of an additional spray event would have not had a significant effect on the measured SMD value. However, the base fuel standard deviation over 19 measured base fuel SMDs was on average ± 0.43 μm and ± 0.47 μm at minimum and 50 % transmission cases, respectively. Total peak to peak variability around ± 1.2 μm across the measured pressure range was noted. Although these figures are based on gasoline SMD measurements, it was assumed similar repeatability characteristics would be seen with alternative fuels as identical equipment and experimental conditions were employed in the study.

For additive analysis, the base fuel mean value with its standard deviation was chosen as the basis for identifying additive effects. Anything beyond standard deviation was thought to represent a significant change. However, as demonstrated in Section 5.1.3, the variability in base fuel SMD values meant that additive readings could be outside the identified window while changes from the respective base fuel measurements were still within ± one standard deviation. As such, it was not possible to identify with confidence any changes in gasoline direct injection atomisation quality with additive bearing fuels.

The variability in the study can be assumed to result from the injector characteristics. Injector needle movement variability due to control timing and voltage characteristics changes are likely to be the primary causes although small changes in ambient conditions could also have had an effect on the readings. However, what is clear, is that the effect that additives have on the base fuel properties is very small and any further characterisation of the system would not have provided additional benefits. This also applied to the alternative fuel study, where general trends in SMD sizes could be identified but further system characterisation was not thought to be valuable.

5.3 Viscosity and Surface Tension Measurement of Experimental Fuels

The measured and literature based values of viscosity and surface tension are presented in Table 5.3. The fuel was controlled at 19.6 °C for all viscosity measurements while surface tension readings were carried out under ambient conditions that for the current set of experiments meant fuel temperature of 17.5 °C. Measurements for gasoline fuel mixed with additives were carried out only for ten time treat rate levels.

Apart from fuels with low viscosity, the viscosity measurements were in good agreement between experimental and literature based values. Heptane and toluene measurements showed difficulties can arise with very low viscosity liquids, where values approximately twice as high as those reported in literature were measured.

Unlike the viscosity measurements where only low viscosities appeared to be overestimated compared to literature based values, surface tension measurements were higher throughout the measured range. Two potential sources of error can be used to explain the measurements.

Firstly, the surface tension equation as proposed by the apparatus manufacturer (Equation 3.1, page 79) does not take into account of the contact angle, ϑ, between the liquid surface and the wall of the capillary tube. Contact angle can be included in Equation 3.1 as [251]:

$$\sigma = \frac{1}{2}\frac{\rho g h r}{\cos\vartheta} \qquad 5.1$$

where the symbols are as stated in Section 3.1.4. It should be noted that difficulties in measuring the contact angle and the assumption that the liquid completely ‘wets’ the capillary wall (especially in cases where density of liquid is significantly larger than the density of air), the angle ϑ is often assumed as 0^{o} and Equation 5.1 is represented as Equation 3.1. Furthermore, the contact angle is defined as $\vartheta < 90$ for liquids that ‘wet’ the tube wall and the term is likely to increase the calculated surface tension

Fuel	Additive/Fuel Concentration	Dynamic Viscosity, cP (@ T = 19.6°C)	Literature Viscosity, cP	Surface Tension, dyn/cm (@ T = 17.5°C)	Literature Surface Tension, dyn/cm
Gasoline	Base	0.84	0.88	34.9	21
	AS-A	0.84	-	34.9	-
	C-B	0.85	-	34.9	-
	CI-E	0.86	-	34.9	-
	CI-F	0.85	-	34.9	-
	CI-H	0.84	-	34.9	-
	CI-I	0.85	-	34.9	-
	DCA-A	0.85	-	34.9	-
	DCA-B	0.84	-	34.9	-
	DCA-C	0.83	-	34.9	-
	DCA-G	0.84	-	34.9	-
	DCA-M	0.85	-	34.9	-
	DCA-N	0.86	-	34.9	-
	DRA	2.25 (@ 20.5°C)	-	34.9	-
	DRA (After Injection)	1.18 (@ 20.5°C)	-	-	-
	DRB	2.20 (@ 20.5°C)	-	34.9	-
	DRB (After Injection)	1.25 (@ 20.5°C)	-	-	-
	FM-A	0.85	-	34.9	-
	FM-N	0.88	-	34.9	-
	FM-O	0.85	-	34.9	-
	Lauric Diethanolamide	0.85	-	34.9	-
Diesel	Base	3.54	2-4.5	44.9	26.5
Alternative Fuels	100% Hexene	0.68	0.51	29.7	20.13
	75% Hexene/25% Dodecane	0.78	-	32.3	-
	50% Hexene/50% Dodecane	0.92	-	34.9	-
	25% Hexene/ 75% Dodecane	1.04	-	37.6	-
	100% Dodecane	1.25	1.36	40.5	25.35
	100% Heptane	0.79	0.386	31.9	20.14
	50% Heptane/50% Toluene	0.89	-	38.0	-
	100% Toluene	1.02	0.55	46.8	28.4

Table 5.3: Measured and literature based viscosity and surface tension values of all fuels used in experiments, including base and additive bearing fuels and pure fuels with binary mixtures. Gasoline additive measurements were only carried out for 10 time treat rate

value further resulting in even greater discrepancies between the measured and literature based values.

The other source of error could originate from the definition and measurement of capillary rise (term h in the equation) in the tube. As shown in Figure 5.16, in the literature, the capillary rise has been defined as the distance between the surrounding liquid surface to:

a) the bottom of the miniscule (h_1) [252],
b) to the miniscule-wall interface (h_3) [253]
c) an unknown distance between the bottom and top of the miniscule (h_2) [251]

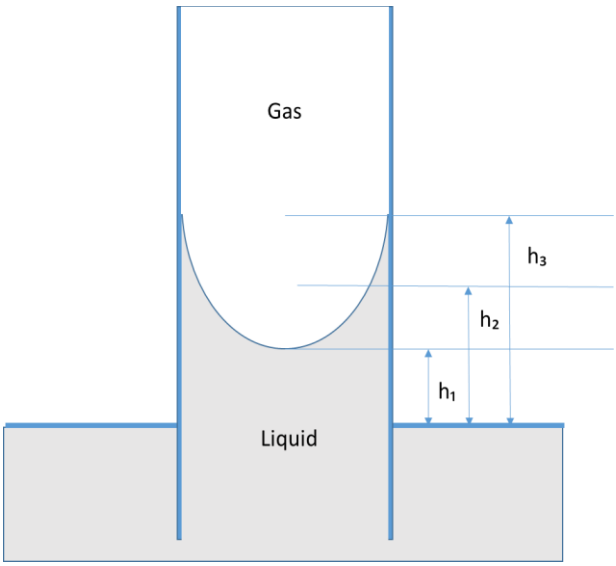

Figure 5.16: Liquid rise in capillary tube and proposed h definitions

The equipment manufacturer had not specified which to use and in the current study the distance was taken as the one from the surrounding liquid surface to the miniscule-wall interface (h_3) which gives the highest h value. Should the lowest point of miniscule have been selected (h_1), reduced surface tension values could have been calculated. However, with the existing methods it was difficult to determine the lowest point of the miniscule. Moreover, since the results based on the liquid-wall interface to surrounding liquid level showed consistently proportionally higher surface tension values (~1.6 x literature values for all fuels) and the present study was interested in comparative changes in fuel properties, the method was seen as adequate.

As was mentioned previously, changes in droplet sizes of binary mixtures of pure fuel seemed to change proportionately to the quantity of the component fuels.

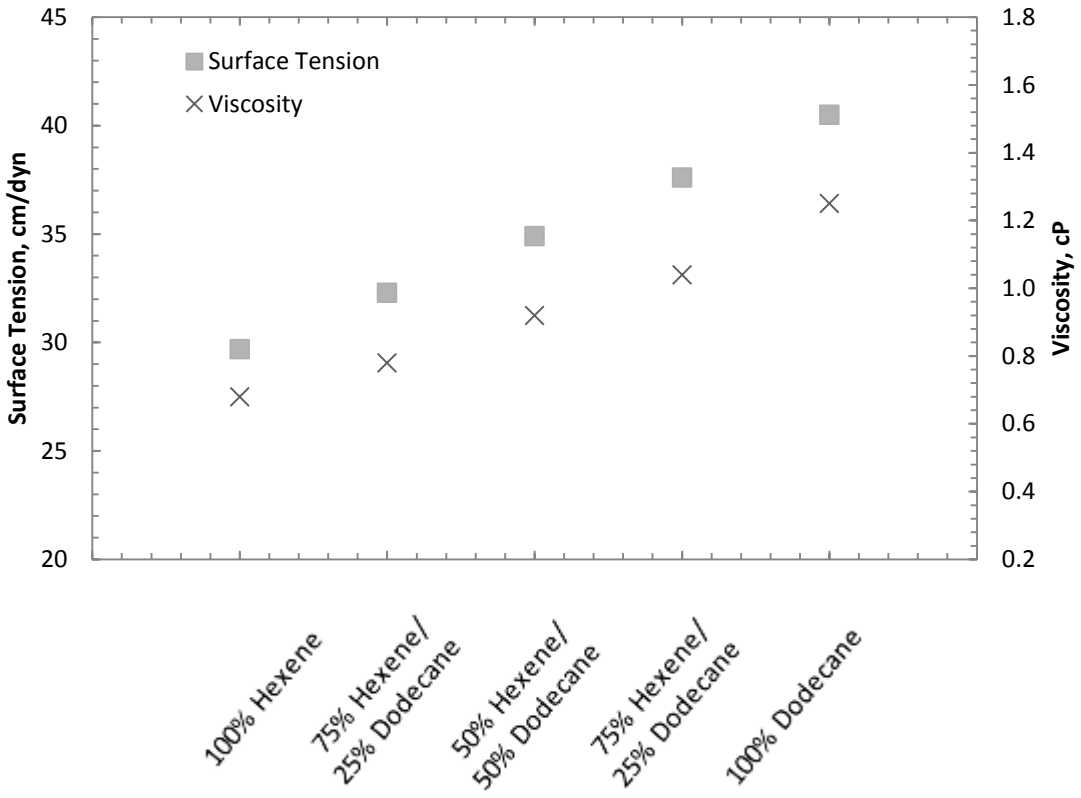

Figure 5.17: Surface tension and viscosity of hexene and dodecane binary mixtures

Furthermore, as described in Section 5.2.2.1, a linear relationship between different fuel blend viscosities, surface tensions and densities has been measured by several researchers. It was, therefore, expected that a linear relationship between the mixtures and pure components would also be detected in the surface tension and viscosity measurements. Figure 5.17 displays this relationship for the hexene and dodecane pure forms and binary mixtures. It can be seen that surface tension measurements displayed a strong linear relationship.

Viscosity measurements of additive carrying gasoline with the drag reducing agents DRA and DRB provided some noteworthy results. As expected from literature survey, the additives increase the viscosity of the base fuel. In case of both the additives, the base fuel viscosity nearly tripled to 2.25 cP for DRA and 2.20 cP for DRB. Since the SMD investigations with these additives demonstrated no distinguishable change Section 5.1.3, further analysis on post injection fuels was carried out. For both additives, a fuel sample consisting of 200 injections at 110 bar injection pressure was analysed. The measurements showed a large drop in viscosity to 1.18 cP and 1.20 cP for DRA and DRB additives, respectively. This reduction was thought to originate from additive break-up/degradation during the highly turbulent

flow through the injector nozzle at high pressures during injection events. Reader is advised to refer to Appendix B for estimated turbulence level calculations. Although viscosity remained nearly 50% higher than the base fuel, it was assumed that at such low fuel viscosities the change in droplet size is unidentifiable with the measured SMD repeatability levels experienced in current study.

It is likely that the fuel volatility also played an important part. Although fuel atomisation study was carried out at ambient temperature, as seen from Table 5.2, it is significantly higher than the flash point of gasoline. Since the SMD measurements were taken at large distances from the injector nozzle, any additive effects might have been overpowered by the fuel evaporation rates.

5.4 Conclusion

This chapter has presented the results of an investigation into the effects of fuel additives on the physical properties of base gasoline fuel. Fundamental gasoline spray formation characteristics were investigated for 17 fuel additives from 6 functional groups in two different additive concentrations through the use of a Malvern laser diffraction system. Additionally, a non-fuel bound viscosity modifying additive was investigated. The study, based on the measured SMD values, indicated that effects from fuel additives are too small to be quantified under the chosen conditions by the selected methods.

Surface tension and viscosity measurements of base gasoline fuel with the higher concentration of additive revealed that the fuel additives, in quantities used in the industry, are unlikely to affect their physical properties. Only exceptions to this were the drag reducing agents that are meant to increase fuels viscosity to reduce turbulent flows in pipe lines. However, their effectiveness is greatly reduced during high pressure injection events where the fuels lost more than 45 % of their viscosity as a result of probable shear degradation. Furthermore, due to their purpose in the distribution systems and their tendency to break up in turbulent flows, likelihood of the drag reducing agents making their way into the vehicle fuel systems in the tested concentrations is practically non-existent.

Additional investigations with single component fuels and their binary mixtures were carried out to confirm the extent to which fuel blend components affect the mixture properties. As initially anticipated, the mixture properties were affected

proportionately to their constituent components. On this basis, it is clear that even at maximum quantities (CI-I 10X, 10g/L of fuel), the proportion of additive in the fuel mixture remains too low to affect their physical properties.

The findings agree with the study carried out by Patel [113], who found that at ambient environmental conditions DCA and CI additives did not have an effect on high pressure diesel sprays. The present study added several new additives to gasoline fuel but again found the additives to not alter the spray characteristics from the base fuel. Therefore, the only effects seen from the additives under high pressure GDI environments are expected to occur within their functional areas.

Chapter 6

Effect of Fuel Additives on Gasoline Combustion

In this chapter, the effects of fuel additives on gasoline combustion characteristics are discussed. Initially, the results from gasoline vapour combustion are presented. The chapter concludes with the outcomes from the experiments in the single cylinder research engine.

6.1 Experimental Additives

Additives employed in the combustion investigations can be seen in Table 6.1. Although additives from all functional groups could in theory affect combustion, it was thought their main influence would come through changes to atomisation characteristics. Chapter 5 analysed the effects of additives on the physical properties of the base fuel and found the viscosity and surface tension not to be affected to an extent where changes in atomisation characteristics could be identified. As such, only CI additives were investigated. The additives in question were named as CI-A, CI-I and CI-Additional. CI-A was a commercially available diesel ignition improver 2-EHN. Its main aim is to provide chain-branching and carrying radicals at low

Additive Group	Additive	Treat Rate (1X), mg/L	Increase in Cetane/ Octane Number at 1X
Combustion Improvers	CI-A	250	2-3 CN
	CI-I	1000	0.2-0.4 RON
	CI-Additional	7000	1.5-2.5 RON

Table 6.1: Additives used in combustion investigations. CI-A is a cetane improver, CI-I and CI-Additional are octane improvers

temperatures to shorten diesel ignition delay. In gasoline, it was likely to cause knocking behaviour, although as shown by Colucci et al. [11], in low concentrations benefits in the form of reduced misfires and cyclic variation could be observed. CI-I was an organic anti-knock additive and CI-Additional a ferrocene antiknock with potassium spark aider. Although CI-Additional has very good anti-knocking properties, it is often also used in power generation and naval applications where it is used as an anti-soot agent [254]. Due to high treat rate of CI-Additional (resulting from high base dilution), CI-Additional was only tested at 1X levels while CI-A and CI-I were additionally analysed at 10X.

6.2 Gasoline Vapour Combustion

Figure 6.1 displays sample images of the flames captured with high speed imaging. The flames for CI-A at 1X and 10X concentration produced similar if not slightly brighter luminosity compared to the base fuel. CI-I flame burned at much lower brightness with the flame for 10X fuel being while CI-Additional seemed to be affected the most by the additive. As described by ATC [255], organometallic anti-knock additives are utilised as catalysts for the burn-out of soot particles. This was represented by localised bright spots throughout the combustion event.

The main outcomes of combustion vessel investigations are presented in Figures 6.2 – 6.7. Figure 6.2 displays the relationship between the peak pressure and peak heat release rates. It can be seen that a positive correlation exists. This is due to factors described in Section 2.4.1. A positive relationship was also experienced between NO_x emissions and peak pressures, as presented in Figure 6.3. This was expected, as higher pressure results from higher temperature which is a precursor for

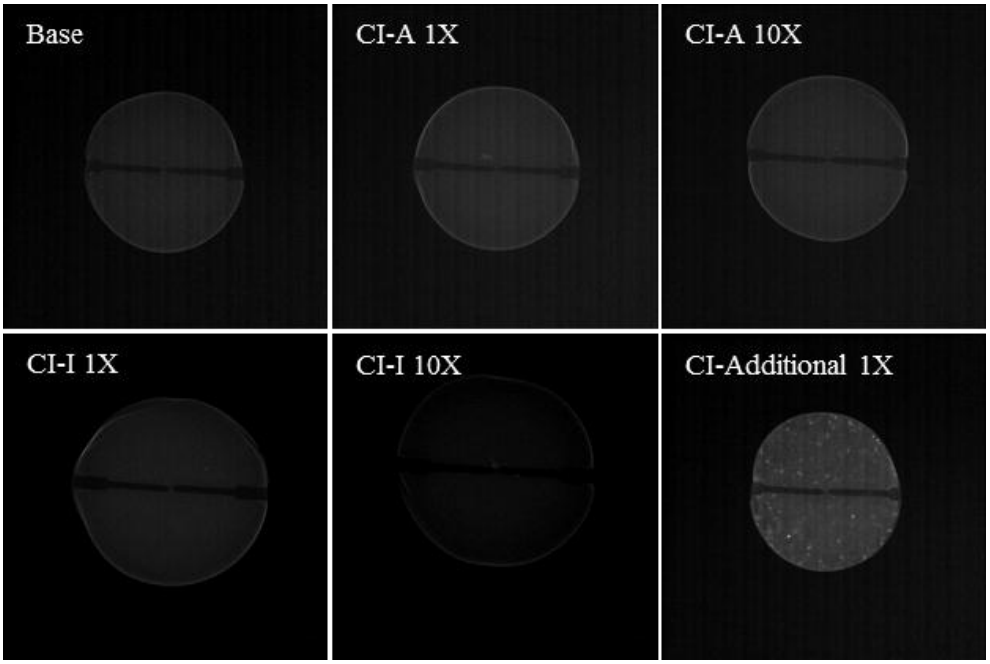

Figure 6.1: Sample flames of additive combustion at t = 29 ms after ignition

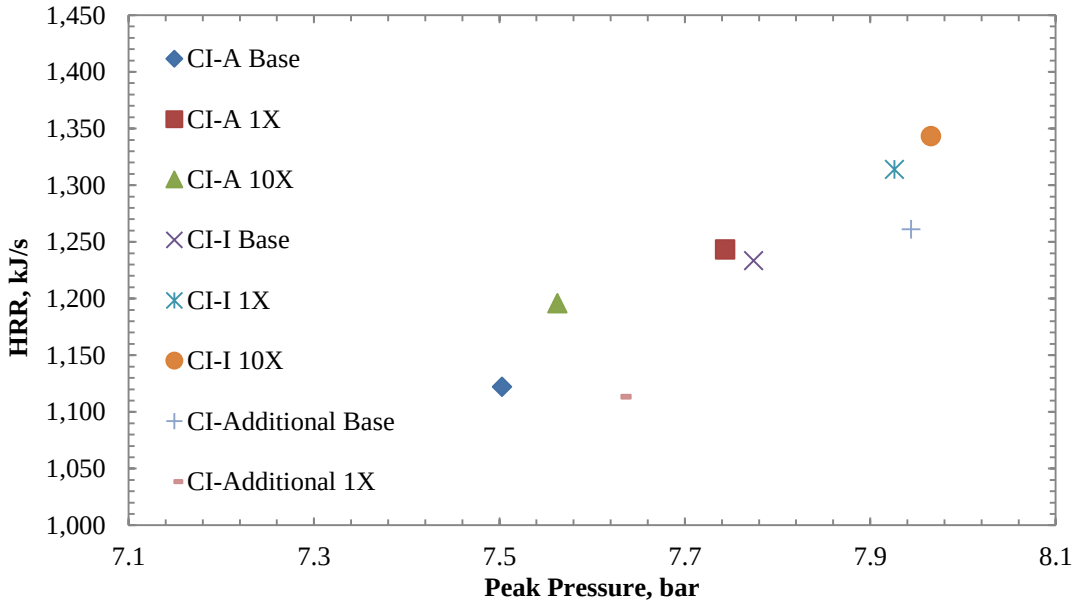

Figure 6.2: Relationship between peak heat release rate and peak pressure reached within the combustion chamber

NO_x formation during combustion. Although it has been suggested by some researchers [48, 49] that additive bound nitrogen compounds can increase NO_x emissions, the results of current study have not provided evidence to support the claims.

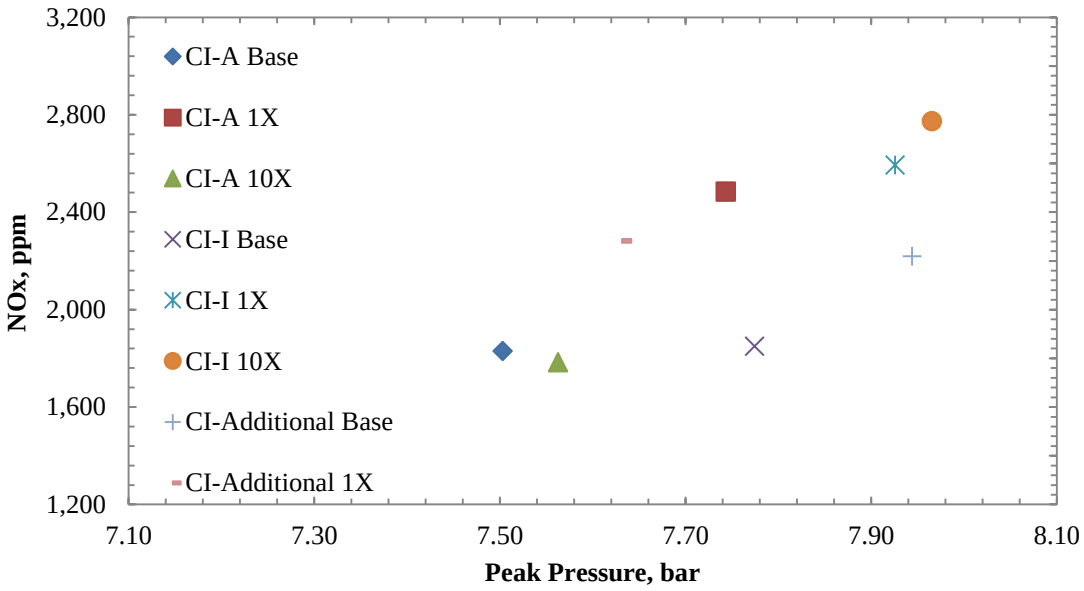

Figure 6.3: Relationship between NO_x emissions and recorded peak pressure

In Figure 6.4, the dependence of peak pressure on initial pressure is displayed. It can be seen that initial conditions were within a small range and seemed not to affect the final pressures within the combustion vessel. Furthermore, similar correlations

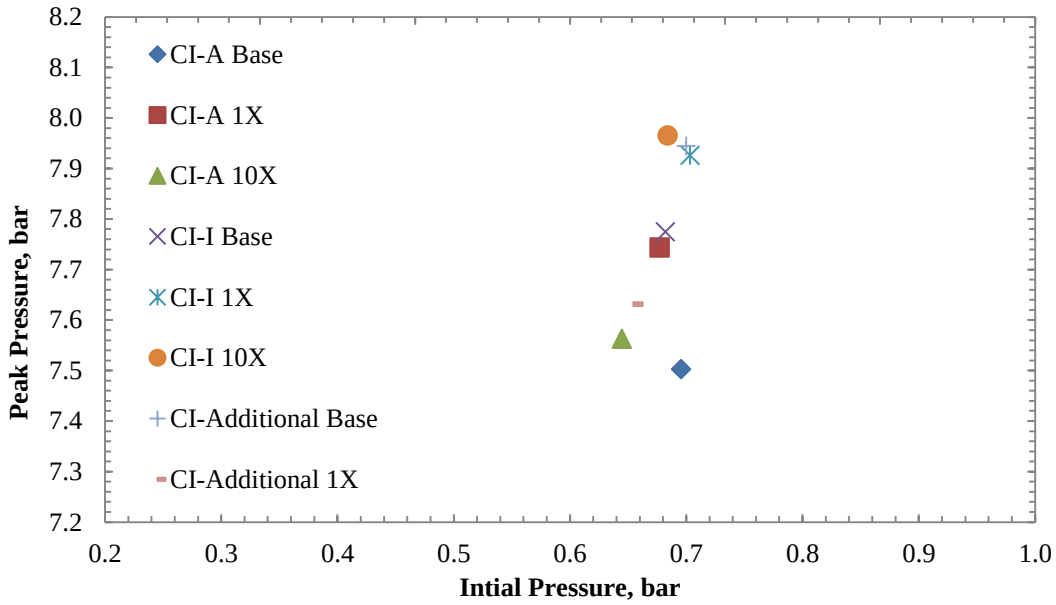

Figure 6.4: Peak pressure dependence on initial pressure conditions

were seen between the vessel wall/ initial air temperature and the final pressure, heat release rate and flame speed. Since pre-ignition gas mixture preparation protocol was

the same for all fuels, it was expected that any changes in combustion characteristics would be a resultant of an additive action.

Overall, the experimental investigation of additives produced inconclusive results. Although changes were seen between base fuels and the following additive tests, comparison of the three base fuel tests that were carried out, revealed the changes could have instead been caused by low experimental repeatability. The CI-A, CI-I and CI-Additional base fuel results extended over much of the recorded range for all fuels. The largest effect from an additive on combustion characteristics was seen for CI-A at 1X concentration. Figure 6.5 displays the relationship between the CO emissions and burning velocity for all fuels. Compared to the next best recorded result, fuel bound CI-A at 1X concentration reduced the CO emissions by 37.7% and increased burning velocity by 5.4%. It was thought that the reduction in the CO emissions could have originated from reduced flame quenching at the inner surfaces of the combustion vessel. The low temperature of the walls compared to the flame front temperature could have resulted in flame being extinguished due to insufficient energy levels available for subsequent reactions. As described in Section 2.1.2, CI-A additive provides ignition promoting radicals at low temperatures, thus, making it possible that in the current set of experiments the flame quenching took place closer to the wall surfaces and a more complete oxidation occurred as a result.

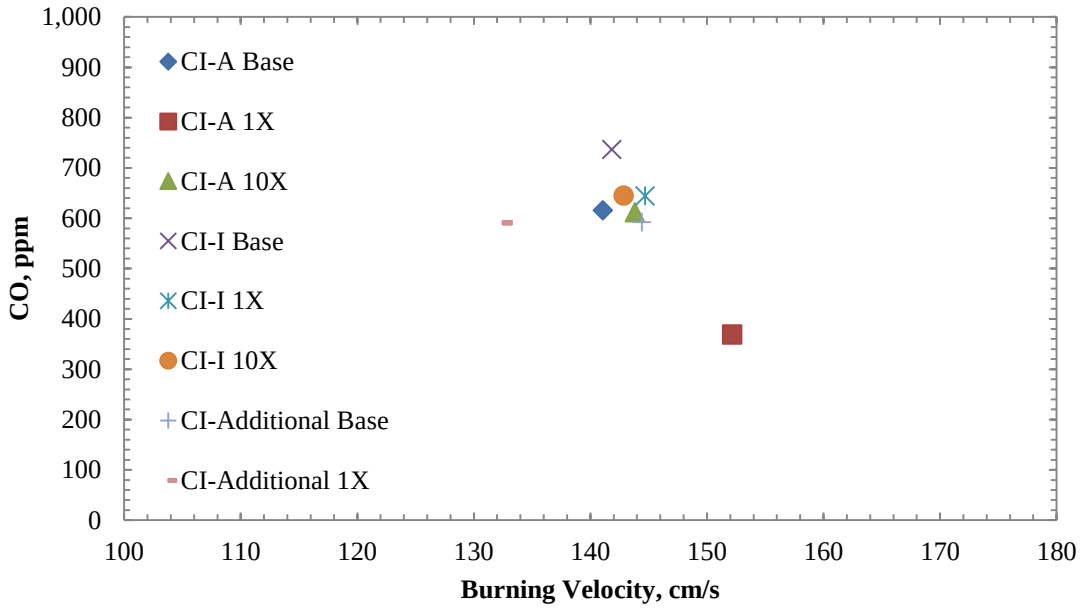

Figure 6.5: Relationship between CO emissions and calculated flame speed

CO emissions could also have been reduced by improved reaction rate throughout the combustion event which could also explain the increase in burning rate. Reduced timescales needed to achieve complete oxidation of hydrocarbons would allow for more of the CO to be turned into CO_2. Although an increase in heat release rate would subsequently be expected, as seen in Figure 6.6, the peak heat release rate experienced for CI-A 1X was not the highest result recorded. Moreover, it is evident that CO emissions in the current study where independent of heat release rate. This can be explained by the study of Aradi and Roos [62] , who found that 2-EHN only survives at temperatures up to 625 K, which is much lower than the expected flame temperatures for the current investigations. Furthermore, Higgins et al. [10] showed that high-temperature chemistry of combustion remained unaffected by the additive, suggesting reduced flame quenching near the vessel walls to be the more probable cause for CO reduction.

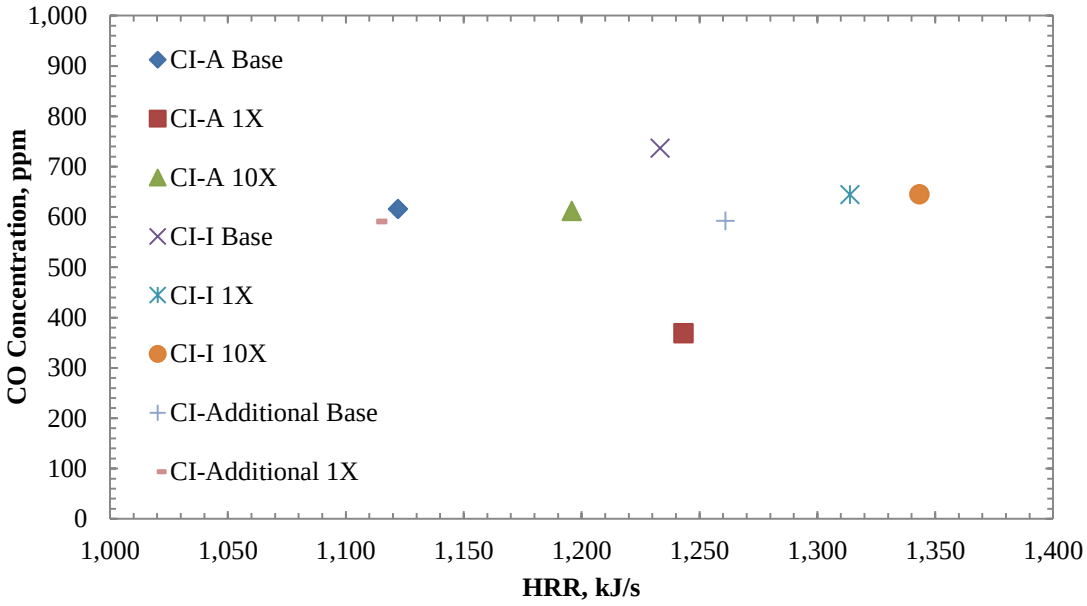

Figure 6.6: Relationship between CO emissions and peak heat release rate

With decreasing CO levels, a reduction in unburnt hydrocarbon emissions would also be expected. However, since unburnt hydrocarbon content in the emissions was not measured and at 10X concentration the CI-A additive effect seemed to disappear, it is not possible to confirm the theory.

Addition of CI-Additional to the base fuel also produced notable results. Lowest burning velocity and peak heat release rate as well as the longest time taken to peak heat release rate and peak pressure were observed. Reductions in flame speeds

have been also noted by other researchers when metallic antiknock additives have been used. TEL containing n-heptane flame speeds were investigated in an engine by Curry [256] and flame propagation speed reductions of up to 50 % were witnessed. An extensive review carried out by Linteris et al. [257] reveals that the main processes responsible for reductions in flame speeds are gas-phase catalytic cycles which involve oxides and hydroxides. The concentration of chain-carrying radicals is reduced by reactions with inhibitors provided by the metallic additives in the flame reaction zone. Furthermore, it has been found that the existence of the inhibitors and subsequent reactions produces additional scavenging species, thus, creating an amplifying effect [258].

An additional factor that could have had an effect on combustion was thought to originate from the spark energy input at the beginning of the combustion event. The applied spark discharge energy was measured for all events except for CI-A Base. Although a small change was experienced in fuel burning velocity for CI-A 1X, Figure 6.7 shows that throughout all tests no correlation between applied spark energy and burning velocity could be seen. Furthermore, since higher spark energy could improve early flame development, it was thought that the time needed to reach peak heat release rate and pressure could have been reduced.

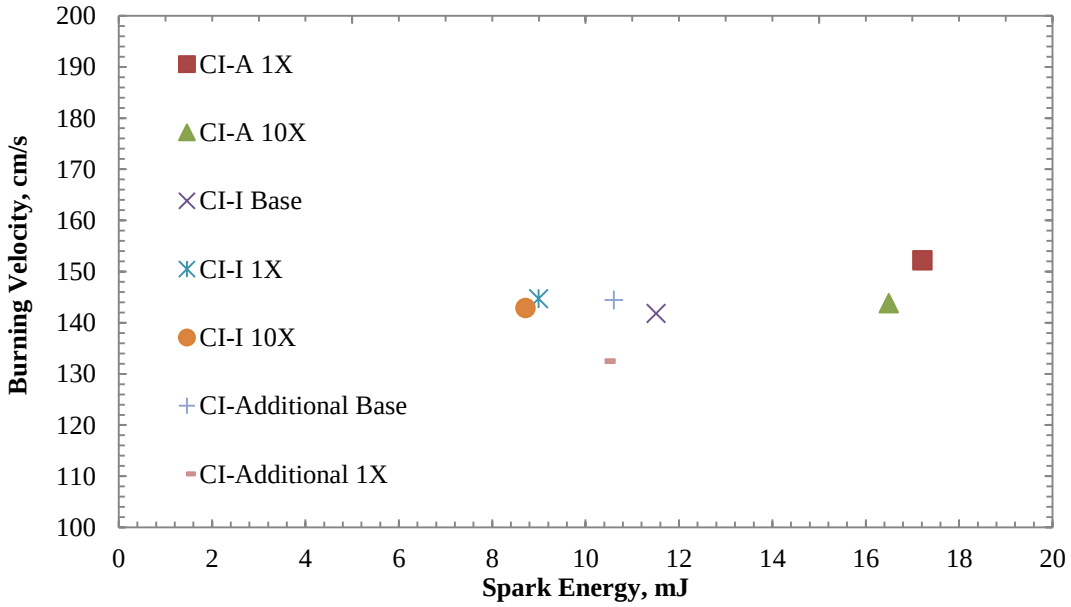

Figure 6.7: Burning velocities for different applied spark energies

Figures 6.8 and 6.9 display, however, that the time taken from spark discharge to maximum heat release rate and pressure, respectively, was not affected by the

energy input. These result compare favourably to several researchers [221, 259], who found the benefit of increased ignition energy to manifest in better lean burning capabilities due to assistance in flame kernel development rather than improvements in the following reaction rates.

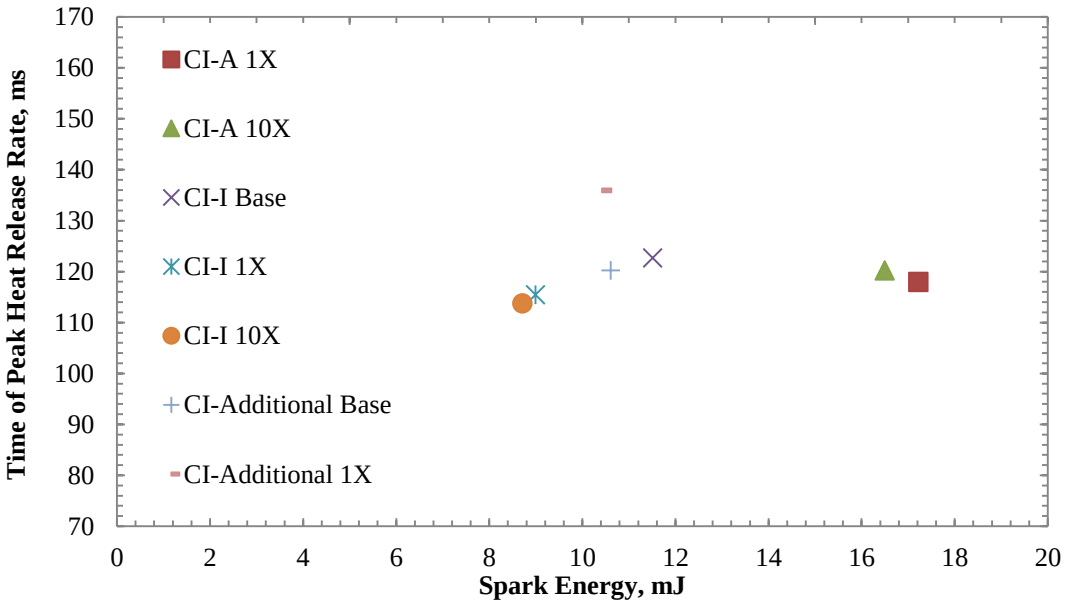

Figure 6.8: Time taken to peak heat release rate for applied spark energies

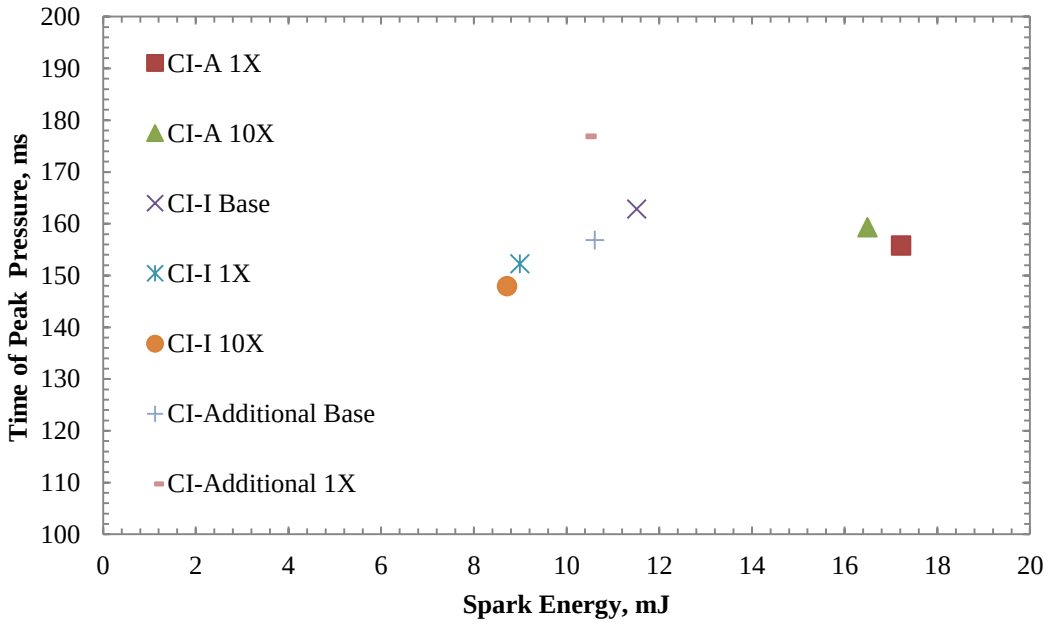

Figure 6.9: Time taken to peak pressure for applied spark energies

The smallest spark energy measured during the experiments was 8.7 mJ for CI-I 10X while minimum ignition energy required to ignite gasoline-air mixtures has been

reported to be 0.8 mJ [260]. Therefore, it can be concluded that irrespective of available spark energy, combustion characteristics for a homogeneous air-fuel mixture in gaseous form remain unaffected as long as the minimum ignition energy is achieved.

6.3 Engine Testing

Following the investigations in the combustion vessel, it was evident that no definite conclusions on additive effectiveness on chemical reactions during combustion could be made. Therefore, the same additives were tested further under engine conditions in a single cylinder research engine. Due to difficulties with the stability of the employed lambda sensor readings, the equivalence ratio could only be kept constant for a set of tests, thus, results are presented for each additive and the corresponding base fuel test separately from other additives. All fuels were tested at a range of different spark advance angles and followed methods described in Chapter 4. The findings of the engine investigations are presented in Figures 6.10 – 6.27.

Figures 6.10 – 6.12 display the knock intensities (KI) for the test fuels. It can be observed that, as expected, the CI-A additive promotes auto ignition in gasoline fuel. For the tested range of spark timings, the base fuel and CI-A 1X behaved similarly up to spark advance angle of 50 CAD after which about a 39.4 % increase in KI could be seen. CI-A 10X demonstrated similar combustion characteristics only at very late spark advance angles. Advancing spark earlier than 35 CAD caused a sudden increase in the KI that peaked at 45 CAD. At that point a 185.2 % increase in knock intensity was experienced.

KI measurements for CI-I are displayed in Figure 6.11. Up to spark timing of 45 CAD all fuels exhibited similar characteristics. However, advancing the spark further caused an increase in KI for both the base and 1X concentration fuels. Very similar characteristics were seen throughout the measured range for the two fuels except for very early spark timing where a 28.6% decrease in KI was seen. At 10X concentration, CI-I displayed strong anti-knocking properties with no spark advance points in the measured range where sudden increase in KI could be seen. Largest decrease in the KI level of 73.3% compared to the base fuel was experienced at the ignition advance of 65 CAD.

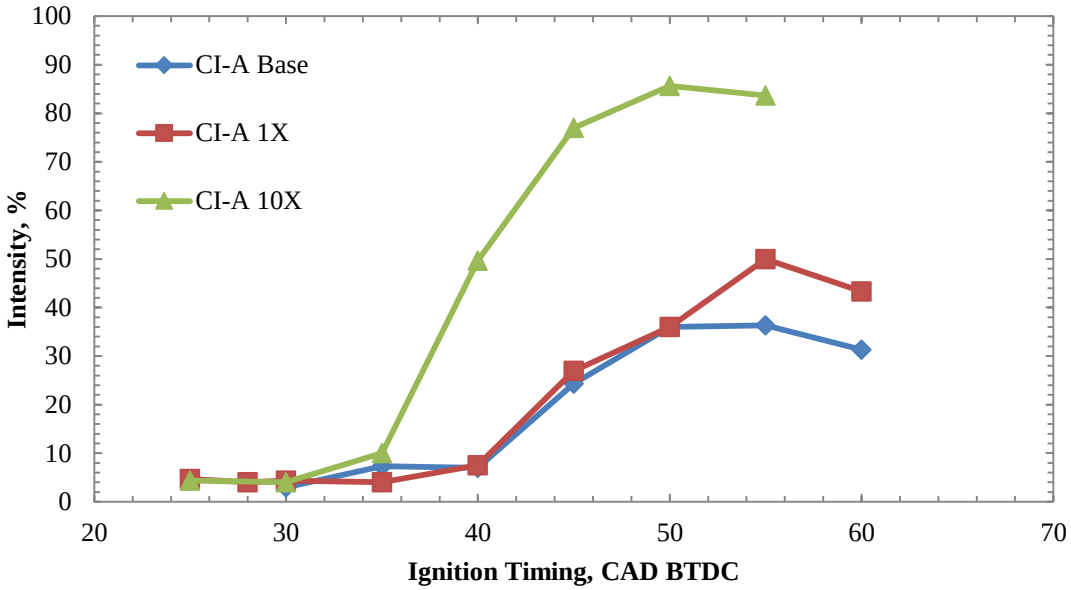

Figure 6.10: Knock intensity CI-A

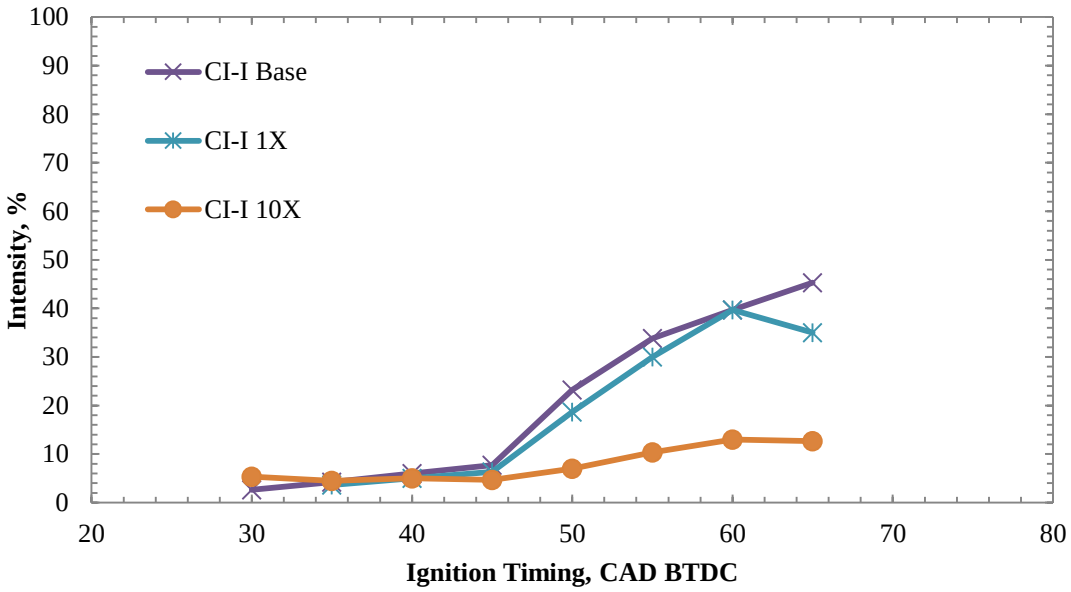

Figure 6.11: Knock intensity CI-I

KI properties for CI-Additional are displayed in Figure 6.12. CI-Additional was found to be the more effective antiknock improver between the two tested gasoline additives. At 65 CAD spark, the reduction in KI was 81.1 %. An anticipated likeness in KI characteristics for CI-I 10X and CI-Additional 1X was observed. As seen in Table 6.1, CI-I at 10X treat rate was expected to produce comparable RON changes to CI-Additional at 1X.

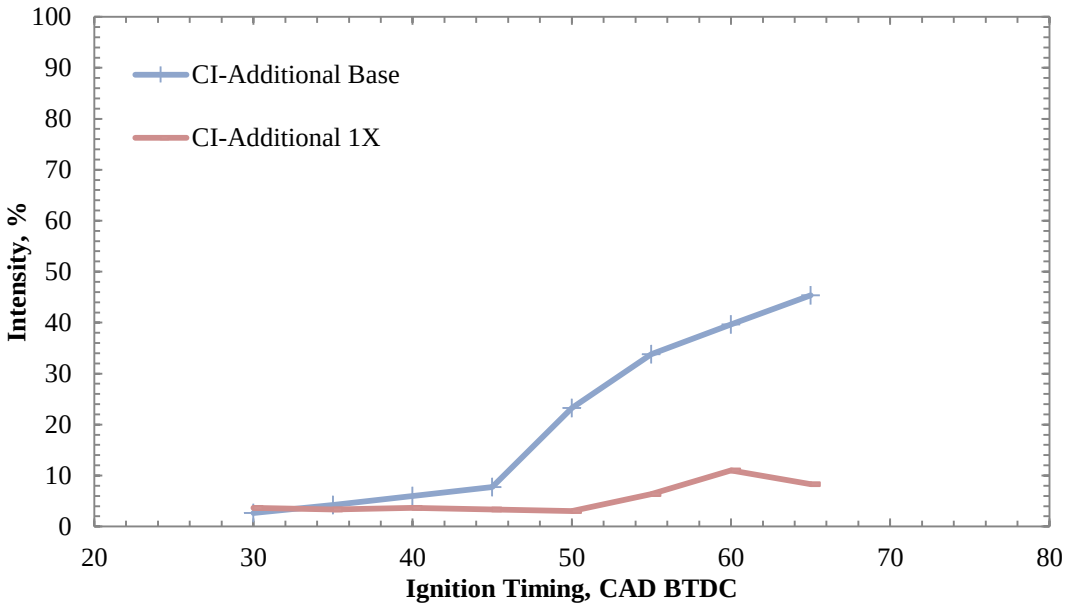

Figure 6.12: Knock intensity CI-Additional

Figures 6.13 – 6.15 display the IMEP results for all the tested fuels. CI-A at both 1X and 10X treat rates caused a reduction in the values. A probable cause for this was a reduction in ignition delay. As a result of an increased presence of ignition promoting radicals in the air-fuel mixture, it is likely more of the combustion occurred in the compression stroke. Furthermore, as KI investigations demonstrated, advancing spark timing beyond 35 CAD BTDC caused end gases to auto-ignite at higher rate than the base fuel. This would have additionally increased the proportion

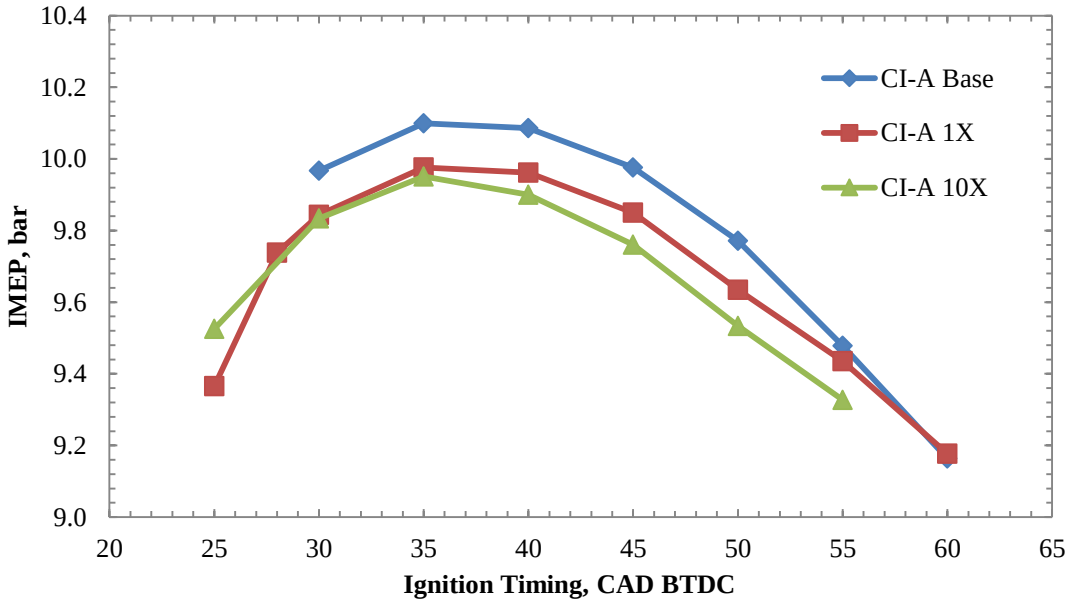

Figure 6.13: IMEP for different spark timing, CI-A

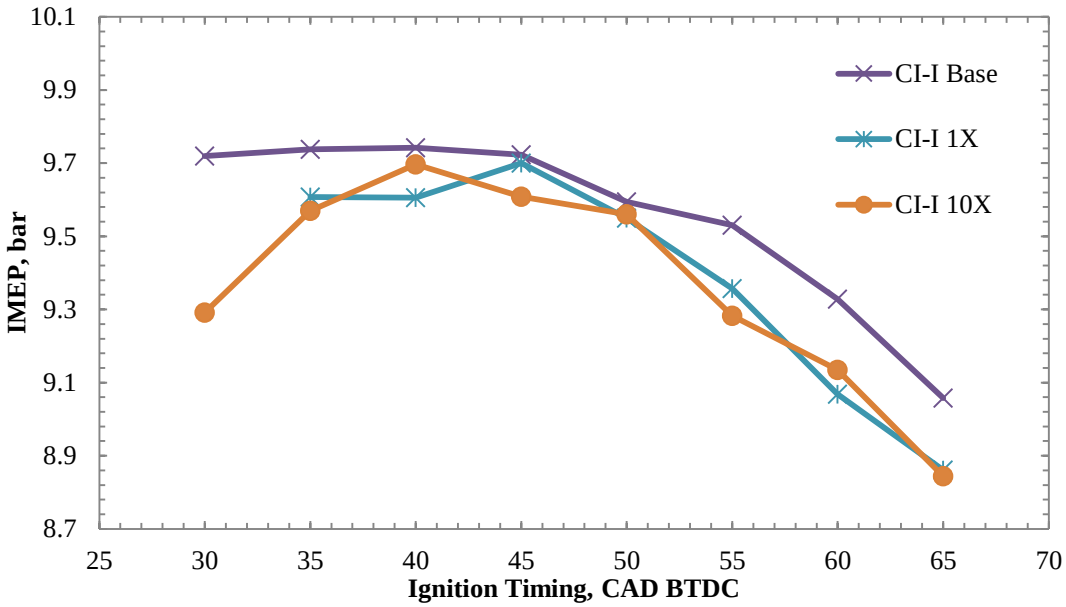

Figure 6.14: IMEP for different spark timing, CI-I

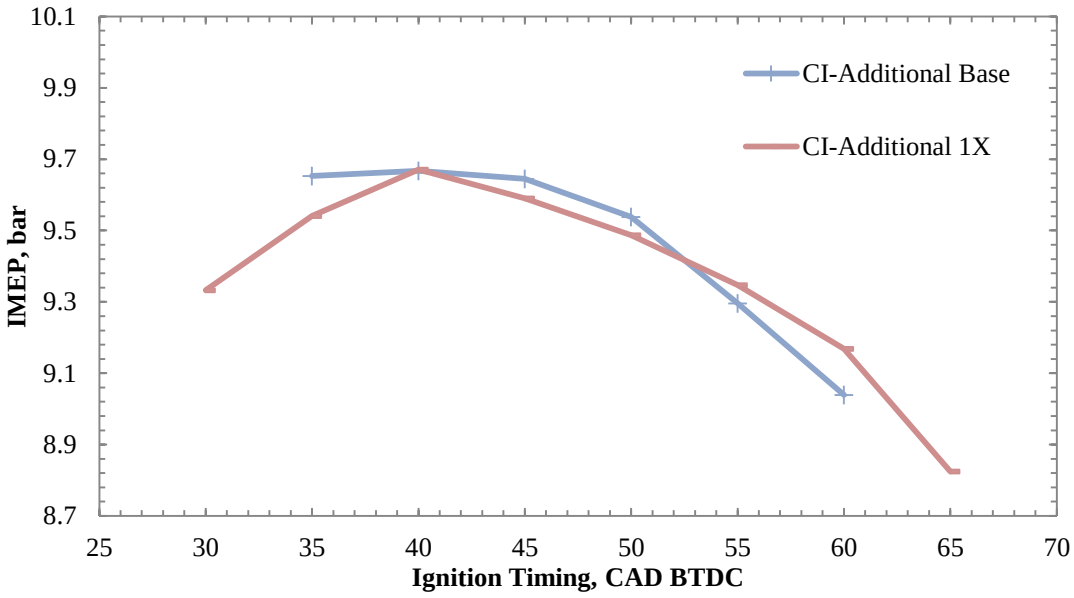

Figure 6.15: IMEP for different spark timing, CI-Additional

of combustion occurring before the power stroke, which would have inherently had an effect on the IMEP. Interestingly, the reduction in IMEP between the base fuel and 1X concentration of the additive is larger than between 1X and 10X concentrations for all but the most advanced sparking point, suggesting a diminishing effectiveness of the additive at high treat rates. Figures 6.14 and 6.15 display IMEP for CI-I and CI-Additional, respectively. In both cases a small decrease in IMEP was experienced for majority of the tested range. It is probable this was caused by the radical absorbing

nature of the antiknock additives that could have reduced the reaction rates. CI-I 1X and 10X exhibited very similar behaviour throughout the investigated range. CI-Additional at ignition advance angles of more than 55 CAD seemed to improve IMEP compared to base fuel.

In-cylinder peak pressures measurements are presented in Figures 6.16 – 6.18. It can be seen that CI-A at neither of the treat rates affected the pressures reached, while both CI-I and CI-Additional reduced the measured peaks. The reductions could

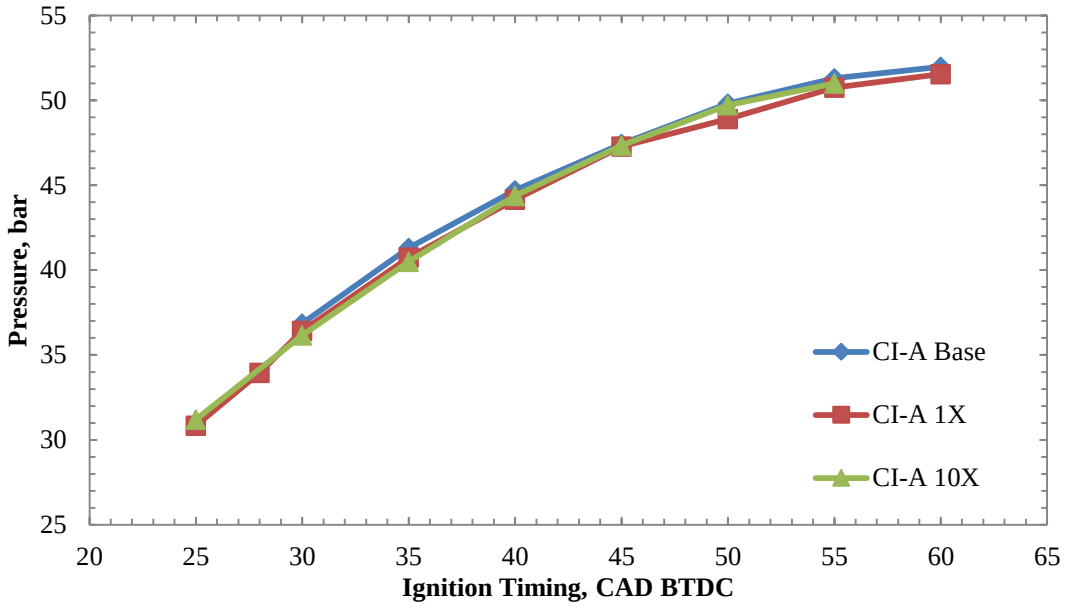

Figure 6.16: Peak in-cylinder pressure at different spark retardation angles for CI-A

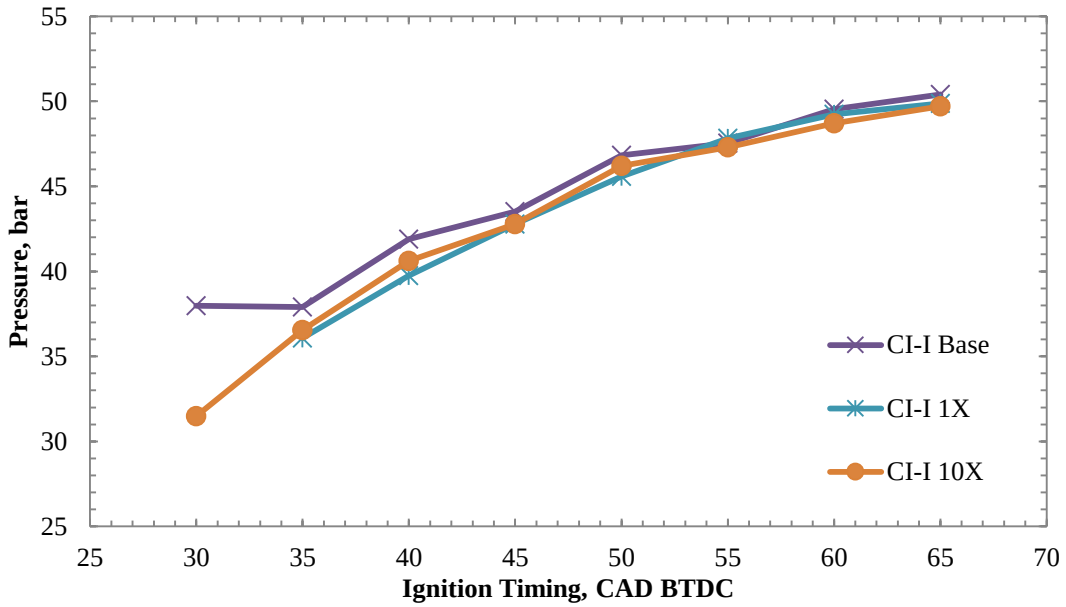

Figure 6.17: Peak in-cylinder pressure at different spark retardation angles for CI-I

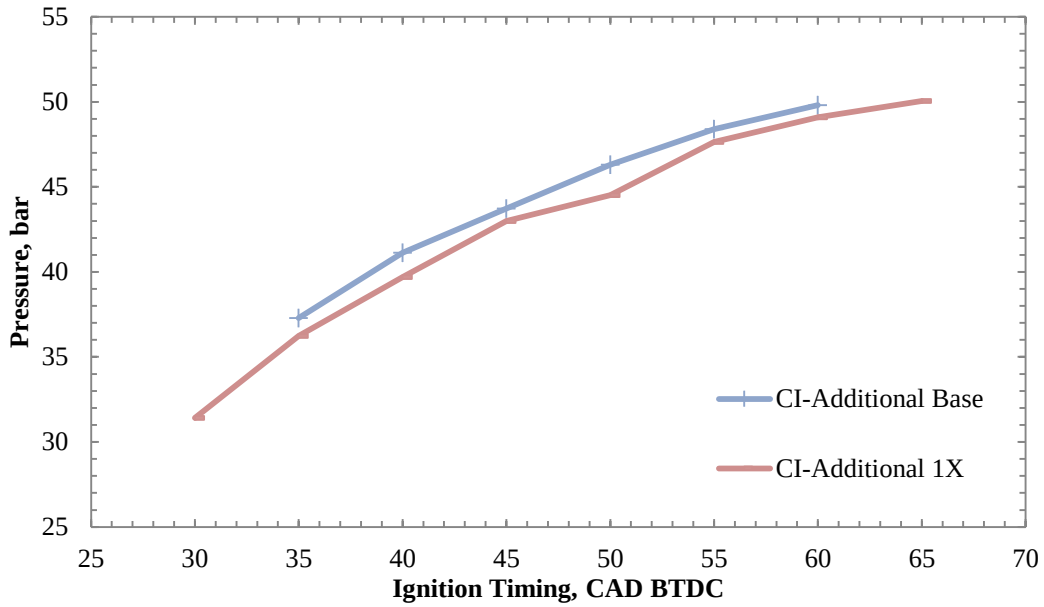

Figure 6.18: Peak in-cylinder pressure at different spark retardation angles for CI-Additional

have been caused by slower pressure rises caused by ignition inhibiting properties of antiknock additives. This would have caused more of the combustion to occur in the expansion stroke where increasing volume would mean lower peak pressure. However, the reduced IMEP values suggest that this was not the case.

Peak heat release rates displayed in Figures 6.19 – 6.21 seemed not to have been affected by the additives either. The unaffected peak pressure accompanied by reduced IMEP and increased KI for CI-A additive could be explained by the low

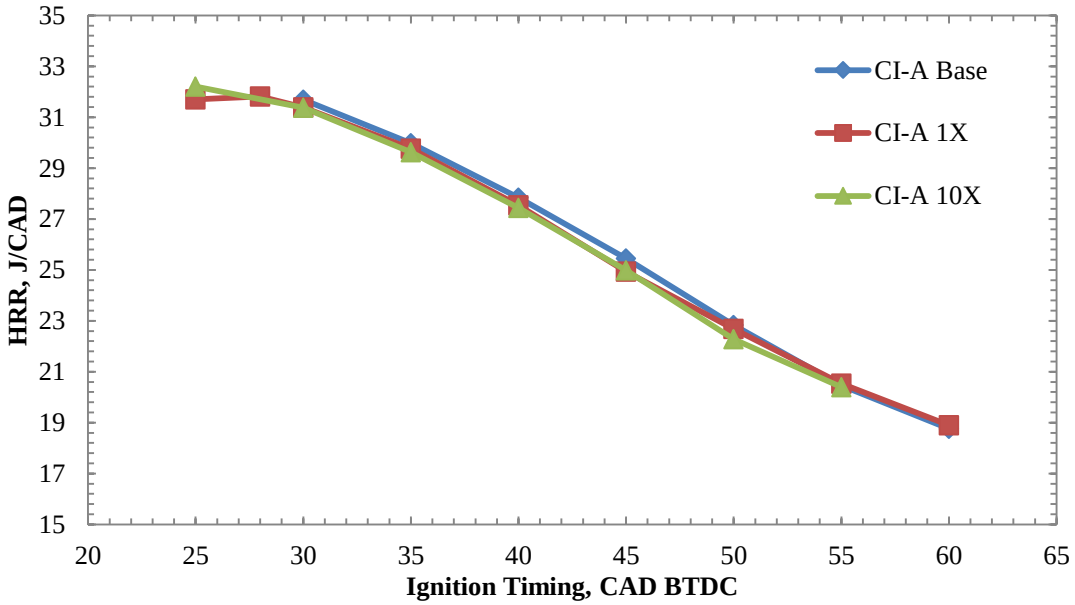

Figure 6.19: Peak heat release rate at different spark retardation angles for CI-A

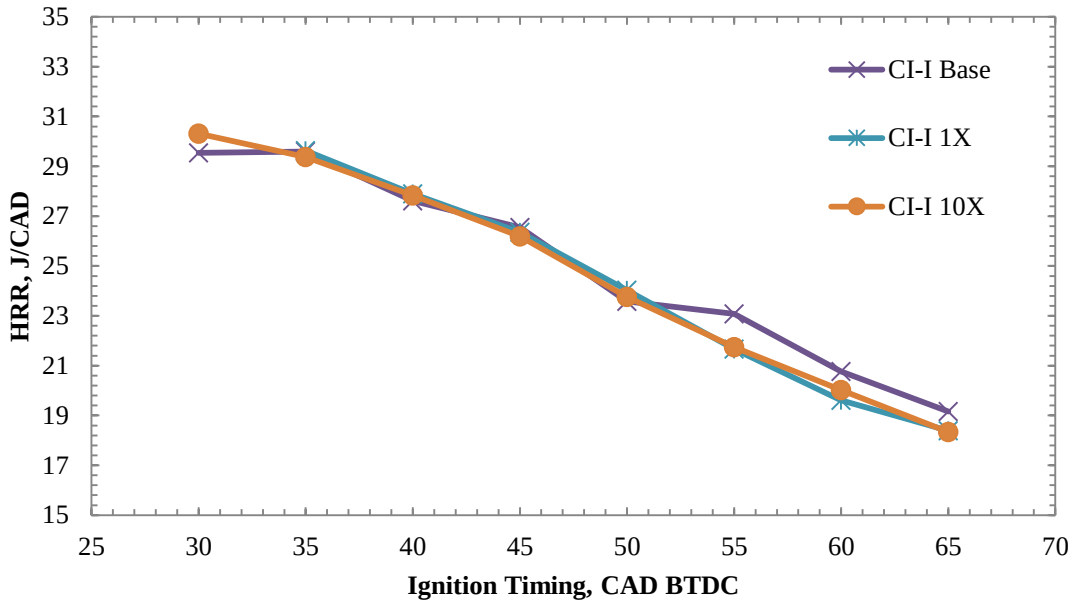

Figure 6.20: Peak heat release rate at different spark retardation angles for CI-I

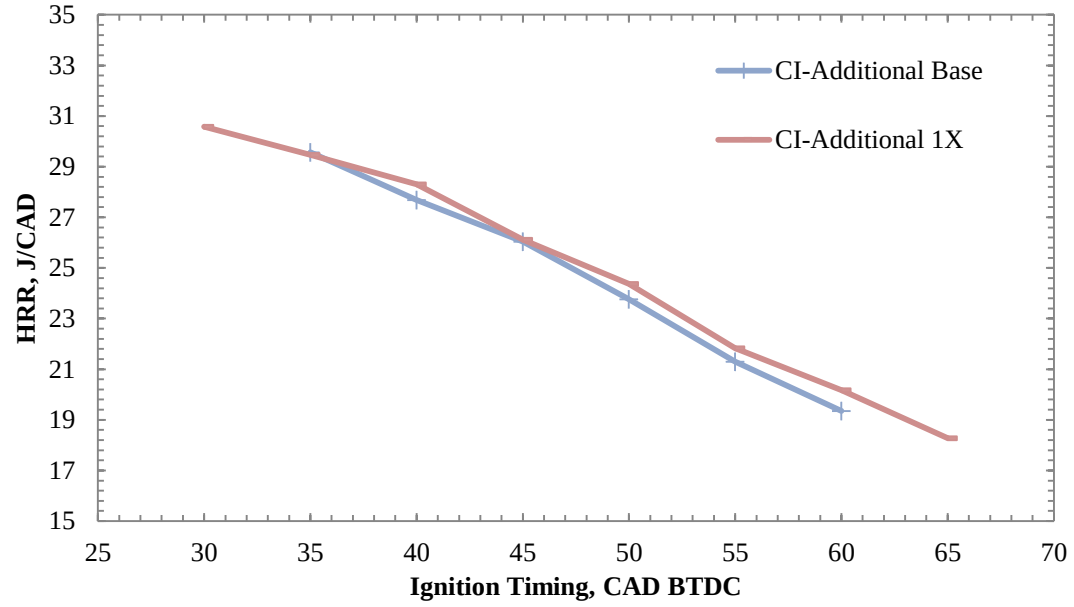

Figure 6.21: Peak heat release rate at different spark retardation angles for CI-Additional

temperature reactions. Iverson [261] explains that such reactions provide a radical pool to support following high temperature reactions and dependent upon conditions, up to 10 % of the available fuel could be consumed in the process. Should this have been the case in current investigations, less fuel would have been left to combust, subsequently resulting in lower IMEP and negligible changes to peak pressures, irrespective of the knock characteristics observed.

Figures 6.22 – 6.30 display the emissions analysis results. CI-A exhibited similar characteristics in the engine to those seen the in the combustion vessel. For 1X concentration, an improved oxidation was seen through reduced CO output and increased CO_2, while at 10X treat rate, the fuel possessed characteristics closer to base gasoline. Reduced CO output could be explained through reduced flame quenching near cylinder walls which would increase CO_2 and also likely the NO_x emissions. However, it is again unclear as to why at 10X concentration the benefits could not be seen. It has been suggested by Linteris et al. [257] that for metallic antiknock additives

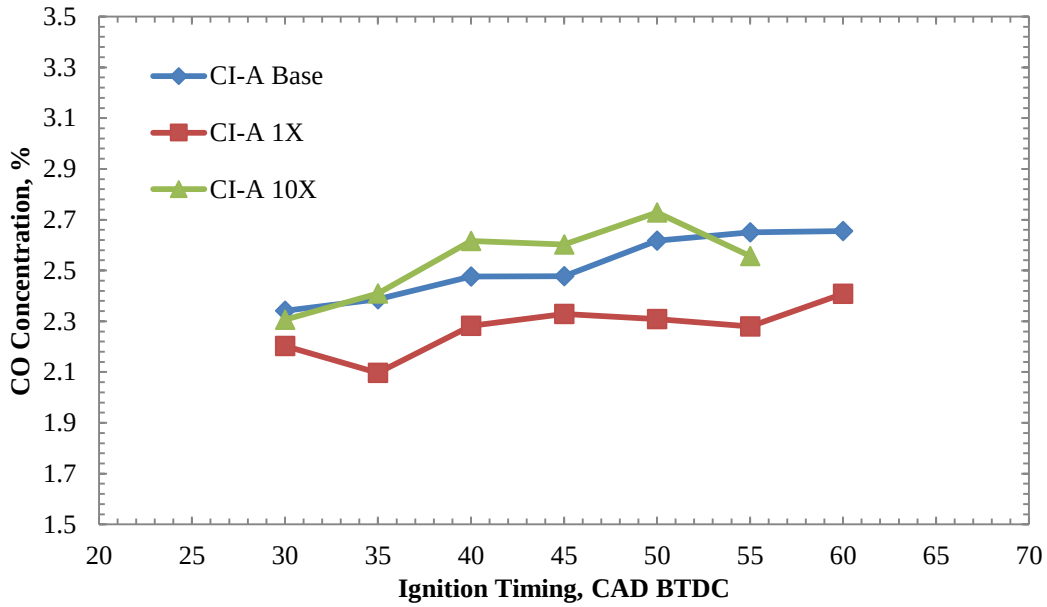

Figure 6.22: CO emissions CI-A

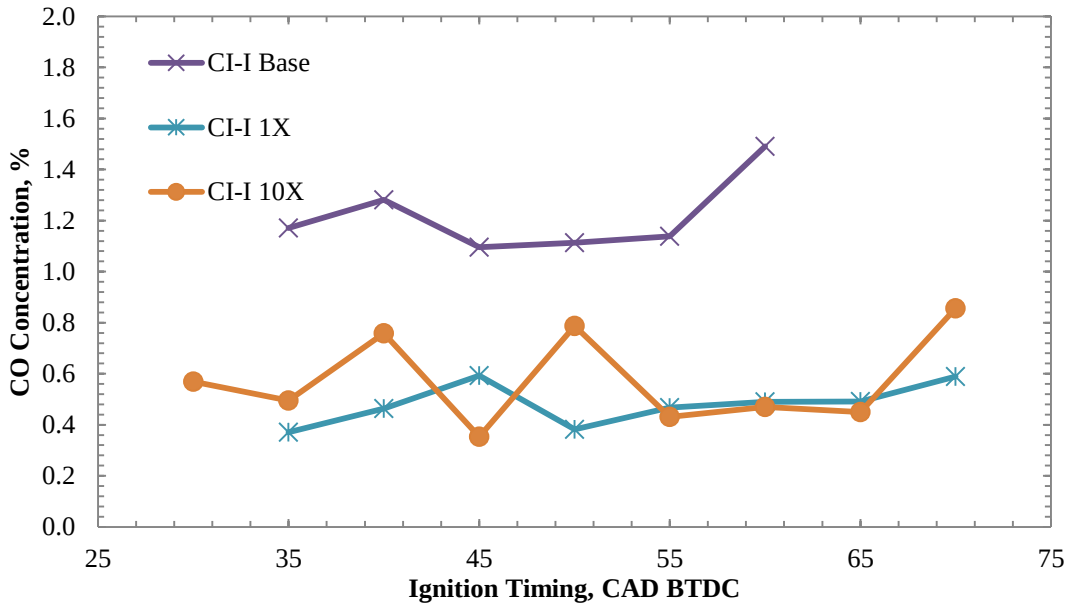

Figure 6.23: CO emissions CI-I

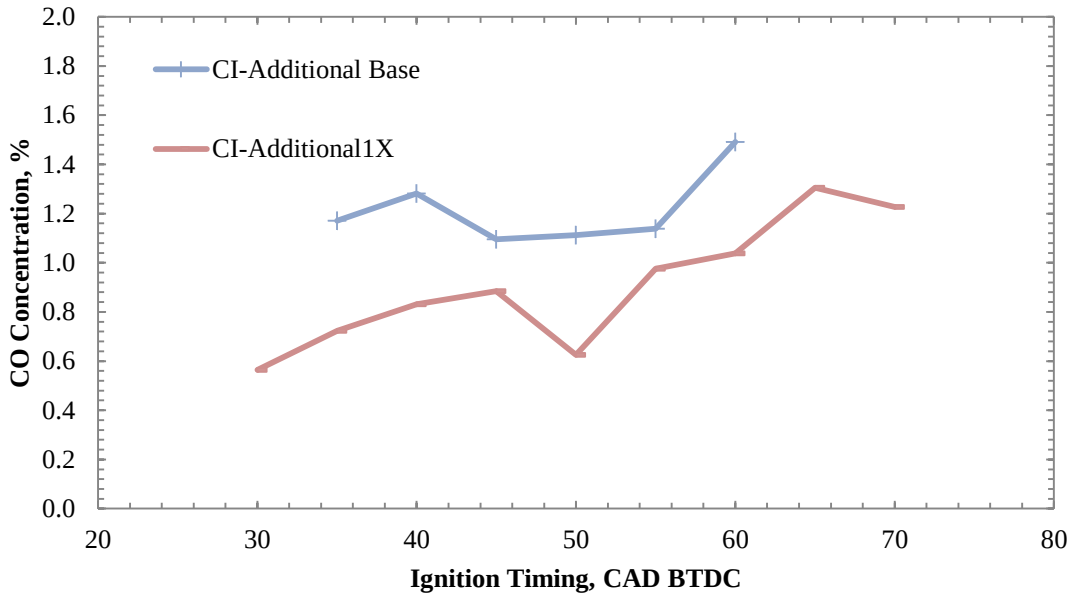

Figure 6.24: CO emissions CI-Additional

an optimum volumetric fraction of additive exists above which condensation processes occur, although, no published data on non-metallic compounds on the matter could be found.

Emissions analysis for antiknock additives suggested a more complete combustion compared to base fuels. The CO levels reduced while increased CO_2 levels were experienced. Also, an increase in NO_x emissions was observed. Although typically this could be explained by higher in cylinder pressures, as seen from Figures 6.17 and 6.18, this was not the case in present study.

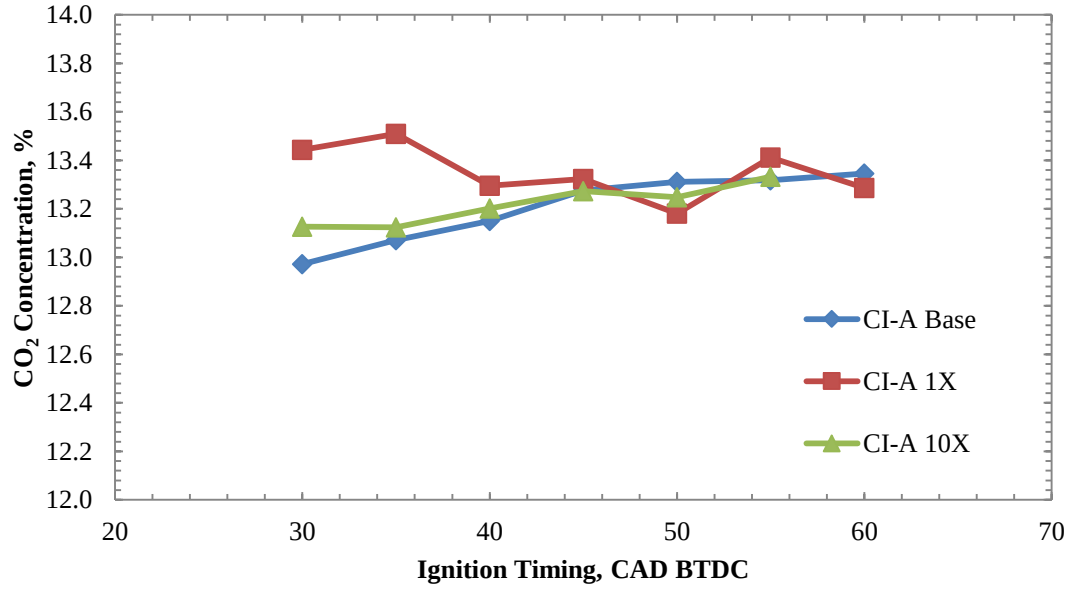

Figure 6.25: CO_2 emissions CI-A

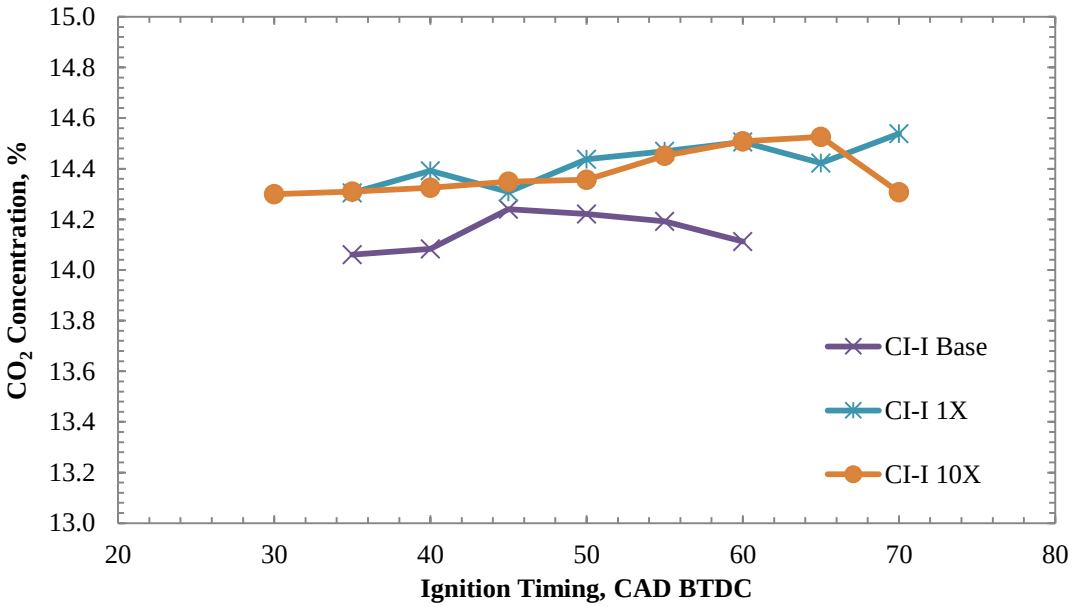

Figure 6.26: CO_2 emissions CI-I

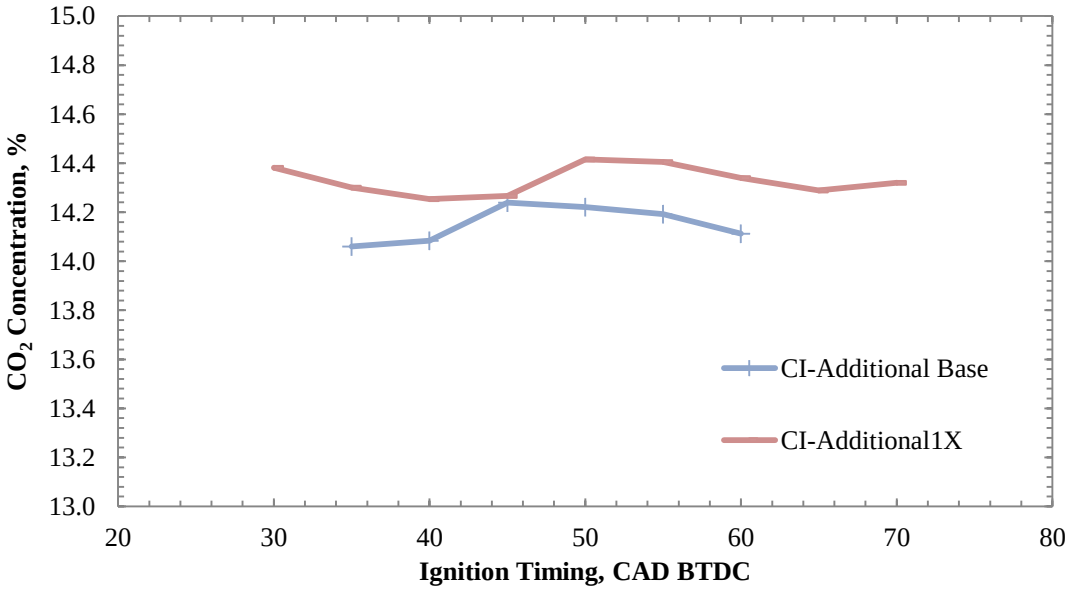

Figure 6.27: CO_2 emissions CI-Additional

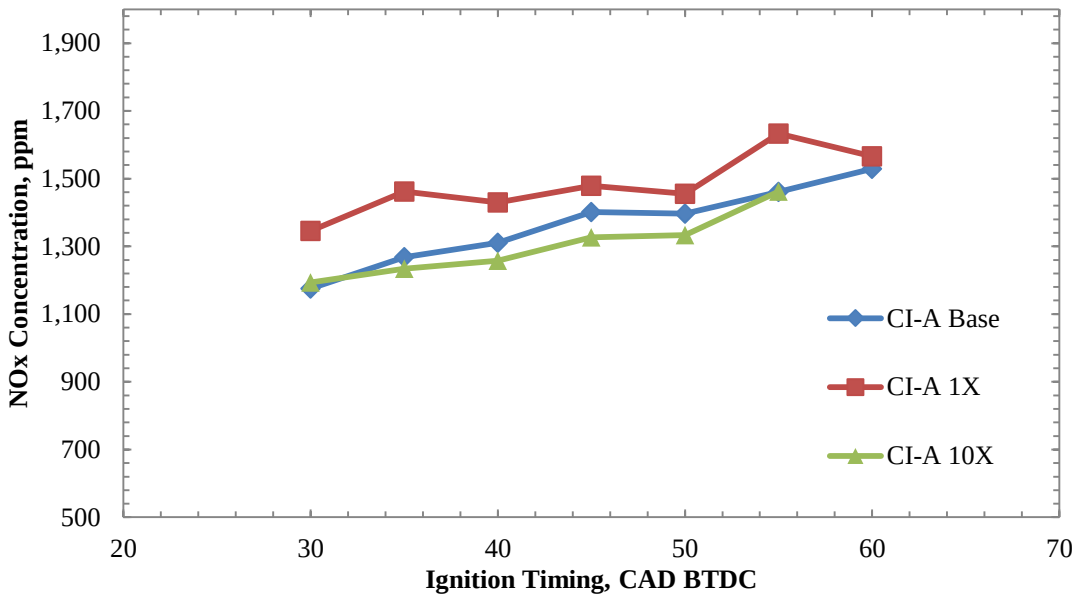

Figure 6.28: NO_x emissions CI-A

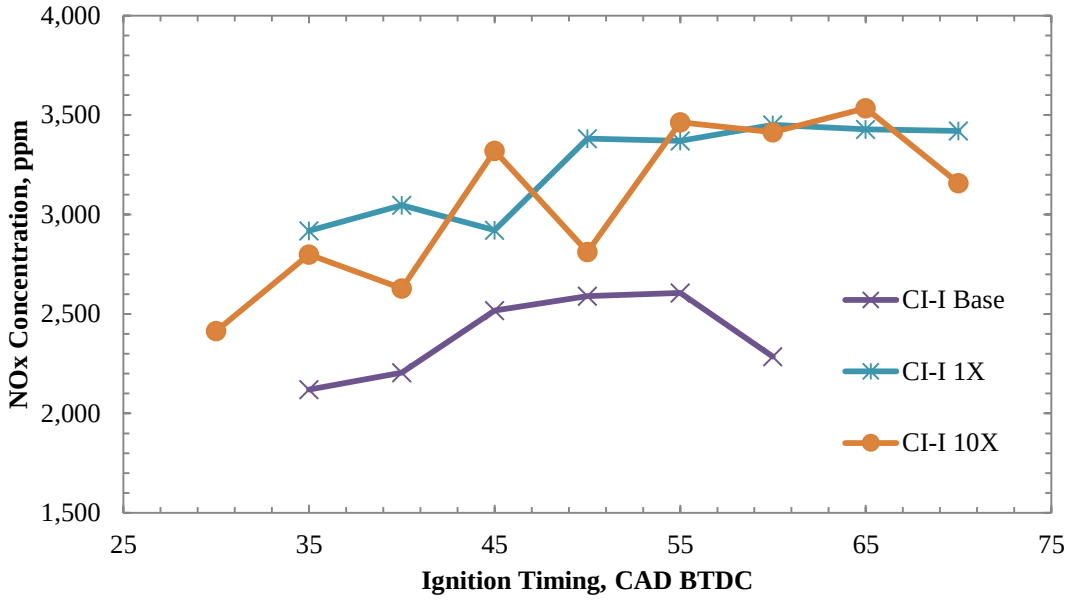

Figure 6.29: NO_x emissions CI-I

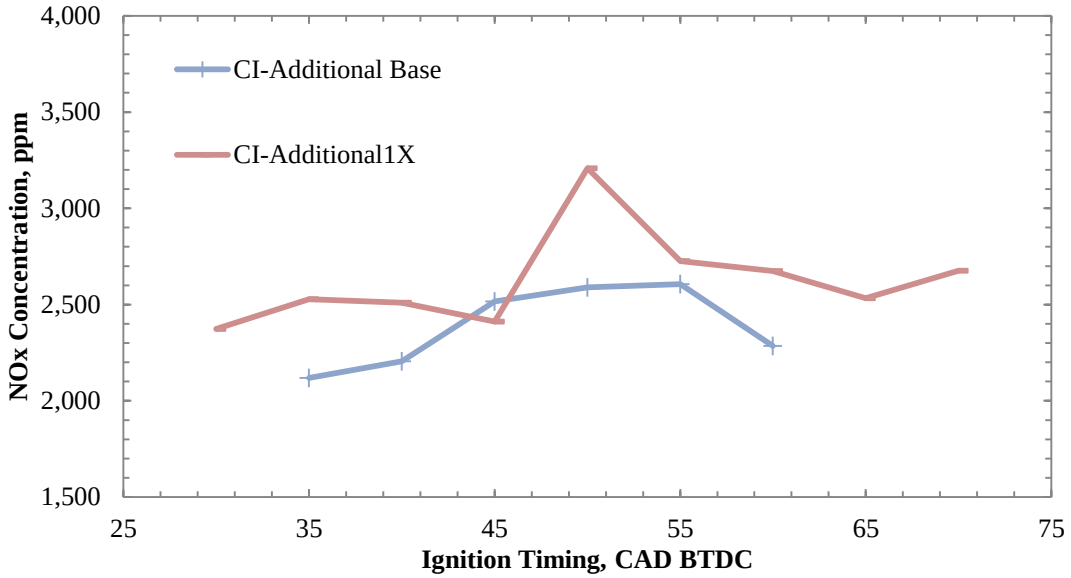

Figure 6.30: NO_x emissions CI-Additional

Figures 6.31 – 6.33 show the relationship between the time to reach peak HRR and ignition timing and in Figures 6.34 – 6.36 the relationship between the time to reach peak pressure and ignition timing is displayed. For CI-A additive at either 1X or 10X concentration, no noticeable change could be seen in the time to reach peak pressure or HRR. Although the peak pressure and HRR during knocking conditions were likely to be higher than non-knocking combustion, each combustion event was processed with a low-pass filter set below the cylinder natural frequency, thus, excluding the knocking behaviour from further analysis.

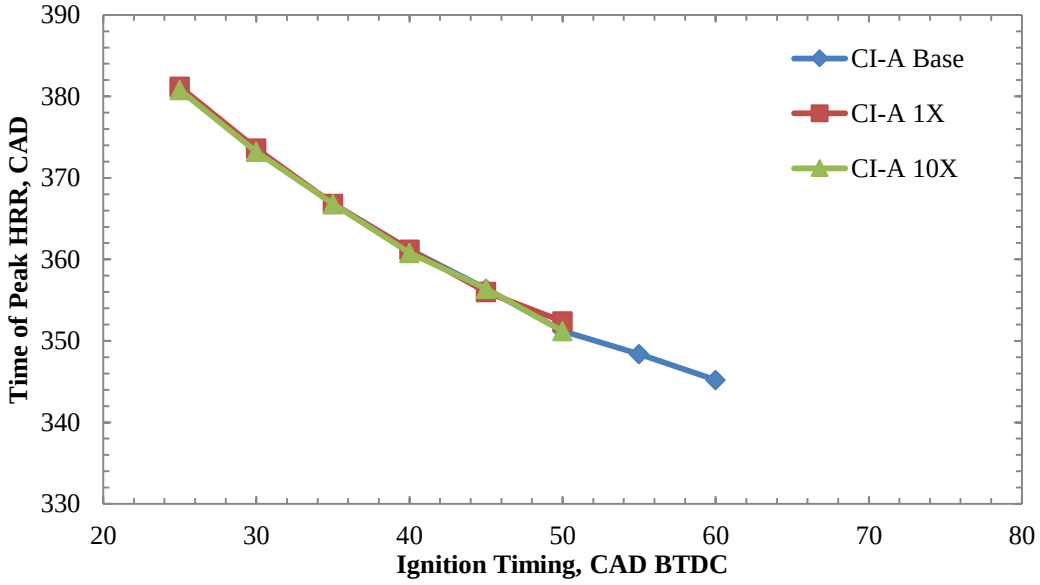

Figure 6.31: Time of peak HRR CI-A

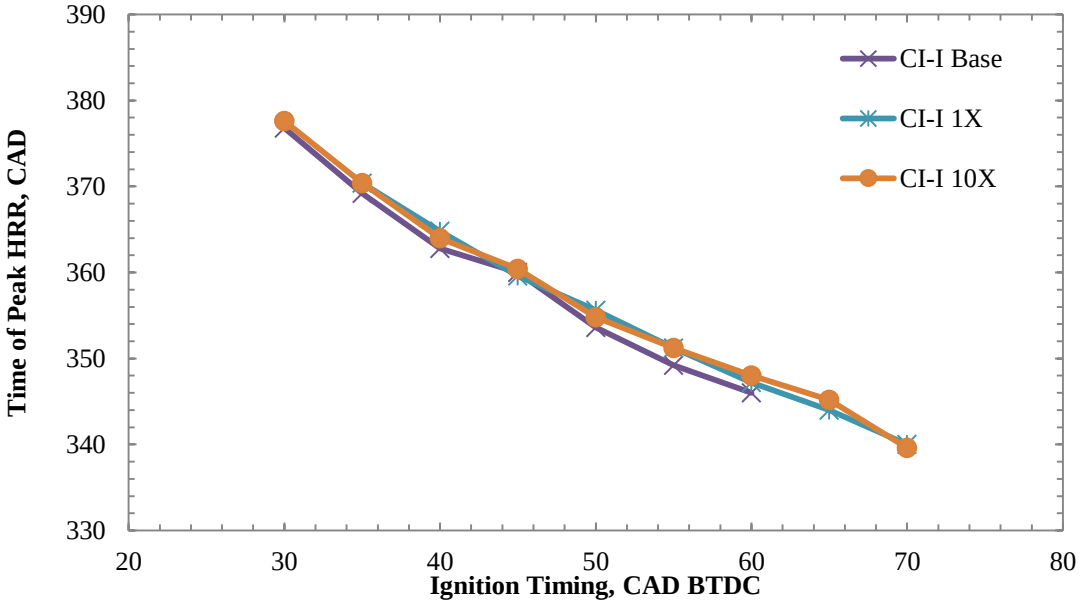

Figure 6.32: Time of peak HRR CI-I

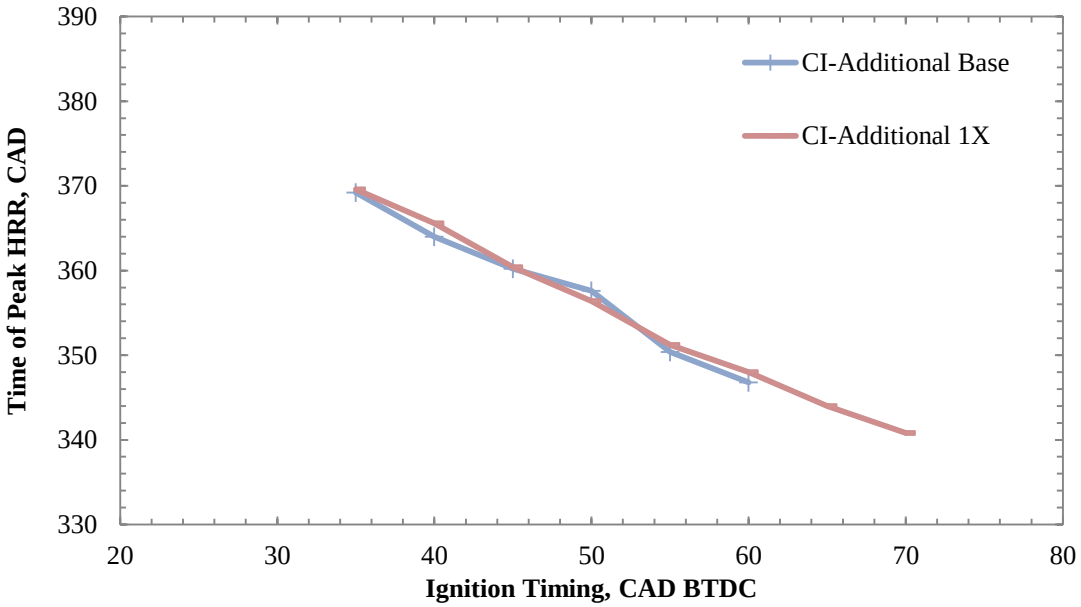

Figure 6.33: Time of Peak HRR CI-Additional

Figures 6.32 – 6.35 display the time of peak HRR and pressure with CI-I additive. At 1X and 10X similar characteristics could be observed and on average compared to the base fuel, the peak HRR and pressure were delayed by 1.3 CAD and 1.4 CAD, respectively. Savaranan and Nagarajan [262] explain that longer residency of high temperature gases in the cylinder could explain increased NO_x emissions. Furthermore, Sayin [263] found increased ignition delay to enable better air-fuel mixing that would result in reduced CO emissions.

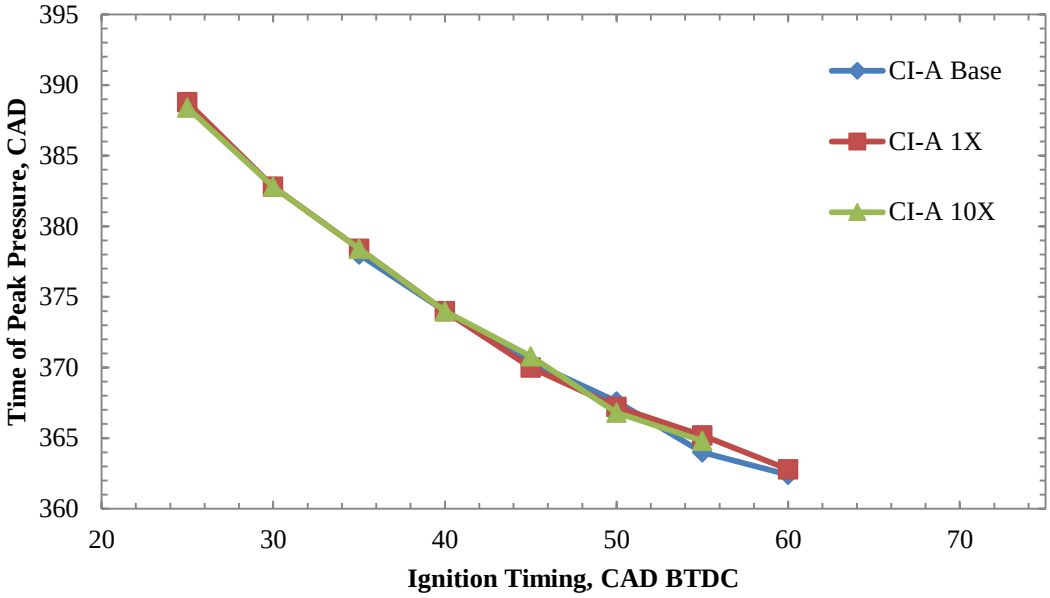

Figure 6.34: Time of peak pressure CI-A

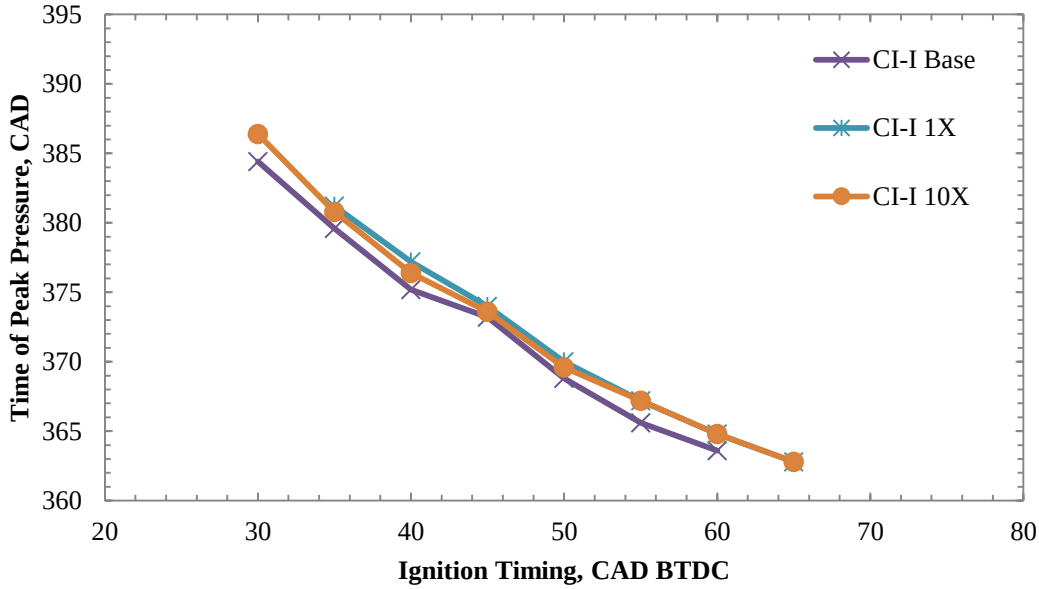

Figure 6.35: Time of peak pressure CI-I

Similar explanation could be used to explain the emissions from CI-Additional bearing gasoline, although as seen in Figures 6.33 and 6.36, the delays in reaching peak HRR and pressure compared to base fuel are shorter than for CI-I additive bearing fuel, at 0.5 CAD and 0.93 CAD on average, respectively. Similar magnitude percentage changes to the timings of peak pressure and HRR between the anti-knock additive bearing fuels and the base fuel also apply for CO, CO_2 and NO_x emission characteristics.

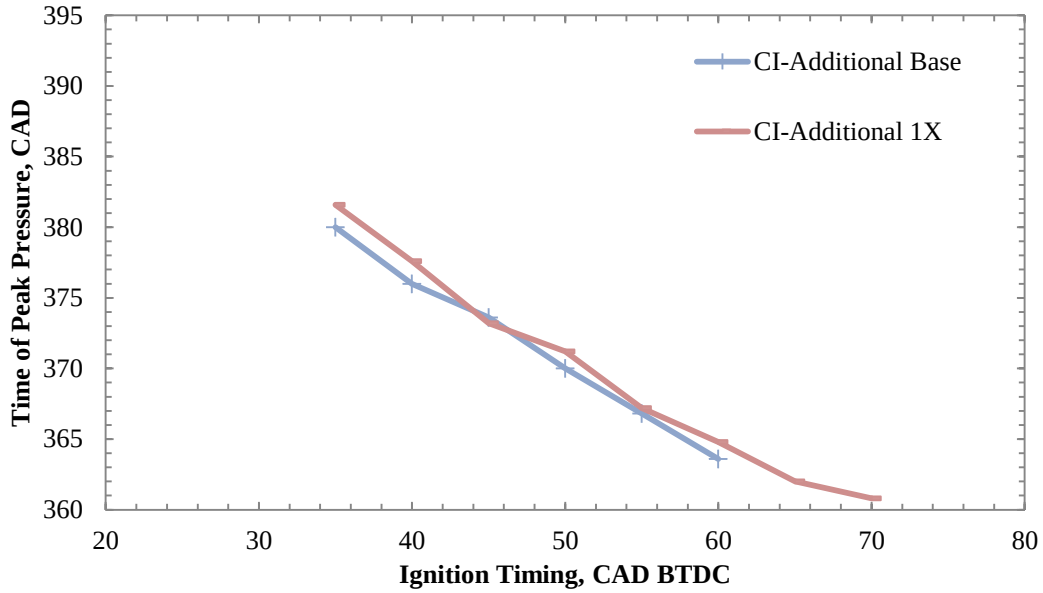

Figure 6.36: Time of peak pressure CI-Additional

6.4 Experimental Error Assessment for Combustion

Similarly to droplet sizing experiments, standard deviation around the measured mean value for a specific characteristic was used to identify any significant additive effects. Gasoline vapour combustion study was carried out on a 5 event average. Initial base fuel analysis showed that mixture preparation to within 1.3 % of measured fuel equivalence ratio could be achieved, while the peak pressure variability was within 2 % of the mean value over the same number of combustion event. This variability was shown to be larger at the final results analysis stage, where peak pressure variability throughout the base fuel tests was seen to be 4.8 %. Similar variability values were found for initial temperature and pressure conditions. Peak HRR was seen to exhibit a standard deviation of 16.3 % while flame speed measurements had a variability of 11.3 %. It can be seen from Section 6.2 that this meant the additive bearing fuel characteristics were within these variability limits and as such no effect from the additives beyond the experimental error could be identified. The variability in emissions characteristics was 16.4 % for CO, 20.6 % for NO_x and 3.2 % for CO_2. The maximum reduction in the CO emissions from the additive study was 37.7 % which was found to be the only measured parameter from the gasoline vapour combustion experiments to exhibit characteristics beyond experimental variability.

The combustion study in the research engine was carried out over a 300 cycle average which for the IMEP values meant that a maximum error of 1.7 % was noted. Since the emissions study was carried out continuously during engine running, only a single reading was taken per test and since each test was carried out under slightly different conditions it was not possible to estimate the variability in the measurements. From Section 6.3 it could be seen that erratic emissions reading were taken, especially for the anti-knock additives. This was thought to result from misfiring cycles where increased oxygen levels reduced CO, CO_2 and NO_x emissions. Although this effect could be taken out of analysis of pressure and HRR, it was not possible for emissions measurements. However, the large number of repeat cycles over which the analysis was carried out meant that the emissions readings were taken over about a 60 second period which was thought to be sufficient to enable identification of general trends in measured parameters.

6.5 Conclusion

Chapter 6 has presented the results of an investigation into the effects of fuel additives on the chemical properties of base fuel in combusting environments. Initially, gasoline vapour combustion with homogeneous mixtures in the constant volume combustion vessel was analysed. The study included heat release, burning velocity, ignition energy and emissions analysis. Subsequently, tests were carried out in a research engine and analysed based on heat release and emissions analysis. Several noteworthy results were observed.

The effectiveness of CI-A additive was most noticeable at 1X concentration. In both, the combustion vessel and engine experiments, the CO level reduced by up to 40 % compared to the base fuel. Also, in both cases at 10X treat rate, the emission characteristics were closer to base fuel. Based on results observed in current study, it was assumed the drop in CO originated from reduced flame quench layer thickness near combustion vessel and combustion chamber walls. It is unclear as to why the benefits of the additive could only be seen at 1X and not 10X treat rates. Higgins et al. [10] observed improvements in combustion characteristics when the base treat rate used was 60 % higher than the 10X used in the current study. The CO characteristics are especially remarkable since engine testing revealed increased low temperature reactions at 10X concentration compared to 1X through increased knock intensity.

Although it has been suggested that additive bound nitrogen can contribute towards increased NO_x emissions [48, 49], current investigation cannot support the claim due to emissions at 10X treat rate being significantly lower than at 1X. It is worth mentioning, however, that comparisons are made to research carried out on diesel fuels and changes in chemical reaction pathways compared to gasoline could exist.

CI-I antiknock additive results in the combustion vessel did not produce conclusive results. Highest peak heat release rate and pressure were seen. However, it is unclear if this was caused by limitations in experimental repeatability, as based on literature the opposite should have been observed. This was not the case in the engine tests. Reductions in knock intensity with increasing additive concentrations could be observed as well as reductions in IMEP and peak in-cylinder pressures. Furthermore, improvements in emissions characteristics were seen which was thought to result from reduced reaction rates that enabled improved air-fuel mixing in the combustion chamber due to longer time scales available. Similar results to CI-I were observed for CI-Additional, although improved antiknock properties at similar RON changes were experienced.

The results found from present study have shown the suitability of the methods employed for the analysis of fuel additive effects on fundamental combustion characteristics although some improvements could be implemented. Vapour combustion displayed that changes in emissions and flame speed to an extent could be observed, although low experimental repeatability suggested a larger number of repeats should be carried out. In the engine, a good coefficient of variance was achieved through the use of a 300 cycle average. However, as was the case with CI-I and CI-Additional, slightly lean air-fuel ratios affected the emissions readings. It is possible that this was due to misfires that caused increases in the oxygen levels and subsequent changes to all measured emissions.

Chapter 7

Conclusion and Suggestions for Further Studies

The previous chapters have offered an in-depth description of the work carried out throughout the present study. The work has focused on investigating the effect additives have on base fuel physical and chemical characteristics with the primary objective being to involve experimental methods to improve on the existing understanding of the de-coupled effects of additives on the combustion processes. Chapter 7 seeks to provide concluding notes on the findings as well as suggest directions in which future investigations could improve on the existing body of knowledge on fuel additives.

7.1 Spray Investigations

Fundamental DI spray characteristics were analysed for a range of additives and fuels at varying conditions. A laser diffraction system was utilised to produce SMD data that enabled quantification of spray quality differences and a novel fuel quantity based comparison method was developed to take into account of temporal variation of spray characteristics at various injection pressures.

The investigations were carried out on 17 fuel additives from 6 functional groups in two concentrations. Additionally, a non-fuel bound viscosity modifier was studied along with a selection of single component fuels and their binary mixtures. Due to the proprietary nature of the additives in present study, only restricted evidence regarding their chemistry was available. The limited information offered was summarised in Section 5.1.1 (Page 117). Additionally fuel viscosity and surface tension was measured for the base fuel and its additive bearing derivatives at concentrations ten times higher than the commercially suggested rate. Similarly to previously published studies on diesel sprays with additives, it was concluded that the effect of additives on gasoline atomisation characteristics is too small to be identified within the experimental error. The key findings can be summarised as follows:

- Fuel atomisation characteristics remained unaffected by fuel additives even in concentrations ten times higher than the commercially suggested rates under high fuel injection pressure and ambient temperature conditions.
- Other than drag reducing agents, fuel viscosity remained unaffected by the addition of fuel additives in concentrations ten times higher than the commercially suggested rate. Drag reducing agents increased the base fuel viscosity by nearly 200 % due to their high molecular weight molecules and resulting molecule agglomerates. Due to their nature, however, the high pressure DI environment meant the molecules went through shear degradation resulting in a more than 45 % loss in viscosity. This drop in viscosity was enough to make capturing changes to SMD indistinguishable with the chosen methodology.
- No fuel additive seemed to affect the surface tension of the base fuel.
- Studies of the binary mixtures of single component fuels showed that fuel physical properties (surface tension and viscosity) change proportionately to their constituent components and have a similar effect on the fuel atomisation characteristics. This result was important from additives point of view. Applying the proportionality to additive quantities in fuel explains why no change in spray characteristics could be identified. The exceptions in this case were the drag reducing additives that affected physical properties of fuels beyond the proportionality due to their high molecular weight molecules and

resulting molecule agglomerates. However, as mentioned, these agglomerates break up during high pressure DI processes.

Although, as shown in Chapter 4, the 50 spray events over which the averaging was carried out reduced moving average changes to below 0.3 %, each of the base fuel measurements demonstrated limitations in overall experimental repeatability levels. The variability could have been induced by small fluctuations in ambient temperature conditions or injector operational characteristics. Although measures such as controlling temperature beyond ambient conditions and characterising injector coil current and voltage, injector needle lift and mass flow rate of the nozzle would enable reduced experimental error and improved analysis of results, the effects additives impose on the physical properties of the base fuel are very small and the potential benefits of refining analysis further are limited.

In conclusion, the study into the effect of additives on gasoline high pressure sprays demonstrated that fuel additives, in commercially used quantities, impose no undesirable properties on fuel atomisation characteristics that could hinder combustion efficiency and their only effect can be assumed to occur within their intended functionality.

7.2 Combustion with Additives

Investigations into the effects of additives on combustion characteristics were carried out in a constant volume combustion vessel with pre-mixed gasoline vapour and in a single cylinder research engine. The study concentrated on investigating combustion improvers and their effects on gasoline heat release rate, flame speed, knock intensity and emissions. Although initially spray combustion in the combustion vessel was planned, preliminary results showed small pressure rises and low experimental repeatability and consequently vaporised gasoline combustion was carried out.

The additives investigated included an organic and an organometallic anti-knock additive and an organic ignition improver. A detailed description of the additives used was given in Section 6.1 (Page 138). Similarly to spray investigations, two additive concentrations were studied except for the organometallic anti-knock

additive that was only investigated at commercially used treat rate. The main observations of the study on CI additive effects on combustion characteristics are:

- CO emissions from pre-mixed gasoline vapour combustion for CI-A additive at 1X treat rate reduced by 37.7 %. In the engine testing a maximum of 12.8% reduction was experienced at spark timing of 35 CAD BTDC. At 10X treat rate, no improvements in the characteristics over base fuel were noted. Although it is unclear why improvements in the 10X concentration were not experienced, at 1X it is believed the reductions originate from reduced flame quenching near the combustion chamber walls. The lower level of CO reduction in the engine experiments can be explained by a smaller wall surface area of the combustion chamber compared to the combustion vessel.
- Improved CO to CO_2 conversion was seen with antiknock additives. This was thought to result from increased combustion duration that allowed for longer periods for the combustion reactions to take place. On average, compared to base fuel peak HRR was reached 1.3 CAD later with CI-I additive at both 1X and 10X concentrations and 1.4 CAD later for peak in-cylinder pressure. An increase with both anti-knock additives was observed for NO_x emissions which was thought to be caused by longer residence of hot gases within the combustion chamber as a result of increased combustion durations.
- Burning velocity for premixed gasoline vapour combustion with CI-A additive at 1X treat rate increased by 5.4 % when compared to the base fuel. At 10X treat rate no change could be noted. However, the results are based on a small sample and no definite conclusions can be made on the additive effects on flame speed.
- Investigation into the effect of ignition energy revealed that no effect could be determined on premixed gasoline vapour combustion. This compares favourably to several researcher who showed that as long as minimum ignition energy (MIE) is supplied by the spark discharge, no changes to the subsequent reactions can be seen. MIE for a gasoline-air mixture is said to be 0.8 mJ while minimum recorded energy in the present study was 8.7 mJ. No measurements of spark energy were completed in the engine experiments.

- Measured knock intensity in the engine for CI-A 1X was very similar to base fuel except for advanced spark timings (>55 CAD BTDC). Greatly increased KI for CI-A 10X could be seen with ignition timing of 35 CAD BTDC or earlier. CI-I 1X KI was very similar to that of the base fuel. CI-I 10X and CI-Additional 1X behaved similarly with greatly suppressed knocking observed throughout the tested range of ignition timings. This is in line with estimated RON increases described in Table 6.1 (Page 139).

The combustion investigation demonstrated, mainly due to the number of samples involved, engine testing to be a better suited method for studying the effect of additives on combustion characteristics than the combustion vessel. It was evident from results that initial conditions in the combustion vessel had a large effect on the combustion characteristics and a significantly larger sample needs to be utilised to confidently draw conclusions from the study.

The most significant result noted from the study was the effect of ignition promoter CI-A (2-EHN) on gasoline combustion. Engine and combustion vessel investigations demonstrated significant reductions in CO levels throughout the tested range with an increase in engine KI levels only occurring at ignition advance of 55 CAD BTDC or earlier at concentrations usually utilised in diesel fuels. As a result, there is basis to suggest that in low concentrations, ignition promoters can offer potential emissions benefits in spark ignited combustion systems without compromising fuel's resistance to auto-ignition.

7.3 Further Work

Although the current study has covered an extensive selection of additives and experimental methods, a number of improvements to the analysis could be implemented to advance the understanding of the effects of additives on fundamental combustion processes.

Among the main enhancements to the spray investigations would be to study atomisation in higher back pressure and temperature conditions. Such environment possesses greater likeness to engine working conditions, especially that of late injection timing under stratified injection strategy. Since current investigations have shown no significant effect on fuel atomisation to result from additive usage in

ambient conditions, the higher energy environment would highlight the additive effect on evaporation characteristics. The only limitation of higher evaporation rates is the increased beam steering effect with a laser diffraction system, though, as in current work, the effect can be taken into account with appropriately selected settings on the equipment.

Present investigations on the effects of additives on combustion characteristics only included compounds that are intended to modify combustion reactions. Although work on fuel atomisation suggested that additives have no unwanted effects on the physical properties of the base fuel, carrying out combustion investigations with a range of additives from all functional groups would facilitate similar judgment on their effects on combustion characteristics. Additionally lower concentrations of CI-A additive than the currently employed 1X could be investigated with regards to its effect on CO emissions and KI.

A final suggestion for future experiments on fuel additives would be to undertake engine testing with a direct injection fuel metering system. Although carburettor equipped engine testing permits investigation into combustion characteristics of fuels well and the lack of electronic fuel metering systems results in low hardware variability, with ever stringent emissions and fuel consumption regulations, an understanding of the fuel additive effects in engines equipped with state-of-the-art technology is paramount. While it is evident that DI fuel metering systems can suffer from large shot-to-shot variability, DI engine testing with additives would demonstrate their effect in real life conditions on combustion and emissions characteristics. Moreover, DI engine testing would tie together spray and combustion analysis from current study whereby, with the addition of particulate matter and unburnt hydrocarbon content in the emissions, the correlation between atomisation quality and combustion performance and their dependence on fuel additives could be evaluated.

References

[1] R. Schmer, The Motor Gasoline Industry: Past, Present and Future, Washington, DC: Energy Information Admisnistration, 1991.

[2] Federal Higway Administration, Highway Statistics 2003, U.S. Department of Transportation, 2003.

[3] European Commission, 2014. [Online]. Available: ec.europa.eu/environment/air/transport/road.htm.

[4] K. Barnes, W. D. Byfleet, S. King, H. Mach, N. J. Tilling, T. Russell and H. P. Sengers, "Fuel Additives and the Environment," Fuel Additives Group, 2004.

[5] A. A. Aradi, J. W. Roos, H. M. Scull and M. W. Meffert, "Fuels Compositions for Direct Injection Gasoline Engines Containing Manganese Compounds". USA Patent US 7,533,343 B2, 30 June 2009.

[6] K. Svensson, "Effects of Fuel Molecular Structure and Composition on Soot Formation in Direct-Injection Spray Flames," 2005.

[7] A. Lefebvre, "The Prediction of Sauter Mean Diameter for Simplex Pressure Swirl Atomisers," *Atomisation and Spray Technology,* vol. 3, no. 1, pp. 37-51, 1987.

[8] P. Felton, G. Pan, F. Bracco and L. Yeh, "Additive Effects on Atomization and Evaporation of Diesel Fuel Under Engine Conditions," 1997.

[9] B. Higgins, D. Siebers and C. Mueller, "Effects of 2-Ethylhexyl Nitrate on Diesel-Spray Processes," 1998.

[10] B. Higgins, D. Siebers, C. Mueller and A. Aradi, "Effects of an Ignition-Enhancing, Diesel-Fuel Additive on Diesel-Spray Evaporation, Mixing, Ignition, and Combustion," *Twenty-Seventh Symposium (International) on Combustion/The Combustion Institute,* pp. 1873-1880, 1998.

[11] W. Colucci, J. Smith and A. Aradi, "Gasoline Compositions Containing Ignition Improvers". USA Patent 5,782,937, 21 July 1998.

[12] R. da Silva, R. Cataluna, E. W. de Menezes, D. Samios and C. M. Piatnicki, "Effect of Additives on the Antiknock Properties and Reid Vapour Pressure of Gasoline," *Fuel,* no. 84, pp. 951-959, 2005.

[13] W. H. Stewart Jr., "Carbon in Motor Causes Many Ills," *The New York Times,* 10 March 1918.

[14] H. Rang and J. Kann, “Advances in Petrol Additive Research,” *Proceedings of the Estonian Academy of Sciences, Chemistry,* no. 52, pp. 130-142, 2003.

[15] M. Dubeck and J. P. Kleiman, “Emission Control Additive”. New York, USA Patent US Patent, 3,434,814, 25 March 1969.

[16] S. Herbstman, T. E. Hayden, T. Nalesnik and N. Benfaremo, “Gasoline Detergent Additive”. New York, USA Patent US Patent, 5,030,249, 9 July 1991.

[17] C. B. Campbell, “Deposit Control Additives - Hydroxy Polyether Polyamines”. San Fransisco, USA Patent US Patent, 4,527,996, 9 July 1985.

[18] “Lubricant Additives and the Environment,” 2007.

[19] R. Lewis and L. Honnen, “Carbamate Deposit Control Additives”. San Fransisco, USA Patent US Patent, 4,236,020, 25 November 1980.

[20] R. Lewis, “Depsoit Control and Dispersant Additives”. San Fransisco, USA Patent US Patent, 4,198,306, 15 April 1980.

[21] M. Schick, Handbook of Detergents, Part E: Applications, volume 141 ed., U. Zoller, Ed., CRC Press, Taylor and Francis Group, 2009.

[22] J. Galle, S. Verhelst, R. Sierens, L. Goyos, R. Castaneda, M. Verhaege, L. Vervaeke and M. Bastiaen, “Failure of Fuel Injectors in a Medium Speed Diesel Engine Operating on Bio-Oil,” *Biomass and Bioenergy,* no. 40, pp. 27-35, 2012.

[23] D. J. Smith, “Development of a Test Method to Evaluate Fuel Quality with Respect to Injector Fouling in Direct Injection Gasoline Engines,” 2007.

[24] K. Corkwell, “Additives Keep It Business as Usual with E85,” *Ethanol Producer Magazine,* April 2008.

[25] M. Fukui, T. Sato, N. Fujita and M. Kitano, “Examination of Lubricant Oil Components Affecting the Formation of Combustion Chamber Deposit in a Two Stroke Engine,” *JSAE Review,* no. 22, pp. 281-285, 2001.

[26] T. W. Zerda, X. Yuan and S. Moore, “Effects of Fuel Additives on the Microstructure of Combustion Engine Deposits,” *Carbon,* no. 39, pp. 1589-1597, 2001.

[27] J. D. Colwell and A. Reza, “Hot Surface Ignition of Automotive and Aviation Fluids,” *Fire Technology,* no. 41, pp. 105-123, 2005.

[28] K. Mogi, K. Hashizume, K. Arisawa and H. Kobayashi, “Analysis and Avoidance of Pre-Ignition in S.I. Engines,” *JSAE Review,* no. 19, pp. 9-14, 1998.

[29] J. B. Heywood, Internal Combustion Engine Fundamentals, McGraw-Hill, 1988.

[30] J. A. Bert, J. A. Gething, T. J. Hansel, H. K. Newhall, R. J. Peyla and D. A. Voss, "A Gasoline Additive Concentrate Removes Combustion Chamber Deposits and Reduces Vehicle Octane Requirement," *SAE Technical Paper: Fuels and Lubricants,* 1983.

[31] H. Haidar, "Combustion Chamber Deposit Effects on Hydrocarbon Emissions from a Spark-Ignition Engine," Boston, 1997.

[32] A. D. Zand, G. Nabi bidhendi, A. T. Mikaeili and H. Pezeshk, "The Influence of Deposit Control Additives on Exhaust CO and HC emissions from Gasoline Engines(Case Study: Tehran)," *Transportation Research,* vol. Part D, no. 12, pp. 189-194, 2007.

[33] G. Kalghatgi and D. Bradley, "Pre-Ignition and 'Super-Knock' in Turbocharged Spark-Ignition Engines," *International Journal of Engine Research,* vol. 13, no. 4, pp. 399-414, August 2012.

[34] W. Newby and L. Dumont, "Mechanism of Combustion Chamber Deposit Formation with Leaded Fuels," *Industrial and Engineering Chemistry,* vol. 45, no. 6, pp. 1336-1342, June 1953.

[35] G. Totten, S. Westbrook and R. Shah, Fuels and Lubricants Handbook: Technology, Properties, Performance and Testing, West Conshohocken, PA: ASTM International, 2003.

[36] J. Bartleson and E. Hughes, "Combustion Chamber Deposits - As Related to Carbon Forming Properties of Motor Oils," *Industrial and Engineering Chemistry,* vol. 45, no. 7, pp. 1501-1508, July 1953.

[37] T. W. Zerda, X. Yuan, S. M. Moore and C. A. Leon y Leon, "Surface Area, Pore Size Distribution and Microstructure of Combustion Engine Deposits," *Carbon,* vol. 37, no. 12, pp. 1999-2009, 1999.

[38] A. Danilov, "Fuel Additives. Development and Use in 2001-2005," *Chemistry and Technology of Fuels and Oils,* vol. 43, no. 2, pp. 155-171, 2007.

[39] R. A. Lewis and L. R. Honnen, "Fuel Compositions Containing Deposit Control Additives". San Fransisco, USA Patent US Patent, 4,160,648, 10 July 1979.

[40] P. Martin, L. De Lima and A. Rojas, "Characterisation and Deposit Forming Tendency of Polar Compounds in Cracked Components of Gasoline. Identification of Oxidized Sulfur Compounds," Caracas, Venezuela.

[41] X. Zhen, Y. Wang, S. Xu., Y. Zhu, C. Tao, T. Xu and M. Song, "The Engine Knock Analysis," *Applied Energy,* vol. 92, pp. 628-636, April 2012.

[42] C. Westbrook, “Chemical Kinetics of Hydrocarbon Ignition in Practical Combustion Systems,” *Proceedings of the Combustion Institute,* vol. 28, pp. 1563-1577, 2000.

[43] S. Benson, “The Mechanism of Inhibition of Knock by Lead Additives, a Chain Debranching Reaction,” *Journal of Physical Chemistry*, vol. 92, pp. 1531-1533, 1988.

[44] J. T. Gidney, M. V. Twigg and D. B. Kittelson, “Effect of Organometallic Fuel Additives on Nanoparticle Emissions from Gasoline Passanger Car,” *Environmental Science & Technology,* vol. 44, no. 7, pp. 2562-2569, 2010.

[45] D. B. Menkes and J. P. Fawcett, “Too Easily Lead? Health Effects of Gasoline Additives,” *enviromental Health Perspectives,* vol. 105, no. 3, pp. 270-273, March 1997.

[46] J. F. Rosen, “Adverse Health Effects of Lead at Low Exposure Levels: Trends in the Management of Childhood Lead Poisoning,” *Toxicology,* vol. 97, no. 1-3, pp. 11-17, March 1995.

[47] W. Dabelstein, A. Reglitzky, A. Schütze and K. Reders, “Automotive Fuels,” in *Ullmann's Encyclopedia of Industrial Chemistry,* Weinheim, Wiley - CVH Verlag, 2012, pp. 425-458.

[48] H. Sarv and N. Cernansky, “NOx Formation from the Combustion of Monodisperse n-Heptane Sprays Doped with Fuel Nitrogen Additives,” *Combustion and Flame,* vol. 76, pp. 265-283, 1989.

[49] J. Appleton and J. Heywood, “The Effects of Imperfect Fuel-Air Mixing in a Burner on NOx Formation from Nitrogen in the Air and the Fuel,” *Symposium (International) on Combustion*, vol. 14, no. 1, pp. 777-786, 1973.

[50] A. Ickes, S. Bohac and D. Assanis, “Effect of 2-Ethylhexyl Nitrate Cetane Improver on NOx Emissions from Premixed Low-Temperature Diesel Combustion,” *Energy Fuels,* vol. 23, pp. 4943-4948, 2009.

[51] W. May, “Catalyst for Improving the Combustion Efficiency of Petroleum Fuels,” Dhahran, Saudi Arabia, 2003.

[52] M. de Carvalho, E. Morgado, Jr., H. Cerqueira, N. de Resende and M. Schmal, “Behavior of Fresh and Deactivated Combustion Promoter Additives,” *Industrial & Engineering Chemistry Research,* no. 43, pp. 3133-3136, 2004.

[53] W. Haney, III and J. Sullivan, “Method and Apparatus for Improving Combustion, Thermal Efficiency and Reducing Emissions by Treating Fuel”. Patent US Patent, 4,629,472, 16 December 1986.

[54] W. Lyons and L. McKone, “Method of Operating Internal Combustion Engines”. Patent US Patent, 2,151,432, 21 March 1939.

[55] W. May and J. Lang, “The Function of Fuel Borne Metallic Catalysts in the Reduction of Thermal and Prompt NOx in Exhausts of Natural Gas Fuel Engines”.

[56] F. Gonzales, “Catalytic Clean Combustion Promoter Compositions for Liquid Fuels Used in Internal Combustion Engines”. Patent US Patent, 5,141,524, 25 August 1992.

[57] F. Gonzales, “Catalytic Clean-Combustion-Promoter Compositions for Liquid Hydrocarbon Fuels Used in Internal Combustion Engines”. Patent US Patent, 5,316,558, 31 May 1994.

[58] Kirk-Othmer Encyclopedia of Chemical Technology: Combustion Science and Technology, John Wiley & Sons, Inc., 2009.

[59] J. Oxley, J. Smith, E. Rogers and W. Ye, “Fuel Combustion Additives: A Study of Their Thermal Stabilities and Decomposition Pathways,” *Energy and Fuels,* vol. 14, pp. 1252-1264, 2000.

[60] P. Clothier, B. Aguda, A. Moise and H. Pritchard, “How Do Diesel-Fuel Ignition Improvers Work,” *Chemical Society Reviews,* vol. 22, no. 2, pp. 101-108, 1993.

[61] W. May, “Nitrogen Oxide Suppression with Combustion Catalysts,” 2009.

[62] A. Aradi and J. Roos, “Compositions Comprising Combustion Improvers and Methods of Use Thereof”. Patent EP 2 267 103 A2, 29 December 2010.

[63] M. Morsy, “Ignition Control of Methane Fueled Homogeneous Charge Compression Ignition Engines Using Additives,” *Fuel,* vol. 86, no. 4, pp. 533-540, march 2007.

[64] K. Becker, “The Influence of an Ignition Quality and Anti-Knock Properties of Light Hydrocarbons in the Diesel Engine,” 1977.

[65] H. Webb, “Catalytic Fuel Additive for Jet, Gasoline, Diesel, and Bunker Fuels”. Patent US Patent, 4,129,421, 12 December 1978.

[66] R. Carroll, N. Carroll, W. Carroll and M. Carroll, “Method and Composition for Improving Fuel Combustion”. Patent US Patent, 7,503,944 B2, 17 March 2009.

[67] G. Kitchen, III, “Combustion Improver Fuel Additive”. Patent US Patent, 4.585,462, 29 April 1986.

[68] J. Roos, L. Cunningham and X. Fuqiang, “Fuel Additives for Future Fuel and Vehicle Technologies,” *J Automotive Safety and Energy,* vol. 1, no. 2, pp. 107-114, 2010.

[69] J. Knepper and D. Sallee, “Anti-Static Compositions”. Patent US Patent, 4,356,002, 26 October 1982.

[70] J. Leonard, “Static Electricity in Hydrocarbon Liquids and Fuels,” *Journal of Electrostatics,* no. 10, pp. 17-30, 1981.

[71] J. Leonard, “Generation of Electrostatic Charge in Fuel Handling Systems: A Literature Survey,” Washington, D.C., 1981.

[72] N. Thompson, “Antistatic Agents for Organic Liquids”. Patent US Patent, 4,416,668, 22 November 1983.

[73] G. Turman, “Antistatic Gasoline Dispensing Nozzle”. Denver, USA Patent US Patent, 2,108,759, 15 February 1938.

[74] P. Koch and K. Belz, “Filter Element which Conducts Static Electricity”. Patent US Patent, 4,999,108, 12 March 1991.

[75] A. Cooney, *Additive Samples,* November 19, 2011.

[76] L. Britton, Avoiding Static Ignition Hazards in Chemical Operations, New York: American Institute of Chemical Engineers, 1999.

[77] S. Schwab and R. Kyaw, “Diesel Fuel Additive Compositions for Prolonged Antistatic Performance”. Patent EP 2 042 584 A2, 1 April 2009.

[78] N. S. Berman, “Drag Reduction by Polymers,” *Annual Review of Fluid Mechanics,* no. 10, pp. 47-64, 1978.

[79] D. N. Schulz, D. G. Peiffer, R. M. Kowalik and J. J. Kaladas, “Drag Reduction Agent”. United States of America Patent US Patent, 4,560,710, 24 December 1985.

[80] W. Brostow, “Drag Reduction in Flow: Review of Applications, Mechanism and Prediction,” *Journal of Industrial and Engineering Chemistry,* no. 14, pp. 409-416, 2008.

[81] A. Al Sarkhi, “Drag Reduction with Polymers in Gas-Liquid/Liquid-Liquid Flows in Pipes: A Literature Review,” *Journal of Natural Gas Science and Engineering,* no. 2, pp. 41-48, 2010.

[82] M. D. Warholic, H. Massah and T. J. Hanratty, “Influence of Drag-Reducing Polymers on Turbulence: Effects of Reynolds Number, Concentration and Mixing”.

[83] M. Al-Yaari, A. Soleimani, B. Abu-Sharkh, U. Al-Mubaiyedh and A. Al-sarkhi, "Effect of Drag Reducing Polymers on Oil-Water Flow in Horizontal Pipe," *International Journal of Multiphase Flow,* no. 35, pp. 516-524, 2009.

[84] S. R. Deshmukh, P. N. Chaturvedi and R. P. Singh, "The Turbulent Drag Reduction by Graft Copolymers of Guargum and Polyacrylamide," *Journal of Applied Polymer Science,* vol. 30, pp. 4013-4018, 1985.

[85] J. Shanshool and H. M. T. Al-Qumaje, "Effect of Molecular Weight on Turbulent Drag Reduction with Polyisobutylene," in *The 1st Regional Conference of Engineering Science*, 2008.

[86] H. Al-Arji, "The Effect of Drag Reducing Agent on Intake Valve Deposit," 2007.

[87] J. Hoyt, J. Taylor and C. Runge, "The Structure of Jets of Water and Polymer Solution in Air," *Journal of Fluid Mechanics,* vol. 63, no. 4, pp. 635-640, 1974.

[88] K. Chao, C. Child, E. Grens II and M. Williams, "Antimisting Action of Polymeric Additives in Jet Fuels," *Journal of American Institute of Chemical Engineers,* vol. 30, no. 1, pp. 111-120, January 1984.

[89] R. Little, R. Pratt and J. Romans, "The Effect of Additives on the Aerosolization of JP-5 Jet Fuel," *Fire Safety Journal,* vol. 5, pp. 145-156, 1983.

[90] F. Liotta and Y. Han, "Production of Ultra-Low Sulfur Fuels by Selective Hydroperoxide Oxidation," 2003.

[91] D. Wei, H. Spikes and S. Korcek, "The Lubricity of Gasoline," *Society of Tribologists and Lubrication Engineers - Tribology Transaction,* vol. 42, no. 4, pp. 813-823, 1999.

[92] F. Gustavsson, P. Forsberg and S. Jacobson, "Friction and Wear Behaviour of Low-Friction Coatings in Concentional and Alternative Fuels," *Tribology International,* no. 48, pp. 22-28, 2012.

[93] J. Williams, Engineering Tribology, New York: Oxford University Press, 1994.

[94] D. Dowson, "Developments in Lubrication - The Thinning Film," *Journal of Physics D: Applied Physics,* no. 25, pp. A334-A339, 1992.

[95] F. Bowden and D. Tabor, Friction and Lubrication of Solids, Clarendon Press, 1950.

[96] B. Davis and J. Retzloff, "Friction Modifier for Gasoline". USA Patent US Patent, 4,236,898, 2 December 1980.

[97] A. Horodysky, J. Kaminski, H. Ashjian and H. Gawel, “Friction Reducing Additives and Compositions Thereof”. Patent US Patent, 4,328,113, 4 May 1982.

[98] G. Abramo, N. Avery and J. Trewella, “Deposit Control Additives and Fuel Compositions Containing the Same”. Patent US Patent, 5,089,028, 18 February 1992.

[99] G. McLean, “Additive Concentrate for Fuel Compositions”. Patent European Patent Application, EP 0 829 527 A1, 18 March 1998.

[100] D. Palmer and S. Heikoff, “Coating Material and Method”. Patent US Patent, 4,071,639, 31 January 1978.

[101] T. Mitusova, S. Loginov, E. Polina, K. Rudyak, V. Kapustin, A. Lugovskoi and B. Vyzhgorodskii, “Improvement of the Lubricating Properties of Diesel Fuels,” *Chemistry and Technology of Fuels and Oils,* vol. 38, no. 3, pp. 167-170, 2002.

[102] ASTM International, “Standard Test Method for Electrical Conductivity of Liquid Hydrocarbons by Precision Meter,” 2012.

[103] A. Lefebvre, “Properties of Sprays,” in *International Conference on Mechanics of Two-Phase Flows,* Taiwan, 1989.

[104] A. Defrance and P. Versille, “Charge-Mixing Device”. France Patent United States Patent Office, 1,790,854, 3 February 1931.

[105] Robert Bosch GmbH, Automotive Handbook, 6th ed., Plochingen: Robert Bosch GmbH, 2004.

[106] F. Zhao, M.-C. Lai and D. Harrington, “Automotive Spark-ignited Direct-Injected Gasoline Engines,” *Progress in Energy and Combustion Science,* vol. 25, no. 5, pp. 437-562, October 1999.

[107] Delphi Corporation, “Delphi Multec GDi Multi-Hole Fuel Injectors,” 2009.

[108] S. Merola, P. Sementa, C. Tornatore and B. Vaglieco, “Effect of the Fuel Injection Strategy on the Combustion Process in a PFI Boosted Spark-Ignition Engine,” *Energy,* vol. 35, no. 2, pp. 1094-1100, February 2010.

[109] T. Anand, A. Mohan and R. Ravikrishna, “Spray Characterization of Gasoline-Ethanol Blends from a Multi-Hole Port Fuel Injector,” *Fuel,* vol. 102, pp. 603-623, December 2012.

[110] N. Fdida, J.-B. Blaisot, A. Floch and D. Dechaune, “Drop-Size Measurement Techniques Applied to Gasoline Sprays,” *Atomization and Sprays,* vol. 2, no. 20, pp. 141-162, 2010.

[111] A. Aziz and M. Ali, “Conceptual Development of a Pressure-Swirl Injector for a Two-Stroke GDI Engine,” in *1st Regional Conference on Vehicle Engineering & Technology*, Kuala Lumpur, 2006.

[112] J. Serra-Pereira, Z. van Romunde, P. Aleiferis, D. Richardson, S. Wallace and R. Cracknell, “Cavitation, Primary Break-Up and Flash Boiling of Gasoline, iso-Octane and n-Pentane with Real-Size Optical Direct-Injection Nozzle,” *Fuel*, vol. 89, no. 9, pp. 2592-2607, September 2010.

[113] P. Patel, “Development of an Optical Facility for an Investigation into the Effect of Fuel Additives on Diesel Sprays,” London, 2013.

[114] R. Baert, P. Frijters, B. Somers, C. Luijten and W. de Boer, “Design and Operation of a High Pressure, High Temperature Cell for HD Diesel Spray Diagnostics: Guidelines and Results,” *SAE Technical Paper,* 2009-01-0649 2009.

[115] C. Dumouchel, “On the Experimental Investigation on Primary Atomisation of Liquid Streams,” *Experiments in Fluids*, vol. 45, no. 3, pp. 371-422, June 2008.

[116] R. van Romunde, “Factors Affecting the Development of Sprays Produced by Multihole Injectors for Direct-Injection Engine Applications,” London, 2011.

[117] M. Pilch and C. Erdman, “Use of Breakup Time Data and Velocity History Data to Predict the Maximum Size of Stable Fragments for Acceleration-Induced Breakup of a Liquid Drop,” *International Journal of Multiphase Flow,* vol. 13, no. 6, pp. 741-757, 1987.

[118] M. Jaalal and K. Mehravaran, “Fragmentation of Falling Liquid Droplets in Bag Breakup Mode,” *International Journal of Multiphase Flow*, vol. 47, pp. 115-132, 2012.

[119] C. Acroumanis, M. Gavaises and B. French, “Effect of Fuel Injection Processes on the Structure of Diesel Sprays,” 1997.

[120] S. Lin and R. Reitz, “Drop and Spray Formation from a Liquid Jet,” *Annual Review of Fluid Mechanics,* no. 30, pp. 85-105, 1998.

[121] J. Strutt and Lord Rayleigh, “On the Instability of Jets,” in *Proceedings of the London Mathematical Society*, London, 1878.

[122] G. Faeth, L.-P. Hsiang and P.-K. Wu, “Structure and Breakup Properties of Sprays,” *International Journal of Multiphase Flow,* vol. 21, pp. 99-127, 1995.

[123] A. Yule and I. Filipovic, “On the Break-Up Times and Lengths of Diesel Sprays,” *International Journal of Heat and Fluid Flow*, vol. 13, no. 2, pp. 197-206, June 1992.

[124] S. Som and S. Aggarwal, "Effects of Primary Breakup Modelling on Spray and Combustion Characteristics of Compression Ignition Engines," *Combustion and Flame,* vol. 157, no. 6, pp. 1179-1193, June 2010.

[125] I. Roisman, L. Araneo and C. Tropea, "Effect of Ambient Pressure on Penetration of a diesel Spray," *International Journal of Multiphase Flow,* vol. 33, no. 8, pp. 904-920, August 2007.

[126] S. Yao, J. Zhang and T. Fang, "Effect of Viscosities on Structure and Instability of Sprays from a Swirl Atomizer," *Experimental Thermal and Fluid Science,* vol. 39, pp. 158-166, May 2012.

[127] A. Datta and S. Som, "Numerical Prediction of Air Core Diameter, Coefficient of Discharge and Spray Cone Angle of a Swirl Spray Pressure Nozzle," *International Journal of Heat and Fluid Flow,* vol. 21, no. 4, pp. 412-419, August 2000.

[128] P. Patel, R. Balachandran, N. Ladommatos and P. Richards, "An Investigation into Transient Diesel Spray Development Using High Speed Imaging in a Novel Optical Pressure Chamber," *SAE Technical Paper 2011-01-1836,* 2011.

[129] W. Zeng, M. Xu, G. Zhang, Y. Zhang and D. Cleary, "Atomization and Vaporization for Flash-Boiling Multi-Hole Sprays with Alcohol Fuels," *Fuel,* vol. 95, pp. 287-297, 2012.

[130] C. Park, S. Kim, H. Kim and Y. Moriyoshi, "Stratified Lean Combustion Characteristics of a Spray-Guided Combustion System in a Gasoline Direct Injection Engine," *Energy,* vol. 41, no. 1, pp. 401-407, May 2012.

[131] Malvern Instruments Limited, "A Basic Guide to Particle Characterization," 2012.

[132] A. Rawle, "Basic Principles of Particle Size Analysis," 2011.

[133] G. Zhang, X. Qiao, X. Miao, J. Hong and J. Zheng, "Effects of Highly Dispersed Spray Nozzle on Fuel Injection Characteristics and Emissions of Heavy-Duty Diesel Engine," *Fuel,* vol. 102, pp. 666-673, 2012.

[134] H. Willauer, R. Ananth, J. Hoover, A. Foote, C. Whitehurst, W. Williams and G. Mushrush, "Flammability of Aerosols Generated by a Rotary Atomizer," *Combustion Science and Technology,* vol. 179, pp. 1303-1326, 2007.

[135] K. Tuntivoranukul, P. Vallikul, B. Fungtammasan, P. Yongyingsakthavorn and C. Dumouchel, "Application of teh D2-Law to Determine Time Evolution and Burn-Out Time of Evaporating Biodiesel Spray Drop-Size Distribution," *Journal of Sustainable Energy & Environment,* vol. 1, pp. 59-63, 2010.

[136] H. Hiroyasu, "Diesel Engine Combustion and its Modelling," in *Diagnostics and Modeling of Diagnistics of Combustion in Reciprocating Engines*, Tokyo, 1985.

[137] A. Lefebvre, "Airblast Atomization," *Progress in Energy and Combustion,* vol. 6, pp. 233-261, 1980.

[138] A. Lefebvre and D. Ballal, Gas Turbine Combustion - Alternative Fuels and Emissions, 3rd ed., Boca Raton: CRC Press, 2010.

[139] R. Tolman, "The Effect of Droplet Size on Surface Tension," *The Journal of Chemical Physics,* vol. 17, no. 3, pp. 333-337, March 1949.

[140] S. Lin and Z. Lian, "Mechanisms of the Breakup of Liquid Jets," *AIAA Journal,* vol. 28, no. 1, pp. 120-126, January 1990.

[141] X.-C. Lu, X.-Q. Qiao, J. Cheng and Z. Huang, "Experimental Investigation of the Influence of Fuel Viscosity on the Spray Characteristics of Diesel Nozzle," *Journal of Shanghai Jiaotong University(Science),* Vols. E-12, no. 1, pp. 61-65, 2007.

[142] M. Elkotb, "Fuel Atomization for Spray Modelling," *Progress in Energy and Combustion Science,* vol. 8, pp. 61-91, 1982.

[143] H. Hiroyasu and T. Kadota, "Fuel Droplet Size Distribution in Diesel Combustion Chamber," *SAE Technical Paper 740715,* 1974.

[144] S. Sazhin, W. Abdelghaffar, E. Sazhina and M. Heikal, "Models for Droplet Transient Heating: Effects on Droplet Evaporation, Ignition and Break-Up," *International Journal of Thermal Sciences,* vol. 44, no. 7, pp. 610-622, July 2005.

[145] L. Araneo, L. Brunello, A. Coghe and R. Donde, "Effects of Fuel Temperature and Ambient Pressure on a GDI Swirled Injector Spray," Milan, 2009.

[146] X. Wang and A. Lefebvre, "Influence of Ambient Air Pressure on Pressure-Swirl Atomization," *Atomisation and Spray Technology (ISSN 0266-3481),* vol. 3, no. 3, pp. 209-226, 1987.

[147] X. Wang and A. Lefebvre, "Mean Drop Sizes from Pressure-Swirl Nozzles," *Journal of propulsiun,* vol. 3, no. 1, pp. 11-18, January 1987.

[148] J. Kashdan, J. Shrimpton and A. Whybrew, "Two-Phase Flow Characterization by Automated Digital Image Analysis. Part 1: Fundamental Principles and Calibration of the Technique," *Particle and Particle Systems Characterization,* vol. 20, no. 6, pp. 387-397, November 2003.

[149] J. Kashdan, J. Shrimpton and A. Whybrew, "Two-Phase Flow Characterization by Digital Image Analysis. Part 2: Application of PDIA for Sizing Sprays,"

Particle and Particle Systems Characterization, vol. 21, no. 1, pp. 15-23, May 2004.

[150] G. Castanet, P. Dunand, O. Caballina and F. Lemoine, "High-Speed Shadow Imagery to Characterize the Size and Velocity of the Secondary Droplets Produced by Drop impacts onto a Heated Surface," *16th International Symposium on Applications of Laser Techniques to Fluid Mechanics,* July 2012.

[151] H. Zhao and N. Ladommatos, "Optical Diagnostics for In-Cylinder Mixture Formation Measurements in IC Engines," *Progress in Energy and Combustion,* vol. 24, pp. 297-336, 1998.

[152] N. Damaschke, G. Gouesbet, G. Grehan, H. Mignon and C. Tropea, "Response of Phase Doppler Anemometer Systems to Nonspherical Droplets," *Applied Optics,* vol. 37, no. 10, pp. 1752-1761, 1998.

[153] N. Fdida, J. Blaisot , D. Dechaume and A. Floch, "Drop Size Measurment Techniques Applied to Gasoline Sprays: Determination of the Relevant Parameters for Application to Spray Combustion Computations," *Paper ID ICLASS06-105,* 2006.

[154] L. Dodge, D. Rhodes and R. Reitz, "Drop-Size Measurement Techniques for Sprays: Comparison of Malvern Laser-Diffraction and Aerometrics Phase/Doppler," *Applied Optics,* vol. 26, no. 11, pp. 2144-2154, 1987.

[155] H.-E. Albrecht, M. Borys, N. Damaschke and C. Tropea, Laser Doppler and Phase Doppler Measurement Techniques, Springer, 2002.

[156] Malvern Instruments, "Spraytec - Accurate Particle Sizing of Aerosols and Sprays," 2007.

[157] L. Dodge, "Comparison of Performance of Drop-Sizing Instruments," *Applied Optics,* vol. 26, no. 7, pp. 1328-1341, 1987.

[158] L. Kranendok and S. Sanders, "Optical Design in Beam Steering Environments with Emphasis on Laser Transmission Measurements," *Applied Optics,* vol. 44, no. 31, pp. 6762-6772, 2005.

[159] A. Jones, "A Review of Drop Size Measurement - The Application of Techniques to Dense Fuel Sprays," *Progress in Energy and Combustion,* vol. 3, pp. 225-234, 1977.

[160] C. Dumouchel, P. Yongyinsakthavorn and J. Cousin, "Light Multiple Scattering Correction of Laser-Differaction Spray Drop-Size Distribution Measurements," *International Journal of multiphase Flow,* vol. 35, pp. 277-287, 2009.

[161] K. Triballier, C. Dumouchel and J. Cousin, “A Technical Study on the Spraytec Performances: Influence of Multiple Light Scattering and Multi-Modal Drop-Size Distribution Measurements,” *Experiments in Fluids,* vol. 35, pp. 347-356, 2003.

[162] A. de Risi, R. Di Sante and G. Colangelo, “Optical Characterisation of a Diesel Spray at High Temperature and Pressure,” Lecce, 2004.

[163] R. Stone, Introduction to Internal Combustion Engines, 2nd ed., Macmillan, 1992.

[164] J. Wang, Z. Huang, H. Miao, X. Wang and D. Jiang, “Characteristics of Direct Injection Combustion Fuelled by Natural Gas-Hydrogen Mixtures Using a Constant Volume Vessel,” *International Journal of Hydrofen Energy,* vol. 33, no. 7, pp. 1947-1956, 2008.

[165] C. Espen and J. Dec, “Diesel Engine Combustion Studies in a Newly Designed Optical-Access Engine Using High-Speed Visualization and 2-D Laser Imaging,” *SAE Technical Paper 970795,* 1993.

[166] C. Tornatore, L. Marchitto, G. Valentino, F. Corcione and S. Merola, “Optical Diagnostics of the Combustion Process in a PFI SI Boosted Engine Fueled with Butanol-Gasoline Blend,” *Energy,* vol. 45, no. 1, pp. 277-287, 2012.

[167] S. Merola and B. Vaglieco, “Optical Investigation of Fuel Deposition Burning in Ported Fuel Injection (PFI) Spark-Ignition (SI) Engine,” *Energy,* vol. 34, no. 12, pp. 2108-2115, 2009.

[168] A. Cheng, A. Upatnieks and C. Mueller, “Investigation of the Impact of Biodiesel Fuelling on NOx Emissions Using an Optical Direct Injection Diesel Engine,” *International Journal of Engine Research,* vol. 7, pp. 297-318, 2006.

[169] E. Mancaruso, S. Merola and B. Vaglieco, “Study of the Multi-Injection Combustion Process in a Transparent Direct Injection Common Rail Diesel Engine by Means of Optical Techniques,” *International Journal of Engine Research,* vol. 9, pp. 483-498, 2008.

[170] S. Eisen, B. Ofner and F. Mayinger, “Investigations of Common-Rail Fuel Injection Technique in DI-Diesel-Engines,” *Proceedings of Symposium on Energy Engineering in the 21st Century (SEE2000),* vol. 4, pp. 1366-1378, 2000.

[171] G. Mittal and C.-J. Sung, “A Rapid Compression Machine for Chemical Kinetics Studies at Elevated Pressures and Temperatures,” *Combustion Science and Technology,* vol. 179, no. 3, pp. 497-530, 2007.

[172] M. Donovan, X. He, B. Zigler, T. Palmer, M. Woolridge and A. Atreya, “Demonstration of a Free-Piston Rapid Compression Facility for the Study of

High Temperature Combustion Phenomena," *Combustion and Flame,* vol. 137, no. 3, pp. 351-365, 2004.

[173] P. Prechtl, F. Dorer, B. Ofner, S. Eisen and F. Mayinger, "Modern optical Measurement Techniques Applied in a Rapid Compression Machine for the Investigation of Internal Combustion Engine Concepts," *Ercoftac Bulletin,* no. 38, 1998.

[174] Z. Hu, L. Somers, T. Davies, A. McDougall and R. Cracknell, "A Study of Liquid Fuel Injection and Combustion in a Constant Volume Vessel at Diesel Engine Conditions," *Fuel,* vol. 107, pp. 63-73, 2013.

[175] D. Segawa, T. Kadota, S. Nakaya, K. Takemura and T. Sasaki, "A Liquid Film or Droplet of Miscible Binary Fuel Burning on a Heated Surface at Elevated Pressures," *Proceedings of the Combustion Institute,* vol. 32, no. 2, pp. 2187-2194, 2009.

[176] D. Oren, S. Wahiduzzman and C. Ferguson, "A Diesel Combustion Bomb: Proof of Concept," *SAE Technical Paper 841358.*

[177] K. Nakanishi and T. Hirano, "The Effects of Charge Dilution on Combustion and Its Improvement - Flame Photograph Study," *SAE Technical Paper 750054,* 1975.

[178] E. Winklhoffer, "An Experimental Database for Diesel Spray Combustion," *26th Symposium (International) on Combustion/The Combustion Institute,* pp. 2541-2547, 1996.

[179] G. Beretta, M. Rashidi and J. Keck, "Turbulent Flame Propagation and Combustion in Spark Ignition Engines," *Combustion and Flame,* no. 52, pp. 217-245, 1983.

[180] E. Winklhofer and H. Fuchs, "Laser Induced Flourescence and Flame Photography - Tools in Gasoline Engine Combustion Analysis," *Optics and Lasers in Engineering,* vol. 25, pp. 379-400, 1996.

[181] G. Settles, Schlieren and Shadowgraph Techniques - Visualizing Phenomena in Transparent Media, Springer, 2001.

[182] A. Moghaddas, K. Eisazadeh-Far and H. Metghalchi, "Laminar Burning Speed Measurement of Premixed n-Dedacane/Air Mixtures using Spherically Expanding Flames at High Temperatures and Pressures," *Combustion and Flame,* vol. 159, no. 4, pp. 1437-1443, 2012.

[183] B. Bougie, M. Tulej, T. Dreier, N. Dam, J. Ter Meulen and T. Gerber, "Optical Diagnostics of Diesel Spray Injections and Combustion in a High-Pressure High-Temperature Cell," *Applied Physics B - Lasers and Optics,* vol. 80, pp. 1039-1045, 2005.

[184] D. Mowbray, “The Use of Schlieren and Shadowgraph Techniques in the Study of Flow Patterns in Density Stratified Liquids,” *Journal of Fluid Mechanics,* vol. 27, no. 3, pp. 595-608, 1967.

[185] M. Drake, T. Fansler and A. Lippert, “Stratified-Charge Combustion: Modeling and Imaging of a Spray-Guided Direct-Injection Spark-ignition Engine,” *Proceedings of the Combustion Institute,* vol. 30, no. 2, pp. 2683-2691, January 2005.

[186] D. Floryan, J. Hofferth and W. Saric, “Design, Assembly, and Calibration of a Focused Schlieren System,” *Technical Paper,* 2012.

[187] L. Kostiuk and R. Cheng, “Imaging of Premixed Flames in Microgravity,” *Experiments in Fluids,* vol. 18, pp. 59-68, 1994.

[188] J. Sjöholm, J. Rosell, B. Li, M. Richter, Z. Li, X.-S. Bai and M. Alden, “Simultaneous Visulization of OH, CH, CH2O and Toluene PLIF in a Methane Jet Flame with Varying Degrees of Turbulence,” *Proceedings of the Combustion Institute,* vol. 34, no. 1, pp. 1475-1482, 20132.

[189] K. Yamamoto, S. Isii and M. Ohnishi, “Local Flame Structure and Turbulent Burning Velocity by Joint PLIF Imaging,” *Proceedings of the Combustion Institute,* vol. 33, no. 1, pp. 1285-1292, 2011.

[190] F. Tinaut, M. Reyes, B. Gimenez and J. Pastor, “Measurements of OH* and CH* Chemiluminescence in Premixed Flames in a Constant Volume Combustion Bomb under Autoignition Conditions,” *Energy Fuels,* vol. 25, pp. 119-129, 2011.

[191] M. Reyes, F. Tinaut, C. Andres and A. Perez, “A Method to Determine Ignition Delay Times for Diesel Surrogate Fuels from Combustion in a Constant Volume Bomb: Inverse Livengood-Wu Method,” *Fuel,* vol. 102, pp. 289-298, 2012.

[192] W. Hetschell, “Optical Diagnostics for Combustion Process Development of Direct-Injection Gasoline Engines,” *Proceedings of the Combustion Institiute,* vol. 28, pp. 1119-1135, 2000.

[193] U. Spicher and A. Velji, “Measurements of Spatial Flame Propagation and Flow Velocities in a Spark Ignition Engine,” *20th Symposium (International) on Combustion/The Combustion Institute,* pp. 19-27, 1984.

[194] C. Ji and S. Wang, “Experimental Study on Combustion and Emissions Performance of a Hybrid Hydrogen-Gasoline Engine at Lean Burn Limits,” *International Journal of Hydrogen Energy,* vol. 35, no. 3, pp. 1453-1462, February 2010.

[195] R.-H. Chen, L.-B. Chiang, C.-N. Chen and T.-H. Lin, "Cold-Start Emissions of and SI Engine Using Ethanol-Gasoline Blended Fuel," *Applied Thermal Engineering,* vol. 31, no. 8-9, pp. 1463-1467, June 2011.

[196] M. Al-Hasan, "Effect of Ethanol-Unleaded Gasoline Blends on Engine Performance and Exhaust Emissions," *Energy Conversion and Mangement,* vol. 44, no. 9, pp. 1547-1561, June 2003.

[197] D. Han, A. Ickes, S. Bohac, Z. Huang and D. Assanis, "HC and CO Emissions of Premixed Low-Temperature Combustion Fueled by Blends of Diesel and Gasoline," *Fuel,* vol. 99, pp. 13-19, September 2012.

[198] S. Hochgreb, "Combustion Related Emissions in SI Engines," in *Handbook of Air Pollution from Internal Combustion Engines,* E. Sher, Ed., Academic Press, 1998, pp. 118-170.

[199] Y. Shen, S. Shuai, J. Wang and J. Xiao, "Optimization of Gasoline Hydrocarbon Compositions for Reducing Exhaust Emissions," *Journal for Environmental Sciences,* vol. 21, no. 9, pp. 1208-1213, 2009.

[200] N. Henein and M. Tagomori, "Cold-Start Hydrocarbon Emissions in Port-Injected Gasoline Engines," *Progress in Energy and Combustion Science,* vol. 25, no. 6, pp. 563-593, December 1999.

[201] R. Farrauto and R. Heck, "Catalytic Converters: State of the Art and Perspectives," *Catalyst Today,* vol. 51, no. 3-4, pp. 351-360, July 1999.

[202] S. Atmur and T. Strasser, "Exhaust Manifold with Integral Catalytic Converter". USA Patent US Patent, 5,692,373, 2 December 1997.

[203] G. Lavoie, J. Heywood and J. Keck, "Experimental and Theoretical Study of Nitric Oxide Formation in Internal Combustion Engines," *Combustion Science and Technology,* vol. 1, pp. 313-326, 1970.

[204] J. Bozzelli and A. Dean, "O + NNH: A Possible New Route for NOx Formation in Flames," *International Journal of Chemical Kinetics,* vol. 27, pp. 1097-1109, 1995.

[205] R.-H. Chen, L.-B. Chiang, M.-H. Wu and T.-H. Lin, "Gasoline Displacement and NOx Reduction in an SI Engine by Aqueous Alcohol Injection," *Fuel,* no. 3, pp. 604-610, March 2010.

[206] S. Wang, C. Ji, J. Zhang and B. Zhang, "Improving the Performance of Gasoline Engine with the Addition of Hydrogen-Oxygen Mixtures," *International Journal of Hydrogen Energy,* no. 36, pp. 11164-11173, 2011.

[207] J. Jang, Y. Lee, C. Cho, Y. Woo and C. Bae, "Improvement of DME HCCI Engine Combustion by Direct Injection and EGR," *Fuel,* vol. 113, pp. 617-624, 2013.

[208] J. Hepburn, E. Thanasiu, D. Dobson and W. Watkins, "Experimental and Modelling Investigations of NOx Trap Performance," *SAE Technical Paper Series, 962051,* October 1996.

[209] J. Heywood, "Automotive Engines and Fuels: A Review of Future Options," *Progress in Energy and Combustion Science,* vol. 7, no. 3, pp. 155-184, 1981.

[210] Y. Wang, S. Raman and J. Grizzle, "Dynamic Modelling of a Lean NOx Trap for Lean Burn Engine Control," 1999.

[211] C. Scholz, "NOx Storage and Reduction Over a Lean-Burn Automotive Catalyst," Eindhoven, 2007.

[212] P. Forzatti and L. Lietti, "The Reduction of NOx Stored on LNT and Combined LNT-SCR Systems," *Catalysis Today,* vol. 155, no. 1-2, pp. 131-139, October 2010.

[213] C.-K. Seao, H. Kim, B. Choi and M. Lim, "The optimal Volume of a Combined System of LNT and SCR Catalysts," *Journal of Industrial and Engineering Chemistry,* vol. 17, no. 3, pp. 382-385, May 2011.

[214] G. Abd-Alla, "Using Exhaust Gas Recirculation in Internal Combustion Engines," *Energy Conversion and Management,* vol. 43, no. 8, pp. 1027-1042, May 2002.

[215] C.-L. Myung, J. Kim, K. Choi, I. Hwang and S. Park, "Comparitive Study of the Engine Control Strategies for Particulate Emissions from Direct Injection Light-duty Vehicle Fueled with Gasoline and Liquefied Petroleum Gas (LPG)," *Fuel,* vol. 94, pp. 348-355, April 2012.

[216] W. Wilke, "Uber die Beziehung zwischen Oktanzahl und Cetanzahl (In German)," *Automobiltechn.,* vol. 43, no. 6, pp. 148-149, 1940.

[217] B. Duboc, "The Effect of Diesel Fuel Additives on Engine Efficiency and Performance," London, 2014.

[218] Brookfield Engineering Laboratories Inc., "Brookfield Digital Rheometer," Stoughton, 2014.

[219] Kimble & Chase, "Surface Tension Analyzer," Rochester, 2008.

[220] S. Marshall, "Measuring Laminar Burning Velocities," Oxford, 2010.

[221] J. Dale, M. Checkel and P. Smy, "Application of High Energy ignition Systems to Engines," *Progress in Energy and Combustion Science,* vol. 23, pp. 379-398, 1997.

[222] Ricardo & Co., "Ricardo E6/US Variable Compression Engine," Shoram, 1970.

[223] Cambustion, "DMS500 Fast Aerosol Size Spectrometer," Cambridge, 2008.

[224] F. Catapano, P. Sementa and B. Vaglieco, "Optical Characterization of Bio-Ethanol Injection and Combustion in a Small DISI Engine for Two Wheels Vehicles," *Fuel,* vol. 106, pp. 651-66, April 2013.

[225] D. Hung, D. Harrington, A. Gandhi, L. Markle, S. Parrish, J. Shakal, H. Sayar, S. Commings and J. Kramer, "Gasoline Fuel Injector Spray Measurement and Characterization - A New SAE J2715 Recommended Practice," *SAE Technical Paper 2008-01-1068,* 2008.

[226] H. Suh, S. Park and C. Lee, "Effect of Piezo-Driven Injection System on the Macroscopic and Microscopic Atomization Characteristics of Diesel Fuel Spray," *Fuel,* vol. 86, pp. 2833-2845, 2007.

[227] P.-C. Chen, W.-C. Wang, W. Roberts and T. Fang, "Spray and Atomization of Diesel Fuel and its Alternatives from a Single-Hole Injector Using a Common Rail Fuel Injection System," *Fuel,* vol. 103, pp. 850-861, August 2013.

[228] S. Moon, C. Bae, J. Choi and E. Abo-Serie, "The Influence of Airflow on Fuel Spray Characteristics from a Slit Injector," *Fuel,* vol. 86, no. 3, pp. 400-409, February 2007.

[229] S. Lee and S. Park, "Experimental Study on Spray Break-Up and Atomization Processes from GDI Injector Using High Injection Pressure up to 30 MPa," *International Journal of Heat and Fluid Flow,* vol. 45, pp. 14-22, February 2014.

[230] A. Elwardany, S. Sazhin and A. Farooq, "Modelling of Heating and Evaporation of Gasoline Fuel Droplets: A Comparitive Study," *Fuel,* vol. 111, pp. 643-647, 2013.

[231] I. Pribicevic and T. Sattelmayer, "Investigation of the Diesel Spray Atomization Process with the Use of Phase Doppler Anemometry at High Injection Pressures and at Engine-Like Gas Densitiy," in *16th International Symposium on Applications of Laser Techniques to Fluid Mechanics,* Lisbon, 2012.

[232] J. Qian and K. Law, "Regimes of Coalescence and Separation in Droplet Collision," *Journal of Fluid Mechanics,* vol. 331, pp. 59-80, 1997.

[233] A. Ghasemi, R. Barron and R. Balachandar, “Spray-Induced Air Motion in Single and Twin Ultra-High Injection Diesel Sprays,” *Fuel,* vol. 121, pp. 284-297, April 2014.

[234] B. Deng, J. Fu, D. Zhang, J. Yang, R. Feng, J. Liu, K. Li and X. Liu, “The Heat Release Rate Analysis of Bio-Butanol/Gasoline Blends on a High Speed SI (Spark Ignition) Engine,” *Energy,* vol. 60, pp. 230-241, 2013.

[235] H. Wei, D. Feng, G. Shu, M. Pan, Y. Guo, D. Gao and W. Li, “Experimental Investigation on the Combustion and Emissions Charactersitics of 2-Methylfuran Gasoline Blend Fuel in Spark-Ignition Engine,” *Applied Energy,* vol. 132, pp. 317-324, 2014.

[236] C. Ferguson and A. Kirkpatrick, Internal Combustion Engines, 2nd ed., J. Hayton, Ed., John Wiley & Sons, Inc., 2001.

[237] C. Ji, S. Wang and B. Zhang, “Effect of Spark Timing on the Performance of a Hybrid Hydrogen-Gasoline Engine at Lean Conditions,” *International Journal of Hydrogen Energy* , vol. 35, pp. 2203-2212, 2010.

[238] W. Winkler, “Shampoo Compositions,” 1984.

[239] D. Cole, “Homogeneous; Containing Water, Microbiocide in Uniform Dispersion,” 1999.

[240] Bosch Compact, “Overview of Diesel Markets from China to the U.S.,” 2013.

[241] B. Esteban, J.-R. Riba, G. Baquero, A. Rius and R. Puig, “Temperature Dependence of Density and Viscosity of Vegetable oils,” *Biomass and Bioenergy,* vol. 42, pp. 164-171, 2012.

[242] P. Hellier, N. Ladommatos, R. Allan and J. Rogerson, “Combustion and Emissions Characteristics of Toluene/n-Heptane and 1-Octene/n-octane Binary Mixtures in a Direct Injection Diesel Engine,” *Submitted to Combustion and Flame,* 2012.

[243] E. Apltekin and M. Canakci, “Determination of the Density and the Viscosities of Biodiesel-Diesel Fuel Blends,” *Renewable Energy,* vol. 33, no. 12, pp. 2623-2630, December 2008.

[244] M. E. Tat and J. H. Van Gerpen, “The Kinematic Viscosity of Biodiesel and Its Blends with Diesel Fuel,” *Journal of the American Oil Chemists' Society,* vol. 76, no. 12, pp. 1511-1513, December 1999.

[245] M. Vidal, W. Rogers and M. Mannan, “Prediction of Minimum Flash Point Behaviour for Binary Mixtures,” *Process Safety and Environmental Protection,* vol. Part B, no. 84, pp. 1-9, 2006.

[246] M. Hristova, "Measurement and Prediction of Binary Mixture Flash Point," *Central European Journal of Chemistry,* vol. 11, no. 1, pp. 57-62, 2013.

[247] M. Hristova and D. Damgaliev, "Flash Point of Organic Binary Mixtures Containing Alcohols: Experiment and Prediction," *Central European Journal of Chemistry,* vol. 11, no. 3, pp. 388-393, 2013.

[248] J. Goodrum, D. Geller and S. Lee, "Rapid Measurement of Boiling Points and Vapour Pressure of Binary Mixtures of Short-Chain Triglycerides by TGA Method," *Thermochimica Acta,* vol. 311, no. 1-2, pp. 71-79, 1998.

[249] T. Vittal Prasad, B. Sankar, R. Pavan Kumar and D. Prasad, "Boiling Temperature Measurements on the Binary Mixtures Formed by Tert-Butanol with some Chloroethanes and Chloroethylenes at 94.6 kPa," *Fluid Phase Equilibria,* vol. 213, no. 1-2, pp. 147-152, 2003.

[250] X. Wang and A. Lefebvre, "Influence of Fuel Temperature on Atomization Performance of Pressure-Swirl Atomizers," *International Symposium on Air Breathing Engines,* pp. 193-199, 1987.

[251] G. Batchelor, An Introduction to Fluid Dynamics, Cambridge University Press, 1967.

[252] P. Hiemenez and R. Rajagopalan, Principles of Colloid and Surface Chemistry, New York: Marcel Dekker, Inc, 1997.

[253] K. Han, Fundamentals of Aqueous Metallurgy, Littleton: SME, 2002.

[254] T. Cooney and T. Russell, *Presentation of Results,* 2014.

[255] Technical Committee of Petroleum Additive Manufacturers in Europe, "Fuel Additives: Use and Benefits," 2013.

[256] S. Curry, "Effect of Antiknocks on Flame Propagation in a Spark Ignition Engine," *Symposium (International) on Combustion,* vol. 9, no. 1, pp. 1056-1068, 1963.

[257] G. Linteris, M. Rumminger and V. Babushok, "Catalytic Inhibition of Laminar Flames by Transition Metal Compounds," *Progress in Energy and Combustion Science,* vol. 34, no. 3, pp. 288-329, June 2008.

[258] M. Day, D. Stamp, K. Thompson and G. Dixon-Lewis, "Inhibition of Hydrogen-Air and Hydrogen-Nitrous Oxide Flames by Halogen Compounds," *Symposium (International) on Combustion,* vol. 13, no. 1, pp. 705-712, 1971.

[259] T. Alger, J. Gingrich, C. Roberts, B. Mangold and M. Sellnau, "A High-Energy Continuous Discharge Ignition System for Dilute Engine Applications," *SAE Technical Paper,* no. 2013-01-1628, 2013.

[260] V. Babrauskas, Ignition Handbook, 1st ed., Issaquah: Fire Science Publishers, 2003.

[261] R. Iverson, "The Effects of Intake Charge Stratification on HCCI Combustion," Madison, 2004.

[262] N. Savaranan and G. Nagarajan, "Experimental Investigation on Performance and Emission Characteristics of Dual Fuel DI Diesel Engine with Hydrogen Fuel," 2009.

[263] C. Sayin, "The Impact of Varying Spark Timing at Different Octane Numbers on the Performance and Emission Characteristic in a Gasoline Engine," *Fuel,* vol. 97, pp. 856-861, 2012.

[264] A. Sonin, The Physical Basis of Dimensional Analysis, 2nd ed., MIT, 2001.

[265] M. Iqbal, M. Ahmad and M. Younis, "Effect of Reynold's Number on Droplet Size of hollow Cone Nozzle of Environment Friendly Univeristy Boom Sprayer," *Pakistan Journal of Agricultural Sciences,* vol. 42, no. 3-4, pp. 106-111, 2005.

[266] DieselNet, March 2012. [Online]. Available: http://www.dieselnet.com/standards/eu/ld.php. [Accessed 3 September 2012].

[267] D. Bradley and G. Hundy, "Burning Velocities of Methane-Air Mixtures Using Hot-Wire Anemometers in Closed-Vessel Explosions," *Symposium (International) on Combustion,* vol. 13, no. 1, pp. 575-583, 1971.

[268] G. Andrews and D. Bradley, "The Burning Velocity of Methane-Air mixture," *Combustion and Flame,* vol. 19, pp. 275-288, 1972.

[269] Driver and Vehicle Licensing Agency, "Rates of Vehicle Tax," 2012.

[270] Y. Tanasawa and S. Toyoda, "On the Atomisation of a Liquid Jet Issuing from a Cylindrical Nozzle," 1955.

[271] X. Feng, J. Lagon, M. Nuckols and M. D. Thomas, "Fuel Additives and Gasoline Containing the Additives". USA Patent US 2012/0180382 A1, 19 July 2012.

[272] S. Agarwal, V. K. Chhibber and A. K. Bhatnagar, "Tribological Behaviour of Diesel Fuels and the Effect of Ant-Wear Additives," *Fuel,* pp. In Press, Corrected Proof, December 2012.

[273] S. Tonini, M. Gavaises and A. Theodorakakos, "The Role of Droplet Fragmentation in High-Pressure Evaporating Diesel Sprays," *International Journal of Thermal Sciences,* vol. 48, pp. 554-572, 2009.

[274] H. Nakamura, T. Ohinouye, K. Hori, Y. Kiyota, T. Nakagami, K. Akishino and Y. Tsukamoto, "Development of a New Combustion System (MCA-JET) in Gasoline Engine," *SAE Technical Paper 780007,* 1978.

[275] K. Saeed, "Laminar Burning Velocity Measurements," 2002.

[276] H. Kobayashi, T. Nakashima, T. Tamura, K. Maruta and T. Niioka, "Turbulence Measurements and Observations of Turbulent Premixed Flames at Elevated Pressures up to 3.0MPa," *Combustion and Flame,* vol. 108, pp. 104-117, 1997.

[277] F. Paschen, "Ueber die zum Funkenübergang in Luft, Wasserstoff und Kohlensäure bei Verschiedenen Drucken Erforderliche Potentialdifferenz," *Annalen der Physik,* vol. 273, no. 5, pp. 69-96, 1889.

Appendix A

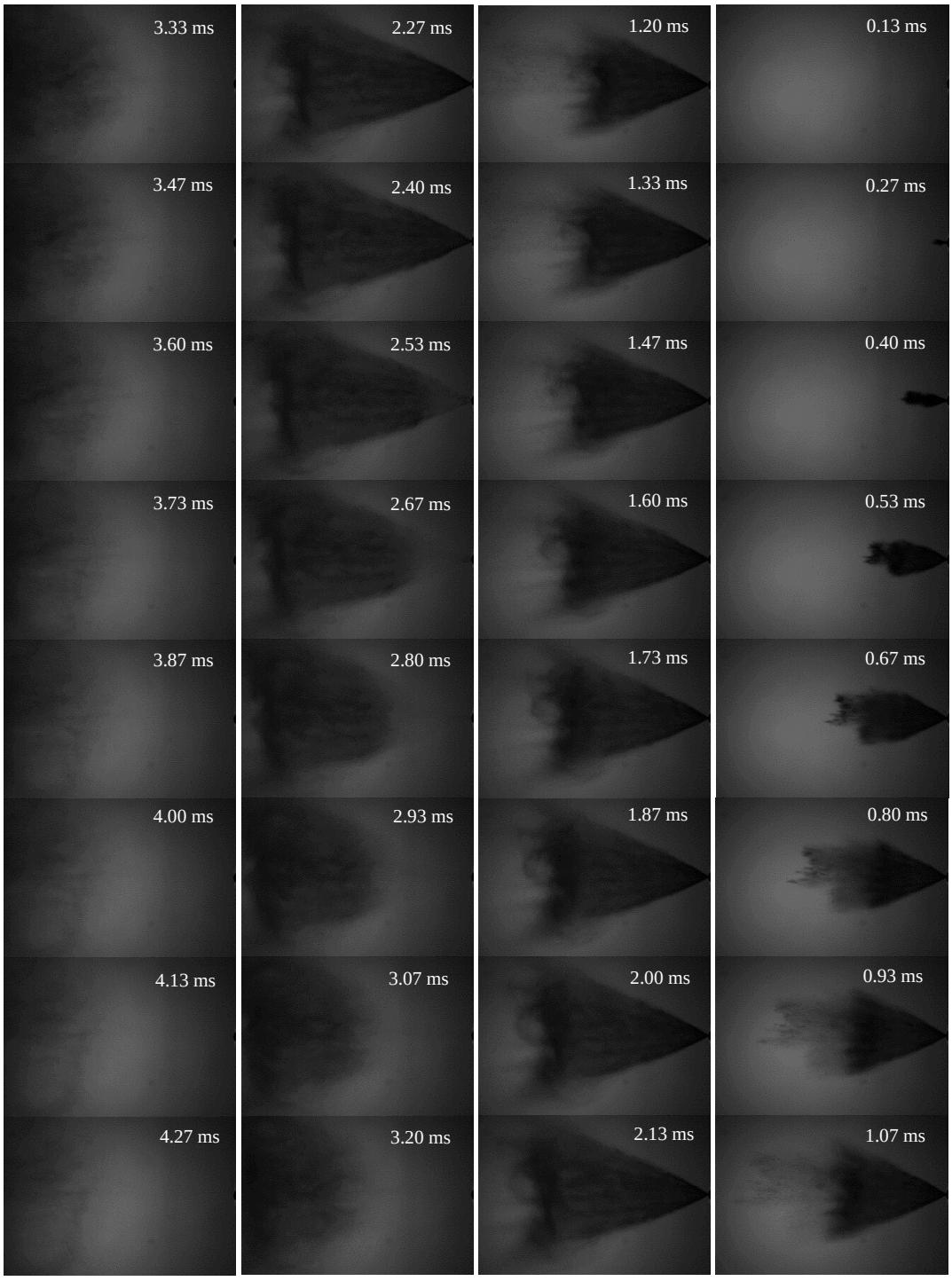

Figure A.1: Shadowgraph images of a fuel spray at 50bar injection pressure with a high speed camera at a capture rate of 7500Hz and 20µs exposure time

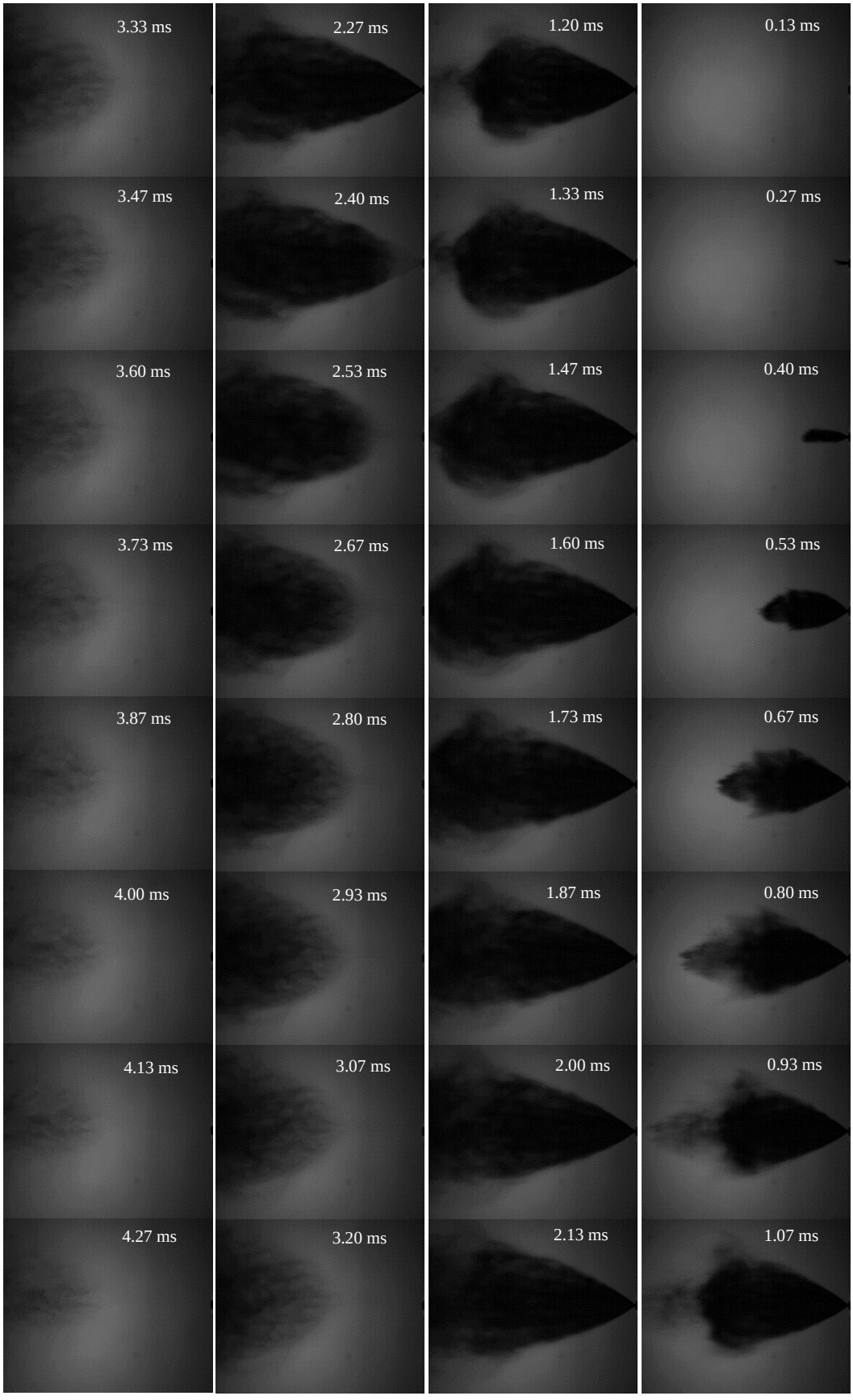

Figure A.2: Shadowgraph images of a fuel spray at 110bar injection pressure with a high speed camera at a capture rate of 7500Hz and 20µs exposure time

Appendix B

Dimensional Analysis

The variables considered relevant to drop size formation are as shown in Table B.1. The dimensions M, L and T stand for mass, distance and time, respectively.

Variable	Symbol	Dimensions
Droplet diameter	d	L
Nozzle diameter	D	L
Fuel density	ρ	ML^{-3}
Fuel viscosity	μ	$ML^{-1}T^{-1}$
Fuel surface tension	σ	MT^{-2}
Fuel spray velocity	u	LT^{-1}

Table B.1: Dimensions of assumed variables

Following the Buckingham's Pi theorem [264], the 6 variables and 3 dimensions give 6 – 3 = 3 dimensionless groups. The three groups were identified as follows:

$$\Pi_1 = \frac{d}{D} \quad \text{B.1}$$

$$\Pi_2 = \frac{\rho u D}{\mu} \quad \text{B.2}$$

$$\Pi_3 = \frac{\rho u^2 D}{\sigma} \quad \text{B.3}$$

Therefore, the relationship between the groups can be expressed as:

$$\frac{d}{D} = f\left[\frac{\rho u D}{\mu}, \frac{\rho u^2 d}{\sigma}\right] \qquad \text{B.4}$$

This relates well to the theory on atomisation as described in Section 2.3 as Π_2 is the Reynolds number and Π_3 the Weber number. A further variable that could be considered is fluid bulk modulus of elasticity and as such a further dimensionless group of Mach number could be used in the analysis. However, as explained by Iqbal et al. [265], Mach number is only relevant if fluid velocity is greater than the speed of sound. As could be seen in Figure 3.5 (page 78), the fuel spray velocity reached in the current study remains below 52 m/s for all pressures up to 110 bar, meaning the Mach number could be excluded from the current study. It is worthwhile noting that the spray tip velocity was calculated from high speed images based on the fuel reaching the measuring point at x = -10 mm and z = 60 mm. Initial spray velocity within the injector nozzle and leaving the nozzle is likely to be higher, thus higher Weber and Reynolds numbers could be computed. Nevertheless, it is a reasonable assumption that the spray velocity would not exceed at any point the speed of sound of 343 m/s at ambient temperature in air.

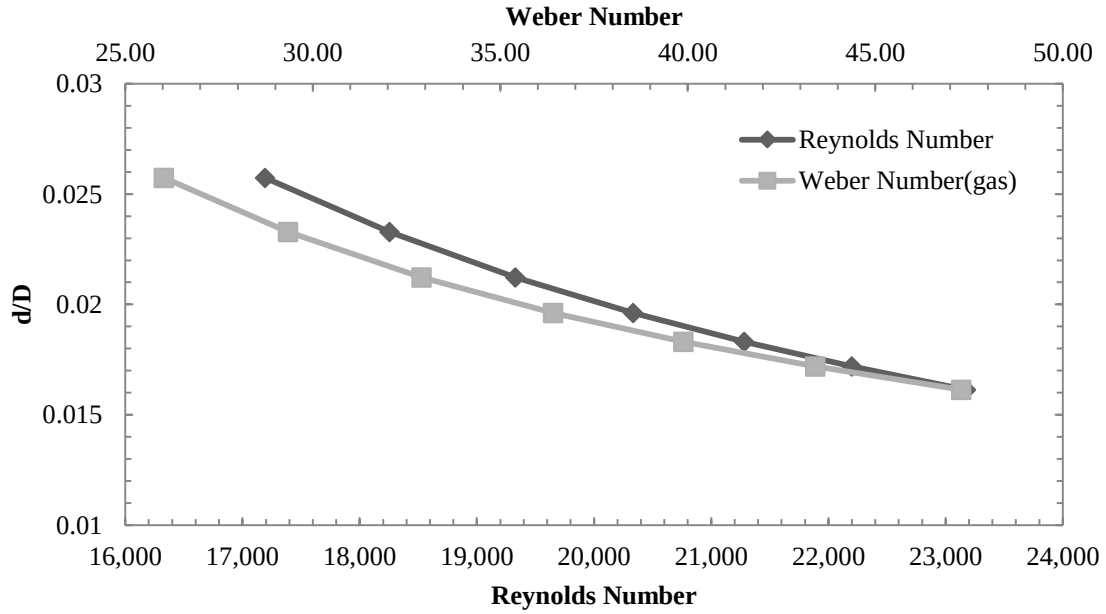

Figure B.1: d/D change with We and Re for sprays at 50-110 bar injection pressure

Figure B.1 displays the change in dimensionless droplet size with respect to the Weber and Reynolds numbers. In both cases, it is evident that an increase in injection pressure results in increased Weber and Reynolds number. This in turn

induces a reduction in droplet size. The calculated Weber number values in the range $26 < We < 47$ suggest that secondary droplet break-up occurs. According to Table 2.2 (Page 47) the mechanisms responsible for the secondary break-up are bag-and-stamen and chaotic.